



**HAL**  
open science

# Computer-Aided Thermofluid Analyses using Excel

Mohamed Musadag El-Awad

► **To cite this version:**

Mohamed Musadag El-Awad. Computer-Aided Thermofluid Analyses using Excel. 2021. halshs-02289507v2

**HAL Id: halshs-02289507**

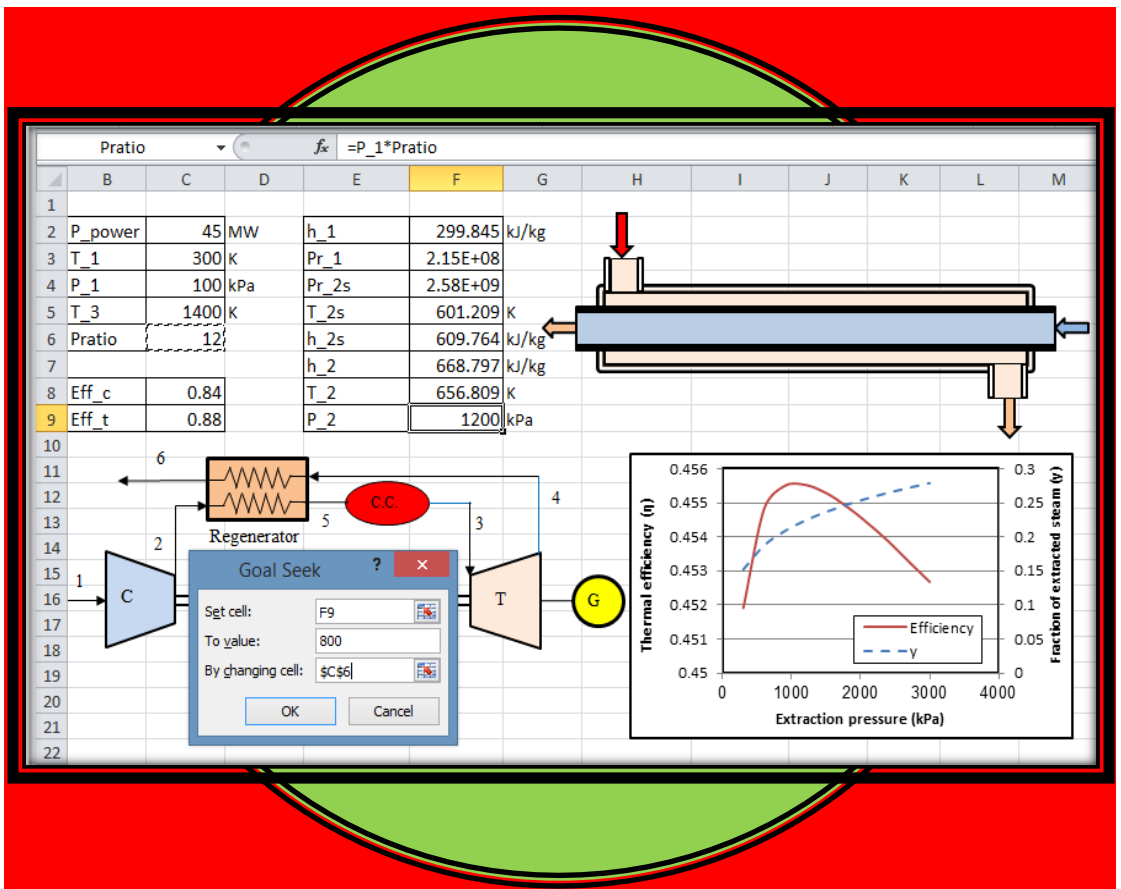
**<https://shs.hal.science/halshs-02289507v2>**

Preprint submitted on 24 Jan 2021

**HAL** is a multi-disciplinary open access archive for the deposit and dissemination of scientific research documents, whether they are published or not. The documents may come from teaching and research institutions in France or abroad, or from public or private research centers.

L'archive ouverte pluridisciplinaire **HAL**, est destinée au dépôt et à la diffusion de documents scientifiques de niveau recherche, publiés ou non, émanant des établissements d'enseignement et de recherche français ou étrangers, des laboratoires publics ou privés.

# Computer-Aided Thermofluid Analyses Using Excel



Mohamed M. El-Awad

Mohamed M. El-Awad (UTAS)

***Computer-Aided Thermofluid Analyses  
Using Excel***

Comouter-Aided Thermofluid Analyses Using Excel

# **Computer-Aided Thermofluid Analyses Using Excel**

**Mohamed M. El-Awad**  
**Associate Professor,**  
**University of Technology and Applied Sciences**  
**College of Applied Sciences, Sohar**

Mohamed M. El-Awad (UTAS)

*This book is dedicated to the memory of my parents*

*Amna and El-Awad*

*May Allah bless their souls in Heaven*

Mohamed M. El-Awad (UTAS)

**January, 2021**

**The Thermax add-in can be downloaded from:**

**[https://www.researchgate.net/publication/334959438\\_Thermax](https://www.researchgate.net/publication/334959438_Thermax)**

## Preface

Microsoft Excel is a general-purpose application that is taught to engineering students in the introductory courses on computer applications. The powerful tools of Excel for data analysis and visualisation, together with its wide availability and simplicity, encouraged its use as an educational tool in various engineering subjects. With respect to thermofluid analyses, a number of articles and research papers have been presented in this regard at various conferences and specialised publications over the past two decades. The lack of built-in functions in Excel for fluid properties also motivated a number of academic institutions and individual researchers to develop relevant Excel add-ins. However, a textbook that presents a general pedagogical approach for using Excel as a platform for computer-aided thermofluid analyses and provides the lecturers and students with sufficiently detailed examples and exercises has, so far, been missing. The aim of this book is to complement the previous efforts by gathering the information needed for using Excel as an effective modelling platform for various types of computer-aided thermofluid analyses.

The Excel-based modelling platform described in the book has four elements; (i) Excel with its user-interface and built-in functions, (ii) the integrated programming language Visual Basic for Applications (VBA), (iii) the Solver add-in that comes with Excel, and (iv) an Excel add-in for fluid properties called Thermax. While Excel and Solver are adequate for most fluid mechanics and heat-transfer analyses, the Thermax add-in helps the students to perform thermodynamic analyses with Excel in an effective and accurate manner. VBA is needed for the development of custom functions when the analytical model cannot be executed by only using Excel's built-in functions and Thermax functions. Proper use of the Excel-based modelling platform minimises the effort of developing the analytical model so that more attention can be paid to the application of the physical and economic principles in thermofluid analyses.

The first three chapters of the book review the basic principles of thermofluid analyses and describe the four components of the Excel-based modelling platform. Chapter 4 is also a general chapter that shows how Excel and its iterative tools can be used for performing iterative solutions in the three thermofluid areas. The following six chapters apply the platform for particular types of thermofluid analyses. Chapters 5 and 6 are dedicated to the hydraulic analyses of pump-pipe systems and pipe-networks, while Chapters 7 and 8 deal with heat-transfer analyses by focussing on the numerical solution of the heat-conduction equation by using the finite-difference method. The application of the Excel-based platform for thermodynamic analyses is demonstrated in Chapters 9 and 10 that use the property functions provided by the Thermax add-in for ideal gases and refrigerant fluids for dealing with the analyses of power-generation and refrigeration cycles.

The book adopts a learning-by-example approach and most of its examples are based on relevant cases or examples given in popular thermofluid textbooks so that the students



can verify their Excel solutions and look for additional applications. Exercises are given at the end of each chapter that help students to sharpen their skills related to the particular topic.

The material covered in the book is adequate for a stand-alone course on computer-aided thermofluid analyses, but the book can also be used to supplement the existing relevant courses by selecting certain chapters or sections from it. Although the book is primarily meant for educational purposes, it is hoped that the material covered in the book can also be useful for practicing engineers in the area of thermofluid systems.

### **Acknowledgements**

The writing of this book would not have been possible without benefitting from the efforts of many colleagues who have made their information and software available in the open literature or their websites. In this respect, a special gratitude goes to the Mechanical Engineering Department at the University of Alabama (USA) whose initiatives both inspired and helped me throughout the preparation of the book. I am also indebted to my colleagues and students at the College of Applied Sciences in Sohar and hope that they find this book a worthy token of appreciation and gratitude. Last, but not least, I am grateful to my beloved family, Ghada, Ahmed, and Ula, for their tolerance and unflinching support that I desperately needed to complete this work.

## CONTENTS

Nomenclature	xi
1. Introduction	1
1.1. A review of thermofluid principles	2
1.1.1. Thermodynamics	2
1.1.2. Fluid dynamics	7
1.1.3. Heat transfer	10
1.2. Advantages of computer-aided thermofluid analyses	13
1.3. The Excel-based modelling platform for thermofluid analyses	16
1.4. Closure	18
References	19
2. Excel	20
2.1. Elements of Excel's user-interface	21
2.2. Excel's formulae	22
2.2.1. Cell reference by location	22
2.2.2. Use of cell labels	24
2.3. Excel's built-in functions	27
2.3.1. Logical functions	28
2.3.2. Functions for matrix operations	29
2.4. Solution of linear systems of equations	33
2.5. Iterative solutions with Excel	35
2.5.1. Iterative solutions with Goal-Seek	35
2.5.2. Iterative solutions with circular calculations	37
2.6. Excel's graphical tools for data presentation and analysis	40
2.7. Closure	43
References	43
Exercises	44
3. Solver, VBA, and Thermax	47
3.1. Solver	48
3.1.1. Activation of Solver	48
3.1.2. The GRG Nonlinear method	50
3.1.3. The Evolutionary method	52
3.1.4. The Simplex LP method	54
3.1.5. The default settings of Solver options	56
3.2. VBA and the development of user-defined functions	58
3.2.1. Activation of VBA	59
3.2.2. Development of UDFs	61
3.3. Thermax installation and use	63
3.4. Closure	67
References	67

Exercises 68

- |   |            |
|---|------------|
| <p>4. Iterative solutions</p> <p>4.1. Iterative solutions by using Goal Seek 72</p> <p>    4.1.1. Type-2 and type-3 pipe flow analyses 72</p> <p>    4.1.2. Thermodynamic analyses involving ideal-gas mixtures 74</p> <p>    4.1.3. Convection heat-transfer analyses 77</p> <p>4.2. Constrained iterative solutions with Solver 80</p> <p>4.3. Iterative solutions involving nonlinear equations 87</p> <p>4.4. Closure 89</p> <p>    References 89</p> <p>    Exercises 90</p>   | <p>71</p>  |
| <p>5. Hydraulic analyses of multi-pipe and pump-pipe systems</p> <p>5.1. Analyses of multi-pipe systems 94</p> <p>    5.1.1. Type-1 flow analyses 95</p> <p>    5.1.2. Type-2 and type-3 flow analyses 99</p> <p>5.2. The operating point for a pump-pipe system 101</p> <p>    5.2.1. A centrifugal pump connected to a single pipe 101</p> <p>    5.2.2. A centrifugal pump connected to two branching pipes 105</p> <p>    5.2.3. A centrifugal pump connected to a simple pipe-network 108</p> <p>5.3. Centrifugal pumps in serial and parallel arrangements 112</p> <p>    5.3.1. Two centrifugal pumps connected in parallel 112</p> <p>    5.3.2. Two centrifugal pumps connected in series 115</p> <p>    5.3.3. A comparison of serial and parallel pump arrangements 117</p> <p>5.4. Closure 118</p> <p>    References 118</p> <p>    Exercises 118</p> | <p>93</p>  |
| <p>6. Hydraulic analyses of pipe networks</p> <p>6.1. The methodology of looped pipe-network analysis 124</p> <p>6.2. Analyses of looped pipe networks by Excel-Solver 129</p> <p>6.3. Analyses of branched pipe networks by Excel-Solver 137</p> <p>6.4. Analyses of mixed pipe networks by Excel-Solver 141</p> <p>6.5. Closure 145</p> <p>    References 146</p> <p>    Exercises 146</p>  | <p>123</p> |
| <p>7. Finite-difference solution of the steady heat-conduction equation</p> <p>7.1. Analytical solutions of the steady one-dimensional conduction equation 150</p> <p>7.2. Application of the FD method to the steady 1D conduction equation 152</p> <p>7.3. Dealing with various boundary conditions 155</p> <p>7.4. Conduction with heat-generation 157</p> <p>7.5. Two-dimensional steady heat conduction 160</p>  | <p>149</p> |

7.6. Application of the FD method using Excel's iterative calculation option	164
7.7. Closure	166
References	167
Exercises	167
8. Finite-difference solution of the transient heat-conduction equation	170
8.1. Transient 1D conduction: the explicit FTCS formulation	171
8.2. Transient 1D conduction: the implicit BTCS formulation	175
8.2.1. Application of the BTCS scheme by assembling the linear system	176
8.2.2. Application of the BTCS scheme by using iterative calculations	178
8.3. Transient 2D heat conduction: A general formulation	178
8.4. The explicit FTCS scheme for 2D conduction	180
8.5. The implicit BTCS scheme for 2D conduction	184
8.6. Closure	187
References	187
Exercises	188
9. Thermodynamic analyses of gas power cycles	191
9.1. The ideal Brayton cycle	192
9.2. The regenerative Brayton cycle	196
9.3. Energy analysis of the Otto cycle	200
9.4. Exergy analysis of the Otto cycle	203
9.5. Closure	206
References	207
Exercises	207
10. Analyses of simple and multi-stage compression VCR cycles	209
10.1. The ideal vapour-compression refrigeration cycle	210
10.2. The actual vapour-compression refrigeration cycle	213
10.3. Optimisation analysis of the two-stage compression cycle	215
10.3.1. The analytical model	215
10.3.2. The optimisation analysis	217
10.4. Optimisation analysis of the three-stage compression cycle	220
10.4.1. The analytical model	222
10.4.2. The optimisation analysis	222
10.5. Closure	224
References	225
Exercises	225
Appendices	227
Appendix A: Properties of air and liquid water at atmospheric pressure	228
Appendix B: The numerical tools provided by Thermax	230
Appendix C: Application of the Hardy-Cross method with Excel	238
Appendix D: Analysis of a gravity-driven network with eight loops	246

Appendix E: Finite-difference analysis of heat transfer from a triangular fin 252

Appendix F: Macros and VBA functions for applying the finite-difference method  
with Excel 258

Subject index

264

## Nomenclature

$A$	Area
$C$	Friction coefficient in Hazen-Williams equation, Equation (1.28)
$c_p$	Specific heat at constant pressure, kJ/kg·°C
$c_v$	Specific heat at constant volume, kJ/kg·°C
$D$	Diameter
$E$	Total energy of the system
$e$	Energy per unit mass of the system
$E_G$	Total energy generated in the system
$e_G$	Energy generated per unit volume
$f$	Darcy friction factor, defined by Equation (1.21)
$f$	Manning friction factor, defined by Equation (1.27)
$F_D$	Drag force, defined by Equation (B.2)
$g$	Acceleration of gravity
$h$	Average heat-transfer coefficient
$h$	Enthalpy, kJ/kg
$h_f$	Major friction in a pipe system
$k$	Thermal conductivity, W/m·°C
$k$	Isentropic exponent, dimensionless ( $k=c_p/c_v$ )
$K$	Minor losses friction coefficient in a pipe system, defined by Equation (1.29)
$L$	Length
$m$	Mass
$\dot{m}$	Mass rate of flow
$P$	Pressure, usually in kPa
$P_r$	Relative pressure (for an ideal gas)
$q$	Heat-transfer per kg of the working fluid, usually kJ
$Q$	Heat, usually in kJ
$Q$	Volume flow rate
$\dot{Q}$	Rate of heat transfer, W or kW
$r$	Radius or radial distance
$R$	Gas constant, kJ/kg.K
$R_{th}$	Thermal resistance, usually °C/W
$R_u$	Universal gas constant kJ/kmol.K
$s$	Entropy
$T$	Temperature
$u$	Internal energy per unit mass, kJ/kg
$U$	Overall heat-transfer coefficient of a heat-exchanger
$v$	Specific volume, m <sup>3</sup> /kg
$V$	Velocity, usually m/s
$w$	Work-done per kg of the working fluid, usually kJ
$\dot{W}$	Power, W or kW
$x,y,z$	Space coordinates in the Cartesian system

### **Greek Characters**

$\gamma$	Specific weight of a fluid
$\delta$	Thickness (e.g. of insulation)
$\Delta$	Difference (e.g. temperature)
$\varepsilon$	Roughness of surface material
$\varepsilon$	Heat-exchanger effectiveness
$\eta$	Efficiency
$\mu$	Dynamic viscosity, kg/m.s
$\nu$	Kinematic viscosity, m <sup>2</sup> /s
$\rho$	Density, kg/m <sup>3</sup>
$\tau$	Time, annual operating hours of a system
$\tau$	Mesh Fourier number in the finite-difference method, defined by Equation (8.6)

### **Dimensionless Numbers and Groups**

$Bi$	Biot number
$C_f$	Friction coefficient, defined by Equation (B.3)
$Fi$	Fourier number
$Nu$	Nusselt number
$Pr$	Prandtl number
$Re$	Reynolds number

### **Subscripts**

$f$	Saturated liquid condition
$fg$	Difference in property between saturated liquid and saturated vapour
$g$	Saturated vapour condition
$lm$	Log-mean
$s$	Saturation temperature or pressure
$s$	Evaluated at the surface
$\infty$	Evaluation at free-stream ambient conditions

# 1

## **Introduction**



Cars, refrigerators, and air-conditioners have become indispensable items for families in both developed and developing countries. The energy required to operate these systems mainly comes from burning fossil fuels in power-generation plants. Apart from being non-renewable energy sources, large-scale combustion of fossil fuels is the main cause for global warming and its increasingly devastating effects at different parts of the world. Therefore, proper design and operation of these and other energy-demanding devices are required for minimising these effects. The design methods of these systems are mainly based on the principles of *thermodynamics*, *fluid mechanics*, and *heat transfer*. This chapter reviews the main principles of these three thermofluid subjects with the objective of showing how they can be used to reduce the losses and minimise energy consumption. For a number of reasons the equations involved in thermofluid analyses are difficult to solve without using computer-aided methods. Therefore, these analyses introduce many simplifications that reduce their accuracy. In this respect, the chapter highlights the advantages of computer-aided methods for thermofluid analyses and describes the Excel-based modelling platform used in this book for these analyses.

### **1.1. A review of the thermofluid principles**

The two main principles that form the framework for thermofluid analyses are the conservation of mass (the continuity equation) and the conservation of energy (the first-law of thermodynamics). These principles take different mathematical forms depending on whether the system under consideration is open or closed and on whether the flow is steady or unsteady, compressible or incompressible, laminar or turbulent, etc. Numerous auxiliary relationships are needed in order to quantify the various parameters involved in the resulting equations such as pressure-variations, friction losses, and rates of heat-transfer. In what follows, the main concepts of thermodynamics, fluid dynamics, and heat-transfer are reviewed by considering typical applications.

#### **1.1.1. Thermodynamics**

The principles of *engineering thermodynamics* allow us to determine the amount of energy transfer in the form of work or heat between any system and its surroundings. They also allow us to determine the efficiency and effectiveness of the system if energy conversion is involved. There are four basic laws for thermodynamics the most important of which are the first and the second laws of thermodynamics. To apply these two basic laws, thermodynamic analyses use many property relationships, tables, and charts that determine the properties of the particular fluid involved and its phase (a liquid, a liquid-vapour mixture, a gas, or a gaseous mixture). To illustrate the application of thermodynamic laws and relationships in a typical analysis, consider the air-compression system shown in Figure 1.1.a. Air enters the system that has two stages of compression separated by an intercooler at a temperature  $T_1$  and pressure  $P_1$ . The first-stage compressor,  $C_1$ , compresses the air adiabatically to state 2, after which it enters the intercooler where its temperature is reduced to  $T_3$ . The second-stage compressor,  $C_2$ , then increases the air pressure to  $P_4$  at which the temperature increases to  $T_4$ . Figure 1.1.b shows the compression process on a temperature-entropy diagram.

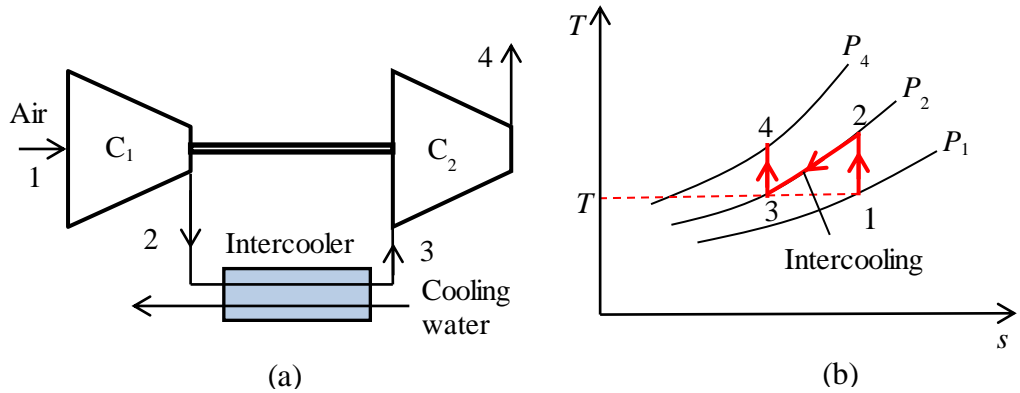


Figure 1.1. Schematic and  $T$ - $s$  diagrams of a two-stage air compressor with inter-stage intercooling

How the total compression work is divided between the two compressor stages depends on their compression ratios and there is a certain value of the intermediate pressure ( $P_i$ ) that minimises the total compression work. The principles of thermodynamics help us to determine this optimum pressure as shown below.

Treating the two compressor stages as steady-flow processes and neglecting changes in kinetic and potential energy, the first-law of thermodynamics is expressed as [1]:

$$q - w = (h_{out} - h_{in}) \quad (1.1)$$

Where  $q$  and  $w$  are the amounts of heat transfer and work transfer per unit mass flow of air, respectively, and  $(h_{out} - h_{in})$  is the resulting enthalpy change over the stage. Equation (1.1) adopts the usual sign convention that heat into the system is positive, while work into the system is negative. Assuming the compression processes in both stages to be isentropic as shown in Figure 1.1.b means that they are adiabatic ( $q=0$ ) and reversible. Therefore, using an average specific heat for air at constant pressure ( $c_p$ ), the compression work per unit mass flow of air in stage 1 ( $w_1$ ) and in stage 2 ( $w_2$ ) can be determined from Equation (1.1) as follows:

$$w_1 = -(h_2 - h_1) = -c_p(T_2 - T_1) \quad (1.2)$$

$$w_2 = -(h_4 - h_3) = -c_p(T_4 - T_3) \quad (1.3)$$

The total compression work ( $w_{total}$ ) is then given by:

$$w_{total} = w_1 + w_2 = -c_p[(T_2 - T_1) + (T_4 - T_3)] \quad (1.4)$$

Assuming perfect intercooling, i.e.,  $T_3 = T_1$ , Equation (1.4) can be rearranged as:

$$w_{total} = c_p T_1 \left[ \left( 1 - \frac{T_2}{T_1} \right) + \left( 1 - \frac{T_4}{T_3} \right) \right] = c_p T_1 \left[ 2 - \left( \frac{T_2}{T_1} \right) - \left( \frac{T_4}{T_3} \right) \right] \quad (1.5)$$

Since the two compression processes are assumed to be isentropic and the specific heat  $c_p$  for air to be constant, the temperature ratios in Equation (1.5) can be converted into pressure ratios by using the following approximate relationships:

$$\frac{T_2}{T_1} = \left( \frac{P_2}{P_1} \right)^{\frac{k-1}{k}} \quad (1.6)$$

$$\frac{T_4}{T_3} = \left( \frac{P_4}{P_3} \right)^{\frac{k-1}{k}} \quad (1.7)$$

Where  $k$  is the ratio of specific heats ( $k=c_p/c_v$ ;  $c_v$  is the specific heat for air at constant volume). With the assumption that there is no pressure loss in the intercooler,  $P_3 = P_2 = P_i$ . Substituting from Equations (1.6) and (1.7), Equation (1.5) becomes:

$$w_{total} = c_p T_1 \left[ 2 - \left( \frac{P_i}{P_1} \right)^{\frac{k-1}{k}} - \left( \frac{P_4}{P_i} \right)^{\frac{k-1}{k}} \right] \quad (1.8)$$

To see how the total compression work varies with the intermediate pressure  $P_i$ , a specific case was considered in which  $T_1=300\text{K}$ ,  $P_1=100\text{ kPa}$ , and  $P_4=900\text{ kPa}$ . Using Equation (1.8), the total compression work in the system was calculated for different values of  $P_i$  and Figure 1.2 shows the result. The figure shows that the value of  $P_i$  at which the total compression work is minimal is around 300 kPa. Increasing and decreasing  $P_i$  from this value both increase the compression work.

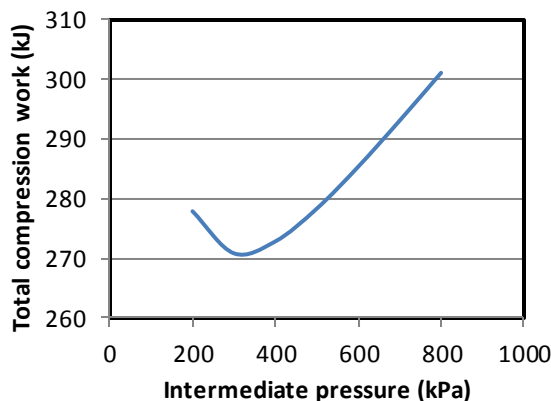


Figure 1.2. Variation of the total compression work with the intermediate pressure

The principles of thermodynamics are particularly useful for performance evaluation and optimisation of power-generation and refrigeration systems. For example, consider the regenerative steam-turbine power plant shown in Figure 1.3. This plant consists of a boiler house for producing superheated steam, a high-pressure steam turbine (HPT), a low-pressure steam turbine (LPT), a condenser, an open feed-water heater (FWH) and two feed-water pumps. A fraction of the steam ( $y$ ) is extracted after the HPT for preheating the feed-water before going back to the boiler house.

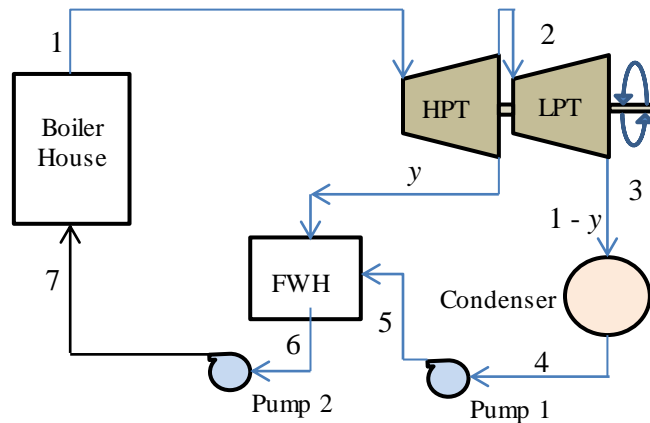


Figure 1.3. Schematic diagram of a regenerative steam-turbine power plant

Although extracted steam reduces the work output from plant, it reduces the amount of heat added in the boiler and its net effect is to increase the thermal efficiency of the plant. There is also a certain extraction pressure for the steam at which the plant's thermal efficiency attains a maximum value. As shown below, the principles of thermodynamics can be used to determine this optimum steam-extraction pressure.

The total specific work output from the two turbines ( $w_{out}$ ) and the total work input to the two pumps ( $w_{in}$ ) are given by:

$$w_{out} = w_{HPT} + w_{LPT} \quad (1.9)$$

$$w_{in} = w_{P1} + w_{P2} \quad (1.10)$$

Where  $w_{HPT}$  and  $w_{LPT}$  are the specific work output from the high-pressure turbine and the low-pressure turbine, respectively, and  $w_{P1}$  and  $w_{P2}$  are the specific work inputs in pump 1 and pump 2, respectively. Assuming the two turbines and the two pumps to be adiabatic and neglecting the changes in kinetic and potential energies, the work output or input for each device can be determined from the enthalpy difference across the device. Per each kg of steam generated in the boiler, these are given by:

$$w_{HPT} = (h_1 - h_2) \quad (1.11)$$

$$w_{LPT} = (1 - y)(h_2 - h_3) \quad (1.12)$$

$$w_{P1} = (1 - y)(h_5 - h_4) \quad (1.13)$$

$$w_{P2} = (h_7 - h_6) \quad (1.14)$$

Mass and energy balance over the open feed-water heater gives:

$$yh_2 + (1 - y)h_5 = 1 \times h_6 \quad (1.15)$$

The net specific work output from the plant ( $w_{net}$ ) is then given by:

$$w_{net} = w_{out} - w_{in} \quad (1.16)$$

Similarly, the specific heat input to the boiler ( $q_{in}$ ) is determined by the relevant enthalpy change as follows:

$$q_{in} = (h_1 - h_7) \quad (1.17)$$

Finally, the thermal efficiency of the plant ( $\eta$ ) can be calculated from:

$$\eta = w_{net} / q_{in} \quad (1.18)$$

Both  $w_{net}$  and  $\eta$  depend on the fraction of steam extracted for regeneration ( $y$ ); which in turn depends on the extraction pressure ( $P_2$ ). Figure 1.4 shows the variation of  $y$  and  $\eta$  with  $P_2$  for an ideal cycle in which  $P_1 = 15$  MPa,  $T_1 = 600^\circ\text{C}$ , and  $P_4 = 10$  kPa. The figure shows that the cycle's efficiency attains a maximum value of 45.55% when  $P_2$  is in the range of 1000 kPa.

It should be mentioned that the working fluid in the above power plant, which is water, changes its phase from a liquid to superheated steam in the boiler, to a saturated mixture of water and steam in the low-pressure turbine, and returns to liquid water in the condenser. Therefore, appropriate property tables or charts are needed for determining the thermodynamic properties of water at the different states. In general, thermodynamic analyses use many tables and charts for various working fluids. The principles of thermodynamics are also needed for the analyses of air-conditioning systems and processes and for the analyses of the processes that involve combustion and other chemical reactions. For such analyses, thermodynamics provides the basic relationships needed to quantify the effects of fluid mixing and chemical reactions on the properties of the working fluids and to determine the transfer of energy and effluents to or from the system.

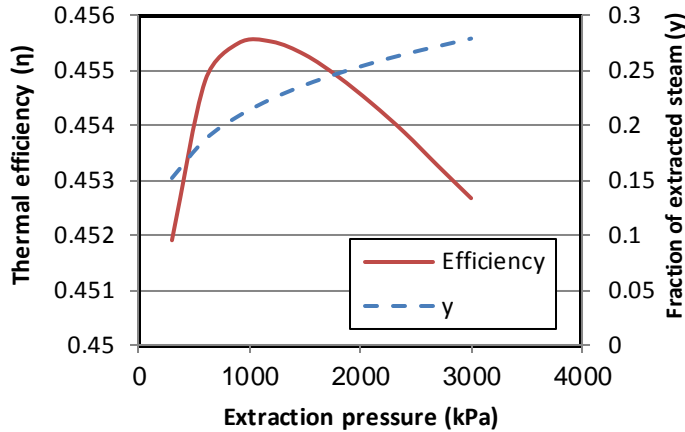


Figure 1.4. The effect of intermediate pressure ( $P_2$ ) on the fraction of extracted steam ( $\gamma$ ) and thermal efficiency ( $\eta$ ) of a regenerative steam-turbine power plant

### 1.1.2. Fluid dynamics

In addition to pipes and ducts, fluid-transporting systems require various equipment such as pumps, compressors, control valves, and flow-measuring devices. The principles of *fluid dynamics* help us to estimate the power needed for overcoming friction in these equipment and to determine suitable types and sizes for them. To illustrate the application of these principles, consider the pump-pipe system shown in Figure 1.5 that conveys a liquid between two non-pressurised tanks A and B through a pipe of known length  $L$ , diameter  $D$ , and roughness  $\varepsilon$ . Suppose that we want to determine the needed pump power for transporting the liquid at a certain flow rate  $Q$ .

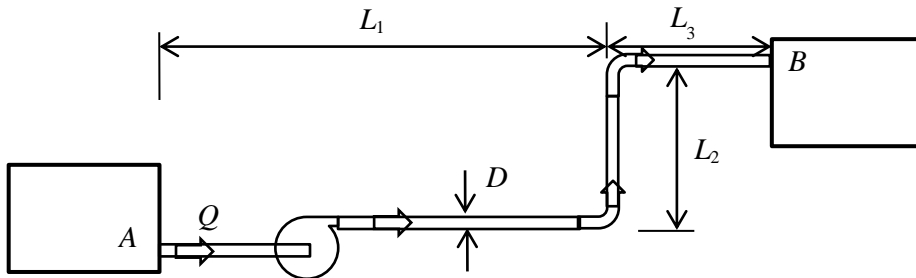


Figure 1.5. Schematic diagram of a simple pump-pipe system

The required pump power ( $\dot{W}$ ) can be determined from the following “power equation”:

$$\dot{W} = \gamma \times Q \times h_p / \eta \quad [\text{W}] \quad (1.19)$$

Where  $\gamma$  is the specific weight of the transported liquid ( $\text{N}/\text{m}^3$ ),  $Q$  is the volume flow rate of the liquid ( $\text{m}^3/\text{s}$ ),  $h_p$  is the pump head (m) needed to circulate the fluid through

the pipe from  $A$  to  $B$ , and  $\eta$  is the combined efficiency of the pump and the electric motor. For a steady flow of an incompressible fluid,  $h_p$  can be determined from the following “energy equation”:

$$h_p = h_{f,total} + (Z_B - Z_A) + \frac{V_B^2 - V_A^2}{2g} \quad [\text{m}] \quad (1.20)$$

Where  $h_{f,total}$  is the total head loss through the system due to friction (m),  $Z_A$  and  $Z_B$  are the elevations (m) at points  $A$  and  $B$ , respectively, and  $V_A$  and  $V_B$  are the corresponding fluid velocities (m/s). If the two tanks are not open to the atmosphere, the energy equation should also include a term for the pressure difference between the tanks.

The total friction head loss  $h_{f,total}$  consists of two parts: the *major friction loss* ( $h_f$ ), which is the part lost in the pipe itself, and the *minor friction head loss* ( $h_c$ ), which is the part lost in other components of the system like nozzles, elbows, valves, etc. The major friction loss can be determined from the following Darcy-Weisbach equation [2]:

$$h_f = f \frac{L}{D} \frac{V^2}{2g} \quad [\text{m}] \quad (1.21)$$

Where  $f$  is the dimensionless Dracy friction factor,  $V$  the fluid velocity (m/s),  $L$  the total length of the pipe (m), and  $D$  the internal diameter of the pipe (m). The value of the friction factor, which depends on the roughness of the pipe surface and on whether the flow is laminar or turbulent, can be obtained from a Moody diagram [2] or calculated from a relevant formula. For laminar flows,  $f$  can be calculated from:

$$f = 64/\text{Re} \quad \text{Re} < 2300 \quad (1.22)$$

Where  $\text{Re}$  is the Reynolds number defined as:

$$\text{Re} = VD/\nu \quad (1.23)$$

Where  $\nu$  is the kinematic viscosity of the flowing fluid ( $\text{m}^2/\text{s}$ ). For a turbulent flow in rough pipes,  $f$  can be obtained from the following Swamee-Jain formula [2]:

$$f = 0.25 / \left[ \log_{10} \left( \frac{\varepsilon}{3.7D} + \frac{5.74}{\text{Re}^{0.9}} \right) \right]^2 \quad \text{Re} > 4000 \quad (1.24)$$

For more accuracy, the friction factor for a turbulent flow can be determined by using the following Colebrook-White formula (frequently referred to as the Colebrook equation):

$$\sqrt{\frac{1}{f}} = -2.0 \log_{10} \left( \frac{\varepsilon/D}{3.7} + \frac{2.51}{\text{Re} \sqrt{f}} \right) \quad (1.25)$$

The Colebrook equation is an example of the implicit equations met in thermofluid analyses that need to be solved iteratively. For turbulent flows in smooth tubes,  $f$  can be determined from the first Petukhov formula [2]:

$$f = (0.790 \ln \text{Re} - 1.64)^{-2} \quad 10^4 < \text{Re} < 10^6 \quad (1.26)$$

Chemical engineers usually determine the pipe friction by using the following Chezy-Manning equation instead of the Darcy-Weisbach equation:

$$h_f = 2f \frac{L}{D} \frac{V^2}{g} \quad [\text{m}] \quad (1.27)$$

Where  $f$  is the Fanning friction factor. Comparison with Equation (1.21) reveals that the value of the Fanning friction factor is 4 times the corresponding value of the Darcy friction factor. Civil engineers determine the friction head loss in water-transporting pipes by using the following Hazen-Williams equation:

$$h_f = \frac{10.67 L Q^{1.852}}{C^{1.852} D^{4.8704}} \quad [\text{m}] \quad (1.28)$$

Where  $C$  is a coefficient that depends on the roughness of the pipe. Unlike Equations (1.21) and (1.27), Equation (1.28) is applicable for both laminar and turbulent flows.

The minor friction losses,  $h_c$ , can be determined from the following equation:

$$h_c = \sum_1^n K \frac{V^2}{2g} \quad [\text{m}] \quad (1.29)$$

Where  $n$  is the total number of components in the fluid system and  $K$  is a coefficient the value of which can be found for each component in relevant tables.

Given the values of the pipe length and diameter, flow rate, fluid viscosity, and pipe material or roughness, the equations described above can be used to determine the required pump power. The equations can also be used to determine the maximum flow rate of the fluid to be delivered via a pipe of a certain diameter such that the friction loss in the system or the needed pump power does not exceed a specified limit. Moreover, by taking into consideration the initial cost of the pump-pipe system that



increases with  $D$ , and the cost of electrical energy needed by the pump that decreases with  $D$ , the equations can be used to determine the economic pipe diameter  $D_{opt}$  that gives the lowest total owning cost for the system over its entire life-time. In general, the equations are also applicable for analysing and optimising pipe-networks.

The principles of fluid dynamics also enable us to select the appropriate type and size of the pump for a given pump-pipe system by matching the “pump curve” with the “system curve”. This is achieved with the help of pump characteristic curves usually provided by the manufacturers. In many situations a single pump or compressor may not be adequate for the required flow rate or delivery pressure and more than one pump or compressor have to be used. In this situation, the principles of fluid dynamics help us to decide when to arrange the pumps/compressors in parallel or in series.

### 1.1.3. Heat transfer

The design practices of energy-conversion equipment that deal with the transfer of thermal energy such as boilers, condensers, and heat exchangers are mainly based on the principles of *heat transfer*. Three independent physical laws are used in heat-transfer analyses to quantify the *rate* of heat transfer between an object and its surroundings depending on whether the heat transfers by conduction (Fourier’s Law), convection (Newton’s law of cooling), or radiation (Stefan-Boltzmann law). The physical properties that determine the rate of heat transfer by conduction, radiation, and convection are the thermal conductivity ( $k$ ), the surface emissivity ( $\varepsilon$ ) and absorptivity ( $\alpha$ ), and the heat-transfer coefficient ( $h$ ), respectively.

While  $k$ ,  $\varepsilon$ , and  $\alpha$  are material or surface-specific,  $h$  depends on both the fluid and the flow. Numerous analytically-obtained relationships and empirical formulae are used for determining  $h$  depending on whether the flow is forced or natural and whether the flow is internal or external to the system being considered. These formulae usually give the Nusselt number ( $Nu$ ) which is related to  $h$  as follows:

$$h = \frac{k}{D} Nu \quad [\text{W/m}^2 \cdot \text{K}] \quad (1.30)$$

Where  $D$  is the pipe diameter and  $k$  is the thermal conductivity of the transported fluid. Many analytical or empirical formulae are used for determining the Nusselt number for forced or natural flows over single tubes, bank of tubes, plates, etc. For example, the following Dittus-Boelter equation is used for determining  $Nu$  inside a fluid-transporting pipe due to forced convection [3]:

$$Nu = 0.023 Re^{0.8} Pr^n \quad (1.31)$$

Where  $Re$  is the Reynolds number,  $Pr$  the Prandtl number, and  $n$  is a constant that takes a value of 0.4 when the pipe is being heated and 0.3 when it is being cooled.

The subject also describes the methods that can be used to minimise or maximise the rate of heat-transfer between the system's components or between the system and its surroundings by means of thermal insulation, fins, heat-pipes, etc. To illustrate the use of heat-transfer concepts in thermal-insulation analyses, consider the metal pipe shown in Figure 1.6 that has an internal radius  $r_1$  and external radius  $r_2$ . The pipe carries a fluid at a temperature  $T_i$ , while the surrounding air is at a different temperature  $T_\infty$ .

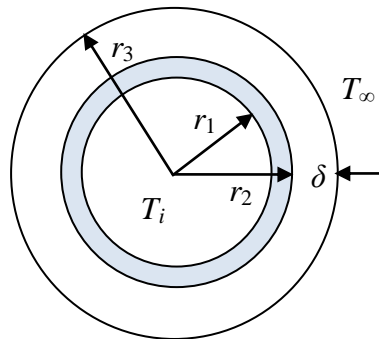


Figure 1.6. Schematic for an insulated metal pipe

The temperature difference between the pipe and the surroundings will cause heat gain or heat loss to/from the pipe and, in order to reduce this heat gain or heat loss, the pipe has to be covered by an insulating material. The principles of heat transfer help us to account for the effect of thermal insulation on the rate of heat-transfer to/from the pipe.

The rate of heat transfer ( $\dot{Q}$ ) can be calculated from [3]:

$$\dot{Q} = (T_i - T_\infty) / R_{th} \quad [\text{W}] \quad (1.32)$$

Where  $R_{th}$  is the combined thermal resistance to heat-transfer by conduction, convection, and radiation, which is given by [3]:

$$R_{th} = \frac{1}{h_i A_1} + \frac{\ln(r_2 / r_1)}{2\pi L k_1} + \frac{\ln(r_3 / r_2)}{2\pi L k_2} + \frac{1}{h_o A_3} \quad [\text{K/W}] \quad (1.33)$$

Where  $h_i$  and  $A_1$  are the heat-transfer coefficient and surface area inside the pipe, respectively,  $h_o$  and  $A_3$  are the heat-transfer coefficient and surface area outside the insulated pipe, respectively,  $L$  is the length of the pipe, and  $k_1$  and  $k_2$  are the thermal conductivities of the pipe and the insulation, respectively. To simplify the analysis,  $h_o$  in Equation (1.33) takes into account the heat-transfer by both convection and radiation to/from the insulation surface. The thickness of the metal pipe is usually small compared to its diameter, while its thermal conductivity is much higher than that of the insulation material. Therefore, the equation can be simplified further by neglecting the term that represents the thermal resistance due to conduction through the pipe.

Equations (1.32) and (1.33) can be used to determine the required thickness of insulation ( $\delta$ ) for reducing the rate of heat transfer to the required tolerance or for controlling the surface temperature within a range that is dictated by safety or other practical considerations. Although the thicker the insulation the lower will be the rate heat transfer, the cost of insulation increases with its thickness and, therefore, adding more insulation will not be economically profitable beyond a certain thickness. By extending the above heat-transfer model so that the cost of insulation and the value of the saved thermal energy can be calculated and compared, the above equations can also be used to determine the economically optimal thickness of insulation ( $\delta_{opt}$ ).

Figure 1.7 shows a metal pipe with circular fins attached to its surface so as to boost the rate of heat-transfer between the fluid being transported with the pipe and the surrounding medium, usually air. The principles of heat transfer can be used to develop the required mathematical equations that determine the the rate of heat transfer from the pipe and, therefore, to evaluate the effectiveness and efficiency of the fin.

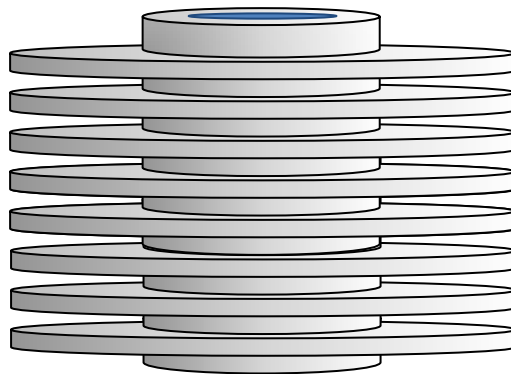


Figure 1.9. Circular fins attached to a metal pipe

Another important application of heat-transfer principles is that related to the design and selection heat-exchangers. A heat-exchanger is any device that allows the transfer of thermal energy between two fluids through a separating surface usually a pipe, a duct, a tube, or a plate. Figures 1.8 and 1.9 show two types of heat-exchangers commonly used in industries and power-plants. Figure 1.8 shows a shell-and-tube heat-exchanger while Figure 1.9 shows a cross-flow heat-exchanger. Heat-exchanger analyses either aim at determining the required size (i.e., surface area) for a specified heat-transfer duty or determining the exit temperatures of the two streams from a specified heat-exchanger type and size. Two methods are used for these two types of analyses which are the log-mean temperature difference (LMTD) method and the effectiveness-number of transfer units ( $\epsilon$ -NTU) method. Complex thermal systems use heat-exchanger networks [HENs] and finding the configuration that minimises the annual cost of the network is based on the principles of heat transfer.

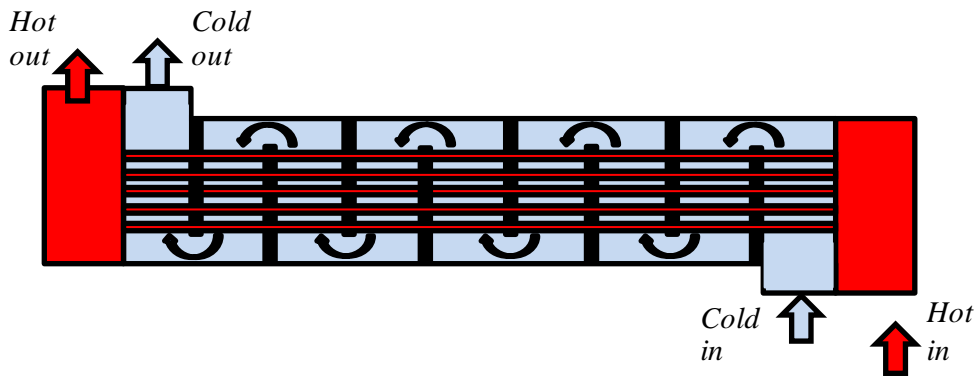


Figure 1.8. A parallel-flow shell-and-tube exchanger

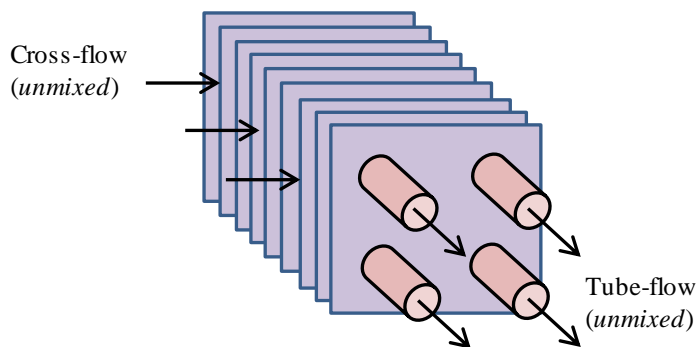


Figure 1.9. A cross-flow exchanger with both streams unmixed

## 1.2. Advantages of computer-aided thermofluid analyses

Apart from saving time and eliminating possible human errors, computer-aided thermofluid analyses offer a number of advantages over traditional methods that use property tables and charts. An important advantage of computer-aided methods is their ability to give more realistic results by avoiding unnecessary simplification of the models and by using more accurate estimations of fluid properties. Moreover, they offer reliable techniques for iterative solutions, optimisation analyses, and the analyses of complex thermofluid systems. In what follows, these advantages are illustrated by means of relevant examples.

### A. Avoiding excessive simplification of the model

In many situations, traditional analytical methods adopt excessive simplifications of the analytical models; which makes their results grossly deviate from the behaviour of real systems. A good example of this situation is given by the models of internal-combustion (IC) engines. Traditional air-standard models of IC engines, such as the Otto cycle and the Diesel cycle, neglect heat-transfer and friction losses, treat the combustion process as heat-addition from an external source, and use constant specific

heats for the working fluids. These assumptions enable the engine processes to be represented by simple closed-form relations for calculating the amount of heat added to the engine and net work from the engine [4]. However, air-standard models usually overestimate the engine's output and thermal efficiency.

By comparison, computer-aided models of IC engines closely mimic the behaviour of actual IC engines by taking into consideration the geometrical as well as the thermodynamic characteristics of the engines. Therefore, these models can be used to investigate the effect of important design and operation factors such the ignition or injection timing on the engine performance or the effect of engine speed on the specific fuel consumption. However, the formulation of these models leads to a set of ordinary differential equations that need to be solved simultaneously by using a numerical method such as the Newton-Raphson method [5].

### **B. Accurate representation of fluid properties and processes**

The ideal-gas law can be used with reasonable accuracy for determining the specific volume of a superheated vapour, but when the temperature approaches the saturation line, the value of the specific volume determined by the ideal-gas law departs significantly from the actual volume. More accurate estimates can be obtained by using the following Soave-Redlich-Kwong (SRK) equation of state [1]:

$$P = \frac{R_u T}{\tilde{v} - b} - \frac{a\alpha}{\tilde{v}(\tilde{v} + b)} \quad (1.34)$$

Where  $P$  is the absolute pressure of the gas,  $\tilde{v}$  is the molar specific volume,  $R_u$  is the universal gas constant,  $T$  is the absolute temperature of the gas, and the constants  $a$ ,  $b$  and  $\alpha$  are fluid-dependent. Figure 1.10 shows the deviations from the tabulated values by those obtained from the ideal-gas law and the SRK equation of state for refrigerant R134a at 0.2 MPa. The figure shows that the error of the ideal-gas law is more than 2% even at high temperatures and increases as the temperature approaches the saturation value, but the accuracy of the SRK equation remained higher than 99% even close to the saturation line. However, since the SRK equation is implicit in  $\tilde{v}$  it cannot be used directly to determine the specific volume. A number of standard iterative procedures (e.g. Newton-Raphson method) can be used to solve the equation, but they are more suitable for computer-aided analyses than hand calculations.

Another important implicit equation for thermofluid analyses is the Colebrook-White equation, Equation (1.25), that determines the friction factor ( $f$ ) for turbulent pipe-flows. Since the equation involves  $f$  on both sides and needs to be solved iteratively, the explicit relationships such as the Swamee-Jain formula are preferred even though the Colebrook-White equation is more accurate. Many other nonlinear equations like the SRK equation and the Colebrook-White equation give advantage to computer-aided thermofluid analyses by enabling more realistic and accurate estimations.

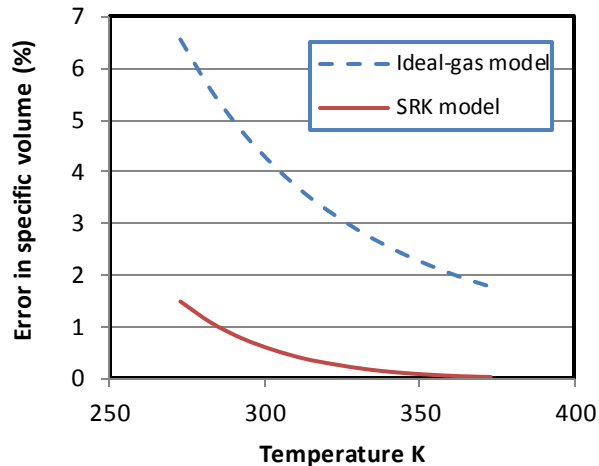


Figure 1.10. Errors in the specific volume of R134a by the ideal-gas law and the SRK equation of state

### C. Dealing with iterative solutions and optimisation analyses

A good example of thermofluid analyses that require iterative solutions is found in pipe-flow analyses. Pipe flow problems that require the friction head loss to be determined when both the diameter and flow rate are known can be solved in a straightforward manner by using Equation (1.21). However, in design analyses of pump-pipe systems we may need to find the flow rate in a given pipe that gives a specified head loss or to find a suitable pipe diameter for specified head loss, flow rate, and pipe length. In these two cases, the friction factor  $f$  cannot be determined in advance because it depends on the Reynolds number. Therefore, these two types of pipe-flow problems, referred to as type-2 and type-3 problems, need to be solved by iteration. It is much easier to carry out the iterative process to the required level of accuracy by using a computer-aided method than by doing it manually. Other types of thermofluid analyses that also require iterative solutions include rating analyses of heat exchanger and the determination of the adiabatic flame temperature by first-law analysis of the combustion process.

Optimisation analyses are needed for determining the best design for a thermofluid system such as the optimum intermediate pressure for a two-stage air-compression system, the optimum steam-extraction pressure for a regenerative Rankine cycle, and the economic thickness of insulation for a pipe. While simple optimisation analyses that involve a single design parameter can be performed by means of calculus techniques and graphic tools, optimisation analyses of complex systems that involve multiple design variables require the use of computer-aided techniques.

### D. Analyses involving complex models

The complexity of modelling certain thermofluid systems makes their analyses only possible with the help of computer-aided methods. The model complexity can be either

due to the complexity of the physical structure of the system itself or the complexity of its mathematical representation. An example of physically complex systems is the pipe network shown in Figure 1.11 that consists of four pipe loops and four consumption points and fed by two water tanks; tank A and tank B. Suppose that the flow rates from the two supply tanks are specified together with the pipe diameters and lengths and it is required to determine the discharges at the four consumption points.

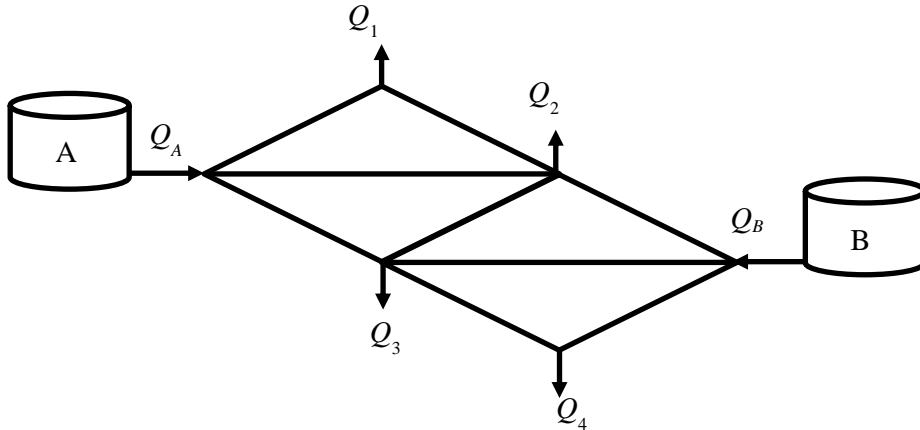


Figure 1.11. A looped pipe network supplied by two tanks

Although the solution is mainly based on the two well-known principles of conservation of mass and conservation of energy, it is difficult to solve the problem by using manual analytical methods especially when a minimum or a maximum pressure level is to be met at the discharge points. In this case, a computer-aided method, such as the Hardy-Cross method presented in Appendix C, has to be used [6, 7]. The optimisation analyses of heat-exchanger networks give another example of the models that deal with physically complex systems [8].

Mathematically complex thermofluid models that need computer-aided numerical methods are found in multi-dimensional fluid-flow and heat transfer analyses. This type of analyses involves coupled and nonlinear partial differential equations that have to be solved by using computational fluid dynamics (CFD) methods such as the finite-volume method or the finite-difference method. Many commercial CFD applications are available nowadays that offer great flexibility and user-friendliness.

### 1.3. The Excel-based modelling platform for the thermofluid analyses

Microsoft Excel is commonly used for data visulation and for dealing with simple computer-based operations like matrix inversion and matrix multiplications [3,9]. However, Excel is equipped with other features that make it a capable modelling platform for a wide range of engineering “What-if” analyses [10-12]. In addition to its Goal Seek command and the Solver add-in, the “Developer” ribbon in Excel provides a programming language called Visual Basic for Applications (VBA) that can be used for developing customised user-defined functions (UDFs) not provided by Excel. The

## Comouter-Aided Thermofluid Analyses Using Excel

Developer ribbon also allows the use of macros to remove the tedium of parametric studies and repetitive calculations. The main limitation of Excel with respect to thermofluid analyses, which is the lack of built-in functions for fluid properties, could be solved by developing suitable add-ins for this purpose [13-15].

This book uses an Excel-based modelling platform for thermofluid analyses that includes in addition to Excel, Solver, and VBA, an educational Excel add-in called Thermax. Thermax provides seven groups of property functions for ideal gases, saturated water and superheated steam, synthetic and natural refrigerants, atmospheric humid air for psychrometric analyses, two aqua solutions for vapour-absorption refrigeration, chemically-reacting substances, and air at standard atmospheric pressure. Thermax also provides two interpolation functions and a Newton-Raphson solver for nonlinear equations that enhance the usefulness of the Excel-based modelling platform. Table 1.1 summarises the roles of the four components of the Excel-based modelling platform as used in this book.

Table 1.1. Roles of the four components of the Excel-based modelling platform

Component	Role
Excel	<ul style="list-style-type: none"> <li>• Provides the basic functions needed for thermofluid analyses including the general mathematical functions and the matrix-operation functions</li> <li>• Provides the Goal Seek command needed for performing unconstrained iterative solutions involving a single parameter</li> <li>• Allows circular calculations which can be a convenient method for dealing with parameter dependency in certain analyses</li> <li>• Provides graphical tools needed for data visualisation and analyses</li> <li>• Allows macros to be recorded for repetitive calculations</li> </ul>
Solver	<ul style="list-style-type: none"> <li>• Allows constrained iterative solutions involving multiple parameters</li> <li>• Allows optimisation analyses with single and multiple design variables</li> <li>• Offers three solution options that suit different types of analyses</li> </ul>
Thermax add-in	<ul style="list-style-type: none"> <li>• Provides the physical properties of various fluids</li> <li>• Provides two interpolation functions for tabulated data and a Newton-Raphson solver for non-linear equations such as the Colebrook-White equation and the SRK equation</li> </ul>
VBA	<ul style="list-style-type: none"> <li>• Needed for developing custom functions for the non-linear equations involved in iterative solutions and optimisation analyses</li> <li>• Needed for developing numerical solvers for large systems of linear equations</li> <li>• Can be used to develop additional fluid property functions or other functions not provided by Excel or the Thermax add-in</li> </ul>



#### 1.4. Closure

The following two chapters describe the Excel-based modelling platform in more details. While Chapter 2 focuses on the features of Excel that are mostly needed for thermofluid analyses such as its matrix functions and its Goal Seek command, Chapter 3 introduces the other three components of the modelling platform. Chapter 3 gives examples of using the three solution methods offered by Solver, describes the development of user-defined functions with VBA, and shows how the property functions provided by Thermax can be used in Excel formulae. Chapter 4 deals with iterative solutions of thermofluid problems and gives examples of using Excel's Goal Seek command and Solver for this type of analyses in the fields of fluid dynamics, heat-transfer, and thermodynamics. The Excel-based platform is then used in Chapters 5 to 10 for various types of thermofluid analyses.

Chapters 5 and 6 deal with fluid systems and illustrate the use of Excel and Solver for the analyses of multi-pipe and pump-pipe systems and pipe-networks. Different pipe and pump arrangements are analysed in Chapter 5 to determine the system's friction losses, power requirement, or operating point. Chapter 6 uses Solver for the analyses of gravity-driven pipe-networks with looped, branched, and mixed configurations. Both Chapters 7 and 8 deal with the numerical solution of the heat-conduction equation by using the finite-difference (FD) method. While Chapter 7 focuses on the steady conduction equation, Chapter 8 focuses on the transient equation. Two approaches are presented in these chapters for applying the explicit and implicit formulations of the FD method by using Excel's matrix functions and iterative calculations.

Chapters 9 and 10 deal with thermodynamic analyses by using the property functions provided by the Thermax add-in. Chapter 9 that deals with the analyses of power-generation cycles focuses on the Brayton cycle for gas-turbines and the Otto cycle for the spark-ignition internal-combustion engines. Using air standard assumptions, this chapter presents both energy and exergy analyses of the Otto cycle. Chapter 10 that deals with the analyses of refrigeration cycles focuses on the vapour-compression refrigeration (VCR) cycle with refrigerant R134a as the working fluid. The chapter considers both the simple single-stage cycle and the multi-stage cycle with two and three stages of compression and shows how the Solver add-in provided by Excel can be used for optimisation analyses of the multi-stage VCR cycles.

#### References

- [1] Y.A. Cengel, and M.A. Boles, *Thermodynamics an Engineering Approach*, McGraw-Hill, 7<sup>th</sup> Edition, 2007
- [2] C. T. Crowe, D. F. Elger, B. C. Williams, and J. A. Roberson, *Engineering Fluid Mechanics*, 9<sup>th</sup> edition, John Wiley & Sons, Inc., 2009.
- [3] Y.A. Cengel and A.J. Ghajar, *Heat and Mass Transfer: Fundamentals and Applications*. 4<sup>th</sup> edition, McGraw Hill, 2011.
- [4] W.W. Pulkrabek, *Engineering Fundamentals of the Internal Combustion Engine*, 2<sup>nd</sup> Edition, Pearson Education International, 2004.

- [5] C.R. Ferguson, *Internal Combustion Engines*, John Wiley & Sons, 1986.
- [6] A. Rivas, T. Gómez-Acebo, and J. C. Ramos. The application of spreadsheets to the analysis and optimization of systems and processes in the teaching of hydraulic and thermal engineering, *Computer Applications in Engineering Education*, Vol. 14, Issue 4, 2006, pp. 256-268.
- [7] D. Brkic, Spreadsheet-Based Pipe Networks Analysis for Teaching and Learning Purpose, *Spreadsheets in Education (eJSiE)*: Vol. 9: Iss. 2, Article 4, 2016. Available at: <http://epublications.bond.edu.au/ejsie/vol9/iss2/4>
- [8] A. Bejan, G. Tsatsaronis, M. Moran, *Thermal Design & Optimisation*, John Wiley & Sons, 1996.
- [9] J. P. Holman, *Heat Transfer*, 10<sup>th</sup> edition, McGraw-Hill. 2010.
- [10] A. Karimi, Using Excel for the thermodynamic analyses of air-standard cycles and combustion processes, ASME 2009 Lake Buena Vista, Florida, USA.
- [11] Z. Ahmadi-Brooghani, Using Spreadsheets as a Computational Tool in Teaching Mechanical Engineering, *Proceedings of the 10<sup>th</sup> WSEAS International Conference on computers*, Vouliagmeni, Athens, Greece, July 1315, 2006, 305-310
- [12] S.A. Oke, Spreadsheet Applications in Engineering Education: A Review, *Int. J. Engng Ed.* Vol. 20, 2004, No. 6, 893-901
- [13] The University of Alabama, Mechanical Engineering, Excel for Mechanical Engineering project, Internet: <http://www.me.ua.edu/excelinme/index.htm> (Last accessed July 11, 2019).
- [14] J. Huguet, K. Woodbury, R. Taylor, Development of Excel add-in modules for use in thermodynamics curriculum: steam and ideal gas properties, American Society for Engineering Education, 2008, AC 2008-1751.
- [15] K. Mahan, J. Huguet, K. Woodbury, R. Taylor, Excel in ME: Extending and refining ubiquitous software tools, American Society for Engineering Education, 2009, AC 2009-2295.

# 2

# Excel

With its user-interface, built-in functions, iterative tools, and graphical tools, Excel forms the backbone of the modelling platform used in this book for thermofluid analyses. This chapter is not intended to review all the features and built-in functions provided by Excel, but to focus on those needed for building analytical models for thermofluid analyses. In this respect, the chapter highlights the use of cell-labelling in writing formulae instead of the usual referencing by location. The chapter also illustrates the use of Excel's matrix functions for the solution of linear systems of equations and the use of Goal Seek and circular calculations for the solution of nonlinear equations. The final section on Excel's graphical tools demonstrates the use of the trendline feature for curve-fitting of tabulated data.

### 2.1. Elements of Excel's user-interface

Excel's user-interface allows us to manipulate the stored data by providing a large set of built-in functions and a number of analytical tools. It also provides numerous commands for adjusting the appearance of the workspace and presenting the primary data and the results in various forms. Figure 2.1 shows a screenshot of an Excel sheet that stores the scores obtained by a group of students in one semester.

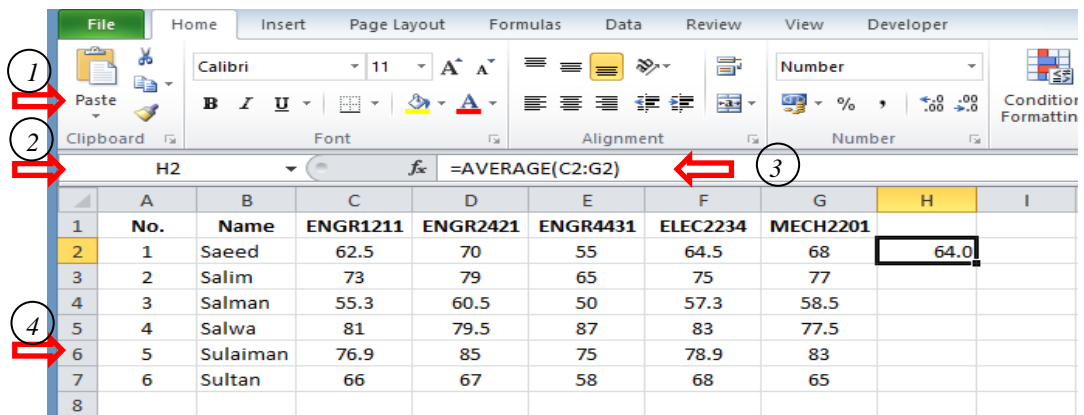


Figure 2.1. The main elements of Excel's user-interface

To allow easy access to the large number of functions, tools, and commands provided by Excel, its interface is divided into a number of elements with different purposes. Figure 2.1 shows four of these elements which are:

1. The ribbon
2. The name box
3. The formula bar
4. The workspace

The **Ribbon**, which occupies the upper part of the sheet, organises the numerous commands provided by Excel into nine "tabs", e.g., the **File**, **Home**, and **Insert** tabs.

Each tab consists of a number of command-groups that have a common purpose. The **Workspace**, which is the main part of the sheet, is divided into a grid of columns and rows that form separate “**cells**” at their intersections. A cell is referred to by a letter and a number, e.g., A1, B3, H2, etc. The letter represents the cell’s column while the number represents its row. The **Name box** shows the location of the current cell.

As Figure 2.1 shows, a cell can simply contain a character data, such as “Saeed” and “Salim”, or a numerical data, such as 62.5 and 70. A cell can also contain a formula for data manipulation using the numerous built-in functions provided by Excel. The formula bar in Figure 2.1 reveals the formula typed in cell H2 that uses the built-in function “**AVERAGE**” to determine the average score of the first student in the list (Saeed) in the five subjects as 64.0. Note that, unlike simple numerical or character cells, a cell that includes a formula must include the equal sign “**=**”. The role of the **Formula bar** will be explained in more details in the following section.

## 2.2. Excel’s formulae

In general, Excel’s formulae include mathematical or logical operators, built-in functions, and cell references. Excel provides two ways to refer a particular cell; either by its location in the sheet, e.g., A2, C10, etc., or by giving it a relevant name, e.g., efficiency, diameter, etc. The two methods will be illustrated below.

### 2.2.1. Cell reference by location

To illustrate this method, let us write a formula that calculates the area of a circle from its radius. To do this, open a new Excel sheet and type the number 5, which is the radius of the circle, in cell A1 as shown in Figure 2.2.

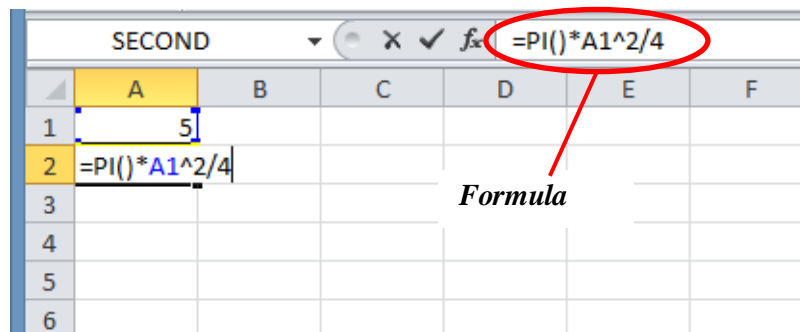


Figure 2.2. Writing an Excel formula to determine the area of a circle

Now, go to cell A2 and type the following formula:

**=PI()\*A1^2/4**

The function “**PI()**” is a built-in function that returns the value of Archimedes’ constant  $\pi$ . The formula also contains a reference to cell A1 that stores the value of the circle’s radius, the multiplication operator \*, the division operator /, the power operator ^, and

the constants 2 and 4. Note that the formula is shown in the formula bar which can also be used to edit the formula. Pressing the **Enter** key after typing the formula, you will obtain the result shown in Figure 2.3; which is 19.63495 square metres.

	A	B	C	D	E	F
1	5					
2	19.63495					
3						
4						
5						
6						

Figure 2.3. The Excel sheet with a formula that determines the area of a circle

The following example shows how Excel’s formulae and built-in functions can be used in a simple thermodynamic analysis.

**Example 2-1. Determining the specific volume of R134a by using the ideal-gas law**

Develop an Excel sheet that calculates the specific volume ( $v$ ) of refrigerant R134a from the ideal-gas law at a pressure of 200 kPa ( $T_{sat} = -10.09^{\circ}\text{C}$ ) and temperatures in the range  $0^{\circ}\text{C}$  to  $100^{\circ}\text{C}$  (273 to 373 K). Compare your results with the tabulated data.

**Solution**

Figure 2.4 shows the Excel sheet prepared for this example. The pressure ( $P$ ), the gas constant ( $R$ ), and the temperature ( $T$ ) are stored in columns A, B, and C, respectively. Column D stores the values of  $v$  obtained from relevant property tables and column E stores the corresponding values obtained from the ideal-gas law:

$$v = RT / P \tag{2.1}$$

Where,  $P$  and  $T$  are the absolute pressure and temperature, respectively, and  $R$  is the gas constant for R134a ( $R = 0.08149 \text{ kJ/kg.K}$ ). The percentage error of the ideal-gas law in estimating the specific volume is given by:

$$Error = \frac{v_{Ideal} - v_{Table}}{v_{Table}} \times 100 \tag{2.2}$$

To determine the percentage error at 273K, go to cell F2 and type the following formula which is equivalent to Equation (2.2):

$$=(E2 - D2)/D2*100$$

F2		fx					
		=(E2-D2)/D2*100					
	A	B	C	D	E	F	G
1	P	R	T	v_table	v_ideal	error v_ideal	
2	200	0.08149	273	0.10438	0.1112339	6.5662483	
3	200	0.08149	283	0.10922	0.1153084	5.5743911	
4	200	0.08149	293	0.11394	0.1193829	4.776944	
5	200	0.08149	303	0.11856	0.1234574	4.1306933	
6	200	0.08149	313	0.12311	0.1275319	3.5917878	
7	200	0.08149	323	0.12758	0.1316064	3.1559414	
8	200	0.08149	333	0.13201	0.1356809	2.7807363	
9	200	0.08149	343	0.13639	0.1397554	2.4674463	
10	200	0.08149	353	0.14073	0.1438299	2.2026931	
11	200	0.08149	363	0.14504	0.1479044	1.974869	
12	200	0.08149	373	0.14932	0.1519789	1.7806389	
13							

Figure 2.4. The sheet developed for determining error in the ideal-gas law for R134a

Note that the formula bar in Figure 2.4 reveals the above formula. When you press the **Enter** key, the number **6.566** will appear in cell F2 as shown in the figure. To find the percentage errors at other temperatures you can simply copy the formula in cell F2 and paste it on cells F3 to F12. The calculated values of the errors show that the maximum error occurs at the lowest temperature, which is 273K. The error decreases gradually as the temperature increases.

### 2.2.2. Use of cell labels

The usual reference to cells by their columns and rows suits perfectly statistical analyses in which the same formula is applied to a large body of data that is stored column-wise or row-wise. For example, we may want to determine the average value, maximum value, or minimum value of the tabulated data. Example 2-1 illustrated this situation. However, thermofluid analyses usually involve numerous formulae but a small set of data, e.g. the diameter of a pipe, the density or viscosity of a fluid, the effectiveness of a heat exchanger, etc. For such analyses, it is more convenient to give the cell a meaningful name or “label” that matches its content. The cell can then be referred to by its label instead of its relative location. This method makes it easier to recognise the quantities involved in the Excel formulae.

For the purpose of illustration, let us develop an Excel sheet to compare the density of air before and after an isentropic compression process from an initial condition of  $P_1 = 100$  kPa and  $T_1 = 300$  K to a final pressure of  $P_2 = 800$  kPa. The two air densities involved can be calculated from the ideal-gas law as follows:

$$\rho_1 = P_1 / RT_1 \tag{2.3}$$

$$\rho_2 = P_2 / RT_2 \tag{2.4}$$

Where  $R$  is the gas constant for air ( $R = 0.287$  kJ/kg.K). For an isentropic process,  $T_2$  is related to  $T_1$  according to the following approximate relationship:

$$T_2 = T_1 \times (P_2 / P_1)^{\frac{k-1}{k}} \tag{2.5}$$

Where  $k$  is the ratio of specific heat at constant pressure ( $c_p$ ) and at constant volume ( $c_v$ ). For air,  $k$  can be taken as 1.4. Note that in Appendix A, Table A.1,  $k$  is used for the thermal conductivity.

Figure 2.5 shows the sheet prepared for this analysis in which the respective cell labels are typed in the column to the left of the different pressures and temperatures, while the corresponding units are written in the column to the right of each quantity. This is also done to the other quantities in the calculations. The sheet also shows the units of the different properties involved for more clarification.

	A	B	C	D	E	F	G
1	<b>Air density before and after an isentriopic compression</b>						
2							
3	$P_1$	100	kPa		$P_2$	800	kPa
4	$T_1$	300	K		$T_2$	543.434	K
5							
6	$R$	0.287	kJ/kg.K		$Density_1$	1.16144	m3/kg
7	$P_r$	8			$Density_2$	5.12934	m3/kg
8	$k$	1.4					
9							
10							

Figure 2.5. Excel sheet for calculating the air densities before and after compression

Placing the cursor on cell F4 makes the formula bar reveal the formula used in the calculation of the temperature  $T_2$  according to Equation (2.5) which is:

$$=B4*B7^{((B8-1)/B8)}$$

The above formula can be made more understandable by using familiar labels to refer to the different cells involved. To do that, select the cells in columns A and B as shown in Figure 2.6, then go to **Formulas** and, at the **Name Manager**, select **Create from Selection**. When the form shown in Figure 2.6 appears to you, tick the “Left column” option. Pressing the “OK” button will make Excel create names for the different values in the selection box according to the labels written on the left column. The cell F3 that stores the value of  $P_2$  can also be associated with its corresponding label in cell E3.



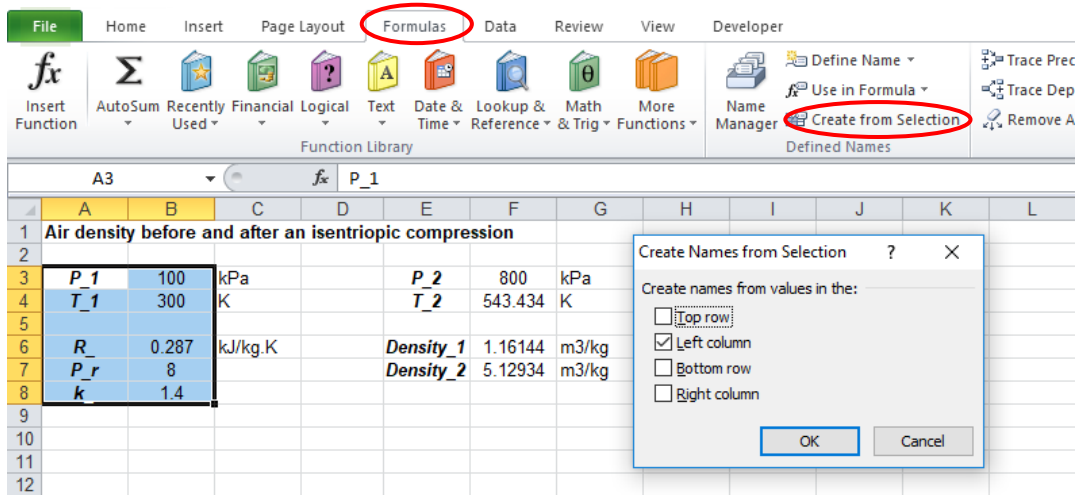


Figure 2.6. Creating names for a selected group of cells

Now, retype the formula in cell F4 that determines  $T_2$  as follows:

$$=T_1 * P_r^{((k_- - 1) / k_-)}$$

The formula bar in the sheet shown in Figure 2.7 reveals the formula with the corresponding labels instead of location references.

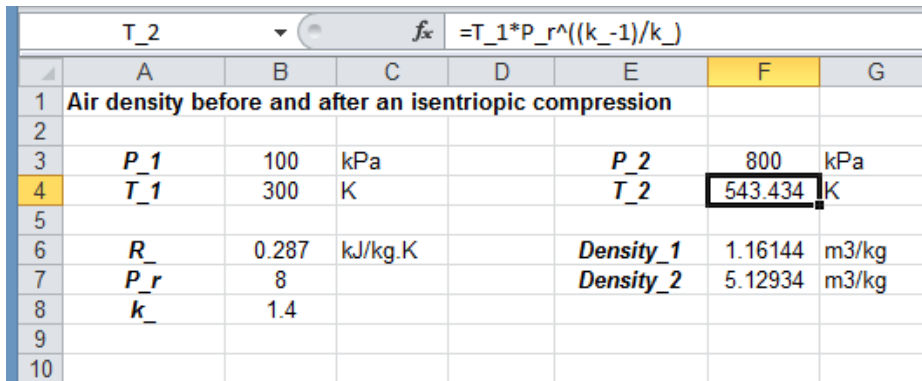


Figure 2.7. Formulae using cells labels instead of locations

Labelled formulae are easier to edit than those using location referencing particularly when intricate formulas are involved. Another advantage of cell-labelling is that if you copy a labelled formula and paste it in any other cell you will get the same answer, but if you copy a formula that uses the usual referencing by location in another cell you will get a different answer. To reveal or hide all the formulae in the sheet, press the control key (ctrl) with the tilde key (~). When naming your cells, choose suitable representative names for the variables involved, e.g. P\_1 and T\_1 for  $P_1$  and  $T_1$ . Note that Excel does not accept "P1" or "T1" as labels since these can be confused with usual cell references

by locations. Therefore, Excel automatically changes these labels to “P1\_” and “T1\_”. More information about Excel formulae can be found in Walkenbach [1].

### 2.3. Excel’s built-in functions

Excel provides a large library of built-in functions for data manipulation, like the **AVERAGE** function, and other functions commonly used in engineering analyses like the **PI**, **SIN**, and **COS** functions. To view the full range of Excel’s functions, type “=” in any Excel cell as shown in Figure 2.8 and then place the cursor on the “**Insert Function**” *fx* button in the formula bar and click it. The dialog box shown in Figure 2.9 will appear to you. List all the categories via the “**Select a category**” slot.

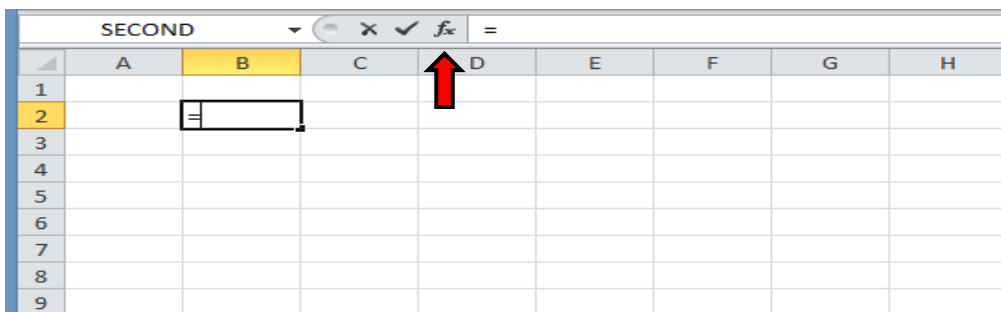


Figure 2.8. Exploring Excel’s built-in functions

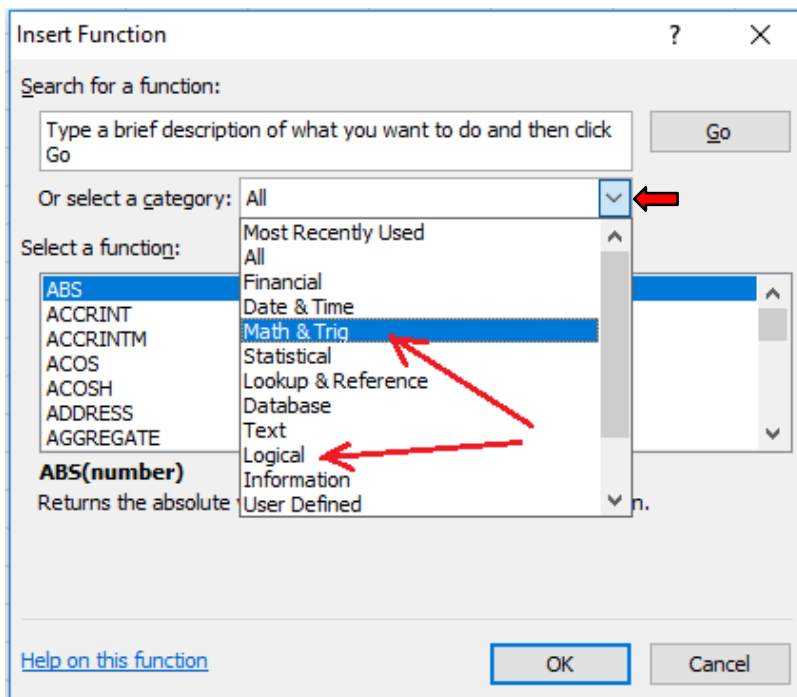


Figure 2.9. The various categories of Excel’s built-in functions

The **Math & Trig** group includes the mathematical and trigonometric functions used in different types of engineering analyses. Figure 2.10 shows some of the numerous functions in this group. Note that the dialog box gives a brief explanation of each function. For example, the explanation given to the **ABS** function is that it returns the absolute value of a number. The functions **ACOS**, **ASIN**, and **ATAN** apply the familiar inverse trigonometric functions:  $\cos^{-1}$ ,  $\sin^{-1}$ , and  $\tan^{-1}$ , respectively. By scrolling down the list, you can find many other familiar functions. The following discussion focuses on two types of functions that are needed for the development of analytical models in subsequent chapters of the book, which are (a) the logical functions and (b) the functions for matrix operations.

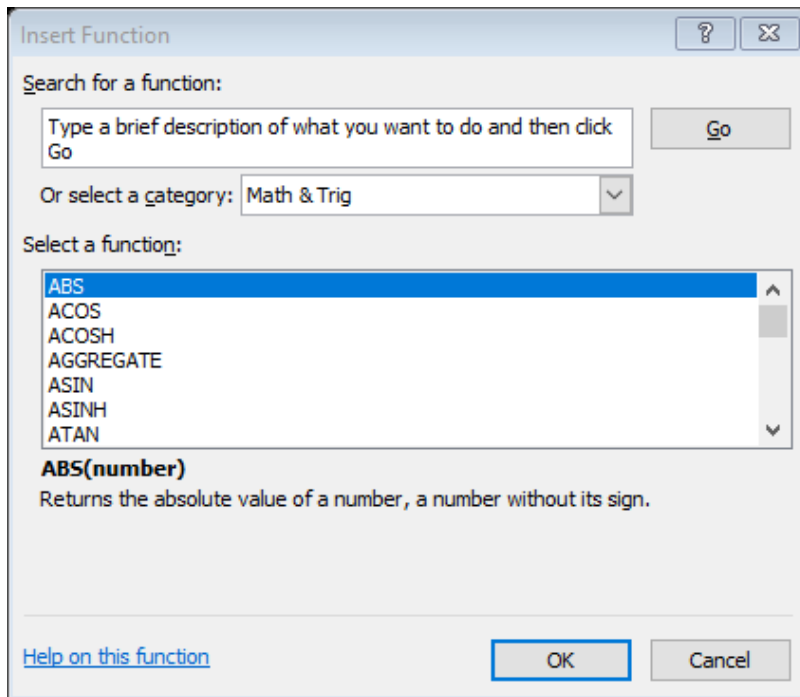


Figure 2.10. Common mathematical functions supported by Excel

### 2.3.1. Logical functions

To determine the major friction loss ( $h_f$ ) in a pipe by using the Darcy-Weisbach equation we have to establish whether the flow is laminar or turbulent so as to select the relevant formula for the friction factor ( $f$ ). The flow remains laminar before the Reynolds number ( $Re$ ) reaches a certain value, which can be taken as 2,000, but the flow can only be considered fully turbulent beyond  $Re = 3000$ . There is a transitional region between laminar and turbulent flows when  $2000 < Re < 3,000$ . Suppose that we want to write an Excel formula that determines the type of flow from the given value of the Reynolds number. Using a simple **IF** function, we can write the following formula:

$$=IF(Re \leq 2000, \text{"Laminar"}, \text{"Turbulent or transitional"})$$

Note that the above **IF**-formula does not differentiate between a turbulent and a transitional flow. Therefore, we need to use a second logical test inside the first logical test. This can be done by using the following nested IF function:

$$=IF(Re \leq 2000, \text{"Laminar"}, IF(Re \geq 3000, \text{"Turbulent"}, \text{"Transitional"}))$$

Figure 2.11 shows an Excel sheet containing the above formula (shown in the formula bar) and the response of the formula when  $Re = 500$ , which is "Laminar". Depending on the value of  $Re$  stored in cell C2, the result of the If-formula can be "laminar", "Turbulent", or "Mixed". Excel supports six other logical functions; **AND**, **FALSE**, **IFERROR**, **NOT**, **OR** and **TRUE** that can be combined in the same formula so as to handle more intricate choices.

	A	B	C	D	E	F	G	H	I	J
1										
2		Re	500							
3										
4		Flow	Laminar							
5										
6										

Figure 2.11. A formula using the nested IF function to determine the type of flow

### 2.3.2. Functions for matrix operations

Adjacent cells can be treated as a matrix or a vector and a group of Excel’s formulae allow for the addition, subtraction, and multiplication of these matrices and vectors according to the established rules of matrix operations. Figure 2.12 shows a 3x3 matrix (A) stored in the cells B3:D5 and a vector (b) stored in cells F3:F5.

	A	B	C	D	E	F	G	H	I	J
1										
2		Matrix A (3x3)				Vector b (3x1)		Vector c (=Axb)		
3		1	2	3		1		=MMULT(B3:D5,F3:F5)		
4		4	5	6		2				
5		7	8	9		3				
6										
7										

Figure 2.12. Step 1 of using the matrix multiplication function

Matrix (A) and vector (b) can be multiplied and the result stored in a third vector (c) by using the matrix function **MMULT**. The procedure is as follows:

1. After keying in the data of matrix (A) and vector (b) as shown in Figure 2.12, position the cursor at cell H3 and type the formula: =MMULT(B3:D5;F3:F5).

- Now press ENTER key and cell H3 will take the value 14, which is the result of multiplying the first row of the matrix with the vector (b) as Figure 2.13 shows.

H3		fx =MMULT(B3:D5,F3:F5)								
	A	B	C	D	E	F	G	H	I	J
1										
2		Matrix A (3x3)				Vector b (3X1)		Vector c (=Axb)		
3		1	2	3		1		14		
4		4	5	6		2				
5		7	8	9		3				
6										
7										

Figure 2.13. Step 2 of using the matrix multiplication function

The other two elements of the result vector will not appear automatically. To view the complete solution vector, do as follows:

- Select the cells H3:H5 as shown in Figure 2.14,
- Press the function key F2 once and then simultaneously hold the (**SHIFT + CONTROL**) keys together and press ENTER. The complete solution vector (c) will now appear as shown in Figure 2.15.

H3		fx =MMULT(B3:D5,F3:F5)								
	A	B	C	D	E	F	G	H	I	J
1										
2		Matrix A (3x3)				Vector b (3X1)		Vector c (=Axb)		
3		1	2	3		1		14		
4		4	5	6		2				
5		7	8	9		3				
6										
7										

Figure 2.14. Step 3 of using the matrix multiplication function

H3		fx {=MMULT(B3:D5,F3:F5)}								
	A	B	C	D	E	F	G	H	I	J
1										
2		Matrix A (3x3)				Vector b (3X1)		Vector c (=Axb)		
3		1	2	3		1		14		
4		4	5	6		2		32		
5		7	8	9		3		50		
6										
7										

Figure 2.15. Step 4 of using the matrix multiplication function

An important matrix-operation function provided by Excel is the matrix-inversion function **MINVERSE** which is needed for the solution of linear systems of equations. The following example illustrates the use of this function.

**Example 2-2. Using the matrix inversion function**

By using the **MINVERSE** function, find the inverse of matrix [A] given by:

$$[A] = \begin{bmatrix} 1 & 0 & 3 \\ 0 & 5 & 6 \\ 7 & 0 & 5 \end{bmatrix}$$

**Solution**

The first step is to enter the elements of the matrix as shown in Figure 2.16. After entering the data, go to cell F2 and type the formula “=MINVERSE(B2:D4)”. When you press **ENTER**, this cell will have the value -0.3125, which is the first element of the inverse matrix  $[A]^{-1}$  shown in Figure 2.17.

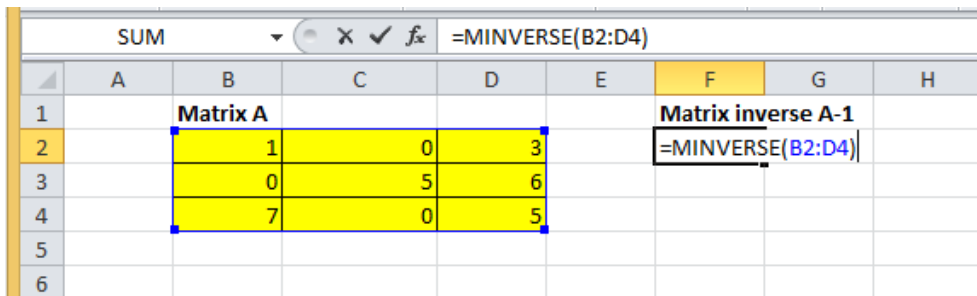


Figure 2.16. Step 1 of using the MINVERSE function

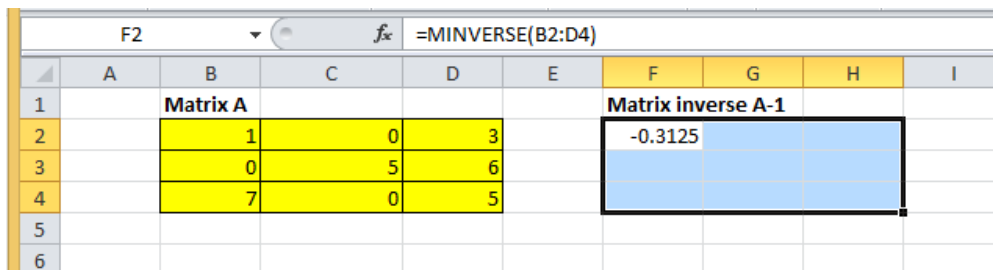


Figure 2.17. Step 2 of using the MINVERSE function

Starting with the formula in cell F2, select the range F2 to H4 as shown in Figure 2.17. Press and release the function key F2 and then simultaneously hold the **CTRL+SHIFT** keys and press **ENTER**. Other elements of the inverse matrix  $[A]^{-1}$  will then appear as shown in Figure 2.18. You can check the solution by multiplying matrix [A] with its inverse by using the **MMULT** functions. The procedure is illustrated by Figures 2.19 to 2.21. As should be expected, Figure 2.21 shows that the resultant matrix is the identity matrix.

		F2				fx {=MINVERSE(B2:D4)}			
	A	B	C	D	E	F	G	H	I
1		Matrix A				Matrix inverse A-1			
2		1	0	3		-0.3125	0	0.1875	
3		0	5	6		-0.525	0.2	0.075	
4		7	0	5		0.4375	0	-0.0625	
5									
6									

Figure 2.18. The complete inverse matrix  $[A]^{-1}$

		SECOND				fx =MMULT(B2:D4,F2:H4)			
	A	B	C	D	E	F	G	H	I
1		Matrix A				Matrix inverse A-1			
2		1	0	3		-0.3125	0	0.1875	
3		0	5	6		-0.525	0.2	0.075	
4		7	0	5		0.4375	0	-0.0625	
5									
6		Matrix AxA-1							
7		=MMULT(B2:D4,F2:H4)							
8		MMULT(array1, array2)							
9									
10									

Figure 2.19. Multiplying matrix  $[A]$  by its inverse  $[A]^{-1}$

		B7				fx =MMULT(B2:D4,F2:H4)			
	A	B	C	D	E	F	G	H	I
1		Matrix A				Matrix inverse A-1			
2		1	0	3		-0.3125	0	0.1875	
3		0	5	6		-0.525	0.2	0.075	
4		7	0	5		0.4375	0	-0.0625	
5									
6		Matrix AxA-1							
7		1							
8									
9									
10									

Figure 2.20. The first element of the product (identity) matrix

		B7				fx {=MMULT(B2:D4,F2:H4)}			
	A	B	C	D	E	F	G	H	I
1		Matrix A				Matrix inverse A-1			
2		1	0	3		-0.3125	0	0.1875	
3		0	5	6		-0.525	0.2	0.075	
4		7	0	5		0.4375	0	-0.0625	
5									
6		Matrix AxA-1							
7		1	0	0					
8		0	1	0					
9		0	0	1					
10									

Figure 2.21. The complete solution which is the identity matrix

### 2.4. Solution of linear system of equations

An example of thermofluid analyses that involve systems of linear equations is the solution of the heat conduction equation with the finite-difference method. Linear systems of equations can be solved with Excel by applying the matrix-inversion method. For illustration, consider the following linear system written in matrix notation:

$$[A]\{x\} = \{y\} \tag{2.6}$$

Where  $[A]$  is the coefficient matrix,  $\{x\}$  the vector of unknowns, and  $\{y\}$  the right-side or “load” vector. By applying the matrix-inversion method, the solution vector  $\{x\}$  can be obtained as follows:

$$\{x\} = [A]^{-1} \{y\} \tag{2.7}$$

Where  $[A]^{-1}$  is the inverse of matrix  $[A]$ . The following example illustrates the procedure of applying the method by using Excel’s matrix functions.

#### Example 2-3. Solution of a system of linear equations

Find the values of  $x_i$  in the following system of linear equations:

$$\begin{bmatrix} 14 & 14 & -9 & 3 & -5 \\ 14 & 52 & -15 & 2 & -32 \\ -9 & -15 & 36 & -5 & 16 \\ 3 & 2 & -5 & 47 & 49 \\ -5 & -32 & 16 & 49 & 79 \end{bmatrix} \begin{Bmatrix} x_1 \\ x_2 \\ x_3 \\ x_4 \\ x_5 \end{Bmatrix} = \begin{Bmatrix} -15 \\ -100 \\ 106 \\ 329 \\ 463 \end{Bmatrix} \tag{2.8}$$

#### Solution

Note that the system is symmetric; which is typically the case with linear systems that arise in the solution of heat-conduction problems by the finite-difference method. For larger systems of equations, the symmetry of the system can be utilised for reducing the required computer memory by storing only one half of the coefficient matrix. However, this requires a complicated computer programming. For small systems like the one considered here, it is more convenient to use Excel’s matrix inversion and multiplication functions. Figure 2.22 shows the Excel sheet that stores both the coefficient matrix  $[A]$  and the load vector  $\{y\}$ . The inverse matrix  $[A]^{-1}$ , which is obtained by following the procedure described in the previous section, is stored below the coefficient matrix as shown in the figure. The inverse matrix  $[A]^{-1}$  is then multiplied with the load vector  $\{y\}$  and the result stored below the load vector as shown in Figure 2.23. The complete solution is shown in Figure 2.24. The first element is practically zero and, therefore, the solution vector is  $\{x\} = (0, 1, 2, 3, 4)$ .



B8		fx {=MINVERSE(B2:F6)}										
	A	B	C	D	E	F	G	H	I	J	K	
1												
2		14	14	-9	3	-5		-15				
3		14	52	-15	2	-32		-100				
4		-9	-15	36	-5	16		106				
5		3	2	-5	47	49		329				
6		-5	-32	16	49	79		463				
7												
8		0.270366	-0.37237	0.248897	0.614204	-0.56509						
9		-0.37237	0.768517	-0.48966	-1.31425	1.202069						
10		0.248897	-0.48966	0.365182	0.880899	-0.80293						
11		0.614204	-1.31425	0.880899	2.355126	-2.13266						
12		-0.56509	1.202069	-0.80293	-2.13266	1.949218						
13												

Figure 2.22. The coefficient matrix  $[A]$ , the load vector  $\{y\}$ , and the inverse matrix  $[A]^{-1}$

SUM		fx {=MMULT(B8:F12,H2:H6)}										
	A	B	C	D	E	F	G	H	I	J	K	
1												
2		14	14	-9	3	-5		-15				
3		14	52	-15	2	-32		-100				
4		-9	-15	36	-5	16		106				
5		3	2	-5	47	49		329				
6		-5	-32	16	49	79		463				
7												
8		0.270366	-0.37237	0.248897	0.614204	-0.56509		=MMULT(B8:F12,H2:H6)				
9		-0.37237	0.768517	-0.48966	-1.31425	1.202069						
10		0.248897	-0.48966	0.365182	0.880899	-0.80293						
11		0.614204	-1.31425	0.880899	2.355126	-2.13266						
12		-0.56509	1.202069	-0.80293	-2.13266	1.949218						
13												

Figure 2.23. Multiplying the inverse matrix  $[A]^{-1}$  with the load vector  $\{y\}$

H8		fx {=MMULT(B8:F12,H2:H6)}										
	A	B	C	D	E	F	G	H	I	J	K	
1												
2		14	14	-9	3	-5		-15				
3		14	52	-15	2	-32		-100				
4		-9	-15	36	-5	16		106				
5		3	2	-5	47	49		329				
6		-5	-32	16	49	79		463				
7												
8		0.270366	-0.37237	0.248897	0.614204	-0.56509		-5.68434E-14				
9		-0.37237	0.768517	-0.48966	-1.31425	1.202069		1				
10		0.248897	-0.48966	0.365182	0.880899	-0.80293		2				
11		0.614204	-1.31425	0.880899	2.355126	-2.13266		3				
12		-0.56509	1.202069	-0.80293	-2.13266	1.949218		4				
13												

Figure 2.24. The complete solution vector  $\{x\}$

It should be mentioned that the procedure described above by using Excel’s functions suits best one-dimensional fluid-flow and heat-transfer analyses. This is because the linear systems generated in multi-dimensional analyses are usually too large to be solved efficiently by using the matrix-inversion method.

## 2.5. Iterative solutions with Excel

Excel offers its user two methods to perform iterative solutions: (i) by using the **Goal Seek** command and (ii) by using **circular calculations**. In what follows the two methods will be illustrated with the help of simple examples.

### 2.5.1. Iterative solutions with Goal Seek

The **Goal Seek** command is used for finding the value of an independent variable ( $x$ ) that yields a specified value of a dependent variable ( $y$ ). It is a simple, yet very useful tool for “What-if” analyses. The following example illustrates how this command can be used to solve a nonlinear equation.

#### Example 2-4. Solution of a nonlinear equation by Goal Seek

A centrifugal pump is used for lifting water from the utility network at the ground level to a tank at the top of a building that is 30-m high as shown in Figure 2.25. The pump’s characteristic curve can be represented by the following formula:

$$h_p = h_0 - aQ - bQ^2 - cQ^3 \quad (2.9)$$

Where  $h_p$  and  $Q$  are the pump’s head (m) and discharge ( $\text{m}^3/\text{s}$ ), respectively, and  $h_0$ ,  $a$ ,  $b$ , and  $c$  are constants the values of which are 47.22,  $2.985 \times 10^3$ ,  $1.549 \times 10^5$ , and  $2.348 \times 10^8$ , respectively.

Neglecting friction losses in the pipe, determine the water flow rate ( $\text{m}^3/\text{s}$ ) that can be delivered by the pump.

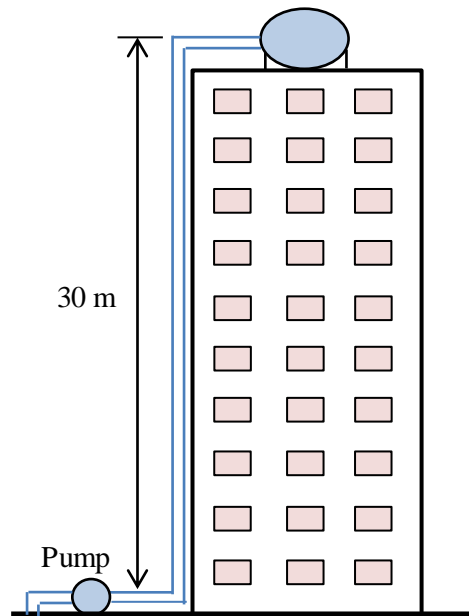


Figure 2.25. Schematic for Example 2-4

#### Solution

Figure 2.25 shows the Excel sheet prepared for this example in which the values of the four constants in Equation (2.9) are stored at the top of the sheet. The pump’s discharge is calculated at various values of the discharge and plotted as shown in the figure. We can see from the plot that the value of  $Q$  that yield  $h_p = 30$  m is approximately  $0.003 \text{ m}^3/\text{s}$ .

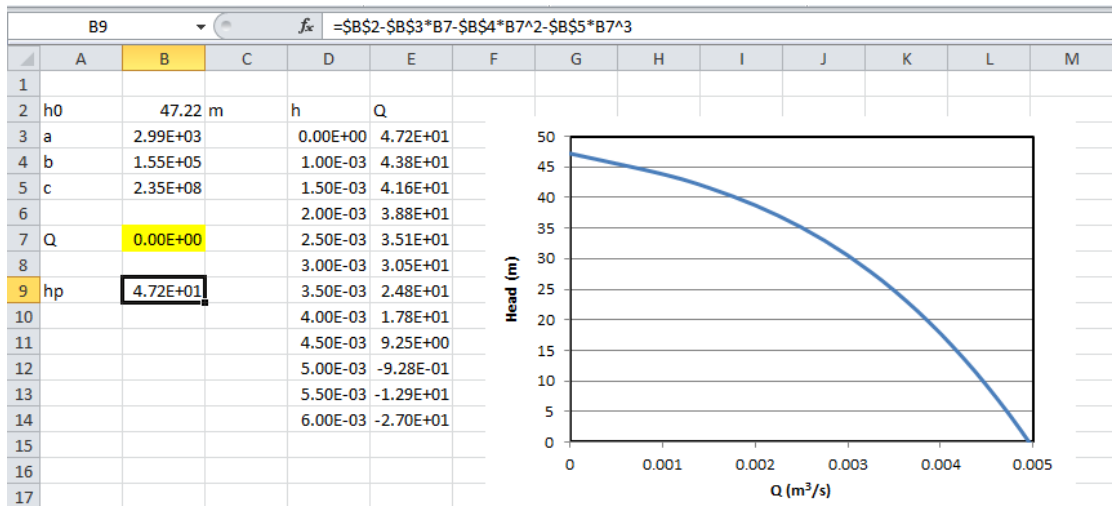


Figure 2.25. Excel sheet for Example 2-4

To solve the problem by using Goal Seek, enter an initial guess for  $Q$  in cell B7, say 0, and then enter the following formula that uses Equation (2.9) to calculate  $h_p$  in cell B9:

$$=B\$2-B\$3*B7-B\$4*B7^2-B\$5*B7^3$$

Note the dollar sign (\$) that has been added to the references of the four constants, e.g. B2 has become B\$2. The formula bar in Figure 2.25 reveals the above formula by placing the cursor at cell B9.

To activate the Goal Seek command, go to the **Data** tab, select the **What-If-Analysis** option in the **Data Tools** group and then select **Goal Seek**, as shown in Figure 2.26. The Goal Seek dialog box shown in Figure 2.27.a will then appear to you. The dialog box asks you to select the “**Set cell**”, i.e. the cell that contains the dependent variable, which is B9 in this case. You also have to specify the value sought for this cell and the adjustable cell that stores the parameter to be changed. In this case, we seek the value in the cell B9 to be 30 by changing the value of the cell B7. The completed form is shown in Figure 2.27.b.

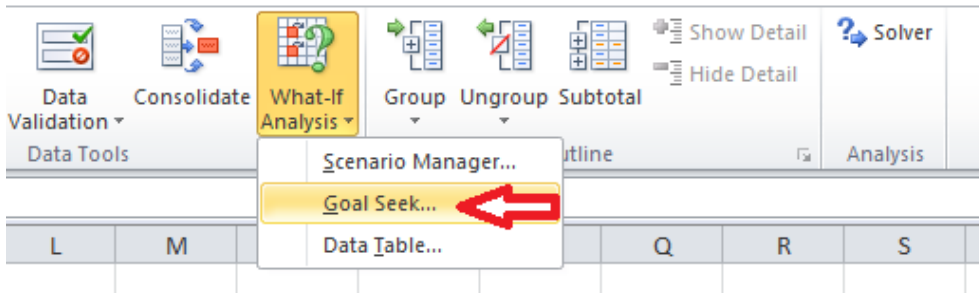


Figure 2.26. Activation of the Goal Seek command

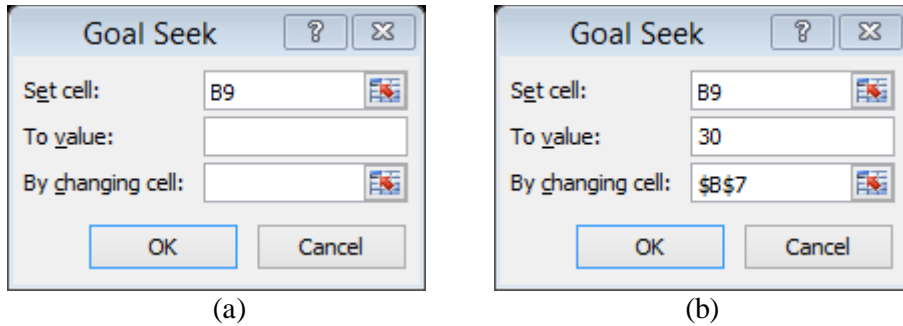


Figure 2.27. Goal Seek Set-up for Example 2-4: (a) before completion (b) the completed box

By pressing the “OK” button after completing the Goal Seek form, Excel will change the value in the adjustable cell (B7) until the Set cell (B9) acquires the required value. As shown in Figure 2.28, the answer obtained is  $Q = 0.003 \text{ m}^3/\text{s}$  which agrees with the estimated value from the plot in Figure 2.25.

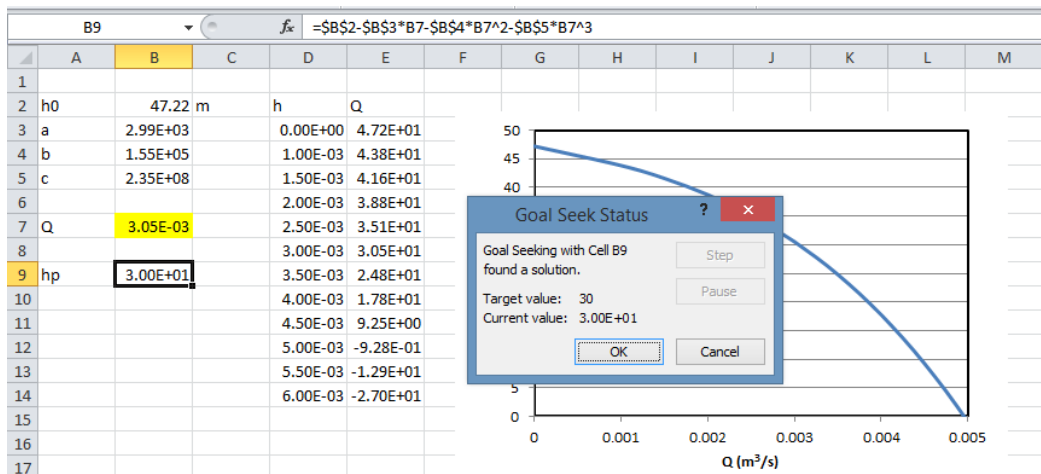


Figure 2.28. Goal Seek solution for Example 2-4

### 2.5.2. Iterative solution with circular calculations

A circular reference occurs when an Excel formula tries to refer to its own cell in a direct or indirect manner. In standard programming this is not allowed, but Excel gives its user the option to use “circular calculation” if intended. In this case, Excel will iterate until all the formulae involved are satisfied. The following example illustrates this special feature which is useful for thermofluid analyses.

#### Example 2-5. Determining the final temperature of heated air

Heat is added to a piston-cylinder device that contains one kg of air initially at 300K. If 100 kJ of heat is added to the air at constant pressure, determine the final temperature of

air taking into consideration that its molar specific-heat ( $\tilde{c}_p$ ) varies with temperature according to the following formula:

$$\tilde{c}_p = a + bT + cT^2 + dT^3 \quad [\text{kJ/kmol}] \quad (2.10)$$

Where  $a = 28.11$ ,  $b = 1.97 \times 10^{-03}$ ,  $c = 4.80 \times 10^{-06}$ , and  $d = -1.97 \times 10^{-09}$ .

**Solution**

From the definition of specific heat, the final temperature ( $T_2$ ) is given by:

$$T_2 = T_1 + Q/(\tilde{c}_p / M) \quad (2.11)$$

Where  $T_1$  is the initial temperature,  $Q$  is the amount of heat added, and  $M$  is the molar mass for air ( $M=29$ ). If the variation of  $\tilde{c}_p$  with temperature is ignored and its value at  $T_1$  alone is used, Equation (2.11) determines  $T_2$  as 399.73K. However, we can be more accurate by using Equation (2.10) to determine  $\tilde{c}_p$  at the average temperature,  $T_{avr} = (T_1+T_2)/2$ . Figure 2.29 shows the Excel sheet developed for this method which reveals the formulae inserted in cells F2, F4, and F6.

	A	B	C	D	E	F	G	H
1	Air							
2		T_1	300 K		T_avr	350	=(T_1+T_2)/2	
3		Q	100 kJ					
4					Cp	1.010428	=(a+b*T_avr+c*T_avr^2+d*T_avr^3)/29	
5		a	28.11					
6		b	1.97E-03		T_2	1+Q/Cp	=T_1+Q/Cp	
7		c	4.80E-06					
8		d	-1.97E-09					
9								

Figure 2.29. Excel sheet developed for Example 2-5

As soon as we type Equation (2.11) in cell F6, Excel will make the warning message that there is a circular reference as shown in Figure 2.30.

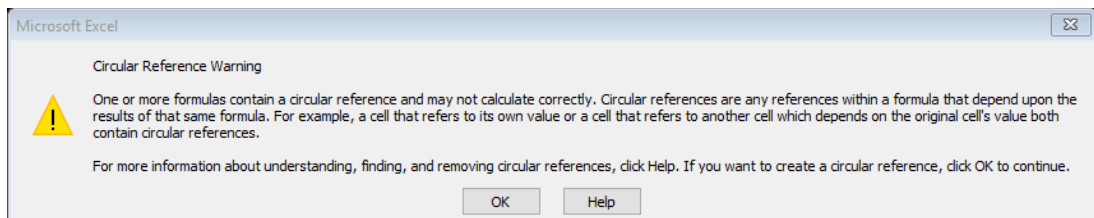


Figure 2.30. The circular-reference prompt

## Computer-Aided Thermofluid Analyses Using Excel

The circular reference occurs because  $T_2$  depends on  $\tilde{c}_p$  according to Equation (2.11) while  $\tilde{c}_p$  itself depends on  $T_2$  according to Equation (2.10). If we press the “OK” button shown in Figure 2.30, the cells involved in the circular reference will be identified as shown in Figure 2.31. In this case, three cells are involved in the circular reference, which are F2, F4, and F6.

T_2		fx		=T_1+Q/Cp				
	A	B	C	D	E	F	G	H
1	Air							
2		T_1	300 K		T_avr	350	=(T_1+T_2)/2	
3		Q	100 kJ					
4					Cp	1.010428	=(a+b*T_avr+c*T_avr^2+d*T_avr^3)/29	
5		a	28.11					
6		b	1.97E-03		T_2	0	=T_1+Q/Cp	
7		c	4.80E-06					
8		d	-1.97E-09					
9								

Figure 2.31. The cells involved in the circular reference

Excel can iterate to determine the values of both  $T_2$  and  $\tilde{c}_p$  that satisfy the relevant equations if permitted because the iterative-calculation option is not allowed by default. To allow it, go to **File** and select **Options**. The **Backstage View** form shown in Figure 2.32 will appear to you. Select **Formulas**, then the form will appear as shown in Figure 2.33. Enable iterative calculations by ticking () the box indicated in the figure and press the “OK” button. Excel can now iterate to find the values of  $T_2$  and  $c_p$  that simultaneously satisfy Equations (2.10) and (2.11). Figure 2.34 shows the solution found by this method, which is  $T_2 = 398.976\text{K}$ .

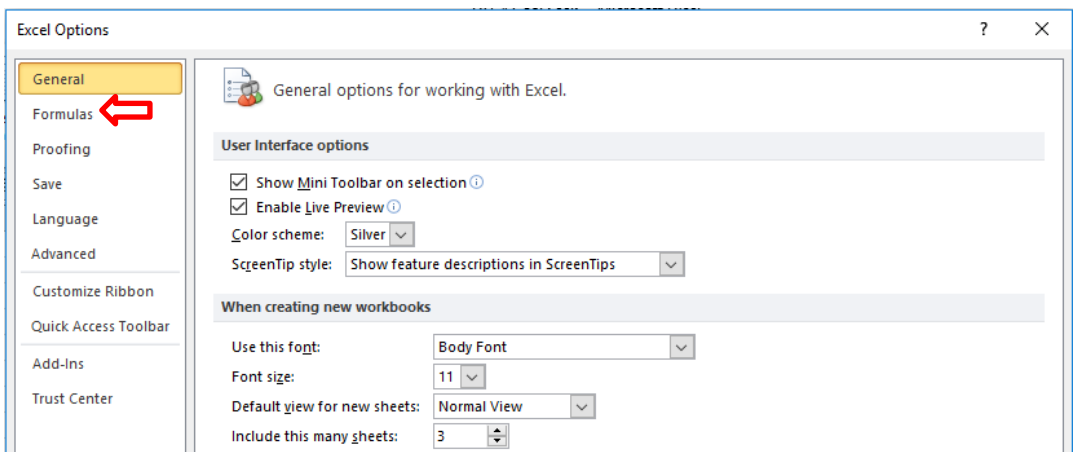


Figure 2.32. Selecting Excel's option (Formulas)

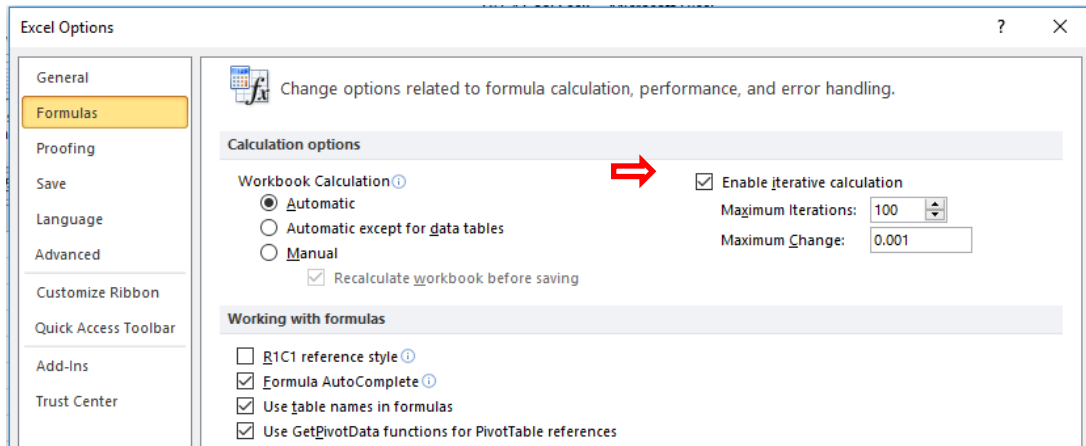


Figure 2.33. Enabling iterative calculations from Excel's Formulas option

	A	B	C	D	E	F	G	H
1	Air							
2		T <sub>1</sub>	300 K		T <sub>avr</sub>	349.488	=(T <sub>1</sub> +T <sub>2</sub> )/2	
3		Q	100 kJ					
4					Cp	1.010346	=(a+b*T <sub>avr</sub> +c*T <sub>avr</sub> <sup>2</sup> +d*T <sub>avr</sub> <sup>3</sup> )/29	
5		a	28.11					
6		b	1.97E-03		T <sub>2</sub>	398.976	=T <sub>1</sub> +Q/Cp	
7		c	4.80E-06					
8		d	-1.97E-09					
9								

Figure 2.34. Solution of Example 2-5 by circular calculations

This example can also be solved by using the Goal Seek command. In this case, we have to start the iterative solution by providing Excel with a guessed value for  $T_2$ , call it  $T_{2o}$ , based on which a new value for  $T_2$  is calculated, called it  $T_{2c}$ . Since the guessed value  $T_{2c}$  is unlikely to be correct, it will be different from  $T_{2o}$ . Goal Seek is then used to adjust the value of  $T_{2o}$  until the difference ( $\text{Diff} = T_{2c} - T_{2o}$ ) vanishes.

Most iterative solutions in this book are obtained by using the Goal Seek command. However, the circular-calculation option is more useful in certain situations as demonstrated in Chapters 8 and 9 that deal with the numerical solution of the heat-conduction equation with the finite-difference method.

## 2.6. Excel's graphical tools for data presentation and analysis

Excel has numerous graphical tools that can be used to present the stored data in a variety of charts. Figure 2.35 shows one type of Excel charts that displays the annual variation of temperature and relative humidity at one location in a certain day. The figure shows a line chart in which the temperature is scaled on the primary y-axis (on the left) while the humidity is scaled on the secondary y-axis (on the right). This arrangement is useful for displaying two or more types of data that differ significantly in magnitude such as the net specific work and thermal efficiency of a power cycle.

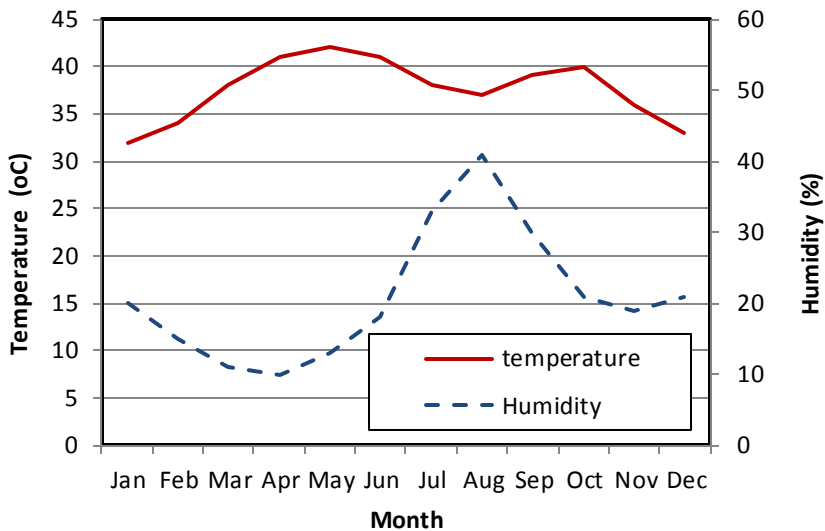


Figure 2.35. An example of line charts

Excel supports other types of charts that allow the user to select the most appropriate way to display his/her data in the form of bar, area, or scatter charts. For more information about the different types of Excel's charts, the reader can refer to specialised references such as Walkenbach [2]. A number of tutorials and videos that show how to create different types of charts can also be found in the internet.

Excel's charts provide a curve-fitting capability of numerical data by using the **Trendline** feature. This capability is particularly useful for computer-aided thermofluid analyses because it can be used to convert tabulated fluid-properties and other data into analytical equations that make the data more suitable for iterative solutions and optimisation analyses. To illustrate the use of this feature, consider Table 2.1 that shows properties of saturated water in the range  $0.001^{\circ}\text{C} - 60^{\circ}\text{C}$ . These values of the saturation pressure ( $P_{\text{sat}}$ ) and saturated liquid enthalpy ( $h_f$ ) are used in psychrometric analyses of air-conditioning applications. For computer-aided analyses, it is useful to convert these data into relevant equations.

The trendline feature provides a number of options, which include exponential, linear, logarithmic, polynomial, and power equations as shown in Figure 2.36. To fit a trendline to the data, we have to create line charts for the two properties as shown in Figures 2.37.a and 2.39.b. Trendlines can then be added on the line charts. Figures 2.37.a and 2.39.b also show the corresponding trendline equations of the tabulated data as determined by using polynomial equations. As Figure 2.37.b shows, a linear equation is adequate for the  $h_f$  data since its variation over the given temperature range is mild. However, a third-order polynomial is required to represent the variation of  $P_{\text{sat}}$  with temperature as shown in Figure 2.37.a.



Table 2.1. Properties of saturated water at temperatures in the range 0°C- 60°C taken from Cengel and Boles [3]

$T^{\circ}\text{C}$	$P_{sat}$ [kPa]	$v_f$ [m <sup>3</sup> /kg]	$v_g$ [m <sup>3</sup> /kg]	$u_f$ [kJ/kg]	$u_g$ [kJ/kg]	$h_f$ [kJ/kg]	$h_g$ [kJ/kg]	$s_f$ [kJ/kg.K]	$s_g$ [kJ/kg.K]
0.01	0.6117	0.001000	206.00	0.000	2374.9	0.001	2500.9	0.0000	9.1556
5	0.8725	0.001000	147.03	21.019	2381.8	21.020	2510.1	0.0763	9.0249
10	1.2281	0.001000	106.32	42.020	2388.7	42.022	2519.2	0.1511	8.8999
15	1.7057	0.001001	77.885	62.980	2395.5	62.982	2528.3	0.2245	8.7803
20	2.3392	0.001002	57.762	83.913	2402.3	83.915	2537.4	0.2965	8.6661
25	3.1698	0.001003	43.340	104.83	2409.1	104.83	2546.5	0.3672	8.5567
30	4.2469	0.001004	32.879	125.73	2415.9	125.74	2555.6	0.4368	8.4520
35	5.6291	0.001006	25.205	146.63	2422.7	146.64	2564.6	0.5051	8.3517
40	7.3851	0.001008	19.515	167.53	2429.4	167.53	2573.5	0.5724	8.2556
45	9.5953	0.001010	15.251	188.43	2436.1	188.44	2582.4	0.6386	8.1633
50	12.352	0.001012	12.026	209.33	2442.7	209.34	2591.3	0.7038	8.0748
55	15.763	0.001015	9.5639	230.24	2449.3	230.26	2600.1	0.7680	7.9898
60	19.947	0.001017	7.6670	251.16	2455.9	251.18	2608.8	0.8313	7.9082

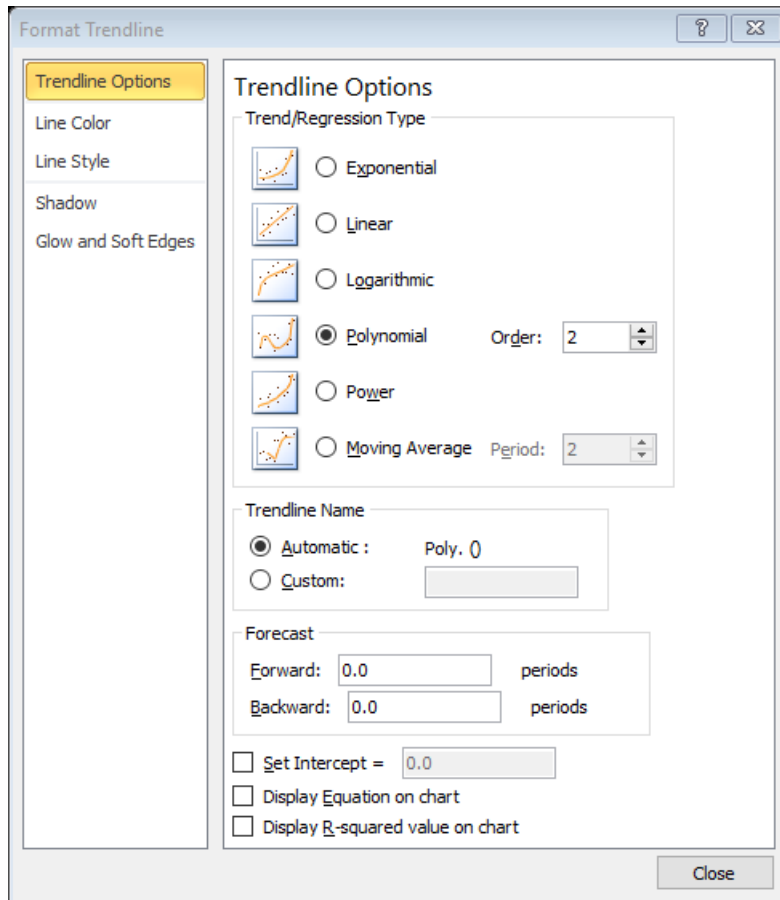


Figure 2.37. The Format Trendline window

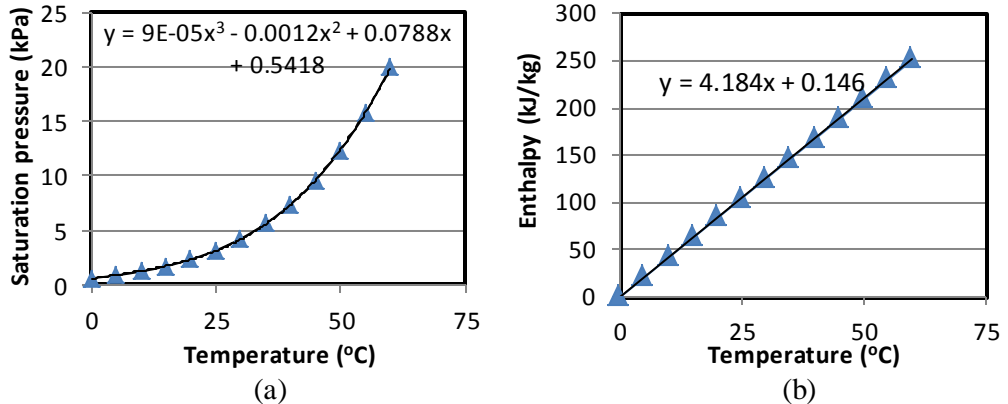


Figure 2.37. Fitting trendlines on tabulated data for water of (a) saturation pressure and (b) saturated liquid enthalpy

## 2.7. Closure

This chapter described the main features of Excel needed for thermofluid analyses. The chapter highlighted the importance of using cell labelling with Excel's formulae and illustrated the use of Excel's general mathematical functions, logical functions, and the functions for matrix operations. The chapter also demonstrated the use of Excel's two iterative tools: Goal Seek and circular calculations. In spite of its simplicity, the Goal Seek command is very useful for iterative solutions as shown in later chapters of this book. Finally, the chapter illustrated the usefulness of Excel's charting tools for the presentation of tabulated data particularly the trendline feature.

It should be mentioned that the **Developer tab** in Excel's user-interface provides a number of other useful features that have not been mentioned in the chapter but needed for enhancing the effectiveness of Excel as modelling platform for thermofluid analyses. One of these features is the ability to record **macros** for conducting repetitive calculations and parametric analyses as illustrated in Appendix F.

## References

- [1] J. Walkenbach, *Excel 2010 Formulas*, Wiley Publishing Inc., 2010
- [2] J. Walkenbach, *Excel 2007 Charts*, Wiley Publishing Inc., 2007
- [3] Y. A. Cengel and M. A. Boles. *Thermodynamics an Engineering Approach*, McGraw-Hill, 7<sup>th</sup> Edition, 2007
- [4] S. C. Chapra and R. P. Canale, *Numerical Methods for Engineers*, 6<sup>th</sup> Edition, McGraw Hill, 2010

**Exercises**

1. The following table shows measured values of the temperature by two different methods compared to the correct corresponding values. Find the average error for each method.

<i>Correct T (°C)</i>	<i>Method 1</i>	<i>Method 2</i>
0	0.1044	0.1112
10	10.1092	10.1153
20	20.1139	20.1194
30	30.1186	30.1235
40	40.1231	40.1275
50	50.1276	50.1316
60	60.1320	60.1357
70	70.1364	70.1397
80	80.1407	80.1438
90	90.1450	90.1479
100	100.1493	100.1520

2. The following table shows the data for the saturation pressure of a certain fluid. Use a nested IF statement to develop an interpolation formula that determines the saturation pressure of the fluid at any temperature in the range  $5^{\circ}\text{C} \leq T \leq 30^{\circ}\text{C}$ .

$T(^{\circ}\text{C})$	$P_{\text{sat}} \text{ (kPa)}$
5	0.872
10	1.228
15	1.705
20	2.339
25	3.169
30	4.246

3. A system of algebraic equations can be expressed in matrix form as follows:

$$\begin{bmatrix} 70 & 1 & 0 \\ 60 & -1 & 1 \\ 40 & 0 & -1 \end{bmatrix} \begin{Bmatrix} a \\ b \\ c \end{Bmatrix} = \begin{Bmatrix} 636 \\ 518 \\ 307 \end{Bmatrix}$$

Solve the system of equations to determine the values of the three unknowns  $a$ ,  $b$ , and  $c$ . This exercise is based on Example 9.11 in Chapra and Canale [4]. The answer is:  $a = 8.5941$ ,  $b=34.4118$ , and  $c = 36.7647$ .

4. Figure 2.P4 shows a triangular fin attached to the surface of a wall. Solution of the conduction heat transfer equation with the finite-difference method resulted in the

following system of linear equations the solution of which gives the temperatures in °C at different distances from the fin base as shown in the figure:

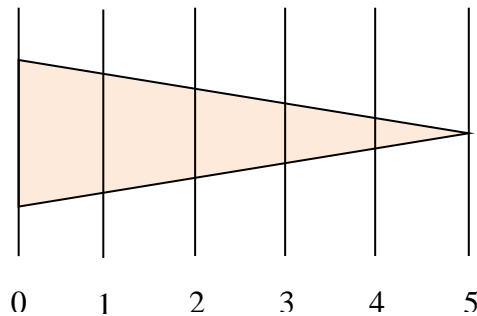


Figure 2.P4. Triangular fin

$$-8.008 T_1 + 3.5 T_2 = -900.209$$

$$3.5 T_1 - 6.008 T_2 + 2.5 T_3 = -0.209$$

$$2.5 T_2 - 4.008 T_3 + 1.5 T_4 = -0.209$$

$$1.5 T_3 - 2.008 T_4 + 0.5 T_5 = -0.209$$

$$T_4 - 1.008 T_5 = -0.209$$

Use Excel functions to solve the above system of linear equations.

- Adopting suitable names in your formulae, prepare an Excel sheet for calculating the frictional loss ( $h_f$ ) in a circular pipe of diameter  $D$ , length  $L$ , and roughness  $k_s$ . Use your sheet to determine  $h_f$  in the following cases:

(a)  $D = 25$  cm,  $L = 150$  m,  $V = 2$  m/s,  $k_s = 0.045$  mm, carrying water at  $20^\circ\text{C}$ .

(b)  $D = 25$  cm,  $L = 150$  m,  $V = 0.2$  m/s,  $k_s = 0.045$  mm, carrying oil at  $20^\circ\text{C}$ .

(c)  $D = 25$  cm,  $L = 150$  m,  $V = 7$  m/s,  $k_s = 0.045$  mm, carrying air at  $20^\circ\text{C}$ .

Use the Dracy-Weisbach equations and determine the values of the kinematic viscosity from relevant property tables.

- Using a line chart, plot the variation of  $\sin \theta$  for  $-180 \leq \theta \leq 180$  in steps of  $10^\circ$  then add  $\cos \theta$  on the same chart.
- Using the data shown in Table 2.1, make a line chart for  $\nu_f$  and  $\nu_g$ . Add polynomial trendlines for both and comment on the trendlines equations.
- The table below shows some of the thermo-physical properties of air at atmospheric pressure and different temperatures. Use Excel charts to show the

variation of the properties  $\rho$ ,  $\beta$ ,  $c_p$ ,  $k$ ,  $\alpha$ ,  $\mu$ ,  $\nu$ , and  $Pr$  with temperature and use trendline to obtain suitable equations for these properties.

$T$ (K)	$\rho$ (kg/m <sup>3</sup> )	$\beta \times 10^3$ (1/K)	$c_p$ (J/kg.K)	$k$ (W/m.K)	$\alpha$ (m <sup>2</sup> /s)	$\mu \times 10^6$ (N S/m <sup>2</sup> )	$\nu \times 10^6$ (m <sup>2</sup> /s)	$Pr$
273	1.252	3.66	1011	0.0237	19.2	17.456	13.9	0.71
293	1.164	3.41	1012	0.0251	22.0	18.240	15.7	0.71
313	1.092	3.19	1014	0.0265	24.8	19.123	17.6	0.71
333	1.025	3.00	1017	0.0279	27.6	19.907	19.4	0.71
353	0.968	2.83	1019	0.0293	30.6	20.790	21.5	0.71
373	0.916	2.68	1022	0.0307	33.6	21.673	23.6	0.71
473	0.723	2.11	1035	0.0370	49.7	25.693	35.5	0.71
573	0.596	1.75	1047	0.0429	68.9	29.322	49.2	0.71
673	0.508	1.49	1059	0.0485	89.4	32.754	64.6	0.72
773	0.442	1.29	1076	0.0540	113.2	35.794	81.0	0.72

9. The volume  $V$  of liquid in a spherical tank of radius  $r$  is related to the depth  $h$  of the liquid by:

$$V = \pi h^2(3r - h)/3$$

Using the Goal Seek command, determine the value of  $h$  for the tank with  $r=1$  m and  $V = 0.5$  m<sup>3</sup>.

This exercise is based on Problem 8.9 in Chapra and Canale [4]. Answer:  $h = 0.431$  m.

# 3

## **Solver, VBA, and Thermax**

As the main component of the present modelling platform for thermofluid analyses, Excel provides the user-interface and built-in functions, two iterative tools, and graphic tools. However, what make Excel an effective platform for thermofluid analyses are the three auxiliary components; Solver, VBA, and Thermax. This chapter focuses on these three components and illustrates their use by means of relevant examples. With respect to Solver, the chapter shows how its three solution methods can be used for performing optimisation analyses and solving systems of linear and nonlinear equations. The chapter also shows how VBA can be used for developing custom functions and how Thermax functions can be used in Excel formulae.

### 3.1. Solver

Solver is a multi-purpose iterative tool developed by Frontline Systems [1] as an Excel add-in for “What-if” analyses. Compared to Excel’s own iterative tool, which is the Goal Seek command described in Chapter 2, Solver offers the following advantages:

1. While Goal-Seek can only be used for simple problems that involve only one decision variable, Solver can deal with more difficult problems in which the objective cell is affected by numerous decision variables.
2. Goal Seek allows only a required value of the objective cell to be achieved, but Solver also enables Excel to perform an optimisation analysis by finding the maximum or minimum value for the formula in the objective cell.
3. Solver allows constraints to be applied on the solution, which is not possible with Goal Seek. The ability to impose constraints is needed for both optimisation analyses and iterative solutions.
4. Solver offers three solution methods that suit different types of problems and gives the user a number of numerical options for applying the same method.

#### 3.1.1. Activation of Solver

Like the Goal Seek command, Solver is found in the **Data tab** as shown in Figure 3.1. If it doesn’t appear in your Data tab, then go to **File** and then click **Options** and select **Add-Ins**. From the **Manage** option at the bottom of the menu select **Excel Add-ins** and then click “Go”. The **Add-Ins** dialog box shown in Figure 3.2 will be shown. To add **Solver** to the add-ins menu, tick (✓) on the “**Solver**” option and return to the **Data tab**. When you click the **Solver** button from the **Data tab**, the **Solver Parameters** dialog box shown in Figure 3.3 will be shown.

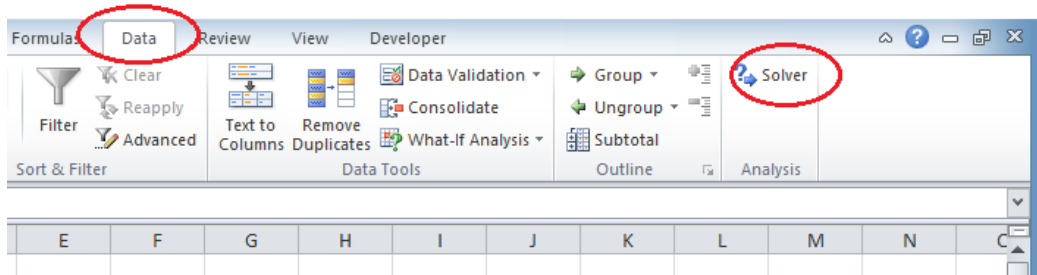


Figure 3.1. The Solver add-in in the Data tab

## Computer-Aided Thermofluid Analyses Using Excel

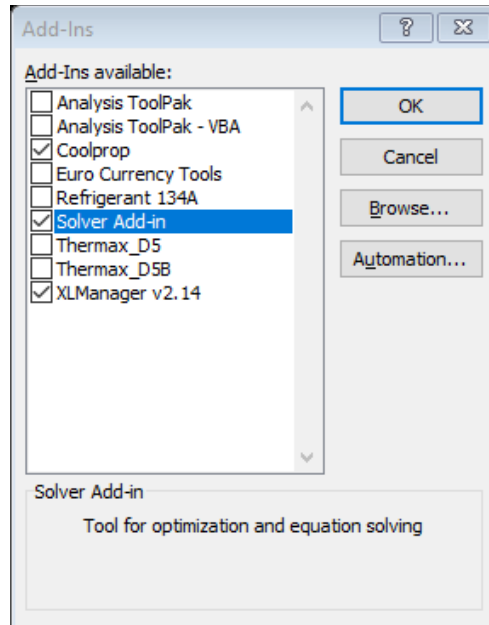


Figure 3.2. Activating Solver from the menu of Excel add-ins

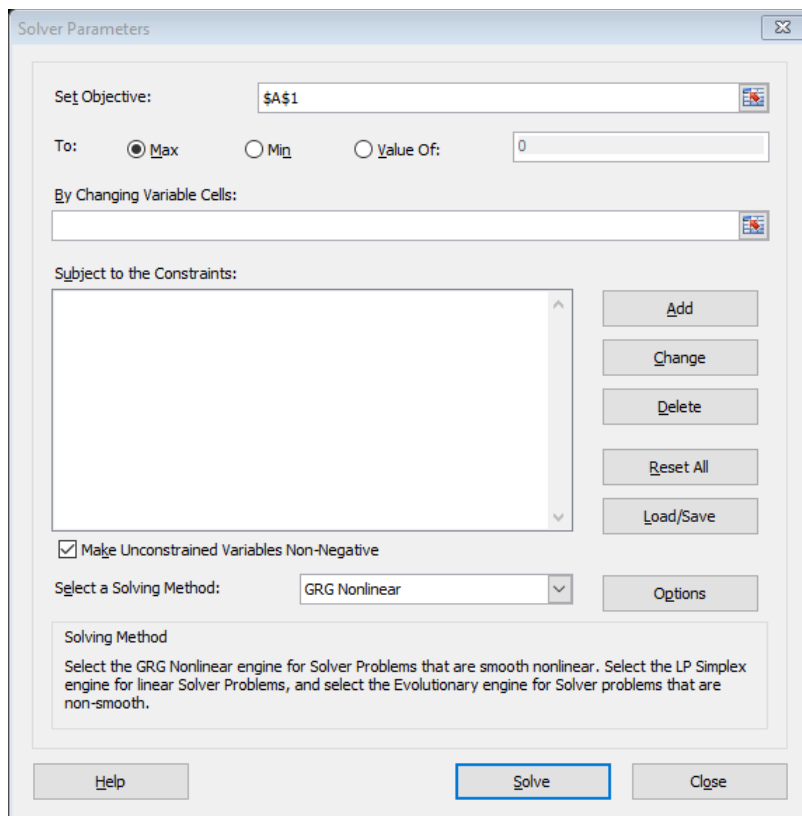


Figure 3.3. Solver Parameters dialog box



**Solver Parameters** dialog box helps the user to select a formula in one cell, called the **objective cell**, and a group of other cells, called **decision variables** or variable cells, which are directly or indirectly related to the formula in the objective cell. By adjusting the **decision variables**, the **objective cell** can be maximised, minimised, or made to acquire a certain value. As shown in Figure 3.3, **constraints** can be applied on the decision variables. To suit different types of problems, Solver offers three solution methods which are:

1. The **GRG Nonlinear** method,
2. The **Evolutionary** method
3. The **Simplex LP** method.

The GRG Nonlinear method involves the determination of the function's gradient like the Steepest Descent method [2, 3]. The **Evolutionary** method adopts a variety of genetic algorithms and local search methods [4, 5]. While both the **GRG Nonlinear** and the **Evolutionary** methods are suitable for non-linear problems, the **Simplex LP** method, which is a linear-programming method, is suitable for linear problems. As shown in Figure 3.3, Solver uses the **GRG Nonlinear** method by default. The following sections give examples of using the three solution methods.

### 3.1.2. The GRG Nonlinear method

In an optimisation analysis we may require the objective function to be maximised or minimised depending on the situation at hand. For example, the optimisation of pipe insulation requires its total cost to be minimised, while the optimisation of a thermal power plant requires its thermal efficiency to be maximised. The following example illustrates the use of the **GRG Nonlinear** method in optimisation analyses.

#### Example 3-1. Finding the minimum value of a quadratic function

Find the minimum value of the following quadratic function in the specified range.

$$f(x) = x^2 - 2x - 1; \quad -2 \leq x \leq 3 \quad (3.1)$$

#### Solution

Figure 3.4 shows the Excel sheet developed for this example. The line chart inserted in the figure shows the variation of  $f$  with  $x$  from which we can see that the minimum value of  $f$  is -2 and occurs at  $x = 1$ . An initial value for  $x$  is entered in cell **B3** based on which the function  $f(x)$  is calculated in cell **B6** according to Equation (3.1). Note the cursor is placed on cell **B6** to reveal the following formula typed in the cell:

$$= B3^2 - 2 * B3 - 1$$

We can now use Solver to determine the minimum value of the function. To do so, select **Solver** from the **Data tab** and fill its parameters dialog-box as shown in Figure 3.5 that shows the top part of the completed box.

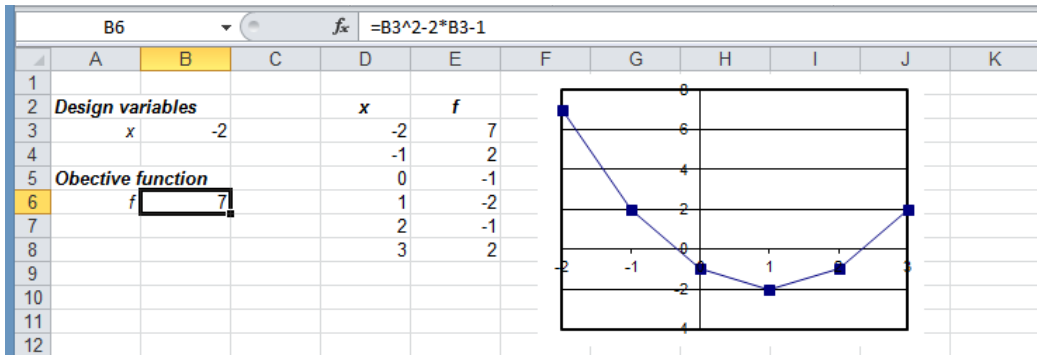


Figure 3.4. Excel sheet for determining the local minimum of the quadratic function

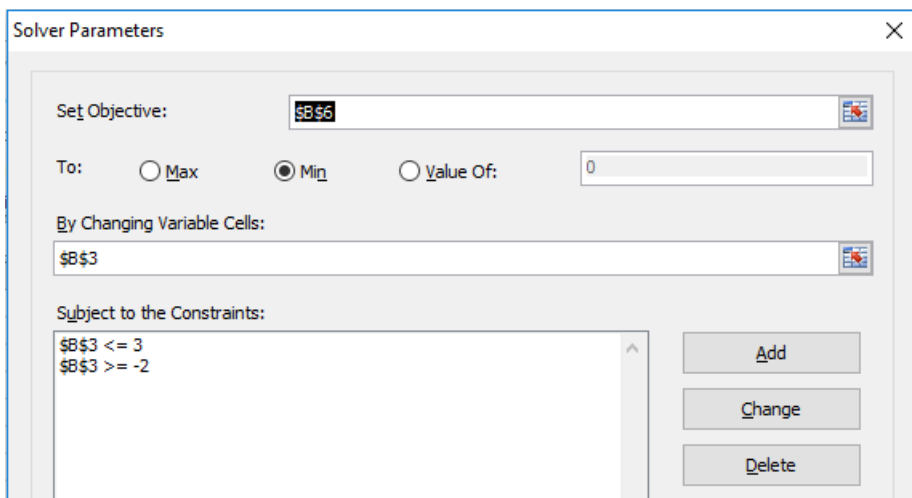


Figure 3.5. The completed Solver dialog box for Example 3-1

The dialog box in Figure 3.5 has been filled as follows:

- Set Objective: **B6** and **Min** have been selected for this option since want the value of the function in cell **B6** is to be minimised
- By Changing Variable Cells: **B3** which is the cell that stores the value of the independent variable  $x$
- Subject to the Constraints: Two constraints have been added that specify the minimum and maximum values of  $x$ , e.g.  $x \geq -2$  and  $x \leq 3$
- Select a Solving Method: The **GRG Nonlinear** method (the default option)

Pressing the “**Solve**” button of the completed parameters box sparks Solver to find the required solution. As shown Figure 3.6, shows, the answer found by Solver, which is  $x = 1, f = -2$ , agrees with the graphical solution shown in Figure 3.4.

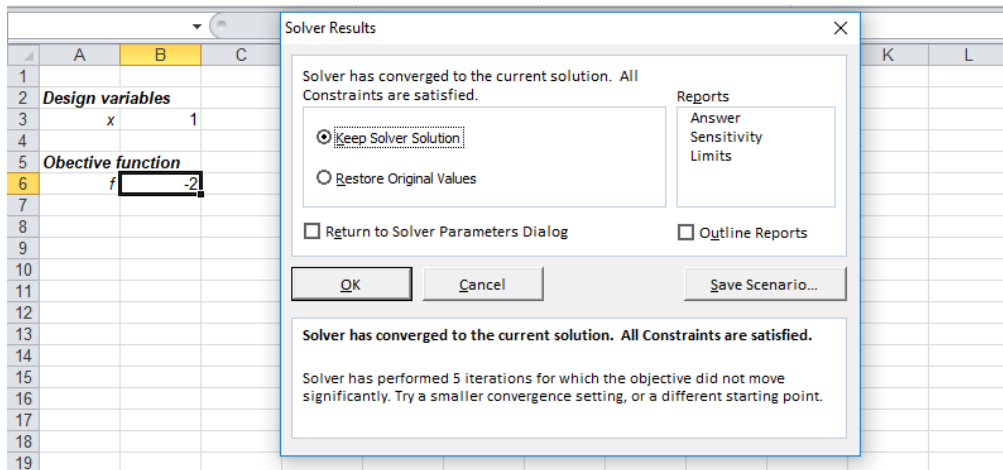


Figure 3.6. Solver solution for Example 3-1

### 3.1.3. The Evolutionary method

When the function to be optimised has more than one point of inflection, the solution found by the **GRG Nonlinear** method may only be a local minimum or maximum. The following example illustrates the capability of the **Evolutionary** method to find the global optimum solution for a simple function.

#### Example 3-2. Finding the global minimum of a function

Determine the global minimum value for the following function:

$$f(x) = x \cos(x) \quad 3 \leq x \leq 14 \quad (3.2)$$

#### Solution

Figure 3.7 shows the Excel sheet developed for solving this example. The insert shows that the function has two minima in the specified range of  $x$ ; one at  $x \approx 5$  and another at  $x \approx 11$ . Let us first try to solve the problem with the **GRG Nonlinear** method. An initial value for  $x$  has been entered in cell **B2** based on which the function  $f$  is calculated in cell **B4**. The formula bar in Figure 3.7 reveals the formula entered in the cell **B4**. Figure 3.8 shows the completed Solver parameters dialog-box with two constraints that specify the upper and lower limits for  $x$ . From Figure 3.9 that shows the solution found by Solver it is clear that it found the local minimum ( $y = -4.81$ ) which is nearer to the initially specified value and not the global minimum.

In order to locate the global minimum by the **GRG Nonlinear** method, the solution has to be started with an initial guess that is closer to the global minimum, e.g.,  $x = 9$ . The advantage of the **Evolutionary** method is that such an arrangement is not required. The set-up shown in Figure 3.8 only needs the solution method to be changed to “**Evolutionary**”. Figure 3.10 that shows the solution obtained by this method confirms that the method produced the global minimum ( $y = -11.041$ ).

# Computer-Aided Thermofluid Analyses Using Excel

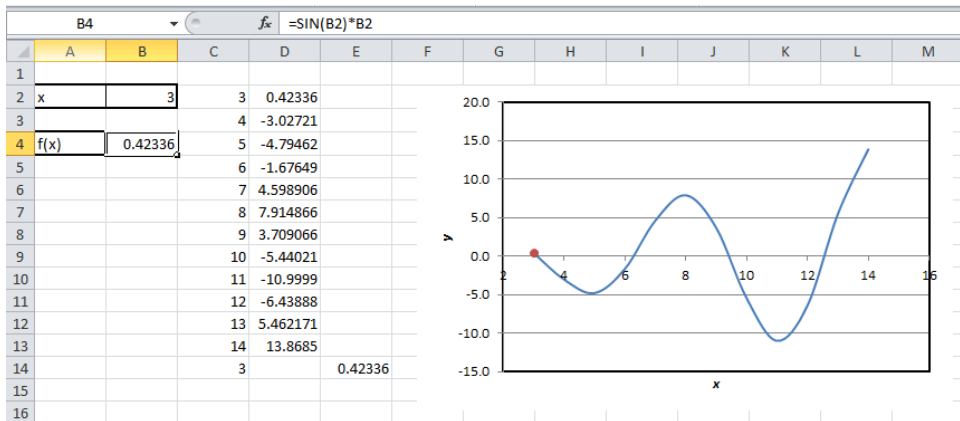


Figure 3.7. The Excel sheet for Example 3-2

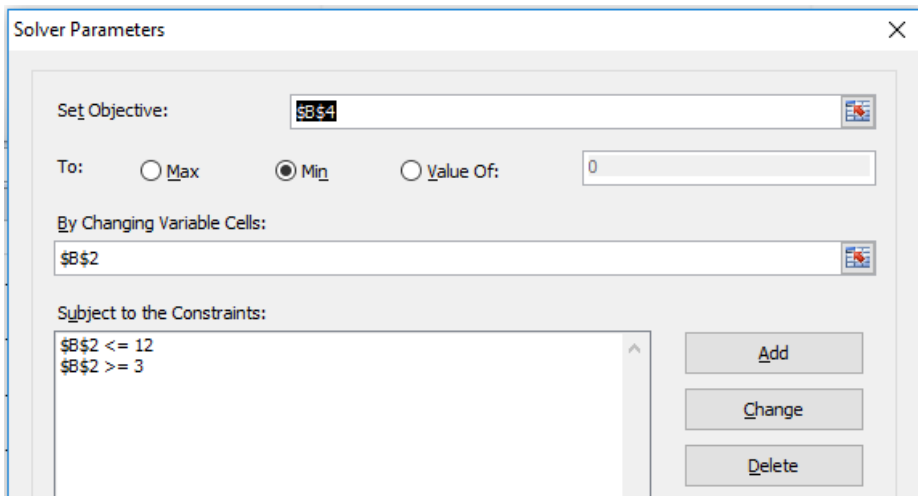


Figure 3.8. Solver set-up for Example 3-2 with GRG Nonlinear method

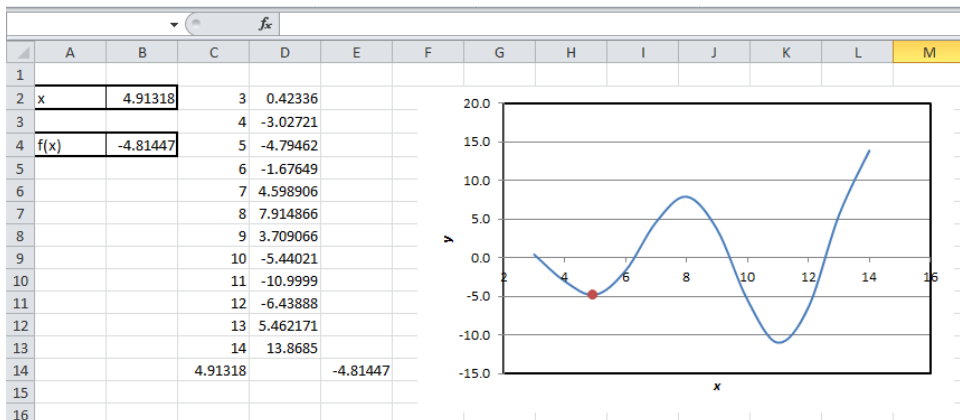


Figure 3.9. Solver solution for Example 3-2 with the GRG Nonlinear method

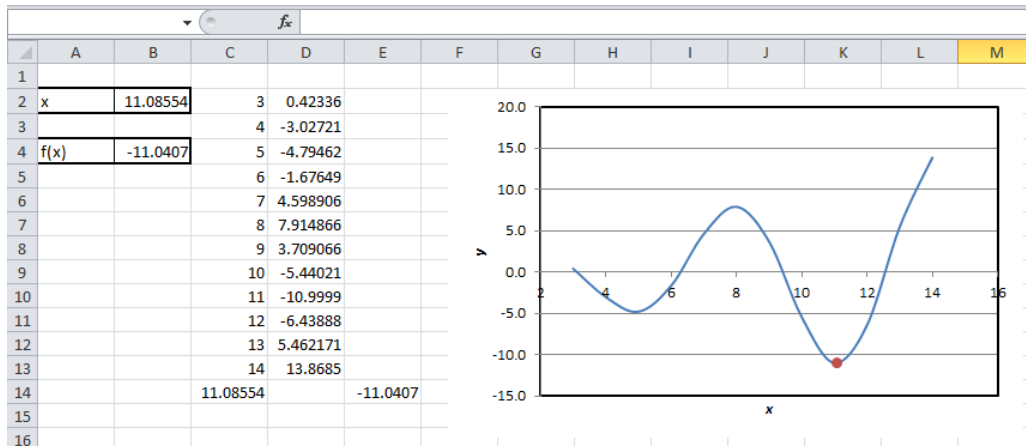


Figure 3.10. Solver solution for Example 3-2 with the Evolutionary method

The **Evolutionary** method is useful for optimisation analyses that involve non-smooth and discontinuous functions, which are difficult to solve with the **GRG Nonlinear** method. However, its disadvantage is that it takes long computer times. While the **GRG Nonlinear** method took less than a second to solve the above problem, the **Evolutionary** method took one minute and 35 seconds.

### 3.1.4. The Simplex LP method

This option provides a method for solving small systems of linear equations that can be used instead of the method described in the Chapter 2 by using Excel’s matrix functions. The method will be illustrated by reconsidering the problem of Example 2-3. Figure 3.11 shows a new Excel sheet for solving the problem with the present method.

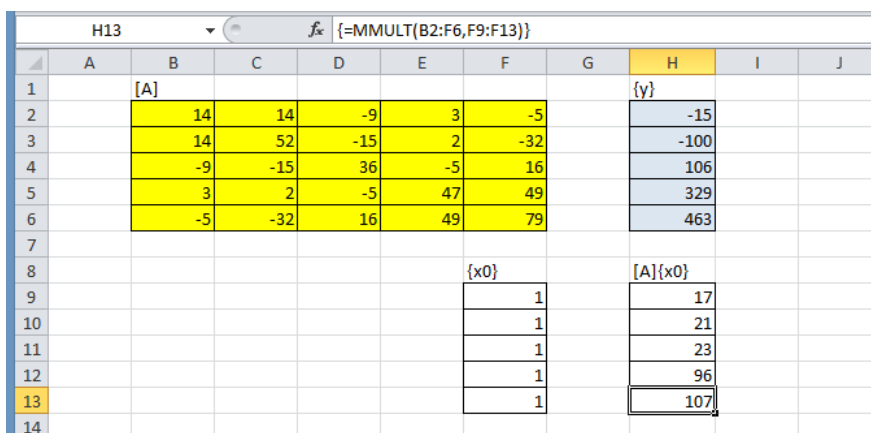


Figure 3.11. Excel sheet for solving Example 2-3 with Solver

The top part of the sheet stores the coefficient matrix [A] and the right-hand vector {y} of the system of linear equations to be solved. The procedure starts with a guessed solution which is stored as vector {x0} in cells F9:F13. All the elements of this vector

are given a value of 1 as shown in Figure 3.11. The coefficient matrix  $[A]$  is then multiplied by the guessed vector  $\{x_0\}$  using Excel's "MMULT" function and the result stored in cells **H9:H13**. If this initial guess is the correct answer, the multiplication  $[A]\{x_0\}$  will be the same as the true right-hand side vector, i.e.:

$$[A]\{x_0\} = \{y\} \quad (3.3)$$

However, Figure 3.11 shows that the vector  $[A]\{x_0\}$  is different from the true right-hand side vector  $\{y\}$  stored in cells **H2:H6**. Solver can now be used to adjust the variable cells **D9:D13** so that all elements of the vector  $[A]\{x_0\}$  become equal to their counterparts in vector  $\{y\}$ , i.e.:

- H9 = H2**
- H10 = H3**
- H11 = H4**
- H12 = H5**
- H13 = H6**

Solver set-up for this task is shown in Figure 3.12.

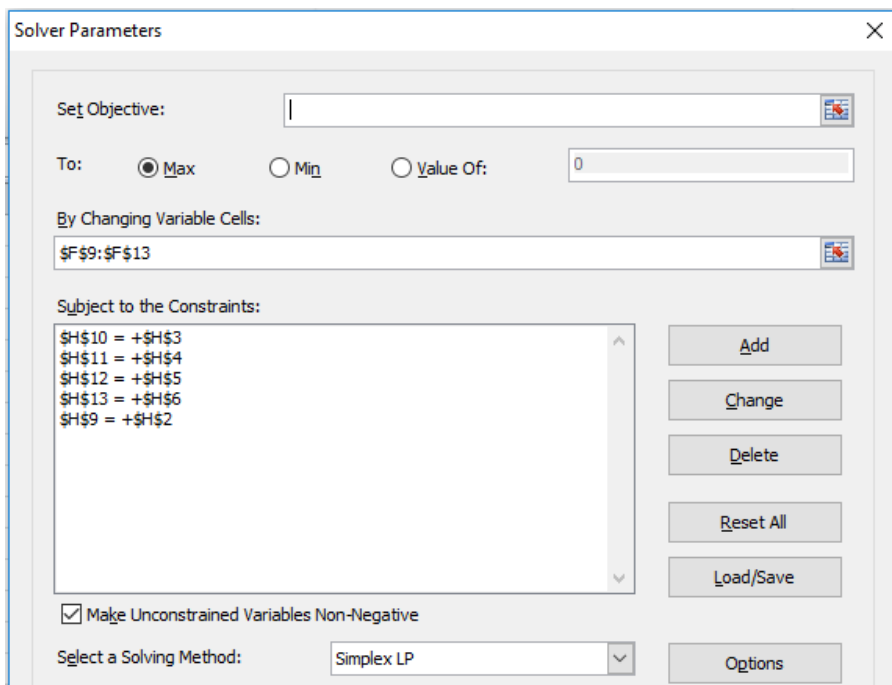


Figure 3.12. Solver set-up for Example 2-3 with the Simplex LP method

Note that the objective cell is left blank and the Simplex LP method is selected as the solution option. In this case, Solver will iterate to find the values of the decision

variables that satisfy all the imposed constraints. The solution found by Solver using the above set-up is shown in Figure 3.13.

	A	B	C	D	E	F	G	H	I	J
1		[A]						{y}		
2		14	14	-9	3	-5		-15		
3		14	52	-15	2	-32		-100		
4		-9	-15	36	-5	16		106		
5		3	2	-5	47	49		329		
6		-5	-32	16	49	79		463		
7										
8						{x0}		[A]{x0}		
9						-6.6E-14		-15		
10						1		-100		
11						2		106		
12						3		329		
13						4		463		
14										

Figure 3.13. Solution of Example 2-3 with the Simplex LP method

All the elements of the  $[A]\{x0\}$  are now equal to their corresponding elements in the vector  $\{y\}$ . The first element of the solution vector, which is  $-6.6 \times 10^{-16}$ , is practically zero. Therefore, the solution is  $[0,1,2,3,4]$ , which is the same as that obtained in Example 2-3 by using the matrix-inversion method. The advantage of Solver compared to the matrix-inversion method is that it can be used for solving systems of nonlinear equations by following a similar procedure (Refer to Problem 3.5 in the Exercises).

### 3.1.5. The default settings of Solver options

Solver gives it user the chance to improve the performance of its three solution methods by allowing alternative options for applying these methods. While some options are common to all three solution methods, others are particular to the **GRG Nonlinear** or the **Evolutionary** method. By clicking the “Options” button in Solver’s parameters dialog box shown in Figure 3.14, the dialog box shown in Figure 3.15 will be shown.

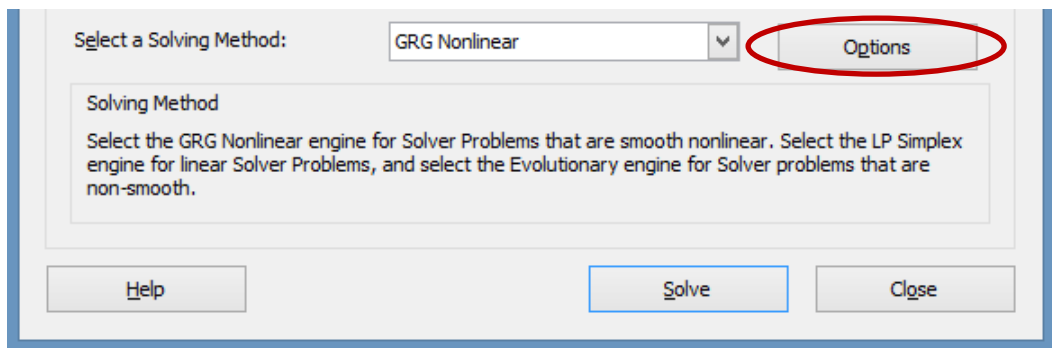


Figure 3.14. Solver options in the Properties dialog box

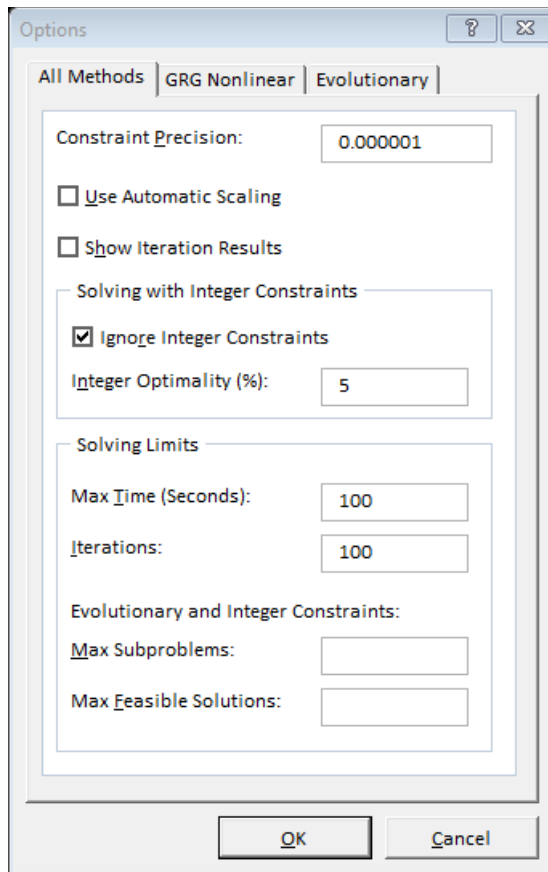


Figure 3.15. Default Solver options adopted in the analyses for all solution methods

Figure 3.15 shows the default settings of the options that are common to all three solution methods. Some of these default settings may have to be changed in order to reduce the computation time or increase the precision of the solution in certain situations. Sometimes, Solver fails altogether to find the solution if the default options are used. For example, certain analyses require the automatic-scaling (AS) option to be used while others require it not to be used. AS enables Solver to handle a poorly-scaled model, i.e. a model in which the values of the objective and constraint functions differ by several orders of magnitude. By using AS, the values of the objective and constraint functions are scaled internally in order to minimise the differences between them.

Figures 3.16.a and 3.16.b show the default settings which are particular to the **GRG Nonlinear** method and to the **Evolutionary** method, respectively. The **GRG Nonlinear** method uses by default the forward difference (FD) approximation of derivatives. Most of the analyses presented in later chapters of the book used the **GRG Nonlinear** method for which the default FD approximation is used.



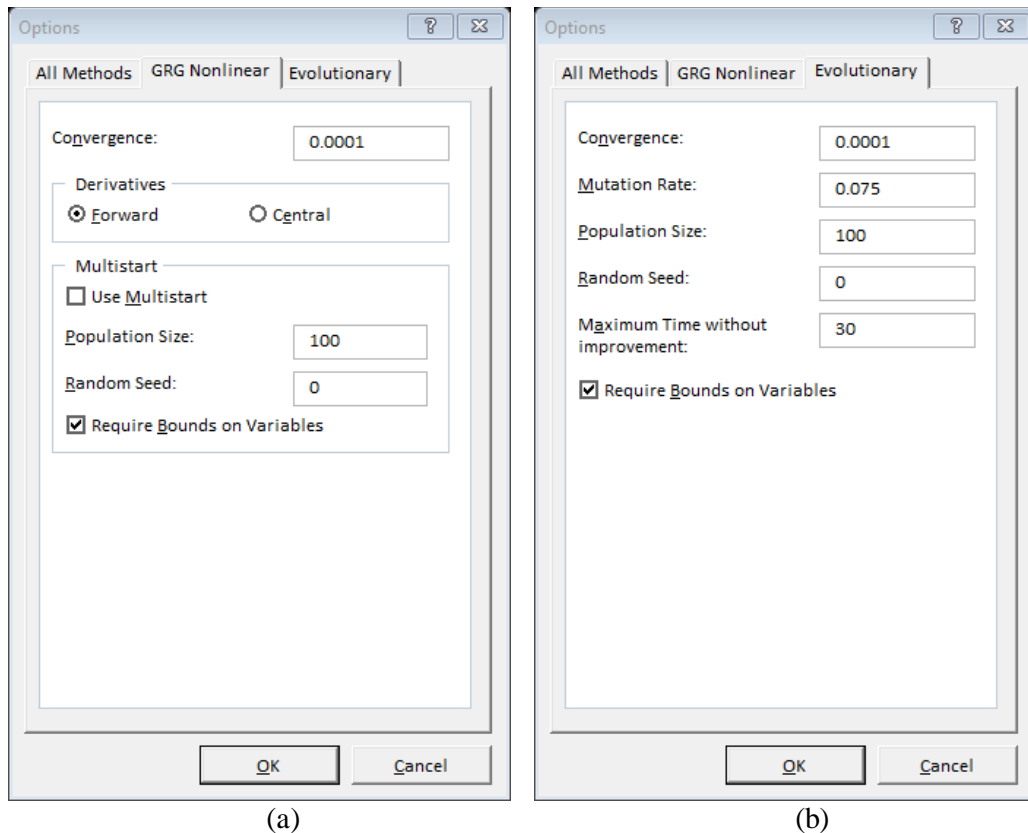


Figure 3.16. The default Solver options specific to: (a) the GRG Nonlinear method and (b) the Evolutionary method

Figure 3.16.b shows the default settings used by the **Evolutionary** method. Note that this method has more adjustable parameters than the **GRG Nonlinear** method. According to the default set-up, the population size is 100 and the maximum allowable time without improvement is 30 seconds. The few cases in this book solved with the **Evolutionary** method show that, with this set-up, the method needs long computer times. Although the time required by the **Evolutionary** method can be reduced by reducing the population size, number of iterations, or the maximum allowable time, the optimisation analyses presented in later chapters do not show a clear advantage to this method over the **GRG Nonlinear** method which is easier to apply.

### 3.2. VBA and the development of user-defined functions

Although Solver and the Goal Seek command enable Excel to deal with a wide range of thermofluid analyses, there are situations where the analytical model requires the development of a customised user-defined function (UDF) that is not provided by Excel. This arises, for example, in thermodynamic analyses that require functions that determine the properties of fluids at various pressures and/or temperatures. This section illustrates the process of activating VBA and using it to develop simple UDFs.

### 3.2.1. Activation of VBA

As shown in Figure 3.17, VBA is found on the left side of the **Developer** tab. This tab gives many other development tools. If the **Developer** tab is not shown in the ribbon of your Excel sheet, then go to **File**, select **Options**, and then select to **Customise Ribbon** from the **Backstage View** shown in Figure 3.18.

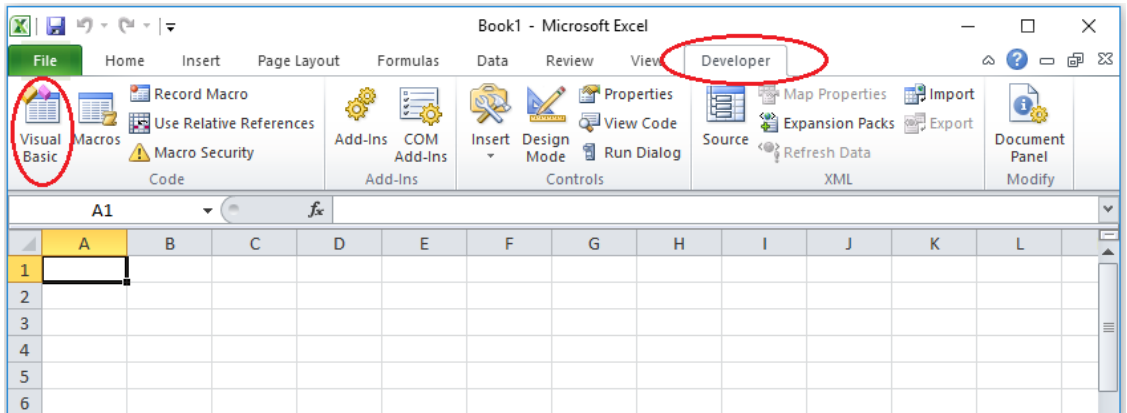


Figure 3.17. Selection of VBA from the Developer tab

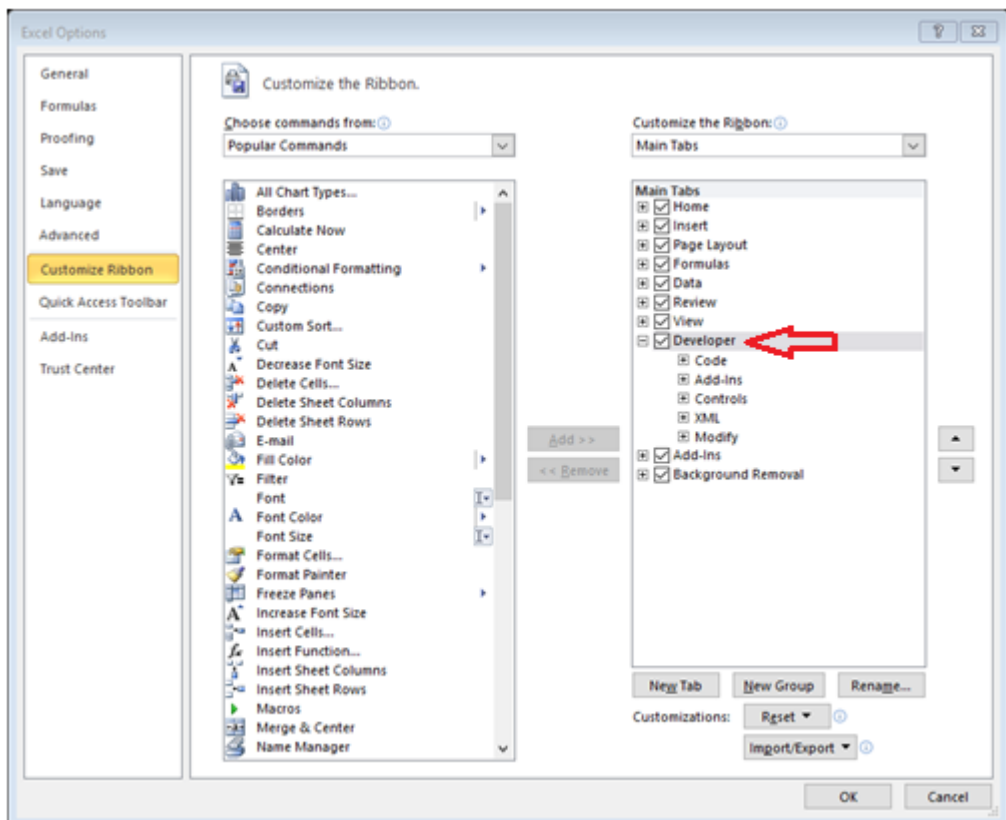


Figure 3.18. Adding VBA to the Developer tab

From the **Main Tabs**, select the **Developer** check box and then click “**OK**”. The **Developer tab** will now be shown in the ribbon of your Excel sheet. To start writing the UDF, go to **Developer** tab menu and select **Visual Basic**. The Visual Basic editor will appear to you as shown in Figure 3.19. Select **Insert** → **Module** and the blank page shown in Figure 3.20 will be open for you to type the VBA code.

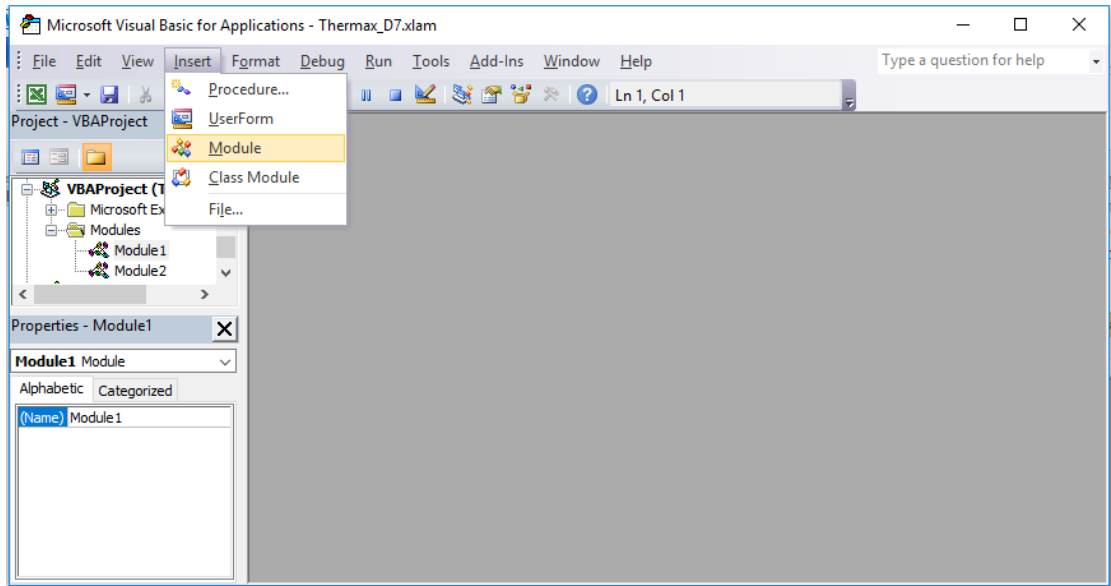


Figure 3.19. Inserting a new module

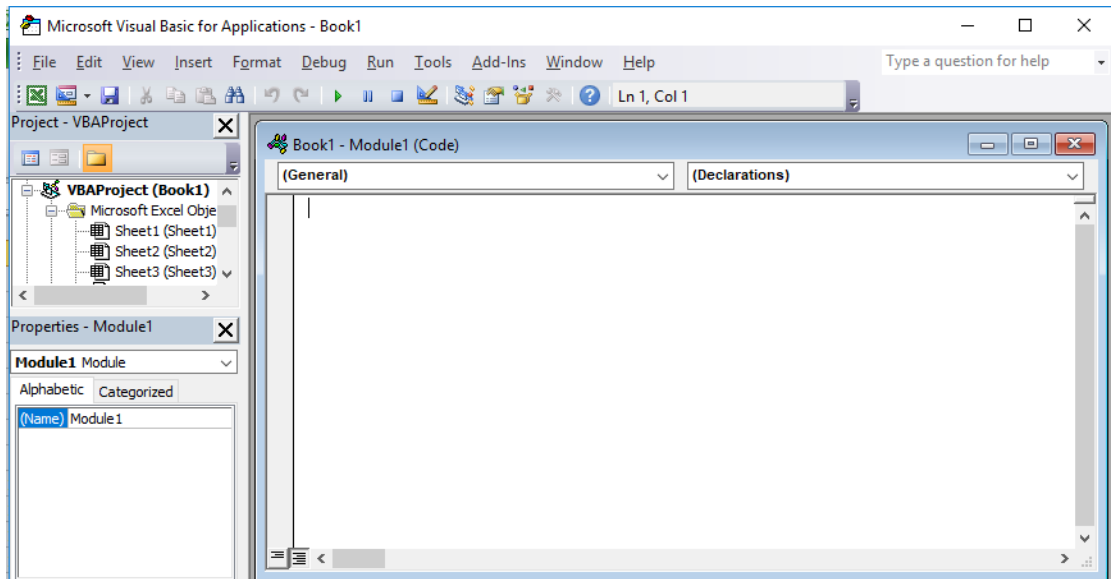


Figure 3.20. A new VBA module

### 3.2.2. Development of UDFs

As a first example let us write a VBA function for determining the area ( $A$ ) of a circle given its diameter ( $D$ ) using the following mathematical equation:

$$A = \pi D^2 / 4 \quad (3.4)$$

The following UDF determines the circle's area according to Equation (3.4):

```
Function Circ_area(Dia)
Pi = 3.141593
Circ_area = Pi * Dia ^2 / 4
End Function
```

Note that the first line in the code starts with the word “**Function**” followed by the name given to the function, which is “**Circ\_area**”. The required input parameters are specified between two brackets after the function name. The present function has only one input parameter, which is the diameter (Dia). As soon as you type the first line of the code and press the “**Enter**” key, the editor will automatically add the **End** line of the function. Now, type the rest of the code as shown in Figure 3.21.

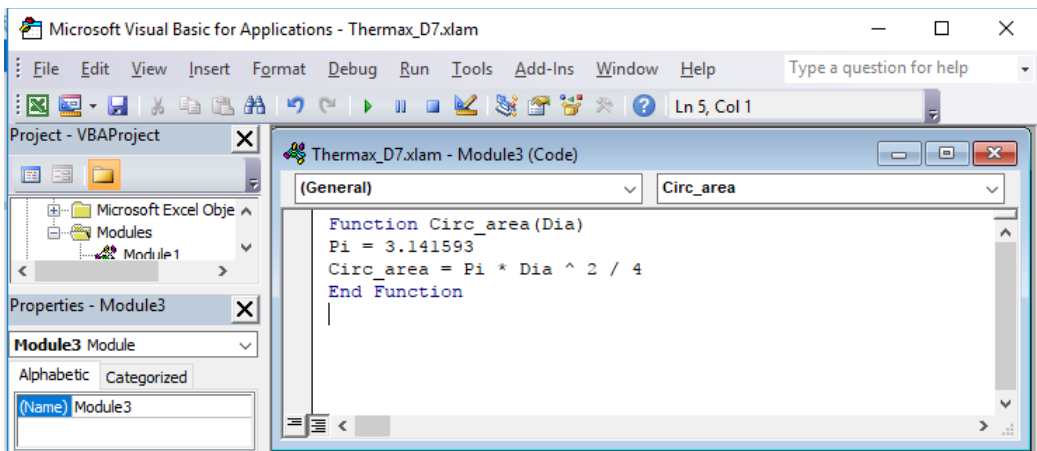


Figure 3.21. A UDF for calculating the area of a circle with a given diameter

After typing the code correctly, the function can be used via Excel UI just like any built-in function as shown in Figure 3.22. Note that the formula bar in Figure 3.22 reveals the formula in cell B2 as:

= **Circ\_area(10)**

Where the number 10 refers to the diameter of the circle, which is the only input to the UDF. You can now check the answer of your user-defined function by calculating the circle's area with a normal Excel formula by typing in any cell “**=pi()\*10^2/4**”.

	A	B	C	D	E	F	G
1							
2		314.1593					
3							
4							
5							
6							
7							

Figure 3.22. Using the “Circ\_area” function in Excel

For thermodynamic analyses, VBA is useful for developing UDFs for fluid properties. As an example, let us develop a UDF that determines the molar specific-heat at constant pressure ( $\tilde{c}_p$ ) for air. For an ideal gas,  $\tilde{c}_p$  is given by the following polynomial [6]:

$$\tilde{c}_p = a_0 + a_1T + a_2T^2 + a_3T^3 \quad [\text{kJ/kmol.K}] \quad (3.5)$$

Where  $T$  is the absolute temperature and  $a_0$ ,  $a_1$ ,  $a_2$ , and  $a_3$  are constants that have different values for different gases. For air, the constants' values are 28.11,  $0.1967 \times 10^{-2}$ ,  $0.4802 \times 10^{-5}$ , and  $-1.966 \times 10^{-9}$  in this order.

The following VBA function, called “cp\_air”, determines  $\tilde{c}_p$  for air based on Equation (3.5). The only input for the function is the absolute temperature (TempK).

```
Function cp_air(TempK)
a0 = 28.11
a1 = 0.00196
a2 = 0.000004802
a3 = -0.000000001966
M = 28.97
cpbar = a0 + a1 * TempK + a2 * TempK ^ 2 + a3 * TempK ^ 3
cp_air = cpbar / M
End Function
```

Figure 3.23 shows the VBA function and the formula bar in Figure 3.24 shows how the function can be used in an Excel formula to determine  $\tilde{c}_p$  for air at 300K. The value returned by the function is 29.0771 kJ/kmol.K. By making suitable extensions, the function can easily be used to determine the values of  $\tilde{c}_p$  for other ideal gases in addition to air (Refer to Exercise 3.8). The various functions provided by Thermax for the thermo-physical properties of water, refrigerants, etc., have been developed by writing similar functions with VBA.

## Computer-Aided Thermofluid Analyses Using Excel

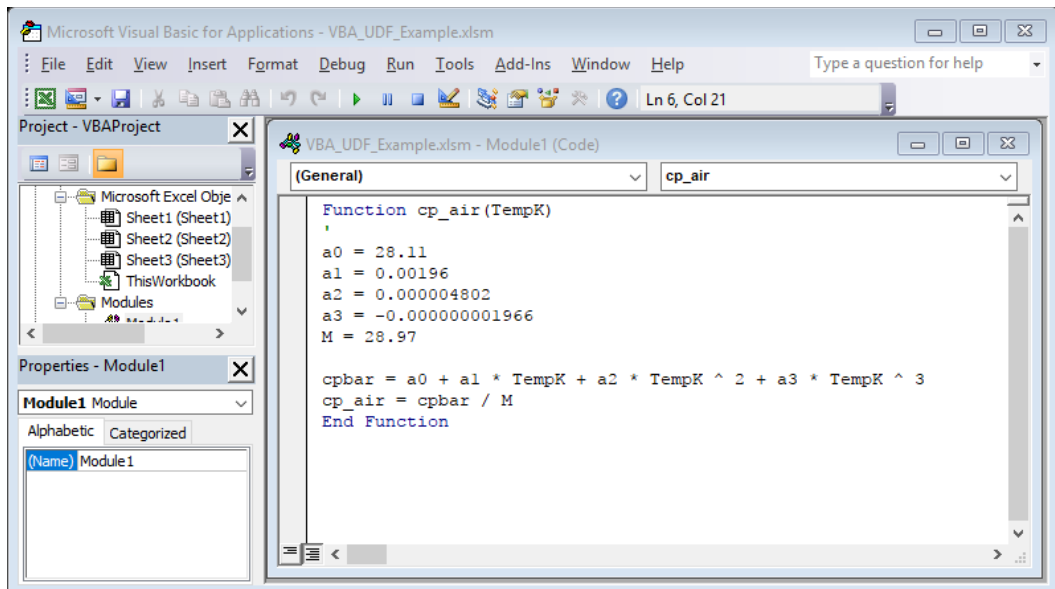


Figure 3.23. A UDF for calculating the molar specific-heat for air

The screenshot shows an Excel spreadsheet with the formula bar displaying  $f_x = =cp\_air(300)$ . The spreadsheet grid shows the following data:

	A	B	C	D	E	F	G
1							
2		29.0771					
3							
4							
5							
6							
7							

Figure 3.24. Using the cp\_air function in Excel

In writing the UDF for the circle's diameter shown in Figure 3.21 we assigned a value for the constant  $\pi$  because VBA does not provide a built-in function for it like Excel. However, this is not necessary since it is possible to use the built-in functions **PI** provided by Excel within the VBA function. This is very useful when built-in functions, like MIN and MAX, can be used to minimise the programming effort needed for developing the required UDF. More information about this and other features of the VBA language can be found in specialised references [7-9].

### 3.3. Thermax installation and use

By providing custom functions for fluid properties, Thermax enables Excel to be used as an educational platform for a wide range of thermofluid analyses [10]. Before Thermax can be recognised by Excel you have to install it in your computer. To do that, open the **Thermax.xla** file and then save it as an "Excel Add-in". Recent Excel versions locate all add-ins in a certain folder in the computer and automatically direct

you to that location when you want to save a new add-in. Save the Thermax add-in in the specified location and **restart** Excel in order to activate it. Open a new Excel sheet and then do the following:

1. Go to **File** and then click **Options**.
2. Select **Add-Ins**. From the **Manage** ribbon at the bottom of the menu select **Excel Add-ins** and then press **Go**. The pull-down menu shown in Figure 3.25 will appear to you.
3. To add **Thermax** to the add-ins menu, tick (✓) the corresponding box.
4. If for any reason you saved the add-in in a location that is different from the default folder, then click on **Browse** and search for it in the destination folder and select it.

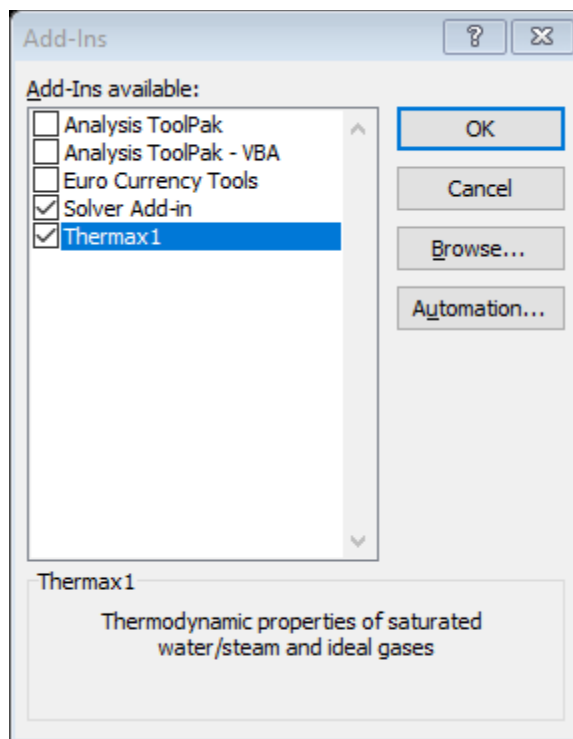


Figure 3.25. Adding Thermax to the menu of Excel add-ins

Once installed, Thermax functions can be used in Excel's formulae just like the built-in functions. For illustration, let us start a formula by entering the equal sign (=) in any cell (say cell B2). If you now press the *fx* button in the formula ribbon, the **Function Wizard** shown in Figure 3.26 will be shown. The Function Wizard first lists the various categories of built-in functions provided by Excel. Scroll down the list of function categories and select the **User-defined** functions. Then, all the functions provided by Thermax will be listed alphabetically as shown in Figure 3.27.

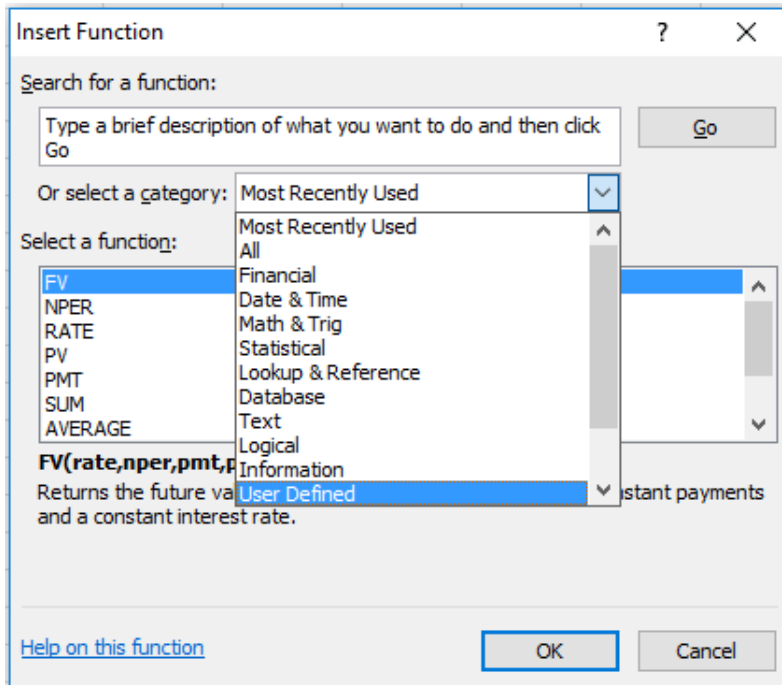


Figure 3.26. Finding the add-in user-defined functions in the Function Wizard

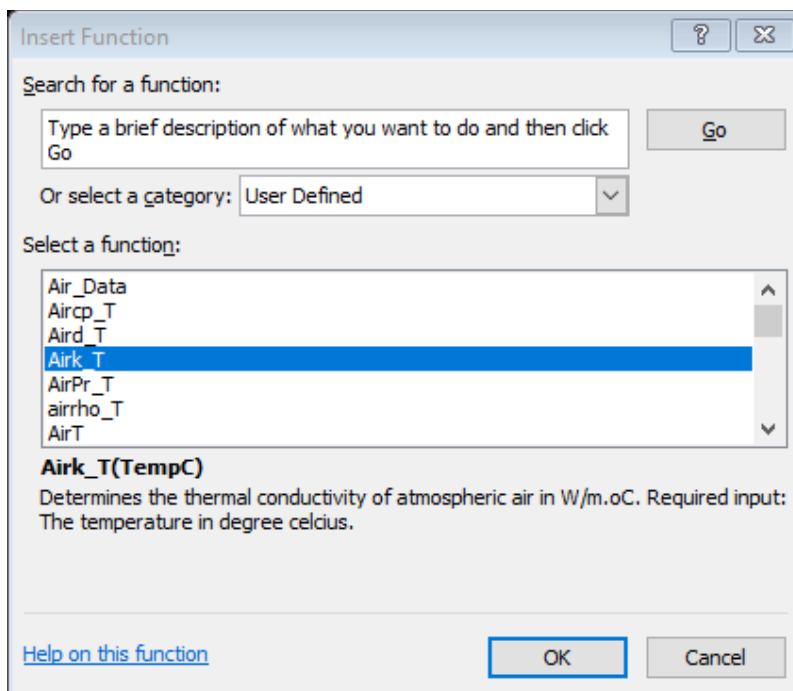


Figure 3.27. Thermax functions listed alphabetically in the User Defined category



The first function in the list, **Air\_Data**, is the auxiliary function that stores the data for the thermo-physical properties of air at standard atmospheric pressure. This function is called by other functions in the same to obtain the values of these properties at the required temperature.

To start using the add-in functions, scroll down the list and select the function **Airk\_T** that determines the thermal conductivity ( $k$ ) of air at a given temperature. Upon pressing the **OK** button, the **Function Arguments** box shown in Figure 3.28 will be shown.

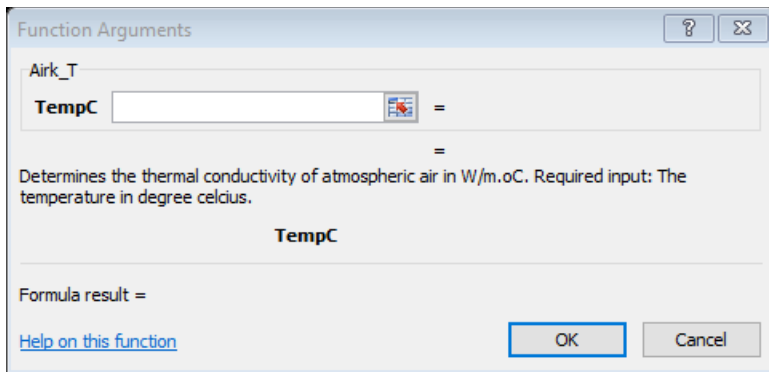


Figure 3.28. The Function Arguments box for the “Airk\_T” function

Figure 3.28 shows that this function has one input parameter, which is the temperature in °C “TempC”, and gives a brief description of its intended use. Let us use the function to determine the thermal conductivity for air at 25°C. Fill the form by entering the value of the temperature, 25, as shown in Figure 3.29.

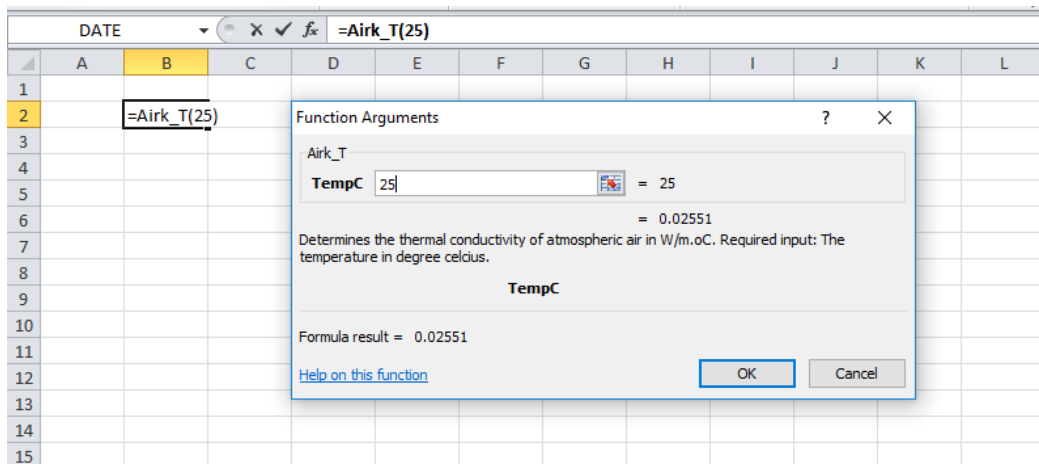


Figure 3.29. Using the function “Airk\_T” to determine the thermal conductivity of atmospheric air at 25°C

Note that the formula ribbon now shows the formula in cell **B2**, which is “=Airk\_T(25)”. The form also shows the calculated value of  $k$ , which is 0.02551 W/m.°C. When you press the “OK” button, this value will appear in the cell **B2**. You can check this value with that given in Table A.1 and try other Thermax functions.

In certain situations the confinement of Excel’s formula to one cell becomes too restrictive for developing the analytical model. This situation arises, for example, when an iterative process involves a non-linear equation such as the Colebrook-White equation or the Soave-Redlich-Kwong equation of state. In this case, a UDF is needed solve the nonlinear equation and return the result to Excel’s formula like any built-in function. For such a case, Thermax provides a Newton-Raphson solver for nonlinear equations in addition to its property functions. Appendix B shows how to use this tool. Appendix B also describes two interpolation functions provided by Thermax for tabulated data which are useful for including additional fluid properties or other tabulated data needed in a thermofluid analysis.

### 3.4. Closure

This chapter introduced the three auxiliary components of the Excel-based modelling platform, Solver, VBA, and Thermax, that make it an effective platform for thermofluid analyses. The chapter gave Examples of using the three solution methods provided by Solver to deal with different types of problems. It also showed how VBA can be used for developing user-defined functions not provided by Excel and explained the procedure for installing Thermax and using its functions in Excel formulae. Appendix B demonstrates the use of the Newton-Raphson solver provided by Thermax for solving nonlinear equations and its two interpolation functions for tabulated data.

### References

- [1] Frontline Systems, internet: <http://www.Solver.com/> (Last accessed November 23, 2015).
- [2] L.S. Lasdon, R.L. Fox, M.W. Ratner, Nonlinear optimization using the generalized reduced gradient method, *Revue Française d'Automatique, Informatique et Recherche Opérationnelle*, tome 8, V3 (1974), p. 73-103. Available at: [http://www.numdam.org/article/RO\\_1974\\_\\_8\\_3\\_73\\_0.pdf](http://www.numdam.org/article/RO_1974__8_3_73_0.pdf)
- [3] Wikipedia, [https://en.wikipedia.org/wiki/Gradient\\_method](https://en.wikipedia.org/wiki/Gradient_method)
- [4] [https://en.wikipedia.org/wiki/Evolutionary\\_algorithm](https://en.wikipedia.org/wiki/Evolutionary_algorithm)
- [5] Wikipedia, [https://en.wikipedia.org/wiki/Evolutionary\\_algorithm](https://en.wikipedia.org/wiki/Evolutionary_algorithm)
- [6] Y. A. Cengel and M. A. Boles. *Thermodynamics an Engineering Approach*, McGraw-Hill, 7<sup>th</sup> Edition, 2007
- [7] J. Walkenbach, *Excel 2013 Power Programming with VBA*, Wiley Publishing, Inc. 2013.
- [8] J. L. Latham, *Programming in Microsoft Excel VBA, An Introduction*, 2008. Internet: <http://ies.fsv.cuni.cz/default/file/download/id/21101> (Last accessed November 29, 2015).
- [9] <http://www.fontstuff.com/vba/vbatut01.htm> (Last accessed November 26, 2017).

- [10] Thermax: An Excel add-in for Thermofluid Analyses. Available at: <https://www.mendeley.com/library/fileproxy?id=04a975bf-59cf-cde5-7abe54d5b118d1e6>
- [11] S.C. Chapra and R.P. Canale, Numerical Methods for Engineers, 6<sup>th</sup> Edition, McGraw Hill, 2010.

### Exercises

1. A system of algebraic equations can be expressed in matrix form as follows:

$$\begin{bmatrix} 70 & 1 & 0 \\ 60 & -1 & 1 \\ 40 & 0 & -1 \end{bmatrix} \begin{Bmatrix} a \\ b \\ c \end{Bmatrix} = \begin{Bmatrix} 636 \\ 518 \\ 307 \end{Bmatrix}$$

Solve the system of equations by using Solver to determine the values of the three unknowns  $a$ ,  $b$ , and  $c$ . This exercise is based on Example 9.11 in Chapra and Canale [11]. The answer is:  $a = 8.5941$ ,  $b = 34.4118$ , and  $c = 36.7647$ .

2. Draw a line chart with Excel to show the variation of the following function in the range  $0 \leq x \leq 4$ :

$$f(x) = 2 \sin x - x^2/10$$

Use Solver to find the maximum of the function in the same range. Based on Example 13.1 in Chapra and Canale [11]. The answer is:  $f(x) = 1.7757$  at  $x = 1.4276$ .

3. The curve shown in Figure 3.P3 is a plot of the function:

$$f = e^{\theta} \sin(2\theta)$$

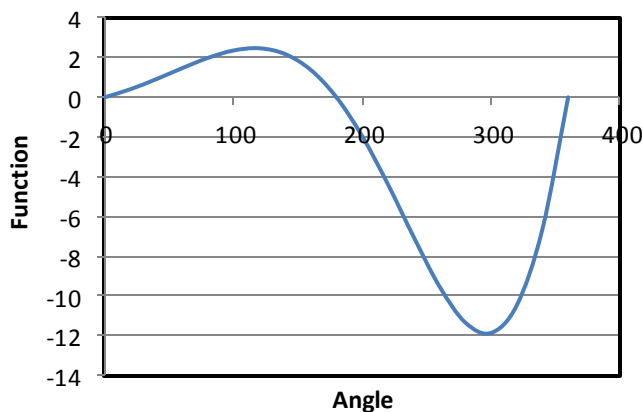


Figure 3.P3 A composite function

## Computer-Aided Thermofluid Analyses Using Excel

Use Solver to find:

- a) The minimum value of the function and the corresponding angle
  - b) The maximum value of the function and the corresponding angle
  - c) The angle at which value of the function equals 4.0
4. Using the Excel sheet developed to solve Example 3-1 by the GRG Nonlinear method, study the effect of using central-difference approximation of derivatives instead of the default forward-difference approximation on the solution.
5. Consider the following set of simultaneous nonlinear equations:

$$x^2 + xy = 10 \quad (\text{A})$$

$$y + 3xy^2 = 57 \quad (\text{B})$$

To solve the system with Solver, rearrange the equations as follows:

$$u(x, y) = x^2 + xy - 10 = 0 \quad (\text{C})$$

$$v(x, y) = y + 3xy^2 - 57 = 0 \quad (\text{D})$$

Create two cells (**B1** and **B2**) to hold initial guesses for  $x$  and  $y$ . Enter the function values themselves,  $u(x, y)$  and  $v(x, y)$  into two other cells (**B3** and **B4**). The initial guesses may result in function values of  $u$  and  $v$  that are far from zero. Determine the sum of the function squares, i.e.  $u^2 + v^2$ , and store it in cell **B5**.

Use Solver to find the values of  $x$  and  $y$  in cells **B1** and **B2** (the Changing cells) that make the value in cell **B5** (the objective cell) equal to zero. Using this procedure, find the roots of the above system starting with initial guesses of  $x = 1$  and  $y = 3.5$ .

This exercise is based on Example 7.5 in Chapra and Canale [11]. The correct pair of roots are  $x=2$  and  $y=3$ .

6. The volume  $V$  of liquid in a spherical tank of radius  $r$  is related to the depth  $h$  of the liquid by:

$$V = \pi h^2(3r - h)/3$$

Using VBA, develop a user-defined function that determines  $h$  at any given values of  $r$  [m] and  $V$  [m<sup>3</sup>]. Check your function with  $r=1$  m and  $V = 0.5$  m<sup>3</sup>. Answer:  $h = 0.431$  m.

7. Extend the UDF developed in Section 3.2 for determining the specific heat for air so that it can be used for other ideal gases as well. Note that in this case, the function will have two input parameter: the name of the gas and the temperature.
8. Using suitable formulae for the thermodynamic properties of superheated steam, develop user-defined functions with VBA for determining the specific enthalpy and entropy of superheated steam from its pressure and temperature.
9. Using suitable formulae for the thermodynamic properties of superheated refrigerant R134a, develop user-defined functions with VBA for determining properties, e.g., enthalpy and entropy, of superheated R134a from its temperature and pressure.

# 4

## **Iterative solutions**

The need for computer-aided iterative solutions is common to all three types of thermofluid analyses and arises for a number of reasons. This chapter gives examples of such analyses and shows how they can be handled by using the two iterative tools provided by Excel; the Goal Seek command and Solver. While the Goal Seek command can be used for the simplest type of iterative solutions that involve a single parameter, Solver is needed for those involving multiple variables and requiring certain constraints to be satisfied by the iterative solution. When the analytical model involves a nonlinear equation, such as the Colebrook-White equation, it becomes difficult to use only Goal Seek and Solver. For such problems, the chapter shows how the Newton-Raphson solver provided by Thermax can be used to deal with the nonlinear equation, leaving the main iteration to Goal Seek or Solver.

#### **4.1. Iterative solutions by using Goal Seek**

Most thermofluid problems that require iterative solutions can be solved by using the Goal Seek command. This section presents three examples that demonstrate its use for typical analyses that require iterative solutions in fluid-dynamics, thermodynamics, and heat-transfer.

##### **4.1.1. Type-2 and type-3 pipe-flow analyses**

The frictional head loss ( $h_f$ ) in a pipe depends on a number of factors that characterise the pipe itself as well as the fluid being transported. For a straight pipe with no fittings carrying a viscous Newtonian and incompressible fluid, the frictional head loss is determined by the following Darcy-Weisbach equation:

$$h_f = f \frac{L V^2}{D 2g} \quad (4.1)$$

Where  $f$  is the Darcy friction factor,  $L$  the length of the pipe,  $D$  its diameter,  $V$  the fluid velocity, and  $g$  the gravity acceleration constant. The friction factor can be obtained from Equation (1.22) if the flow is laminar and from Equation (1.24) or (1.25) if it is turbulent. Practical pipe-flow problems that involve Equation (4.1) can be divided into three types [1]:

1. Type-1 problems – require the determination of  $h_f$  when both the pipe's diameter and fluid velocity (or flow rate) are known.
2. Type-2 problems – require the flow rate to be determined for a specified  $h_f$  and pipe diameter.
3. Type-3 problems – require the pipe diameter to be determined for a given  $h_f$  and flow rate.

Type-1 problems can be solved in a straight-forward manner by using Equation (4.1) to determine the friction head loss. However, both type-2 and type-3 problems require iterative solutions because the Reynolds number and, therefore, the friction factor,  $f$ ,

cannot be determined without knowing  $D$  or  $V$ . For type-2 problems (i.e. unknown flow rate), the iterative procedure can be avoided by using extended Moody diagrams that require the determination of the following dimensionless parameter [2]:

$$\text{Re } f^{0.5} = \frac{D^{1.5}}{\nu} \left( \frac{2gh_f}{L} \right)^{0.5} \quad (4.2)$$

Apart from the inaccuracy of visual chart interpolation, the procedure is difficult to adopt in optimisation or parametric analyses. By using the Goal Seek command, both type-2 and type-3 problems can be solved more accurately. The following example, which is based on Example 8.4 in Cengel and Cimbala [1], shows how Goal Seek can be used to solve a type-3 problem.

#### Example 4-1. Solution of type-3 pipe flow problems

Heated air at 1 atm and 35°C is to be transported in a 150-m-long circular plastic duct ( $\epsilon=0.045$  mm) as shown in Figure 4.1 at a rate,  $Q$ , of 0.35 m<sup>3</sup>/s. If the head loss in the duct is not to exceed 20 m, determine the smallest required diameter for the duct.

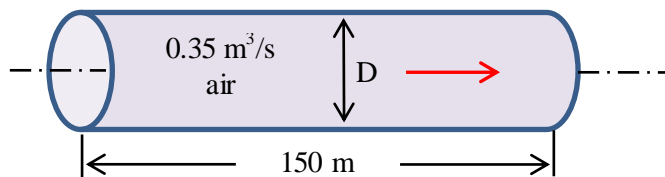


Figure 4.1. Schematic for Example 4-1 (adapted from Cengel and Cimbala [1])

#### Solution with Goal Seek

The problem can be solved by calculating the friction head loss at different diameters of the duct and then selecting the diameter that gives the required head loss which is 20 m. The iterative solution proceeds as follows:

1. Select a diameter for the inner pipe ( $D$ )
2. Calculate the velocity of the hot air ( $V$ ),  $V=Q/A$ ,  $A=\pi D^2/4$
3. Calculate the Reynolds number in the pipe ( $\text{Re}$ ),  $\text{Re}=VD/\nu$
4. Calculate the friction factor ( $f$ ) using Equation (1.22) or (1.24)
5. Calculate the friction head loss ( $h_f$ ) from Equation (4.1)
6. If  $h_f \neq 20$  m, repeat steps 1 to 5

Figure 4.2 shows the Excel sheet developed for this example which is divided into three parts: (i) problem data (ii) calculations, and (iii) results. The data part shows the information given in the question. The value of the kinematic viscosity of air at 35°C ( $\nu = 1.655 \times 10^{-5}$  m<sup>2</sup>/s) was obtained from Cengel and Cimbala [1] and fixed throughout the



calculations. Cell-labelling is applied in the formulae and Figure 4.2 reveals the formulae used in each cell of the calculations part. Note the If-function in cell **F10**.

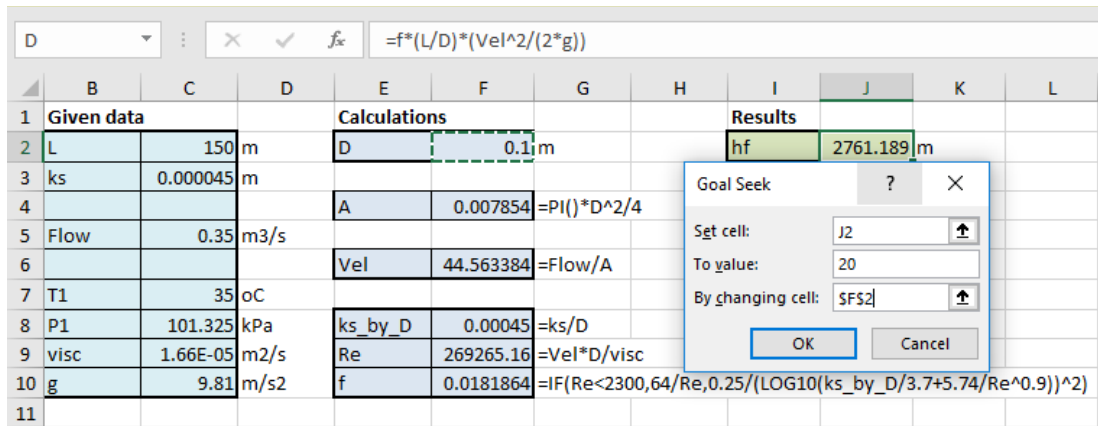


Figure 4.2. Excel sheet and Goal Seek set-up for Example 4-1

As Figure 4.2 shows, for an assumed duct diameter of 0.1 m the friction head loss exceeds 2761 m. Figure 4.2 also shows the completed Goal Seek dialog box that requires Goal Seek to change the diameter in cell **F2** and iterate until the friction head loss in cell **J2** attains the required value of 20 m. Figure 4.3 shows the answer found by Goal Seek, which is  $D \geq 0.27$  m. This answer agrees with that given by Cengel and Cimbala [1]. A similar procedure can be used to solve type-2 flow problems by iterating over the flow rate instead of the diameter.

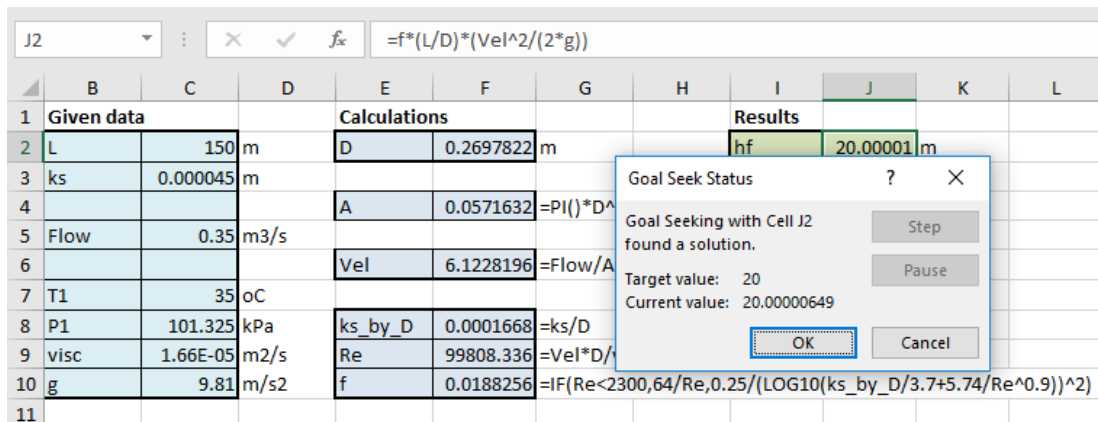


Figure 4.3. Goal Seek solution for Example 4-1

#### 4.1.2. Thermodynamic analyses involving ideal-gas mixtures

Without the usual simplifications and idealisations applied in thermodynamic analyses most of these analyses, if not all, would require iterative solutions. A commonly used thermodynamic approximation is treating air as a pure gas even though it is known to be a mixture of nitrogen, oxygen, and water vapour with small traces of other gases.

Computer-aided analyses with fluid property functions such as those provided by Thermax enable more realistic models to be used by treating air as a mixture of gases instead of a single gas. However, if the temperature of the gas mixture is not known but has to be determined, an iterative solution will be required by this model. The following example shows how the problem can be solved by using Goal Seek.

**Example 4-2. Constant-pressure expansion of air**

Figure 4.4 shows a piston-cylinder device that initially contains a mixture of 21% oxygen and 79% nitrogen by volume. Initially at 100 kPa, 330K, the gas mixture occupies 0.1 m<sup>3</sup>. Fifty kJ of heat is then transferred to the gas causing it to expand at constant pressure. Treating oxygen and nitrogen as ideal gases, determine the final temperature of the gas inside the cylinder.

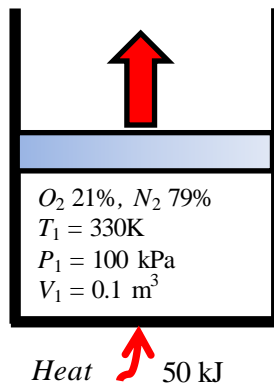


Figure 4.4. Schematic diagram for Example 4-2

**The analytical model**

The solution procedure applies the first-law of thermodynamics to the expansion process. For a mixture of  $O_2$  and  $N_2$ , the first law reads:

$$Q = m_{O_2}(h_{2_{O_2}} - h_{1_{O_2}}) + m_{N_2}(h_{2_{N_2}} - h_{1_{N_2}}) \tag{4.3}$$

Where  $Q$  is the amount of heat added,  $m_{O_2}$  and  $m_{N_2}$  are the masses of oxygen and nitrogen in the device,  $h_{1_{O_2}}$  and  $h_{2_{O_2}}$  are enthalpies of oxygen at the initial and final temperatures, respectively, and  $h_{1_{N_2}}$  and  $h_{2_{N_2}}$  are the corresponding enthalpies for nitrogen. The correct value of the final temperature is that at which the amount of heat added as obtained from Equation (4.3) is equal to the given value, which is 50 kJ.

The values of enthalpy for  $O_2$  and  $N_2$  in Equation (4.3) can be determined by using the relevant Thermax function for ideal gases, **Gash\_TK**, and the masses  $m_{O_2}$  and  $m_{N_2}$  can be obtained from the ideal-gas law using the corresponding partial pressures as follows:

$$m_{O_2} = \frac{(0.21P_1)V_1}{R_{O_2}T_1} \quad (4.4)$$

$$m_{N_2} = \frac{(0.79P_1)V_1}{R_{N_2}T_1} \quad (4.5)$$

Where  $R_{O_2}$  and  $R_{N_2}$  are the gas constants for oxygen and nitrogen, which are 0.2598 kJ/kg.K and 0.2968 kJ/kg.K, respectively.

### Solution with Goal Seek

Figure 4.5 shows the Excel sheet developed for this example. The data part includes the initial pressure, temperature, and volume of the gas mixture together with the mole fractions and gas constants of oxygen and nitrogen. The initial partial pressures of oxygen and nitrogen, P1\_O2 and P1\_N2, are calculated from the total initial pressure (P\_1) and the respective volume fractions, y\_O2 and y\_N2, as shown in cells E2 and E3, respectively. The masses of the two gases in the mixture (m\_O2 and m\_N2) are calculated in cells E5 and E6, respectively, and the total mass (m\_total) in cell E8.

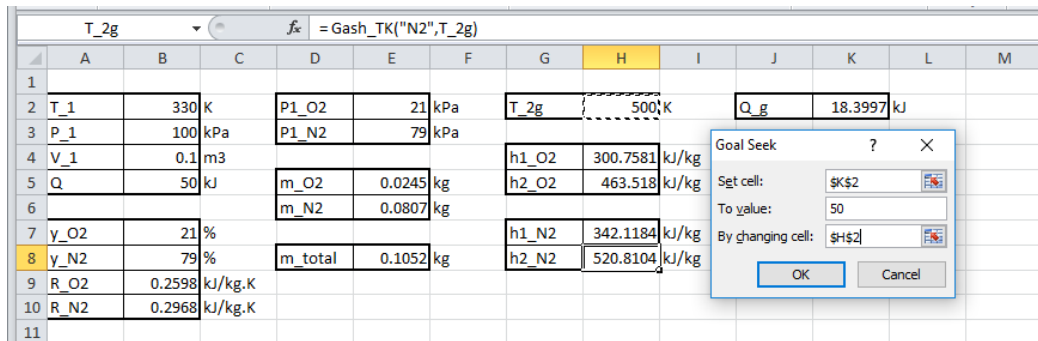


Figure 4.5. The Excel sheet developed for Example 4-2 by using Thermax functions

Starting with a guessed value for the final temperature,  $T_{2g}$ , which is 500K, the initial and final enthalpies of oxygen and nitrogen are determined by using Thermax function **Gash\_TK** at the corresponding temperatures. Equation (4.3) is then used to determine the total amount heat added in the process ( $Q_g$ ). With the guessed final temperature, Equation (4.3) determined the total amount of heat as 18.4 kJ, which is less than the actual values of 50 kJ. To find the appropriate final temperature, the guessed temperature  $T_{2g}$  has to be adjusted by Goal Seek so that the value of  $Q_{2g}$  equals 50 kJ. Figure 4.5 shows the required Goal Seek set-up and Figure 4.6 shows the solution obtained by Goal Seek, which is 780.444K. The value determined for  $T_2$  by treating air as a single pure gas and using the approximate constant specific-heat method ( $c_p = 1.005$  kJ/kg) is 801.2K, which is significantly different, but the value determined by using the exact method is 781.6K. Although these results confirm the accuracy of treating air as a single pure gas with the exact method of analysis, the deviation from the present model is expected to increase as  $T_2$  increases.

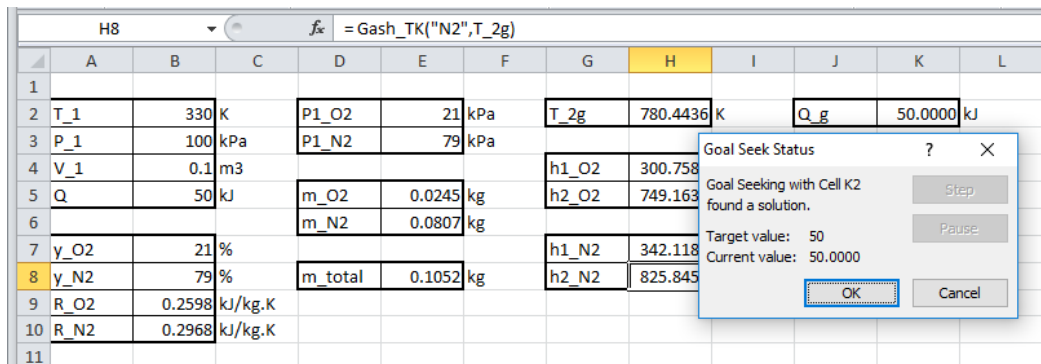


Figure 4.6. Goal Seek solution for Exampe 4.2 by using Thermax functions

### 4.1.3. Convection heat-transfer analyses

Like the friction factor ( $f$ ) in pipe-flow analyses, the convection heat-transfer coefficient ( $h$ ) is not constant but depends on the flow itself. Therefore, convection heat-transfer analyses frequently involve iterative solutions. The following example shows how Excel's Goal Seek command can be used for such analyses. The example is based on Example 10.1 in Holman [3].

#### Example 4-3. Overall heat-transfer coefficient for pipe in air

Hot water at  $98^{\circ}\text{C}$  flows through a 2-in schedule 40 horizontal steel pipe ( $k = 54 \text{ W/m}\cdot^{\circ}\text{C}$ ) and is exposed to atmospheric air at  $20^{\circ}\text{C}$  as shown in Figure 4.7. The water velocity is  $25 \text{ cm/s}$ .

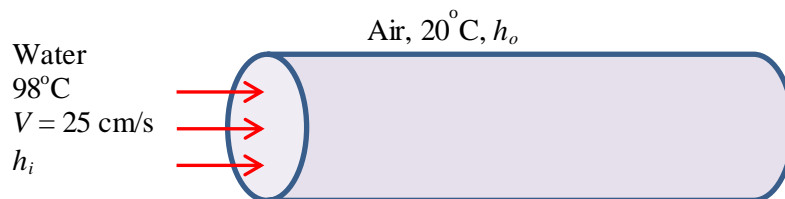


Figure 4.7. Schematic for Example 4-3 (adapted from Holman [3])

Calculate:

- the rate of heat-transfer through the pipe,
- the temperatures at the inside and outside surfaces of the pipe, and
- the overall heat-transfer coefficient based on the outer area of the pipe.

Properties of water at  $98^{\circ}\text{C}$  are:  $\rho = 960 \text{ kg/m}^3$ ,  $\mu = 2.82 \times 10^{-4} \text{ kg/m}\cdot\text{s}$ ,  $k = 0.68 \text{ W/m}\cdot^{\circ}\text{C}$ ,  $\text{Pr} = 1.76$ . For a 2-in schedule 40 pipe,  $D_i = 5.25 \text{ cm}$  and  $D_o = 6.033 \text{ cm}$ .

#### The analytical model

Using the thermal-resistance concept, the rate of heat-transfer through the pipe,  $Q$ , is given by:

$$Q = (T_w - T_\infty) / R_{th} \quad (4.6)$$

Where  $T_w$  and  $T_\infty$  are the water temperature and air-temperature, respectively, and  $R_{th}$  is the total thermal resistance that consists of the thermal resistances due to heat-transfer by convection inside the pipe ( $R_i$ ), by conduction through the steel pipe ( $R_p$ ), and by convection outside the pipe ( $R_o$ ). The three resistances are given by:

$$R_i = \frac{1}{A_i h_i} \quad (4.7)$$

$$R_p = \frac{\ln(D_i / D_o)}{2\pi k} \quad (4.8)$$

$$R_o = \frac{1}{A_o h_o} \quad (4.9)$$

Where  $A_i$  and  $A_o$  are the inside and outside areas of the pipe and  $h_i$  and  $h_o$  are the corresponding heat-transfer coefficients. The internal heat-transfer coefficient  $h_i$  is determined from the corresponding Nusselt number ( $Nu$ ):

$$h_i = Nu \frac{k_w}{D_i} \quad (4.10)$$

Where,  $k_w$  is the thermal conductivity of water. The Nusselt number is determined from empirical equations depending on the type of the flow, i.e., natural or forced, laminar or turbulent. For the turbulent forced internal flow (to be confirmed later),  $Nu$  is obtained from the Dittus-Boelter equation, Equation (1.31), with  $n = 0.4$  [3]:

$$Nu = 0.023 Re^{0.8} Pr^{0.4} \quad (4.11)$$

Where,  $Re$  and  $Pr$  are the Reynolds number and Prandtl number, respectively. For the external flow, Holman [3] used the following simplified equation for free laminar convection from a horizontal pipe to air at atmospheric pressure:

$$h_o = 1.32 \left( \frac{T_o - T_\infty}{D_o} \right)^{1/4} \quad (4.12)$$

Both  $R_i$  and  $R_p$  can be determined directly from the given data, but  $R_o$  depends on  $h_o$  which cannot be determined directly since  $T_o$  is not known. Therefore, the problem has to be solved by adopting an iterative approach by assuming a value for  $T_o$  based on

## Computer-Aided Thermofluid Analyses Using Excel

which  $h_o$  is determined and, consequently,  $Q$ . The value of  $Q$  thus obtained can be used to calculate corresponding values for  $T_i$  and  $T_o$  from:

$$T_i = T_w - Q.R_i \quad (4.13)$$

$$T_o = T_i + Q.R_p \quad (4.14)$$

If the guessed value for  $T_o$  is correct, then it will be the same as that obtained from Equation (4.14). Otherwise, a new guess for  $T_o$  has to be made repeatedly until this condition is met. Once this is achieved, the overall heat-transfer coefficient ( $U_o$ ) based on the outside area ( $A_o$ ) can be obtained from:

$$U_o = \frac{1}{A_o(R_i + R_o + R_p)} \quad (4.15)$$

### Solution with Goal Seek

The Excel sheet developed for this example is shown in Figure 4.8. The given information about the pipe, water, and air properties are entered in the data part on the left side of the sheet. The cells are labelled and the figure shows the formulae used in the calculations. The calculations part at the central part of the sheet starts with a guessed value for the pipe's outside temperature ( $T_{og}$ ) of  $50^\circ\text{C}$ . Based on this value, the sheet determines the outside heat-transfer coefficient ( $h_o$ ) from Equation (4.12) and the thermal resistance associated with it ( $R_o$ ) from Equation (4.9). Following the analytical model described above, the sheet determines the three thermal resistances ( $R_i$ ,  $R_p$ , and  $R_o$ ), and then calculates the rate of heat-transfer ( $Q$ ), inside temperature ( $T_i$ ), outside temperature ( $T_o$ ), and overall-heat transfer coefficient ( $U$ ).

	A	B	C	D	E	F	G	H	I	J	K
1											
2	D_i	0.0525	m	T_og	50	oC					
3	D_o	0.06033	m								
4	k_pipe	54	W/m·C	h_o	6.233341	=1.32*((T_og-T_oo)/D_o)^0.25	Q	35.44258	=T_og-T_oo)/R_o		
5				R_o	0.846439	=1/(h_o*PI()*D_o)					
6	V	0.25	m/s				T_i	97.89039	=T_w-Q*R_i		
7	T_w	98	oC	Re_i	44680.85	=rho*V*D_i/mu					
8	p	960	kg/m3	Nu_i	151.3666	=F(Re_i>2300,0.023*Re_i^0.8*Pr^0.4,64)	T_o	97.87587	=T_i-Q*R_pipe		
9	mu	2.82E-04	kg/m.s	h_i	1960.558	=Nu_i*k/D_i					
10	k	0.68	W/m·C				U	6.207657	=1/(PI()*D_o*(R_i+R_pipe+R_o))		
11	Pr	1.76		R_i	0.003093	=1/(h_i*PI()*D_i)					
12							Diff	0.957517			
13	T_oo	20	oC	R_pipe	0.00041	=LN(D_o/D_i)/(2*PI()*k_pipe)					
14											

Figure 4.8. Excel sheet developed for Example 4-3

As Figure 4.8 shows, the value of  $T_o$  calculated from Equation (4.14) is  $97.876^\circ\text{C}$ , which is different from the initially guessed value ( $T_{og} = 50^\circ\text{C}$ ). The formula bar reveals the formula entered in cell **H12** that calculates the difference between the

calculated exit temperature ( $T_o$ ) and the guesd value ( $T_{og}$ ) as a fraction of  $T_{og}$ . The exit temperature that makes the difference vanishes can be found by using the Goal Seek command and Figure 4.8 shows the required set-up. The solution found by Goal Seek is shown in Figure 4.9. Table 4.1 compares the presents results with those given by Holman [3] to confirm the accuracy of the iterative solution with Goal Seek.

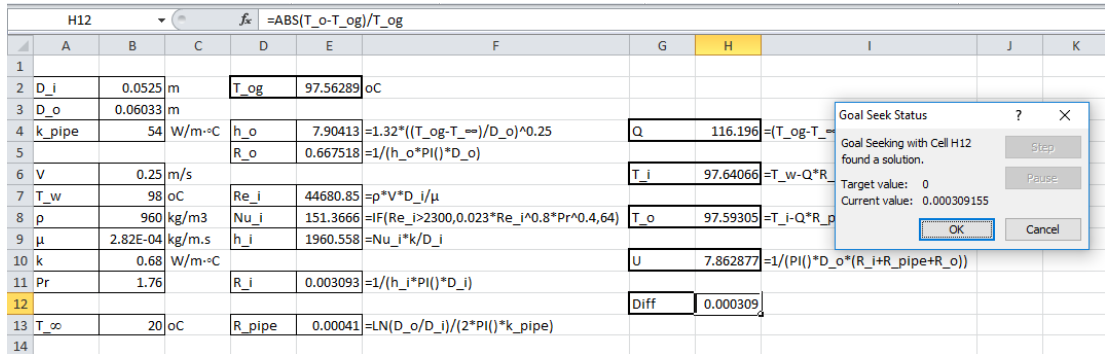


Figure 4.9. Solution obtained by Goal Seek for Example 4-3

Table 4.1. Comparison of the presnt Goal Seek solution with that given by Holman [3]

	Holman [3]	Goal Seek solution
$T_i$	97.65	97.64
$T_o$	97.6	97.59
$h_i$	1961.0	1960.56
$h_o$	7.91	7.90
$U_o$	7.87	7.86

## 4.2. Constrained iterative solutions with Solver

Solver offers greater flexibility than Goal Seek for dealing with iterative solutions because it allows for multiple changeable cells and for constraints to be imposed on the iterative solution. This section illustrates the need for these additional features in thermofluid analyses by means of two examples from the areas of fluid-dynamics and thermodynamics.

### Example 4-4. Determining the maximum water flow rate to avoid cavitation

Water at 20°C ( $\gamma = 9810 \text{ N/m}^3$  and  $\nu = 1.006 \times 10^{-6} \text{ m}^2/\text{s}$ ) is to be pumped from a large reservoir via a pump-pipe system as shown in Figure 4.10. The pump is positioned vertically at a level which is 9 m above the surface of the reservoir and horizontally at 1 m from the vertical section of the pipe. The pipe is made of commercial steel pipe ( $\epsilon = 0.046 \text{ mm}$ ) and has a 2" nominal diameter.

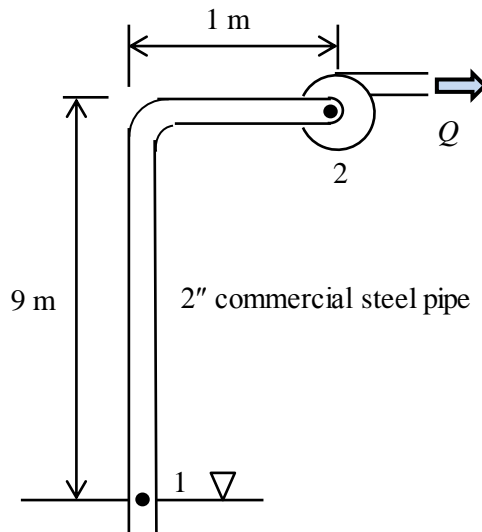


Figure 4.10. Schematic for the pump-pipe system in Example 4-4

Determine the maximum allowable water flow rate ( $Q$ ) such that:

1. The water velocity ( $V$ ) is to be in the range 1.4-2.8 m/s for economic considerations.
2. The pressure at the pump inlet must be greater than the saturation pressure of water at 20°C, which is 2.338 kPa, to avoid cavitation.

This example, which is basically a type-2 pipe flow problem, is based on a similar example given by Schumack [4].

### The analytical model

The energy equation between the pipe inlet (point 1) and the pump inlet (point 2) is:

$$\frac{p_1}{\gamma} + Z_1 + \frac{V_1^2}{2g} = \frac{p_2}{\gamma} + Z_2 + \frac{V_2^2}{2g} + h_f \quad (4.16)$$

Where  $\gamma$  stands for the specific weight of water,  $z$  for the elevation,  $V$  for the water velocity,  $g$  for the gravitational acceleration, and  $h_f$  for the friction loss in the pipe. For a large reservoir  $V_1 = 0$ . Taking point 1 as a reference, i.e.  $Z_1 = 0$ , and noting that the water velocity in the pipe is uniform, i.e.  $V_2 = V$ , the energy equation reduces to:

$$p_2 = \gamma \left( \frac{p_1}{\gamma} - Z_2 - \frac{V^2}{2g} - h_f \right) \quad (4.17)$$



The velocity  $V$  is related to the pipe diameter ( $D$ ) and water flow rate ( $Q$ ) as follows:

$$V = 4Q / \pi D^2 \quad (4.18)$$

Neglecting minor losses, the friction loss can be calculated from the Darcy-Weisbach equation, Equation (4.1), which needs an auxiliary formula to determine the friction factor ( $f$ ) depending on whether the flow is laminar or turbulent.

### Solution with Solver

Figure 4.11 shows the Excel sheet developed for this example. The data part on the left side stores the problem data such as the diameter, roughness, and length of the pipe, etc. The central part stores a guessed value for the water velocity ( $V=1.0$  m/s) in cell E2. Based on the guessed water velocity, the sheet performs the necessary calculations according to the analytical model given above. Figure 4.11 reveals the formulae used in these calculations. Note that an **IF**-statement is used to calculate the friction factor ( $f$ ) depending on the value of the Reynolds number ( $Re$ ). Cell E6 calculates the friction loss ( $hf$ ). Based on the calculated value of friction loss, the pressure at point 2 ( $P_2$ ) is calculated from Equation (4.17) and stored in cell E7. The right side of the sheet contains the single cell I2 that determines the flow rate ( $Q$ ). The formula in this cell is shown in the formula bar.

	A	B	C	D	E	F	G	H	I	J	K
1											
2	D	0.05252	m	V	1.00	m/s		Q	0.0021664	m <sup>3</sup> /s	
3	ε	0.000046	m								
4	L	10	m	Re	52520	=V*D/v					
5	Z <sub>2</sub>	9	m	f	0.023651	=IF(Re<2000,64/Re,0.25/(LOG10(ε/3.7/D+5.74/Re <sup>0.9</sup> ))^2)					
6	P <sub>1</sub>	100	kPa	hf	0.229523	=f*L/D*V^2/(2*gc)					
7	v	1.00E-06	Pa.s	P <sub>2</sub>	8.958382	=(P <sub>1</sub> *1000/γ-Z <sub>2</sub> -V^2/(2*gc)-hf)*γ/1000					
8	γ	9810	N/m <sup>3</sup>								
9	gc	9.81	m/s <sup>2</sup>								
10											

Figure 4.11. Excel sheet developed for Example 4-4

Based on the assumed water velocity of 1.0 m/s, the calculated values of  $hf$  and  $P_2$  are 0.2295 m and 8.958 kPa, respectively. Since the pressure at point 2 is higher than the minimum desired level of 2.338 kPa, while the water velocity ( $V$ ) is less than the minimum economic value of 1.4 m, there is room to increase the flow rate. The task can be left to Solver and Figure 4.12 shows the set-up that requires Solver to maximise the value of the flow rate  $Q$  while satisfying the three constraints shown in the figure. The first constraint on the iterative solution requires the value of  $P_2$  in cell E7 to be higher than or equal to 2.338 kPa. The two other constraints are to satisfy the limits on the water velocity imposed by economic limits, i.e.,  $1.4 \text{ m} \leq V \leq 2.8 \text{ m}$ .

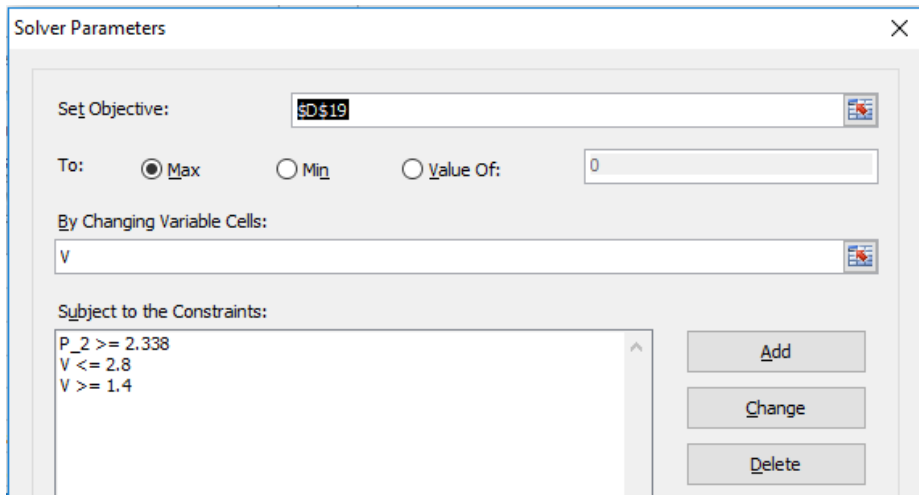


Figure 4.12. Solver parameters dialog box for Example 4-4

Pressing the “Solve” button will trigger Solver to search for the solution. The solution found by the **GRG Nonlinear** method is shown in Figure 4.13. The value determined for the water velocity is 1.90 m/s. Note that this velocity lies within the limits imposed by the economic constraint. The pressure at point 2 is equal to 2.338 kPa which is the minimum pressure level required to prevent cavitation. Therefore, the corresponding flow rate, which is 0.00413 m<sup>3</sup>/s, is the maximum flow rate to be recommended.

	Q		$f_x$	=0.25*PI()*D^2*V							
	A	B	C	D	E	F	G	H	I	J	K
1											
2	D	0.05252	m	V	1.90	m/s		Q	0.004125	m <sup>3</sup> /s	
3	$\epsilon$	0.000046	m								
4	L	10	m	Re	100001.5	=V*D/v					
5	Z <sub>2</sub>	9	m	f	0.021901	=IF(Re<2000,64/Re,0.25/(LOG10( $\epsilon$ /3.7/D+5.74/Re^0.9)))^2					
6	P <sub>1</sub>	100	kPa	hf	0.770567	=f*L/D*V^2/(2*gc)					
7	v	1.00E-06	Pa.s	P <sub>2</sub>	2.338005	=(P <sub>1</sub> *1000/ $\gamma$ -Z <sub>2</sub> -V^2/(2*gc)-hf)* $\gamma$ /1000					
8	$\gamma$	9810	N/m <sup>3</sup>								
9	gc	9.81	m/s <sup>2</sup>								
10											

Figure 4.13. Solver solution for Example 4-4

**Example 4-5. Restrained expansion of air inside a piston-cylinder device**

Figure 4.14 shows a piston-cylinder device that initially contains 0.05 m<sup>3</sup> of air at 200 kPa and 317K. At this state, a linear spring is touching the piston but exerting no force on it before 72.7 kJ of heat is transferred to the air, causing the piston to rise and compress the spring. If the cross-sectional area of the piston is 0.25 m<sup>2</sup> and the spring’s constant ( $k$ ) is 150 kN/m, determine the final volume, pressure, and temperature of the air inside the cylinder after the heat-addition.

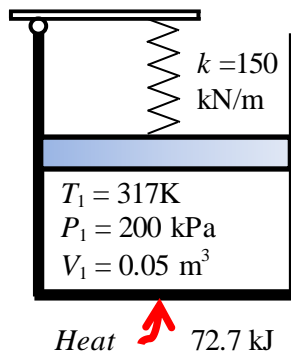


Figure 4.14. Schematic and pressure-volume diagrams for Example 4-5 (adapted from Cengel and Boles [5])

Treat air as an ideal gas with a specific heat at constant volume ( $c_v$ ) that varies linearly with the temperature according to the formula:

$$c_v = 0.645 + 0.0002T \quad (4.19)$$

Where  $T$  is the temperature in K and  $c_v$  is in kJ/kg.K.

### Comment

This example is based of Example 4-4 given by Cengel and Boles [5]. However, unlike the present example, Cengel and Boles [5] specified the final volume to be  $0.1 \text{ m}^3$  instead of specifying the amount of heat added. When the final volume (or final pressure) is given, the problem can be solved in a straightforward manner without iteration. However, in the present example  $T_2$ ,  $V_2$ , and  $P_2$  at the final state depend on the amount of heat added. Another factor that makes the present example more difficult than that given by Cengel and Boles [5] is the use of Equation (4.19) to determine the value of the specific heat  $c_v$  for air. The specific value of 72.7 kJ given in this example has been chosen such that the final volume will be  $0.1 \text{ m}^3$  as specified by Cengel and Boles [5] so that the present final pressure on the piston and total work will be close to their corresponding values even though the data of the two examples are different.

### The analytical model

Like Example 4-2, the problem can be solved by using the first-law of thermodynamics together with the ideal-gas law, but the variation of the specific heat with temperature makes it necessary to adopt an iterative solution. Moreover, the addition of the linear spring in this example introduces a new factor, which is the variation of pressure with air expansion. Since the present iteration process involves both the temperature and the volume (or pressure), the Goal Seek command cannot be used. Therefore, this example requires Solver to start the iterative procedure with assumed values for both the final temperature ( $T_2^*$ ) and the final volume ( $V_2^*$ ).

The final pressure  $P_2$  is given by:

$$P_2 = P_1 - \frac{k\Delta x}{A} \quad (4.20)$$

Where  $A$  is the base area of the piston and  $\Delta x$  is the reduction in the spring's length given by:

$$\Delta x = \frac{V_2^* - V_1}{A} \quad (4.21)$$

The total work ( $W$ ), i.e., the summation of the air expansion work and the work done against the spring, can now be obtained from:

$$W = \frac{(P_1 + P_2)}{2}(V_2^* - V_1) \quad (4.22)$$

The final temperature can be determined by applying the first-law of thermodynamics to the piston-cylinder device as a closed system:

$$Q - W = m(u_2 - u_1) = mc_v(T_2 - T_1) \quad (4.23)$$

Where  $Q$  is the amount of heat added,  $u$  is the internal energy,  $m$  is the mass of air inside the cylinder, and  $\bar{c}_v$  is the average specific heat of air at constant volume. The mass and specific heat of air can be obtained from:

$$m = P_1 V_1 / RT_1 \quad (4.24)$$

$$\bar{c}_v = 0.6 + 0.0002(T_1 + T_2^*)/2 \quad (4.25)$$

Rearranging Equation (4.23), the final temperature  $T_2$  is given by:

$$T_2 = T_1 + \frac{Q - W}{m\bar{c}_v} \quad (4.26)$$

Using the values obtained for  $T_2$  and  $P_2$ , the final volume  $V_2$  can be determined from the ideal-gas law:

$$V_2 = mRT_2 / P_2 \quad (4.27)$$

If the initially guessed volumes of  $T_2^*$  and  $V_2^*$  are correct, then they will be the same as  $T_2$  and  $V_2$  obtained from Equation (4.24) and Equation (4.26), respectively. Otherwise, new values for  $T_2^*$  and  $V_2^*$  have to be used until the differences between the calculated and guessed values become negligibly small. This multi-variable iterative process can be performed with Solver as shown below.

**Solution with Solver**

Figure 4.15 shows the Excel sheet developed for this example and reveals the formulae used in it. The left side of the sheet accommodates the problem data. The calculations part start by an assumed values for the final temperature ( $T_{2g} = 500K$ ) and final volume  $V_{2g} = 0.15 \text{ m}^3$ . Based on the assumed final volume, the sheet determines the compression of the spring ( $\Delta x$ ), spring force ( $F_{spring}$ ), final pressure ( $P_2$ ), and total work involved ( $Work$ ). The final temperature ( $T_2$ ) is then calculated from the first-law according to Equation (4.26), and the final volume ( $V_2$ ) from the ideal-gas law, Equation (4.27). As Figure, 4.15 shows, the calculated values  $T_2$  and  $V_2$  are different from the initial values  $T_{2g}$  and  $V_{2g}$ . Solver can now be used to adjust the guessed value of  $T_{2g}$  and  $V_{2g}$  until they become the same as the calculated values.

		T_2		fx =T_1+(Q-Work)/m/Cv						
	A	B	C	D	E	F	G	H	I	J
1										
2		P_1	200 kPa		T_2g	500		T_2	826.5425	K
3		T_1	317 kPa		V_2g	0.15		V_2	0.059259	m3
4		V_1	0.05 m3							
5					m	0.109915	=P_1*V_1/Rgas/T_1			
6		Q	72.7 kJ							
7		Area	0.25 m		$\Delta x$	0.4	=(V_2g-V_1)/Area			
8					Fspring	60	=kspring*\Delta x			
9		kspring	150 kN/m		P_2	440	=P_1+Fspring/Area			
10					Work	32	=0.5*(P_1+P_2)*(V_2g-V_1)			
11		Rgas	0.287 kJ/kg.K							
12					Cv	0.7267	=0.645+0.0002*(T_1+T_2g)/2			
13										

Figure 4.15. Excel sheet developed for Example 4-5

Figure 4.16 shows the set-up that requires Solver to change the values of  $T_{2g}$  and  $V_{2g}$  in cells F2 and F3, respectively, until the two specified constraints are satisfied: (i)  $T_2 = T_{2g}$  and (ii)  $V_2 = V_{2g}$ . Note that the “Set Objective” option has been left blank. The “Changing Variable Cells” are F2 and F3. Figure 4.17 shows the solution obtained by the **GRG Nonlinear** method of Solver, which is  $T_{2g} = 1014.864K$  and  $V_{2g} = 0.1 \text{ m}^3$ . At this state, the final pressure on the piston is 320.0 kPa and the total work is 13.0 kJ. These values agree with their corresponding values given by Cengel and Boles [5] whose analysis also gave  $P_2 = 320 \text{ kPa}$  and  $W = 13 \text{ kJ}$ .

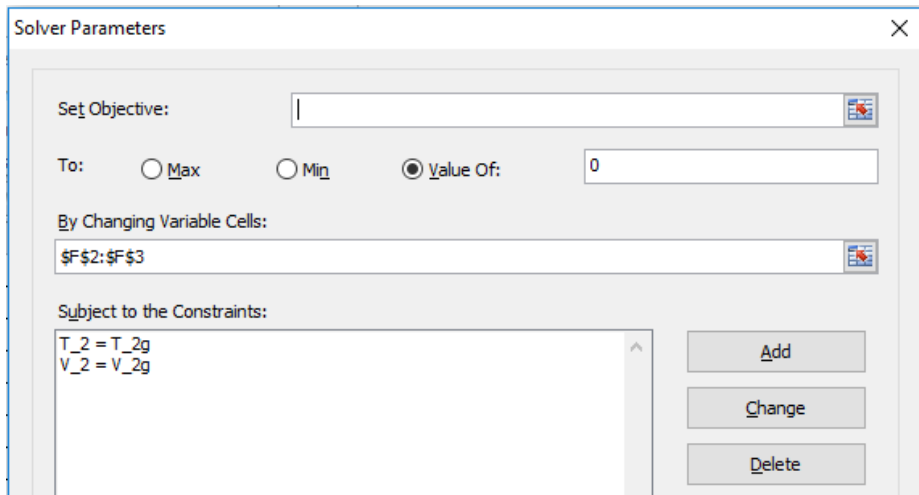


Figure 4.16. Solver set-up for Example 4-5

	A	B	C	D	E	F	G	H	I	J
1										
2		P_1	200	kPa	T_2g	1014.864		T_2	1014.864	K
3		T_1	317	kPa	V_2g	0.100026		V_2	0.100026	m <sup>3</sup>
4		V_1	0.05	m <sup>3</sup>						
5					m	0.109915	=P_1*V_1/Rgas/T_1			
6		Q	72.7	kJ						
7		Area	0.25	m	Δx	0.200105	=(V_2g-V_1)/Area			
8					Fspring	30.0157	=kspring*Δx			
9		kspring	150	kN/m	P_2	320.0628	=P_1+Fspring/Area			
10					Work	13.00837	=0.5*(P_1+P_2)*(V_2g-V_1)			
11		Rgas	0.287	kJ/kg.K						
12					Cv	0.778186	=0.645+0.0002*(T_1+T_2g)/2			
13										

Figure 4.17. Solver solution for Example 4-5

### 4.3. Iterative solutions involving nonlinear equations

To determine the head loss due to friction ( $h_f$ ) in Example 4-1, the friction factor ( $f$ ) for the turbulent pipe flow was obtained from Equation (1.24) which is an explicit equation. However, for a turbulent pipe flow  $f$  can be determined more accurately by using the Colebrook-White equation [1]:

$$\sqrt{\frac{1}{f}} = -2.0 \log \left( \frac{\varepsilon/D}{3.7} + \frac{2.51}{\text{Re} \sqrt{f}} \right) \quad (4.28)$$

Since the equation involves the friction factor  $f$  in both sides, it needs to be solved iteratively in order to determine  $f$ . Therefore, for type-2 and type-3 flow problems using this equation involves two nested iterations; an inside iteration to determine  $f$  and an outside iteration to determine the pipe's diameter or flow rate.

The Newton-Raphson solver (**NRM**) provided by Thermax has been developed so as to allow nonlinear equations such as the Colebrook-White equation to be used in iterative solutions and optimisation analyses. Appendix B illustrates the use of the **NRM** solver by considering another nonlinear equation which is the Benedict-Webb-Rubin equation. In the present situation, the **NRM** solver will be used to solve the Colebrook-White equation leaving the main iteration for Solver or Goal Seek. For illustration, let us reconsider Example 4-1 and solve it by the using Equation (4.28) to determine  $f$  instead of Equation (1.24).

The **NRM** solver requires the intended nonlinear equation to be provided as a separate user-defined function. The one needed for the Colebrook-White equation is listed below:

```
Function colebrook(x, e, Re)
    ' Colebrook equation for the friction factor
    colebrook = 1/Sqr(x) + (2/log(10))*Log(e /3.7 + 2.51/Re/Sqr(x))
End Function
```

Note that in VBA syntax the term “log” is used for the natural logarithm “ln” which is different from Excel. Figure 4.18 shows the Excel sheet developed for solving Example 4-1 with the Colebrook-White equation.

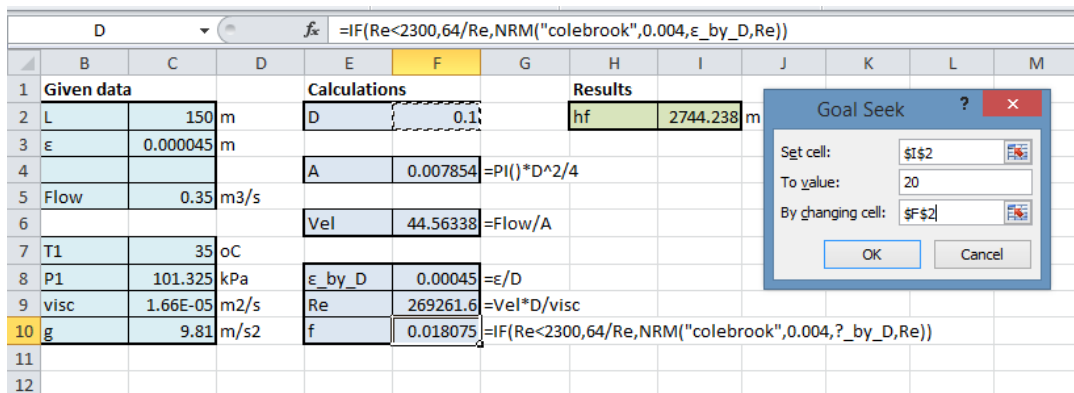


Figure 4.18. Excel sheet for Example 4-1 using the Colebrook-White equation

The only difference from the sheet shown in Figure 4.2 is the content of the cell **F10** that calculates friction factor. Figure 4.18 shows the formula typed in this cell as:

$$=IF(Re<2300,64/Re,NRM('colebrook',0.004,ε_by_D,Re))$$

The first input to the **NRM** solver, “colebrook”, refers to the function that contains the Colebrook-White equation while the second input, **0.004**, is an initial guess for  $f$ . The last two arguments, **ε\_by\_D** and **Re**, respectively, are labels for the cells **F8** and **F9** that store values of the roughness-diameter ratio ( $\epsilon/D$ ) and the Reynolds number ( $Re$ ) at

which  $f$  is to be determined. Figure 4.18, which shows the calculations for a selected diameter of 0.1 m, shows that the value of the friction factor obtained by the Colebrook-White equation is 0.018075 and the corresponding friction loss is 2744.2 m. These values are slightly different from those obtained with Equation (1.24) as shown in Figure 4.2. The diameter that keeps the loss below 20 m can be determined by using Goal Seek and Figure 4.18 also shows Goal Seek set-up for finding the value of  $D$  that makes the friction head loss equal to 20 m. As Figure 4.19 shows, the answer found by Goal Seek is  $D \geq 0.27$  m, which is the same answer obtained earlier in Example 4-1.

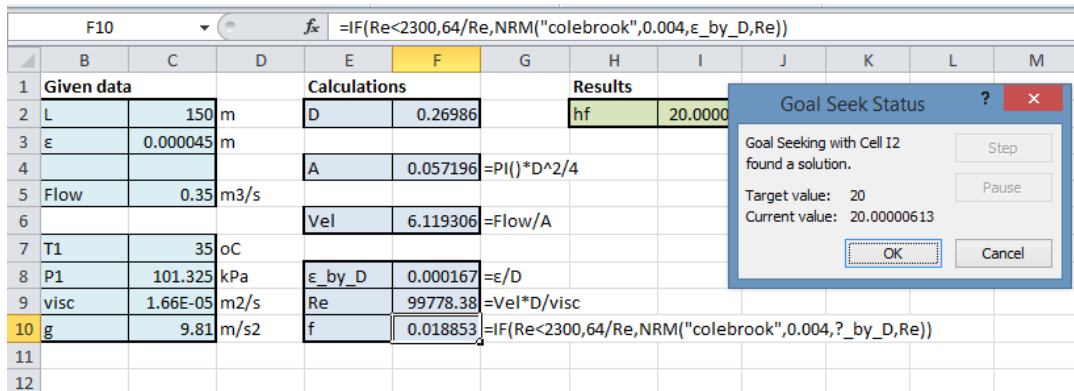


Figure 4.19. Goal Seek solution for Example 4-1 using the Colebrook-White equation

#### 4.4. Closure

This chapter dealt with thermofluid analyses that require iterative solutions and showed how Excel’s Goal Seek command and Solver can be used for solving typical problems from the areas of fluid dynamics, thermodynamics, and heat-transfer. While the Goal Seek command can easily perform the simple type of iterative solutions that involve a single parameter, Solver can perform the more difficult iterative solutions that involve multiple changeable cells and require constraints to be applied to the iterative solution. The chapter also showed how the Newton-Raphson solver provided by Thermax can be used to deal with the solutions that involve nonlinear equations such as the Colebrook-White equation.

#### References

- [1] Y. A. Cengel and J. M. Cimbala, *Fluid Mechanics Fundamentals and Applications*, 3<sup>rd</sup> edition, McGraw-Hill, 2006.
- [2] C. T. Crowe, D. F. Elger, B. C. Williams, and J. A. Roberson, *Engineering Fluid Mechanics*, 9<sup>th</sup> edition, John Wiley, 2009.
- [3] J. P. Holman, *Heat Transfer*, 10<sup>th</sup> edition, McGraw-Hill, 2010.
- [4] M. Schumack, Solution of complex pipe flow problems using spreadsheets in an introductory fluid mechanics course, Proceedings of the 2004 American Society for Engineering Education Annual Conference & Exposition, Session 3666, Pages 9.1108.1 - 9.1108.13. Available at <https://peer.asae.org/solution-of-complex-pipe-flow-problems-using-spreadsheets-in-an-introductory-fluid-mechanics-course>



- [5] Y. A. Cengel, and M. A. Boles, *Thermodynamics. An Engineering Approach*. 5<sup>th</sup> edition, McGraw-Hill, New York, 2006.
- [6] M.J. Moran and H.N. Shapiro, *Fundamentals of Engineering Thermodynamics*, 5<sup>th</sup> edition, John Wiley, & Sons. Inc. 2006.
- [7] M.M. El-Awad, Use of Excel's 'Goal Seek' feature for Thermal-Fluid Calculations, the Electronic Journal of Spreadsheets in Education (eJSiE), Vol. 9, Iss. 1, Article 3, 2016. Available at: <http://sie.scholasticahq.com/article/4657>, last accessed Aug, 4, 2019.

### Exercises

1. Consider the case in Example 4-1. Suppose that the only available pipe diameter is 20 cm and we want to maintain the same maximum limit on the friction head loss of 20 m by reducing the water flow rate. Using the Goal Seek command, determine the water flow rate that gives the required result. Answer: 0.157 m<sup>3</sup>.
2. Using the Excel sheet developed for Example 4-2, determine the final temperature for air when the amount of heat added is 50, 100, 150, and 200 kJ. Also calculate the final temperature from Equation (4.3) by using a constant specific heat ( $c_p$ ) of 1.043 kJ/kg.K. Plot the values obtained for the final temperature ( $T_2$ ) with the amount of heat added by the two methods and comment on the result.
3. A gas mixture consisting of O<sub>2</sub> and CO<sub>2</sub> with mole fractions 0.2 and 0.8, respectively, expands isentropically and at steady state through a nozzle from 700 K, 500 kPa to an exit pressure of 100 kPa as shown in Figure 4.P3. Determine the temperature at the nozzle exit, in K.

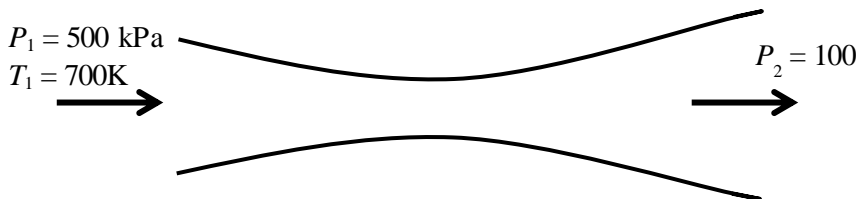


Figure 4.P3. Isentropic expansion in a nozzle

This exercise is based on Example 12.4 in Moran and Shapiro [6]. Using the approximate constant-specific heat method, the exit temperature ( $T_2$ ) can be determined from:

$$T_2 = T_1 \times \left( P_2 / P_1 \right)^{\frac{k-1}{k}} \quad (\text{A})$$

Where  $k$  is the ratio of the specific heats for the mixture. Using  $k = 1.304$ , the resulting exit temperature is 480.9K. Using the exact variable specific heat method,  $T_2$  is determined by requiring the total entropy change to be zero, i.e:

$$y_{O_2} \left[ s_{O_2}^0(T_2) - s_{O_2}^0(T_1) - R_{O_2} \ln \frac{P_2}{P_1} \right] + y_{CO_2} \left[ s_{CO_2}^0(T_2) - s_{CO_2}^0(T_1) - R_{CO_2} \ln \frac{P_2}{P_1} \right] = 0 \quad (B)$$

Where  $y_{O_2}$  and  $y_{CO_2}$  are the volume fractions of  $O_2$  and  $CO_2$ , respectively, and  $R_{O_2}$  and  $R_{CO_2}$  are the molar masses for  $O_2$  and  $CO_2$ , respectively. The values of  $s_{O_2}^0$  and  $s_{CO_2}^0$  can be determined by using the relevant function provided by Thermax. Equation (B), that requires an iterative solution, can be solved by using the Goal Seek command. Answer:  $T_2 = 514.05K$ .

4. Steam is be condensed at  $30^\circ C$  on the shell side of the multi-pass shell-and-tube heat exchanger shown in Figure 4.P4. The condenser has 8-tube-passes with 50 tubes in each pass. Its overall heat transfer coefficient is  $1000 \text{ W/m}^2 \cdot ^\circ C$ . Cooling water ( $C_p = 4180 \text{ J/kg} \cdot ^\circ C$ ) enters the tubes at  $15^\circ C$  at a rate of  $55,000 \text{ kg/h}$ . The tubes are thin-walled, and have a diameter of  $1.5 \text{ cm}$  and length of  $2 \text{ m}$  per pass. Develp and Excel shhet to determine the outlet temperature of the cooling water by using Goal Seek and the LMTD method instead of the  $\epsilon$ -NTU method [7].

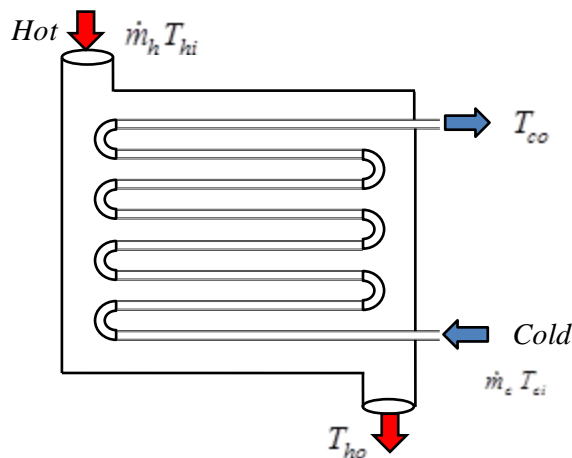


Figure 4.P4. A multi-pass shell-and-tube heat exchanger

5. Reconsider the case in Example 4-5. Show that an alternative solution of this problem that also takes into consideration the variation of specific heat for air with temperature can be obtained by using the ideal-gas property functions provided by Thermax instead of Equation (4.19). Show that this solution can be obtained by using the Goal Seek command instead or Solver and compare your solution with that given in Example 4-5.

6. Consider the semi-infinite slab shown in Figure 4.P6 that is suddenly exposed to convection environment at  $T_\infty$ . The temperature ( $T$ ) at a depth  $x$  from the surface at any time is given by [3]:

$$\frac{T - T_i}{T_\infty - T_i} = 1 - \text{erf}(X) - \left[ \exp\left(\frac{hx}{k} + \frac{h^2\alpha\tau}{k^2}\right) \times \left[ 1 - \text{erf}\left(X + \frac{h\sqrt{\alpha\tau}}{k}\right) \right] \right] \quad (\text{A})$$

Where  $\alpha$  and  $k$  are the diffusivity and thermal conductivity of the slab material, respectively,  $T_i$  is the initial temperature of the solid,  $T_\infty$  is the environmental temperature,  $\tau$  is the elapsed time in seconds, and  $X = (2\sqrt{\alpha\tau})$ .

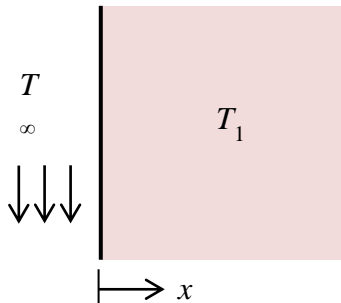


Figure 4.P6. Semi-infinite slab with convection heat-transfer

Equation (A) requires an iterative procedure because the time ( $\tau$ ) appears in both terms on the right-hand side of the equation.

A large slab of aluminium ( $k = 215 \text{ W/m}\cdot^\circ\text{C}$ ,  $\alpha = 8.4 \times 10^{-5} \text{ m}^2/\text{s}$ ) at a uniform temperature of  $200^\circ\text{C}$  is suddenly exposed to a convection-surface environment of  $70^\circ\text{C}$  with a heat-transfer coefficient of  $525 \text{ W/m}^2\cdot^\circ\text{C}$ . Calculate the time required for the temperature to reach  $120^\circ\text{C}$  at the depth of  $4.0 \text{ cm}$  for this circumstance.

This problem is based on Example 4-5 in Holman [3] whose answer is approximately 3000 seconds.

7. Water at  $60^\circ\text{C}$  enters a tube of  $3\text{-cm}$  diameter at a mean flow velocity of  $1.2 \text{ cm/s}$ . If the tube is  $3.0 \text{ m}$  long and the wall temperature is constant at  $80^\circ\text{C}$ , what will be the exit water temperature?

Use Goal Seek to perform the iterative solution of this problem. To determine the viscosity of water at any temperature, develop a user-defined function based on the data shown in Table A.2 in Appendix A. This exercise is based on Example 4-2 in Holman [3]. Answer:  $73.0^\circ\text{C}$ .

# 5

## **Hydraulic analyses of multi-pipe and pump-pipe systems**

The pump-pipe systems used in various applications usually consist of multiple pipes and pumps connected in parallel or in series. The hydraulic analyses of multi-pipe systems are based on the same principles of mass and energy conservation applicable for a single pipe, but simultaneously satisfying the continuity and energy equations in all the pipes usually requires an iterative solution. An iterative solution is also needed for determining the operating point for any pump-pipe system whether it involves a single pump or multiple pumps. This chapter shows how Excel with its iterative tools, Goal Seek and Solver, can be used for analysing multi-pipe systems and determining the operating point for a single pump with various pipe arrangements and for multiple pumps arranged in parallel or in series.

### 5.1. Analyses of multi-pipe systems

Figure 5.1 shows three multi-pipe arrangements in which three pipes are connected (a) in series, (b) in parallel, and (c) at a junction. In general, the pipes may have different lengths, diameters, and roughness. The pipes may also have different elevations at their entrance and exit points.

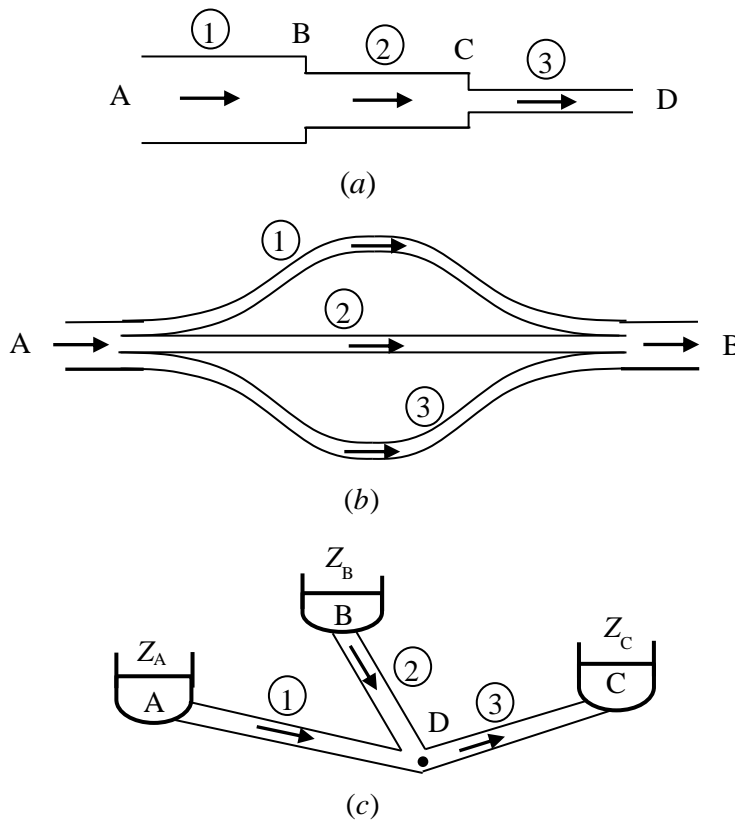


Figure 5.1. Three typical pipe arrangements in a pipe system (adapted from White [1])

### 5.1.1. Type-1 flow analyses

As for the case of a single pipe discussed in Chapter 4, three types of flow problems can arise with multi-pipe analyses depending on whether the pipe diameters and flow rates are known in advance or to be determined. If both the pipe diameters and flow rates are known then the problem is classified as a type-1 flow problem, but if one of these is to be determined, then the problem is classified as a type-2 or a types-3 flow problem. Unlike the case a single pipe, type-1 flow problems for multi-pipe system also require iterative solutions. The following example, which is based on Example 8-7 in Cengel and Cimbala [2], shows how Solver can be used to perform the iterative solution.

#### Example 5-1. Pumping water through two parallel pipes

Water at 20°C is to be pumped from reservoir A to reservoir B through two 36-m-long pipes connected in parallel as shown in Figure 5.2. The elevation of reservoir A is 5 m while that of reservoir B is 13 m. The two pipes are made of commercial steel and their diameters of the two pipes are 4 and 8 cm as shown in the figure. Water is to be pumped by a 70% efficient motor-pump combination that draws 8 kW of electric power during operation. The minor losses and the head loss in the pipes that connect the parallel pipes to the two reservoirs can be neglected. Determine the total flow rate of the pump and the flow rate through each of the two parallel pipes.

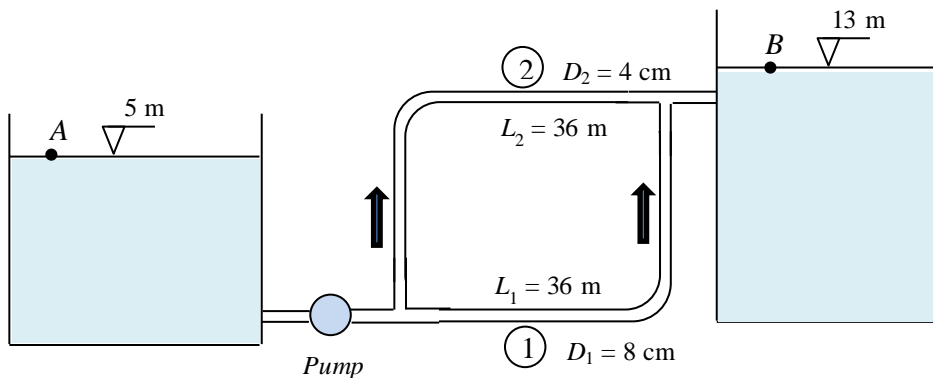


Figure 5.2. The piping system in Example 5-1 (adapted from Cengel and Cimbala [2])

#### The analytical model

Since the fluid at both points A and B are open to the atmosphere,  $P_A = P_B = P_{atm}$ . Also, the fluid velocities at both points are zero ( $V_A = V_B = 0$ ) and, therefore, the energy equation, Equation (1.20), between these two points simplifies to:

$$h_p = h_f + (Z_B - Z_A) \quad (5.1)$$

Where  $h_p$  is the pump head and  $h_f$  is the total friction loss between the two reservoirs. Since the pressures at the entrance and exit points of the two pipes are the same, the friction head losses in the two pipes must be the same:

$$h_{f1} = h_{f2} = h_f \quad (5.2)$$

The friction head loss in each pipe is given by the Darcy-Weisbach equation:

$$h_{f1} = f_1 \frac{L_1}{D_1} \frac{V_1^2}{2g} \quad (5.3)$$

$$h_{f2} = f_2 \frac{L_2}{D_2} \frac{V_2^2}{2g} \quad (5.4)$$

Given the two flow rates  $Q_1$  and  $Q_2$ , the water velocities in two pipes,  $V_1$  and  $V_2$ , can be calculated from:

$$V_1 = Q_1 / A_1 \quad (5.5)$$

$$V_2 = Q_2 / A_2 \quad (5.6)$$

For steady flow of an incompressible fluid, the total flow-rate given by the pump ( $Q$ ) is the summation of the flow-rates in the two parallel pipes ( $Q_1$  and  $Q_2$ ), i.e.:

$$Q = Q_1 + Q_2 \quad (5.7)$$

Finally, the power of the pump ( $\dot{W}_p$ ) is given by the following power equation:

$$\dot{W}_p = \gamma \times Q \times h_p / \eta \quad (5.8)$$

Where  $\gamma$  is the fluid's specific weight and  $\eta$  is the combined pump-motor efficiency. In the present case, the pump-power is known to be 8 kW. This can be used to determine the unknown flow rate ( $Q$ ) and the pump head ( $h_p$ ) by adopting the following iterative procedure:

1. Assume the pipe flow rates  $Q_1$  and  $Q_2$
2. Calculate the corresponding velocities  $V_1$  and  $V_2$  from Equation (5.5) and Equation (5.6), respectively.
3. Based on the two velocities, calculate the friction factors and friction head losses in the two pipes from Equation (5.3) and Equation (5.4), respectively.
4. Calculate the pump power from Equation (5.8)
5. Compare the resulting pipe friction losses to each other, Equation (5.2), and pump power to the specified value of 8 kW. If the pipe friction losses are

different or the pump power is not equal to 8 kW, go back to step 1 and repeat the procedure until the pump power becomes approximately zero.

Cengel and Cimbala [2] determined the friction factors  $f_1$  and  $f_2$  from the Colebrook-White formula. Chapter 4 showed how this implicit equation can be handled within an iterative solution by using the Newton-Raphson solver provided by Thermax.

### Excel implementation

Figure 5.3 shows the Excel sheet developed for this example. The data part, positioned on the left-side of the sheet, shows the given information about the pump-pipe system such as the lengths and diameters of the two pipes, density and viscosity of water, pump efficiency, etc. The calculations part begins at column E with assumed values for the two pipe flow rates ( $Q_1 = Q_2 = 0.01 \text{ m}^3/\text{s}$ ). Based on these assumed flow rates, the sheet determines the corresponding velocities in the two pipes ( $V_1$  and  $V_2$ ), the Reynolds numbers ( $Re_1$  and  $Re_2$ ), and the friction factors ( $f_1$  and  $f_2$ ). For a turbulent flow, the friction factor is obtained from the Colebrook-White formula. The pipes friction losses,  $hf_1$ , and  $hf_2$ , are then calculated and the total pump power ( $P_{\text{pump}}$ ) is determined from Equation (5.8).

	A	B	C	D	E	F	G	H	I	J	K	L
1												
2	L_1	36	m	Q_1	0.01		Re_1	158519.6		Power	2.734141	kW
3	D_1	0.08	m	Q_2	0.01		Re_2	317039.2				
4	L_2	36	m									
5	D_2	0.04	m	Q_total	0.02		ε_by_D_1	0.000563				
6	Z_A	5	m				ε_by_D_2	0.001125				
7	Z_B	13	m	A_1	0.005027							
8	η_p	0.7		V_1	1.989437		f_1	0.019547				
9	ρ	998	kg/m3				f_2	0.02106				
10	μ	1.00E-03	kg/m.s	A_2	0.001257							
11	ε	0.000045	m	V_2	7.957747		hf_1	1.774383				
12	g	9.81	m/s2				hf_2	61.1772				
13												

Figure 5.3. Excel sheet for Example 5-1

With the guessed pipe flow rates, Figure 5.3 shows that the pump power is only 2.734 kW, which is considerably less than the required value. Moreover, the values of  $h_{f1}$  and  $h_{f2}$  are different and, consequently, Equation (5.2) is not satisfied. Solver can now be used to find the correct values of  $Q_1$  and  $Q_2$ . Figure 5.4 shows the required set-up for its parameters dialog-box. Note that the pump power is specified as the **Set Objective** and required to have a value of 8 kW. In this case, Solver will iterate to satisfy the imposed constraint, which is requirement to satisfy Equation (5.2). The solution found by Solver with this set-up is shown in Figure 5.5. According to this solution, the flow rates are  $Q_1 = 0.0258 \text{ m}^3/\text{s}$  and  $Q_2 = 0.00415 \text{ m}^3/\text{s}$ , giving a total pump flow rate of  $0.03 \text{ m}^3/\text{s}$ . Table 5.1 compares the present solution with that obtained by Cengel and Cimbala [2]. The small deviations of the present values confirm the accuracy of the present solution.



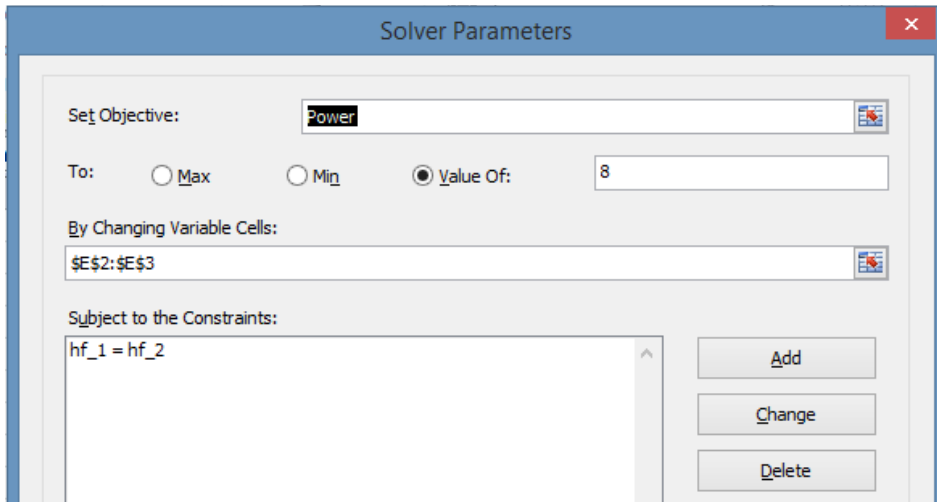


Figure 5.4. Solver's set-up for Example 5-1

	A	B	C	D	E	F	G	H	I	J	K	L
1												
2	L_1	36 m		Q_1	0.025861		Re_1	409944.7		Power	8.000002	kW
3	D_1	0.08 m		Q_2	0.004151		Re_2	131615.1				
4	L_2	36 m										
5	D_2	0.04 m		Q_total	0.030012		$\epsilon_{by\_D\_1}$	0.000563				
6	Z_A	5 m					$\epsilon_{by\_D\_2}$	0.001125				
7	Z_B	13 m		A_1	0.005027							
8	$\eta_p$	0.7		V_1	5.144847		f_1	0.018216				
9	$\rho$	998 kg/m <sup>3</sup>					f_2	0.02209				
10	$\mu$	1.00E-03 kg/m.s		A_2	0.001257							
11	$\epsilon$	0.000045 m		V_2	3.303566		hf_1	11.05859				
12	g	9.81 m/s <sup>2</sup>					hf_2	11.05859				
13												

Figure 5.5. Solver's solution for Example 5-1

Table 5.1. Comparison of the solution determined by Solver with their corresponding values given by Cengel and Cimbala [2]

Parameter	Cengel & Cimbala [2]	Present solution	Deviation (%)
$Q_1$	0.0259	0.025861	-0.151
$Q_2$	0.00415	0.004151	0.024
$Re_1$	410,000	409,944.5	-0.014
$Re_2$	131,600	131,615.3	0.012
$f_1$	0.0182	0.018216	0.088
$f_2$	0.0221	0.02209	-0.045
$h_f$	11.1	11.05861	-0.373

### 5.1.2. Type-2 and type-3 flow analyses

The recommended value for water velocity in commercial pipes lies in the range between 1.4 and 2.8 m/s [3], but Figure 5.5 shows that the velocities in both pipes exceed the upper limit particularly that in pipe 1. Therefore, the values obtained for the pipe flow rates are not acceptable for economic considerations even though they are physically correct based on the given data. Suppose that we decided to replace pipe 2 by a new pipe that has a larger diameter so that the water velocities in the two pipes do not exceed the economic range while maintaining same total water flow rate. The following example shows how Solver can be used to solve this type-3 flow problem.

#### Example 5-2. Determining the economic diameter for a pipe

Pipe 2 in the system shown in Figure 5.2 is to be replaced by a new pipe which is also 36 m long and made of commercial steel. It is required to select the diameter of the new pipe such that the water velocities in both pipes do not exceed 2.8 m/s. For the same data given in Example 5-1 for pipe 1, determine the diameter of pipe 2 and the required pump power for the same total water flow rate of 0.03 m<sup>3</sup>/s.

#### Solution

Figure 5.6 shows the Excel sheet developed for this example with minor modifications to that developed for the previous example. Note that the data part now includes the total flow rate, which is 0.03 m<sup>3</sup>/s. Also note that there are now two changing variables which are Q<sub>1</sub> and D<sub>2</sub> given initial values of 0.01 m<sup>3</sup>/s and 0.04 m, respectively. The sheet calculates the velocities, Reynolds numbers, friction factors, and friction head losses in the two pipes and then determines the pump power (Power).

Power		fx = =p*g_*Q_total*(hf_1+(Z_B-Z_A))/η_p/1000										
	A	B	C	D	E	F	G	H	I	J	K	L
1												
2	Q_total	0.03	m <sup>3</sup> /s	Q_1	0.01	m <sup>3</sup> /s	Re_1	158519.6		Power	4.101211	kW
3	L_1	36	m	D_2	0.04	m	Re_2	634078.4				
4	D_1	0.08	m									
5	L_2	36	m	Q_2	0.02		ε_by_D_1	0.000563				
6	Z_A	5	m				ε_by_D_2	0.001125				
7	Z_B	13	m	A_1	0.005027							
8	η_p	0.7		V_1	1.989437		f_1	0.019547				
9	ρ	998	kg/m <sup>3</sup>				f_2	0.020651				
10	μ	1.00E-03	kg/m.s	A_2	0.001257							
11	ε	0.000045	m	V_2	15.91549		hf_1	1.774383				
12	g_	9.81	m/s <sup>2</sup>				hf_2	239.9489				
13												

Figure 5.6. Excel sheet for Example 5-2

Note that the initial water velocities in the two pipes are above the recommended value while  $h_{f1} \neq h_{f2}$ . Solver can be used to find the solution that satisfies the energy equation while reducing the water velocities in the two pipes to the economic range. Figure 5.7 shows Solver's parameters dialog box for this task. By leaving the **Set Objective** slot

blank, Solver will iterate to satisfy the three imposed constraints. Figure 5.8 shows the solution determined by Solver with this set-up by using the **GRG Nonlinear** method.

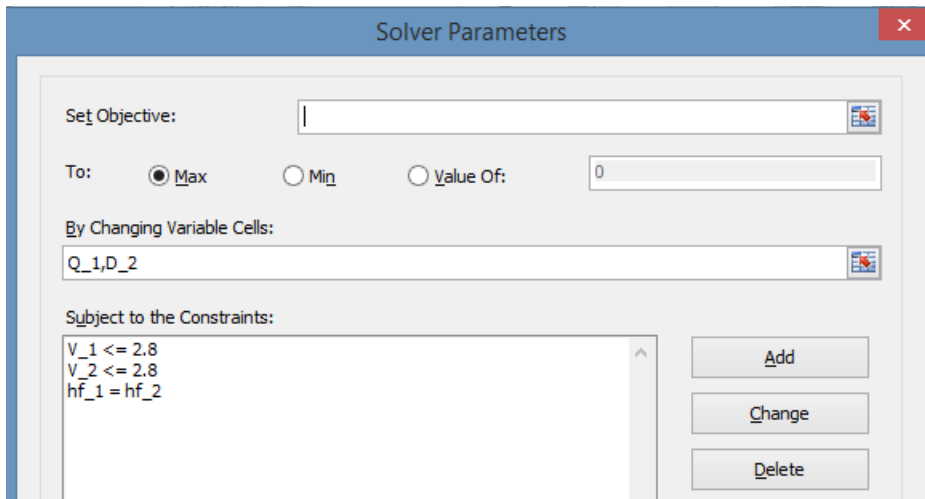


Figure 5.7. Solver set-up for Example 5-2

	A	B	C	D	E	F	G	H	I	J	K	L
1												
2	Q_total	0.03	m <sup>3</sup> /s	Q_1	0.012667	m <sup>3</sup> /s	Re_1	200795.2		Power	4.525542	kW
3	L_1	36	m	D_2	0.090087	m	Re_2	243998.5				
4	D_1	0.08	m									
5	L_2	36	m	Q_2	0.017333		ε_by_D_1	0.000563				
6	Z_A	5	m				ε_by_D_2	0.0005				
7	Z_B	13	m	A_1	0.005027							
8	η_p	0.7		V_1	2.52		f_1	0.019126				
9	ρ	998	kg/m <sup>3</sup>				f_2	0.018496				
10	μ	1.00E-03	kg/m.s	A_2	0.006374							
11	ε	0.000045	m	V_2	2.719334		hf_1	2.785687				
12	g	9.81	m/s <sup>2</sup>				hf_2	2.785793				
13												

Figure 5.8. Solver solution for Example 5-2

According to this solution, the diameter of pipe 2 is 9.0 cm at which the water velocities in the two pipes are  $V_1=2.52$  m/s and  $V_2=2.72$  m/s. Note that the new diameter for pipe 2 is more than twice its initial diameter of 4 cm. Also note that, due to reduced velocities in the two pipes, the pump power has reduced to 4.52 kW. Although the larger diameter increases the pipe's initial cost, it reduces the overall lifetime cost by reducing the pump power and the required energy cost.

With the water velocities now within the economic range, the objective of our present analysis has been achieved. However, the fact that resulting pump power barely exceeds half its capacity, which is 8 kW, raises another issue of practical concern. Running the pump at half its full capacity is bound to reduce its efficiency because

every pump achieves its best efficiency within a certain zone of operating conditions in terms of flow rate and head. The determination of the operating point for a pump-pipe system is dealt with in the following section.

## 5.2. The operating point for a pump-pipe system

The selection of the suitable type and size of a pump for meeting the required fluid flow rate and delivery pressure depends on the characteristics of both the pipe-system and the pump. The operating point for a pump-pipe system is the point at which the fluid's flow rate and pressure supplied by the pump match the required demand. To minimise electricity consumption of a pump, its operating point should be within the zone of its best efficiency. This section deals with the determination of operating point for a single centrifugal pump connected to a single pipe, to two pipes that branch at the pump's discharge, or to a simple branched network that consists of three-pipes.

### 5.2.1. A centrifugal pump connected to a single pipe

Figure 5.9 shows a centrifugal pump that is connected to a single pipe. The pump supplies the pressure needed to overcome friction losses through the pipe so as to maintain the fluid flow.

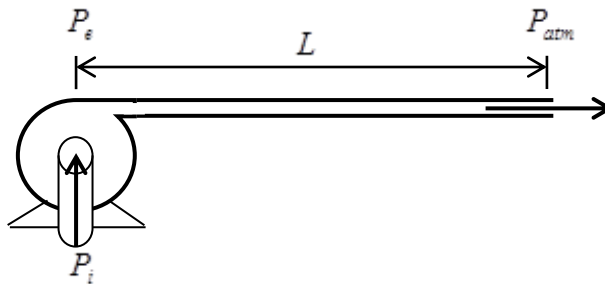


Figure 5.9. Pump-pipe system with a single pipe

The pump head  $h_p$  (in m) is defined as the head of fluid delivered by the pump, i.e.:

$$h_p = (P_e - P_i) / \gamma \quad (5.9)$$

Where  $P_i$  and  $P_e$  are the inlet and exit pressures, respectively, and  $\gamma$  is the specific weight of the fluid. The pump head is not constant for all flow conditions, but depends on the discharge. The curve that shows the relationship between the pump's head and its discharge at a given motor-speed is known as the pump characteristic curve. Figure 5.10 shows a typical characteristic curve for a centrifugal pump. Pump characteristic curves at different motor speeds are supplied by pump manufacturers or can be prepared by direct measurement. Figure 5.10 shows that the maximum pump head is delivered at zero discharge and the head decreases as the discharge is increased. How much pump head is actually needed to overcome the friction loss ( $h_f$ ) and circulate the fluid through the pipe connected to it depends on:

1. The flow rate of the fluid  $Q$
2. The viscosity of the fluid  $\nu$  (which may depend on the fluid's temperature)
3. The diameter of the pipe  $D$
4. The length of the pipe  $L$
5. The roughness ( $\varepsilon$ ) of the pipe inside surface which depends on its material and surface finish

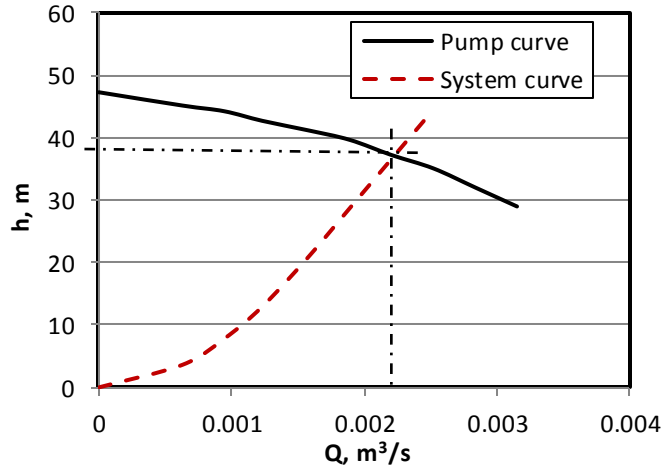


Figure 5.10. The operating point for a centrifugal pump as determined by its characteristic curve and the system curve

The relationship between the frictional losses through the pipe and the flow rate of the fluid being transported is called the system curve. The system curve is obtained by calculating the friction loss  $h_f$  at different fluid flow rates and plotting it versus  $Q$  as shown in Figure 5.10. As the figure shows, the friction loss is zero at no discharge and increases as the discharge is increased. The operating point for the pump is that at which its curve crosses the system curve. At the operating point:

$$h_p = h_{f, total} = h_f + h_c \quad (5.10)$$

Where  $h_f$  and  $h_c$  refer to the friction head losses in the pipe and the components, respectively, which are given by Equation (1.21) and Equation (1.29), respectively.

The power of the pump  $\dot{W}$  at any given flow rate  $Q$  and pump head  $h_p$  is given by the power equation:

$$\dot{W}_p = \rho Q h_p / \eta \quad (5.11)$$

Where  $\eta$  is the pump efficiency. Although the same pump can be used to meet different system curves, the pump efficiency reaches its maximum value at a certain flow rate and a certain head. If we try to operate the pump at load requirements ( $Q$  and  $h_p$ ) which are different those values, then the pump efficiency will drop. Therefore, it is important to have the operating point of the pump-pipe system as close as possible to the point of its best-efficiency.

The operating point of a pump-pipe system can be determined graphically by plotting the pump curve and the system curve on the same graph as shown in Figure 5.10. However, the point can be determined more accurately by representing the pump curve by a mathematical relationship between the pump head  $h_p$  and discharge  $Q$ . Using this  $h_p$ - $Q$  relationship, together with Equation (5.10), the operation point can be determined by iteration. The following example illustrates how Excel's Goal Seek command can be used to determine the operating point for a pump-pipe system that consists of a single pump connected to single pipe. The case is given by Suryanarayana and Arici [4].

**Example 5-3. Operating point for centrifugal a pump connected to a single pipe**

A centrifugal pump is to supply water at ( $\rho = 1000 \text{ kg/m}^3$ ,  $\nu = 1.02 \times 10^{-6}$ ) through a single pipe that has the following specifications:

- Length, 100 m
- Diameter, 2.5 cm
- Roughness, 0.046 mm

According to the manufacturer, the characteristic curve of the pump is given by the following table:

Flow rate (m <sup>3</sup> /s)	Pump head (m)
0.0	47.24
6.3080E-04	45.11
9.4620E-04	44.2
1.2316E-03	42.67
1.5770E-03	41.15
1.8924E-03	39.62
2.2078E-03	37.19
2.5232E-03	35.05
2.8386E-03	32.00
3.1540E-03	28.96

It is desired to determine the operating point and the required power for the pump while ignoring component losses.

**The analytical model**

Since there are no component losses, the friction head is obtained from Equation (1.21) after we establish whether the flow is laminar or turbulent from the value of the Reynolds number. In order to obtain a solution via Goal Seek, the pump head has to be expressed as a function of the flow rate. From the pump data shown above, Suryanarayana and Arici [4] obtained the following polynomial:

$$h_p = 47.22 - 2.985 \times 10^3 Q - 1.549 \times 10^5 Q^2 - 2.348 \times 10^8 Q^3 \quad (5.12)$$

The sought flow rate ( $Q$ ) should be such that the calculated friction head loss in the pipe is equal to pump head as obtained from Equation (5.12). The iterative solution goes as follows:

1. Given an initial guess for the discharge, calculate the water velocity ( $V = Q/A$ )
2. Calculate the Reynolds number and the friction factor  $f$
3. Calculate the corresponding friction loss  $h_f$  from Equation (1.21)
4. Determine the pump head from Equation (5.12)
5. Calculate the difference between the pump head and the friction losses, which is supposed to be zero at the operating point.

It is unlikely that our first guess will be the correct discharge at the operating point. Therefore, the above procedure has to be repeated by using a new value for the discharge until the difference between  $h_f$  and  $h_p$  becomes sufficiently small.

**Excel implementation**

Figure 5.11 shows the Excel sheet developed for solving this example. The data part of the sheet shows the data provided for the pipe and the fluid which is water. Figure 5.11 shows how the calculation part of the Excel sheet executes the iterative procedure described above with an initial guess for the discharge of  $Q = 1.0 \times 10^{-3} \text{ m}^3/\text{s}$ . The figure shows that there is a difference of 21.51 m between the system head ( $h_f$ ) and the pump head ( $h_p$ ).

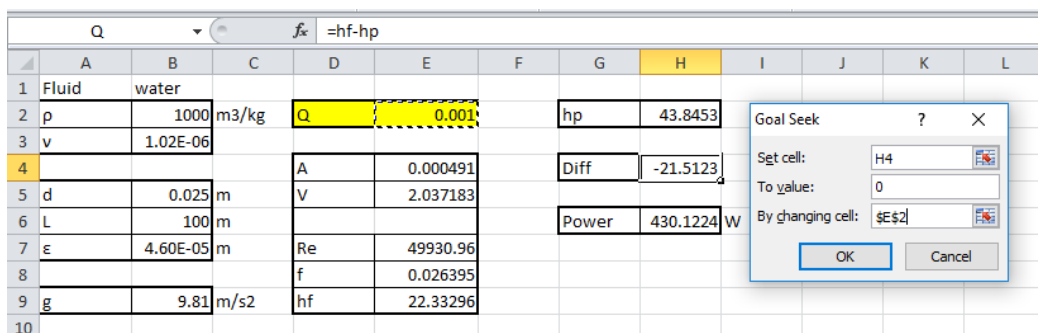


Figure 5.11. Excel sheet and Goal Seek set-up for Example 5-3

Goal Seek can be used to find the value of  $Q$  at which the difference between  $h_f$  and  $h_p$  becomes approximately zero. Figure 5.11 shows Goal Seek set-up for this task and Figure 5.12 shows the solution obtained by it. As the figure shows, Goal Seek finds the operating point at  $Q = 1.395 \times 10^{-3} \text{ m}^3/\text{s}$  and  $h_p = 42.12 \text{ m}$ . The corresponding power is  $576.29 \text{ W}$ . The flow rate is practically the same as that obtained by Suryanarayana and Arici [4] which is  $1.407 \times 10^{-3} \text{ m}^3/\text{s}$ .

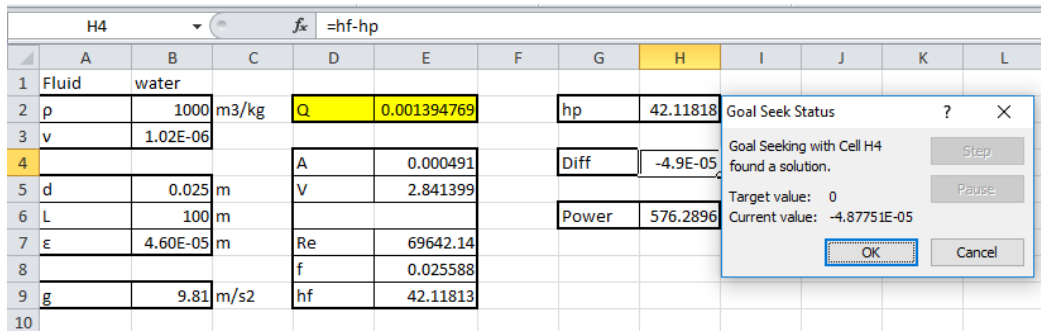


Figure 5.12. Solution obtained by Goal Seek for Example 5-3

### 5.2.2. A centrifugal pump connected to two branching pipes

Figure 5.13 shows a pump that discharges into two branching pipes of different diameters, lengths, and roughness. It is required to determine the operating point for the pump and how the pump's discharge will be divided between the two pipes. To simplify the analysis, it is assumed that the two pipes lie on a horizontal plane and that the two pipes discharge at the atmospheric pressure. This case is also given by Suryanarayana and Arici [4].

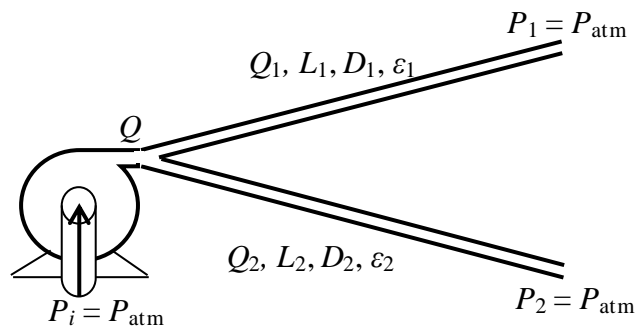


Figure 5.13. A centrifugal pump connected to two parallel pipes

#### The analytical model

From the values of the flow rate in pipe 1 ( $Q_1$ ) and in pipe 1 ( $Q_2$ ), the total flow rate ( $Q$ ) can be calculated as:

$$Q = Q_1 + Q_2 \tag{5.13}$$



The friction head loss in each pipe can be obtained from Equation (1.21):

$$h_{f1} = f_1 \frac{L_1 V_1^2}{D_1 2g} \quad (5.14)$$

$$h_{f2} = f_2 \frac{L_2 V_2^2}{D_2 2g} \quad (5.15)$$

Since the pressures at both ends of the two pipes are the same, the friction head losses in the two pipes must be the same and equal to the pump head, i.e.:

$$h_{f1} = h_{f2} = h_p \quad (5.16)$$

### Excel implementation

Equation (5.16) will be satisfied at the correct values of  $Q_1$  and  $Q_2$ , but both flow rates are unknown and, therefore, the following iterative solution is required:

1. Assume values for  $Q_1$  and  $Q_2$
2. Calculate the total flow rate  $Q$  from Equation (5.12)
3. Calculate  $V_1$  and  $V_2$  and determine the Reynolds number in the two pipes,  $Re_1$  and  $Re_2$
4. Determine the friction factors in the two pipes,  $f_1$  and  $f_2$ , from the corresponding Reynolds numbers using Equation (1.24)
5. Determine the friction losses in the two pipes,  $h_{f1}$  and  $h_{f2}$
6. Determine the pump head  $h_p$  from the pump curve, e.g., Equation (5.12)
7. If  $h_{f1} \neq h_{f2}$ , or  $h_{f1} \neq h_p$ , go back to step 1

After the operating point is determined, the power required by the pump can be obtained from the power equation as follows:

$$\dot{W}_p = \rho g Q h_p \quad (5.17)$$

Alternatively, the pump power can be calculated from the pipes flow rates and friction losses as follows:

$$\dot{W}_p = \rho g (Q_1 h_{f1} + Q_2 h_{f2}) \quad (5.18)$$

Suryanarayana and Arici [4] analysed the performance of the pump-pipe systems shown in Figure 5.13 by following a slightly different iterative process. They also adopted a different formula for the friction factor than Equation (1.24). The data of their example will be used to demonstrate the procedure for using Excel-Solver in the analysis.

**Example 5-4. Operating point for a pump with two parallel pipes**

A pump-two-pipe system as shown in Figure 5.13 has the following dimensions.

$$D_1 = 0.025\text{m} \quad L_1 = 500\text{m} \quad \varepsilon_1 = 15 \times 10^{-6}\text{m}$$

$$D_2 = 0.05\text{m} \quad L_2 = 1,000\text{m} \quad \varepsilon_2 = 46 \times 10^{-6}\text{m}$$

The system carries water ( $\rho = 1000 \text{ kg/m}^3$ ,  $\nu = 1.02 \times 10^{-6}$ ). If the pump has the same characteristic formula expressed by Equation (5.12), determine the flow rates in the two branches and the power required by the pump.

**The Excel sheet**

The Excel sheet developed for this example is shown in Figure 5.14. The data part contains the data for the two pipes and the transported fluid, which is water. The sheet shows the calculations based on assumed values of  $Q_1 = Q_2 = 0.001 \text{ m}^3/\text{s}$ . The velocities, Reynolds number, friction factors and friction head losses are calculated on the basis of these assumed flow rates. With the guessed flow rates, the friction losses in the two pipes,  $h_{f1}$  and  $h_{f2}$ , and the pump head,  $h_p$ , have three different values. The formula bar shows the formula in cell M5 that calculates the difference between the head losses in pipe 1 and the head produced by the pump as 58.066 m. Also, note that Equations (5.17) and (5.18) give two different values for the pump power in cells M7 and M9.

	A	B	C	D	E	F	G	H	I	J	K	L	M	N
1														
2	d_1	0.025	d_2	0.05	Q_1	0.001	Q_2	0.001	Q_p	0.002				
3	L_1	500	L_2	1000										
4	ε_1	1.50E-05	ε_2	4.60E-05	A_1	0.000491	A_2	0.001963	h_p	38.752				
5					V_1	2.037183	V_2	0.509296	Diff	58.06604				
6	ρ	1000												
7	ν	1.00E-06			Re_1	50929.58	Re_2	25464.79	W_pump	760.3142	W			
8	g	9.81												
9					f_1	0.022886	f_2	0.026694	W_pipe	1019.023	W			
10					hf_1	96.81804	hf_2	7.057945						
11														

Figure 5.14. Excel sheet developed for Example 5-4

The required flow rates  $Q_1$  and  $Q_2$  that satisfy Equation (5.16) can be found by using Solver. Figure 5.15 shows the set-up for Solver that requires it to find values of  $Q_1$  and  $Q_2$  that reduces the difference between  $h_{f1}$  and  $h_p$  to zero while satisfying the constraint that the head losses in the two pipes  $h_{f1}$  and  $h_{f2}$  are equal according to Equation (5.16). The solution found by the GRG Nonlinear method is shown in Figure 5.16 according to which the two values of the power required by the pump at the operating point as determined by Equations (5.17) and (5.18) are the same and equal to 894.04 W. The flow rates in the two pipes are  $Q_1 = 0.000547 \text{ m}^3/\text{s}$  and  $Q_2 = 0.002279 \text{ m}^3/\text{s}$ , and  $h_p = 32.24 \text{ m}$ . The corresponding values found by Suryanarayana and Arici [4] are  $Q_1 =$

$0.0005738 \text{ m}^3/\text{s}$ ,  $Q_2 = 0.002325 \text{ m}^3/\text{s}$ , and  $h_p = 32.85 \text{ m}$ . The slight differences can be attributed to the fact that Suryanarayana and Arici [4] used a different formula for calculating the friction factor.

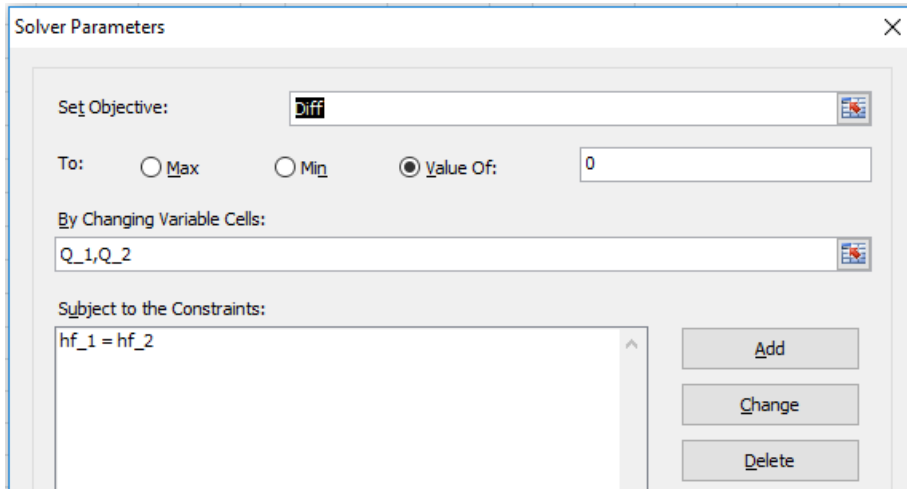


Figure 5.15. Solver set-up for Example 5-4

	A	B	C	D	E	F	G	H	I	J	K	L	M	N
1														
2	d_1	0.025	d_2	0.05	Q_1	0.000547	Q_2	0.002279	Q_p	0.002827				
3	L_1	500	L_2	1000										
4	$\epsilon_1$	1.50E-05	$\epsilon_2$	4.60E-05	A_1	0.000491	A_2	0.001963	h_p	32.2428				
5					V_1	1.114559	V_2	1.160913	Diff	3.01E-06				
6	$\rho$	1000												
7	v	1.00E-06			Re_1	27863.98	Re_2	58045.64	W_pump	894.0446	W			
8	g	9.81												
9					f_1	0.025462	f_2	0.023469	W_pipe	894.0464	W			
10					hf_1	32.2428	hf_2	32.24288						
11														

Figure 5.16. Solver solution for Example 5-4

It should be mentioned that it was necessary in this example to use the automatic-scaling option of Solver with the GRG Nonlinear method so as to find the solution. Apparently, this is due to the use of Equation (5.12).

### 5.2.3. A centrifugal pump connected to a simple-pipe network

Figure 5.17 shows a pump connected to a simple pipe network that consists of three pipes meeting at a junction J as shown in the figure which can either be specified or left to be determined by the analysis. For simplification, the three network pipes are assumed to be in a horizontal plane but they can have different lengths, diameters, and roughness. The operating point for the pump

can be determined by simultaneously satisfying the principles of mass and energy conservation and the pump characteristic curve.

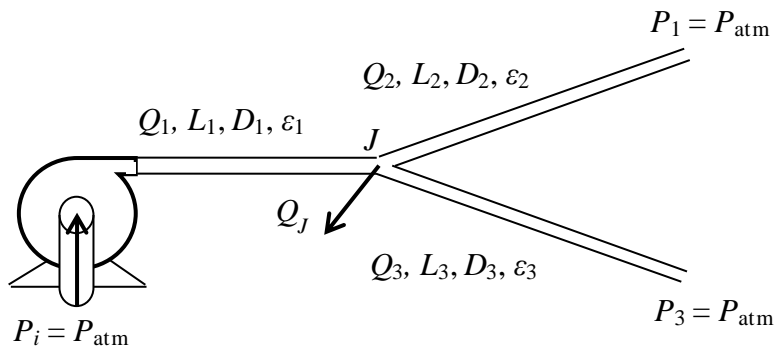


Figure 5.17. A centrifugal pump connected to a simple pipe-network

### The analytical model

The conservation of mass for a steady-flow of an incompressible fluid gives:

$$Q_1 = Q_2 + Q_3 + Q_J \quad (5.19)$$

Where the flow rates  $Q_1$ ,  $Q_2$ ,  $Q_3$ , and  $Q_J$  are as shown in Figure 5.17. If three of the flow rates are specified, the fourth can be calculated from the above equation.

Since the pressures at the inlet of pipe 2 and pipe 3 are the same, and the pressures at their discharge points are both atmospheric, the energy equation leads to:

$$h_{f2} = h_{f3} \quad (5.20)$$

At the operating point, the power required by the pump to balance the friction losses in the network can be calculated from.

$$\dot{W}_p = \rho g Q_1 h_p \quad (5.21)$$

Alternatively, it can be obtained from:

$$\dot{W}_p = \rho g (Q_1 h_{f1} + Q_2 h_{f2} + Q_3 h_{f3}) \quad (5.22)$$

The requirement that the two values of the pump power determined by Equations (5.21) and (5.22) should be equal provides another constraint on the iterative process besides Equation (5.20). The following example shows how Solver can be used to solve the problem.

**Example 5-5. Centrifugal pump connected to a simple-pipe network**

The pump-system shown in Figure 5.17 carries water ( $\rho = 1000 \text{ kg/m}^3$ ,  $\nu = 1 \times 10^{-6}$ ) and its three pipes have the following dimensions.

$$D_1 = 0.05\text{m} \quad L_1 = 500\text{m} \quad \varepsilon_1 = 46 \times 10^{-6}\text{m}$$

$$D_2 = 0.025\text{m} \quad L_2 = 500\text{m} \quad \varepsilon_2 = 15 \times 10^{-6}\text{m}$$

$$D_3 = 0.03\text{m} \quad L_3 = 500\text{m} \quad \varepsilon_3 = 46 \times 10^{-6}\text{m}$$

The network supplies a demand of  $0.0002 \text{ m}^3/\text{s}$  at the junction J. If the pump has the same characteristic formula expressed by Equation (5.12), determine the operating point and the power required by the pump.

**The Excel sheet**

The Excel sheet developed for this example is shown in Figure 5.18. The sheet extends that developed for Example 5-4 by adding the data and the calculations relevant to the third pipe and the flow rate at the junction ( $Q_J$ ). The calculations start by guessed values for  $Q_1 = 0.001 \text{ m}^3/\text{s}$  and  $Q_2 = 0.0005 \text{ m}^3/\text{s}$ . As the formula bar shows,  $Q_3$  is determined from Equation (5.19). The sheet then calculates the velocities, Reynolds numbers, friction factors and friction losses in the three pipes from the Darcy-Weisbach equation using the relevant data. At the guessed value of the flow rate ( $Q = Q_1$ ), the sheet calculates pump power as “W\_pump” on the basis of Equation (5.21) and as “W\_pipe” on the basis of Equation (5.22).

W_pipe		fx = $\rho * g * (Q_1 * hf_1 + (Q_2 + Q_3) * hf_2)$													
	A	B	C	D	E	F	G	H	I	J	K	L	M	N	O
1															
2	d_1	0.05	Q_1	0.001	Q_2	0.0005	Q_3	0.0003	h_p	43.8453					
3	L_1	500													
4	$\varepsilon_1$	4.60E-05	A_1	0.001963	A_2	0.000491	A_3	0.000707	W_pump	430.1224	W				
5	d_2	0.025	V_1	0.509296	V_2	1.018592	V_3	0.424413							
6	L_2	500							W_pipe	250.7246	W				
7	$\varepsilon_2$	1.50E-05	Re_1	24965.48	Re_2	24965.48	Re_3	12482.74							
8	d_3	0.03													
9	L_3	500	f_1	0.026791	f_2	0.026021	f_3	0.031953							
10	$\varepsilon_3$	4.60E-05	hf_1	3.541791	hf_2	27.52033	hf_3	4.889218							
11	Q_J	0.0002													
12	$\rho$	1000													
13	$\nu$	1.02E-06													
14	g	9.81													
15															

Figure 5.18. Excel sheet developed for Example 5-5

Values of  $h_{f1}$ ,  $h_{f2}$ ,  $h_{f3}$ , and  $h_p$  shown in Figure 5.18 indicate that Equation (5.20) is not satisfied with the guessed flow rates. The two values of the pump power determined by Equations (5.21) and (5.22), i.e., W\_pump and W\_pipe, are also different. Solver can be used in order to find the flow rates that satisfy these two conditions. Figure 5.19 shows

the set-up that requires Solver to find the values of  $Q_1$  and  $Q_2$  that makes the difference between  $h_{f2}$  and  $h_{f3}$  diminishes (Equation (5.20)) while making pump power determined by Equation (5.21), which is  $W_{\text{pump}}$ , equal to that determined by Equation (5.22), which is  $W_{\text{pipe}}$ .

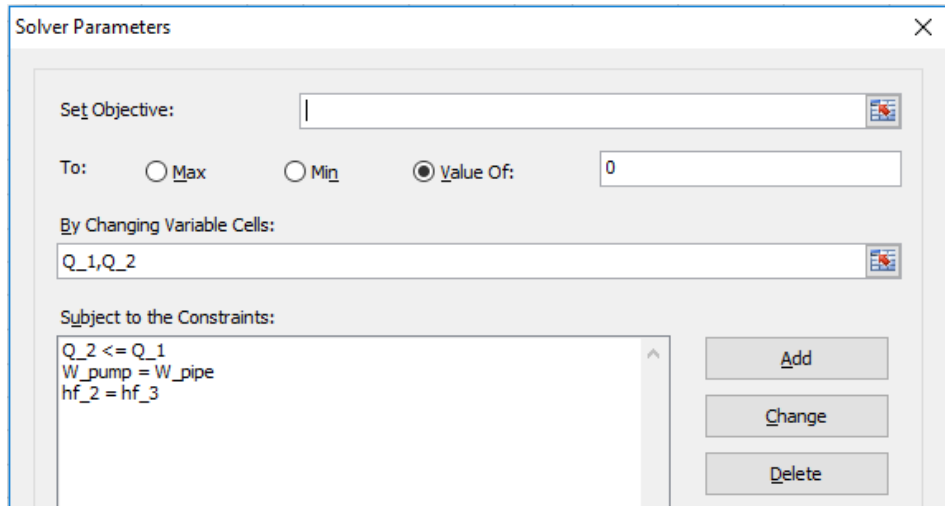


Figure 5.19. Solver set-up for Example 5-5

A third constraint has been added that requires  $Q_2 \leq Q_1$  so as to ensure a physically acceptable solution. By leaving the **Set Objective** blank, Solver will iterate so as to find the solution that satisfies the three specified constraints. Figure 5.20 shows the solution found by Solver with the GRG Nonlinear method with the automatic-scaling option.

	A	B	C	D	E	F	G	H	I	J	K	L	M	N	O
1															
2	d <sub>1</sub>	0.05	Q <sub>1</sub>	0.001671	Q <sub>2</sub>	0.00058	Q <sub>3</sub>	0.000892	h <sub>p</sub>	40.70285					
3	L <sub>1</sub>	500	A <sub>1</sub>	0.001963	A <sub>2</sub>	0.000491	A <sub>3</sub>	0.000707	W <sub>pump</sub>	667.3064	W				
4	ε <sub>1</sub>	4.60E-05	V <sub>1</sub>	0.851141	V <sub>2</sub>	1.180799	V <sub>3</sub>	1.261339	W <sub>pipe</sub>	667.3065	W				
5	d <sub>2</sub>	0.025	Re <sub>1</sub>	41722.6	Re <sub>2</sub>	28941.16	Re <sub>3</sub>	37098.21							
6	L <sub>2</sub>	500	f <sub>1</sub>	0.024584	f <sub>2</sub>	0.025276	f <sub>3</sub>	0.026582							
7	ε <sub>2</sub>	1.50E-05	hf <sub>1</sub>	9.077395	hf <sub>2</sub>	35.9247	hf <sub>3</sub>	35.9247							
8	d <sub>3</sub>	0.03													
9	L <sub>3</sub>	500													
10	ε <sub>3</sub>	4.60E-05													
11	Q <sub>J</sub>	0.0002													
12	p	1000													
13	v	1.02E-06													
14	g	9.81													
15															

Figure 5.20. The solution determined by Solver for Example 5-5

According to this solution,  $Q_1 = 0.001671$ ,  $Q_2 = 0.00058$  and  $Q_3 = 0.000892$  m<sup>3</sup>/s. Judging from the Reynolds numbers in the three pipes, all pipe flows are turbulent. At

the flow rates obtained for the three pipes, the friction losses in pipe 2 and pipe 3 are both equal to 35.9247 m, while the total friction head to be provided by the pump is 40.70285 m. As should be the case, both Equations (5.21) and (5.22) determine the pump power as 667.31 W.

In this example the discharge at the pipes junction has been specified, but it is also possible to allow it to be determined by Solver. In such a case, there will be three adjustable cells for the three flow rates,  $Q_2$ ,  $Q_3$ , and  $Q_J$  or  $Q_1$ . Also note that the method can be applied when the pipes are not on the same horizontal plane.

### 5.3. Centrifugal pumps in serial and parallel arrangements

Practical considerations may require the use of two or more smaller pumps instead of a single large pump. Proper application of the energy equation together with the continuity equation and the pump characteristic equations also enables the pumps operating point to be determined. This section shows how Excel and Solver can be used to determine the operating point for two centrifugal pumps in parallel and in series.

#### 5.3.2. Two centrifugal pumps connected in parallel

Figure 5.21 shows two identical pumps connected in parallel with the characteristic curves for a single pump and for the two parallel pumps. As Figure 5.21.b shows, the operating point shifts from point A for a single pump to point B for the two pumps. The two pumps give a larger flow rate and a higher head compared to the single pump.

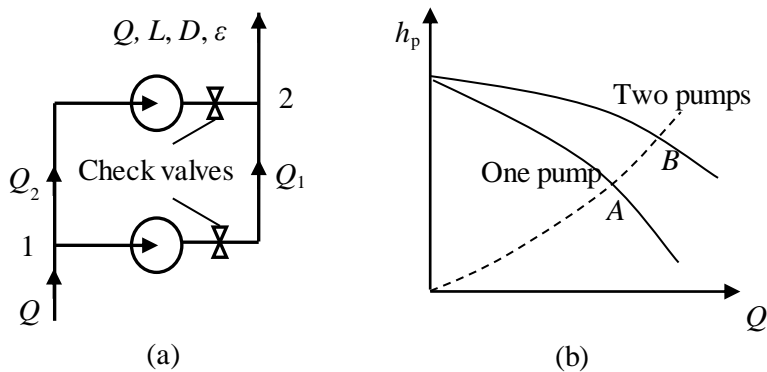


Figure 5.21. Two centrifugal pumps connected in parallel and their characteristic curve

#### Example 5-6. Operating point for two pumps in parallel

The pump-pipe system shown in Figure 5.21 carries water at 25°C in a horizontal pipe. The two pumps are identical and have the characteristic curve given by Equation (5.12). The length and roughness of the pipe are 100 m and 0.046 mm, respectively. For economic reasons it is desired to keep the water velocity in the pipe below 2.8 m/s by selecting a suitable diameter for the pipe. Determine the operating point of the system, the diameter of the pipe, and the power requirement of the two pumps.

**The analytical model**

For a steady flow of an incompressible fluid in the common pipe, mass conservation leads to:

$$Q = Q_1 + Q_2 \tag{5.23}$$

Parallel arrangement of pumps is referred to as "flow-rate additive" [3] because the combined flow rate in the system is the addition of those of the individuals pump as indicated by Equation (5.23). For two identical pumps running at the same speed:

$$Q_1 = Q_2 = Q / 2 \tag{5.24}$$

Neglecting the small loss in the pipe joining the two pumps and assuming no losses within the two pumps, the energy equation applied between points 1 and 2 leads to:

$$h_{p,1} = h_{p,2} = h_p \tag{5.25}$$

At the operating point, the friction head loss in the pipe equals the head delivered by one pump, i.e.:

$$h_f = h_{p,1} = h_{p,2} \tag{5.26}$$

**The Excel sheet**

The data part of the Excel sheet shown in Figure 5.22 gives the length of the main pipe, but not its diameter. The calculations start with assumed values for flow rate,  $Q = 0.001 \text{ m}^3/\text{s}$ , and pipe-diameter,  $d = 0.025 \text{ m}$ . Based on these initial values, the water velocity in the pipe and the corresponding Reynolds number are determined.

	A	B	C	D	E	F	G	H	I
1	Fluid	Water							
2	$\rho$	1000		Q	0.001		Q_1	0.0005	
3	v	1.02E-06		d	0.025 m		Q_2	0.0005	
4									
5	L	100 m		A	0.000491		h_p1	45.65943	
6	$\epsilon$	4.60E-05		V	2.037183		h_p2	45.65943	
7									
8	g	9.81 m/s <sup>2</sup>		Re	49930.96		Power	447.919 W	
9				f	0.026395				
10				hf	22.33296				
11									

Figure 5.22. Excel sheet developed for Example 5-6 (two pumps in parallel)



Since the total flow rate is divided equally between the two pumps as stated by Equation (5.24), the heads delivered by the two pumps,  $h_{p1}$  and  $h_{p2}$ , are equal as required by Equation (5.25). However, the friction head loss in the main pipe ( $h_f$ ) is not equal to the head supported by the pumps as required by Equation (5.26). Therefore, the flow rate,  $Q$ , and pipe diameter,  $d$ , have to be adjusted to values that satisfy Equation (5.25) as well as Equation (5.26) together with the condition that  $V \leq 2.8$  m/s. This can be done by using Solver and the required set-up is shown in Figure 5.23.

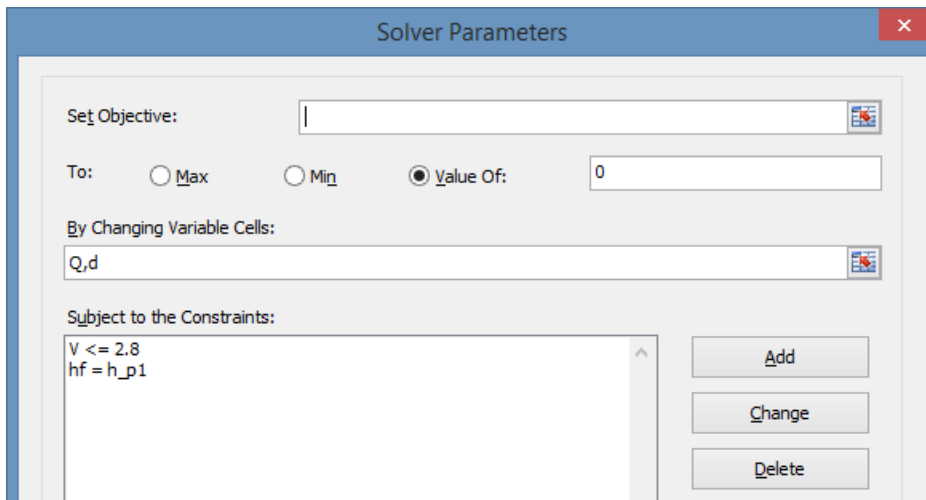


Figure 5.23. Solver set-up for Example 5-6 (two pumps in parallel)

Figure 5.24 shows the solution found by Solver that satisfied the two constraints. According to this solution, the flow rate is  $0.001 \text{ m}^3/\text{s}$ , the pipe diameter is 0.022 m, and the power requirement is 467.08 W. Due to the reduced water velocity, the required power is less than that of the single pump in Example 5-3 even though the pipe diameter is smaller.

	A	B	C	D	E	F	G	H	I
1	Fluid	Water							
2	$\rho$	1000		Q	0.001044		Q_1	0.000522	
3	v	1.02E-06		d	0.022083	m	Q_2	0.000522	
4									
5	L	100	m	A	0.000383		$h_{p1}$	45.58545	
6	$\epsilon$	4.60E-05		V	2.727112		$h_{p2}$	45.58545	
7									
8	g	9.81	m/s <sup>2</sup>	Re	59040.96		Power	467.0778	W
9				f	0.026556				
10				$h_f$	45.58547				
11									

Figure 5.24. Solver solution to Example 5-6 (two pumps in parallel)

### 5.3.3. Two centrifugal pumps connected in series

Two pumps are connected in series when the outlet of the first pump leads directly to the inlet of the second one as shown in Figure 5.25.a. As shown in Figure 5.25.b, the operating point of this arrangement also increases both the system's head and flow rate compared to those of a single pump.

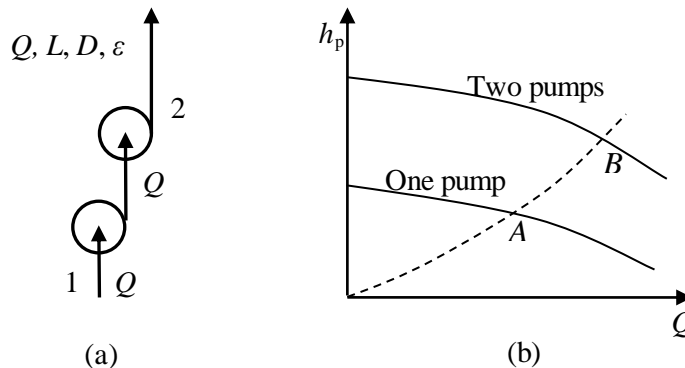


Figure 5.25. Two centrifugal pumps connected in series and their characteristic curve

#### Example 5-7. Operating point for two pumps in series

Two pumps are connected in series to a horizontal pipe that carries water at 25°C. The characteristic curve for both pumps is expressed by Equation (5.12). The pipe length and roughness are 100 cm and 0.046 mm, respectively. For economic reasons, it is desired to keep the velocity in the pipe below 2.8 m/s. Determine diameter of the pipe, the operating point of the system, and the power requirement of the two pumps.

#### The analytical model

For steady flow of an incompressible fluid in the system, mass conservation leads to:

$$Q = Q_1 = Q_2 \quad (5.27)$$

Neglecting the small loss in the pipe joining the two pumps and assuming no losses within the two pumps, the energy equation reduces to:

$$h_p = h_{p,1} + h_{p,2} \quad (5.28)$$

Pumps in series are called "pressure-additive" [3] because the total pressure in the pipe system is the addition of those of the individual pumps as indicated by Equation (5.28). At the operating point, the friction head loss in the pipe equals the head delivered by the two pumps, i.e.:

$$h_f = h_p = h_{p,1} + h_{p,2} \quad (5.29)$$

**Excel sheet**

The sheet developed for this example is shown in Figure 5.26. The data and calculations parts are similar to those in Example 5-6 but, instead of two flow rates in two pipes, in the present sheet the same flow rate  $Q$  passes through both pipes. Given initial values for the flow rate,  $Q$ , and pipe diameter,  $d$ , the sheet calculates the velocity ( $V$ ), Reynolds number ( $Re$ ), friction factor and head losses in the two pipes ( $hf$ ). The sheet then determines the pumps heads  $h_{p1}$  and  $h_{p2}$ , which are identical in this case.

hp		f <sub>c</sub> =h_p1+h_p2							
	A	B	C	D	E	F	G	H	I
1	Fluid	Water							
2	$\rho$	1000		Q	0.001		$h_{p1}$	43.8453	
3	$v$	1.02E-06		d	0.022	m	$h_{p2}$	43.8453	
4									
5	L	100	m	A	0.00038		hp	87.6906	
6	$\epsilon$	4.60E-05		V	2.63066				
7							Power	860.2448	W
8	g	9.81	m/s <sup>2</sup>	Re	56739.73				
9				f	0.026668				
10				hf	42.75617				
11									

Figure 5.26. Excel sheet developed for Example 5-7 (two pumps in series)

Figure 5.26 shows that there is a difference between the pumps' heads and the friction loss in the pipe which indicates that the guessed values are incorrect. Figure 5.27 shows the set-up for Solver for finding the values of  $Q$  and  $d$  that make the friction loss ( $hf$ ) equals the pump head ( $hp$ ) while keeping the velocity below 2.8 m/s. Figure 5.28 shows the solution obtained by Solver according to which the water flow rate is 0.388 litre per second, the pipe diameter is 0.013 m, and the pump power is 350.4 kW.

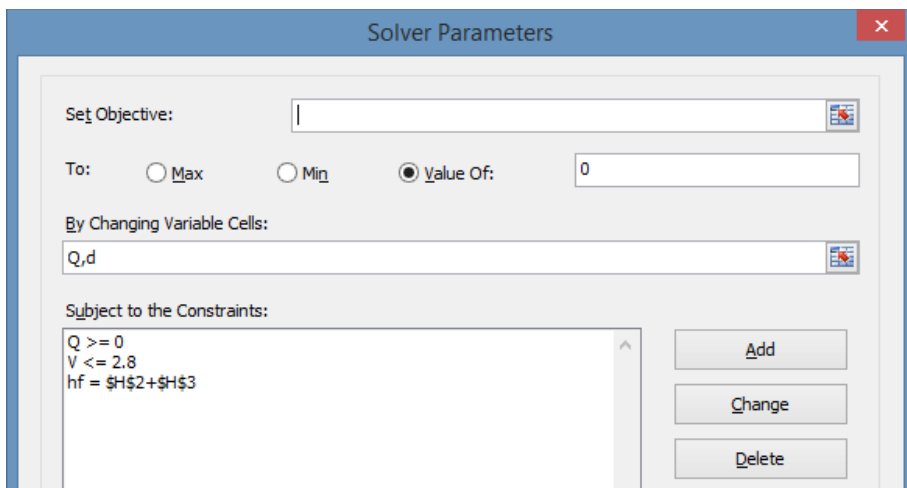


Figure 5.27. Solver set-up for Example 5-7 (two pumps in series)

	A	B	C	D	E	F	G	H	I
1	Fluid	Water							
2	$\rho$	1000		$Q$	0.000388		$h_{p1}$	46.02457	
3	$v$	1.02E-06		$d$	0.013284	m	$h_{p2}$	46.02457	
4									
5	$L$	100	m	$A$	0.000139		$h_p$	92.04913	
6	$\epsilon$	4.60E-05		$V$	2.799998				
7							Power	350.4264	W
8	$g$	9.81	m/s <sup>2</sup>	Re	36465.97				
9				$f$	0.030601				
10				$h_f$	92.04912				
11									

Figure 5.28. Solver solution for Example 5-7 (two pumps in series)

### 5.3.4. A comparison of serial and parallel pumps arrangements

Some general remarks on the performance characteristics of multiple pumps when they are arranged in parallel and in series can be extracted from the results obtained in the previous sections. Table 5.2 compares the calculated values for the water flow rate, pipe diameter, water velocity, friction loss, and pump power for the two pumps arranged in parallel and in series with those of a single pump. The results of shown in Table 5.2 for the single were obtained by modifying the sheet developed in Example 5-3 so as to determine the operating point and pipe diameter with the additional restriction that the pipe velocity does not exceed 2.8 m/s as required for the two pump arrangements. The solution was found with a similar Solver set-up to that shown in Figure 5.23.

Table 5.2. Operating conditions for a single pump, two pumps in parallel, and two pumps in series

Arrangement	$L$ (m)	$Q$ (l/s)	$D$ (m)	$V$ (m/s)	$h_p$ (m)	Power (W)
A single pump	100	1.04	0.022	2.68	43.667	447.295
Two pumps in parallel	100	1.04	0.022	2.72	45.585	467.078
Two pumps in parallel (2)	100	2.08	0.002	2.68	43.667	894.590
Two pumps in series	100	0.34	0.013	2.80	46.025	350.426
Two pumps in series (2)	181	1.06	0.022	2.80	87.168	910.168

The figures in Table 5.2 show that two pumps connected in parallel as shown in Figure 5.21 give the same flow rate as that of the single pump and do not require the pipe diameter to be changed. The slight increase in the water velocity lead to a slight increase in the pump head and, therefore, the required pump power increased from 447.3 W to 467.1 W, i.e., by 4.4 per cent. Since the second pump requires additional initial and maintenance costs, these results indicate that this pump can only be used as a stand-by pump. However, the second pump can be allowed to discharge in a separate pipe. Table 5.2 shows this option as “Two pumps in parallel (2)”. In this case, the water

velocity and pump-head will be the same as those of a single pump, but both the water flow rate and pump power will be doubled.

When the second pump is connected in series, the water flow rate dropped from 1.04 to only 0.34 litres per second and the required pipe diameter dropped from 22 cm to 13 cm. Although the pump-head increased by 5.4 per cent, the required pump power dropped by more than 21 per cent due to the reduced flow rate in the pipe. These results indicate that the two pumps are underutilised with this arrangement under the specified conditions. A more logical use for this pump arrangement is to keep the diameter of pipe unchanged but allow the length of the pipe to increase. A separate Excel sheet was developed for this scenario and its results with the imposed upper limit for the water velocity are shown in Table 5.2 as “Two pumps in series (2)”. As the figures show, the pipe length in this case can be increased to 181 m with a slightly higher water flow rate. However, both the pump head and power will be almost doubled.

#### 5.4. Closure

This chapter presented hydraulic analyses of multi-pipe and pump-pipe systems that require iterative solutions for simultaneously satisfying the continuity equation and the energy equation. The analyses that involved a single variable were solved by using Goal Seek, while the analyses dealing with multiple changing cells were solved by using Solver. All the analyses in this chapter applied the GRG Nonlinear method of Solver and required less than 5 iterations. Determining the operating point for a pump-pipe system by using the third-order pump curve formula in Equation (5.12) required the automatic-scaling feature of Solver to be used. In general, iterative solutions with the GRG Nonlinear method may also require using the multi-start option.

#### References

- [1] F. M., White, *Fluid Mechanics*, Seventh Edition, McGraw-Hill, 2011.
- [2] Y.A. Cengel and J.M. Cimbala, *Fluid Mechanics Fundamentals and Applications*, McGraw- Hill, 2006.
- [3] W.S. Janna, *Design of Fluid Thermal Systems*, 3<sup>rd</sup> Edition, CENGAGE Learning, 2011.
- [4] N. N. Suryanarayana, and O. A. Arici, *Design and Simulation of Thermal Systems*, McGraw-Hill, 2004.

#### Exercises

1. Water at 20°C ( $\rho = 998 \text{ kg/m}^3$  and  $\mu = 1.002 \times 10^{-3} \text{ kg/m}\cdot\text{s}$ ) is to be pumped from reservoir A ( $Z_A = 2 \text{ m}$ ) to reservoir B ( $Z_B = 9 \text{ m}$ ) through two 25-m-long pipes connected in parallel as shown in Figure 5.P1. The diameters of the two pipes are 3 cm and 5 cm. The motor–pump unit draws 7 kW of electric power during operation at 68% efficiency. The minor losses and the head loss in the pipes that connect the parallel pipes to the two reservoirs can be considered to be negligible.

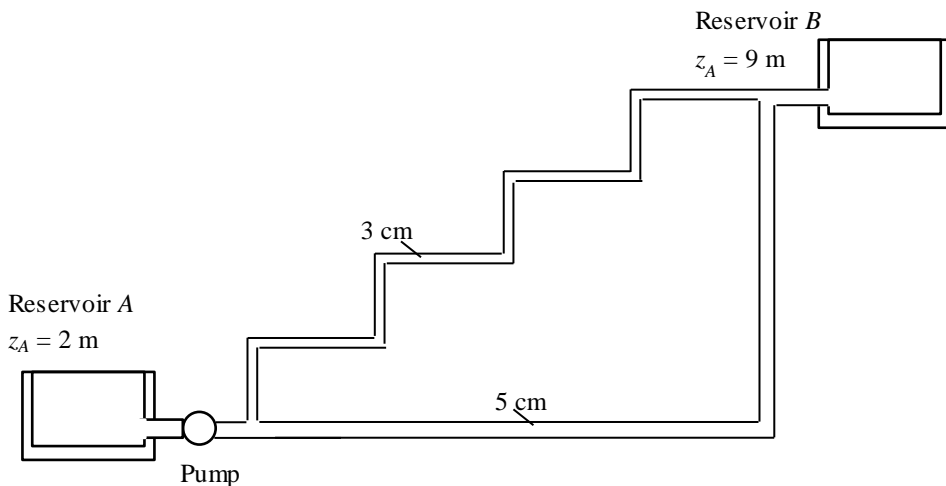


Figure 5.P1. Schematic for problem 5.1

Modify Excel sheet developed for Example 5-1 and use Solver to determine the total flow rate between the reservoirs and the flow rates through each of the parallel pipes for (a) plastic pipes, (b) commercial-steel pipes, and (c) cast-iron pipes. This exercise is based on Problem 8-68 in Cengel and Cimbala [2].

2. A certain part of cast iron piping of a water distribution system involves a parallel section as shown in Figure 5.P2. Both pipes have a diameter of 30 cm and the flow is fully turbulent. One of the branches (pipe A) is 1000 m long, while the other branch (pipe B) is 3000 m long. The flow rate through pipe A is  $0.4 \text{ m}^3/\text{s}$  and the water temperature is  $15^\circ\text{C}$  ( $\rho = 999.1 \text{ kg/m}^3$  and  $\mu = 1.138 \times 10^{-3} \text{ kg/m}\cdot\text{s}$ ).

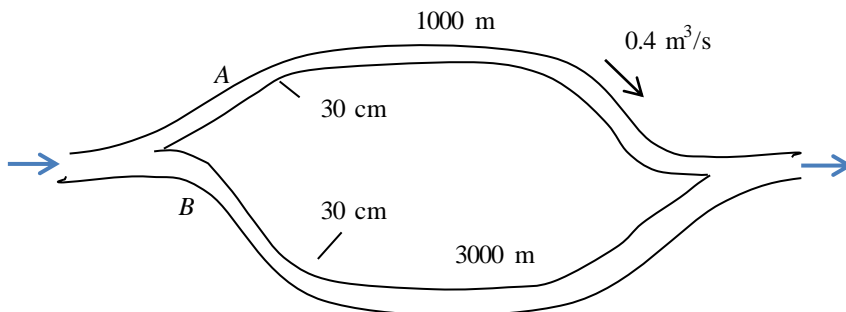


Figure 5.P2. Schematic for problem 5.2

Disregarding minor losses, develop an Excel sheet for analysing the system and use Solver to determine the flow rate through pipe B. Use the Swamee-Jain formula for the friction factor. This exercise is based on Problem 8-82 in Cengel and Cimbala [2]. Answer:  $0.231 \text{ m}^3/\text{s}$ .

3. Figure 5.P3 shows a pipeline that transports oil at  $40^{\circ}\text{C}$  ( $\rho = 876 \text{ kg/m}^3$  and  $\mu = 0.2177 \text{ kg/m}\cdot\text{s}$ ) at a rate of  $3 \text{ m}^3/\text{s}$ . The pipeline branches out into two parallel pipes made of commercial steel that reconnect downstream. Pipe A is 500 m long and has a diameter of 30 cm while pipe B is 800 m long and has a diameter of 45 cm. The minor losses are considered to be negligible. Develop an Excel sheet to determine the flow rate through each of the parallel pipes. This exercise is based on Problem 8-123 in Cengel and Cimbala [2]. Solution:  $Q_A = 0.91 \text{ m}^3/\text{s}$ ,  $Q_B = 2.09 \text{ m}^3/\text{s}$ .

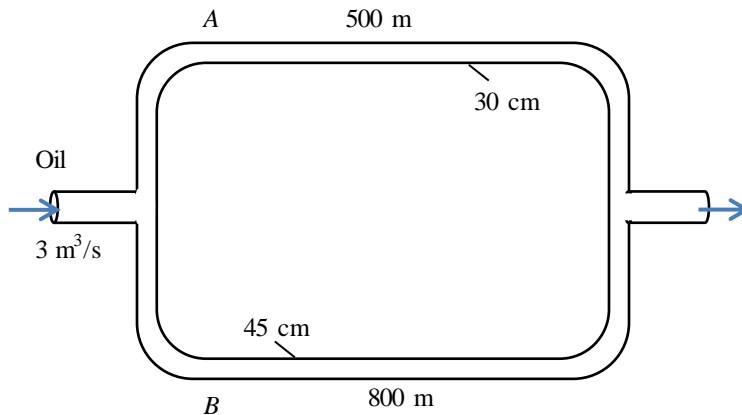


Figure 5.P3. Schematic for problem 5.3

4. The parallel galvanized-iron pipe system of Figure 5.P4 delivers gasoline at  $20^{\circ}\text{C}$  ( $\rho = 680 \text{ kg/m}^3$  and  $\mu = 2.9 \times 10^{-4} \text{ kg/m}\cdot\text{s}$ ) with a total flow rate of  $0.036 \text{ m}^3/\text{s}$ . If the pump is wide open and not running, with a loss coefficient  $K = 1.5$ , determine: (a) the flow rate in each pipe and (b) the overall pressure drop.

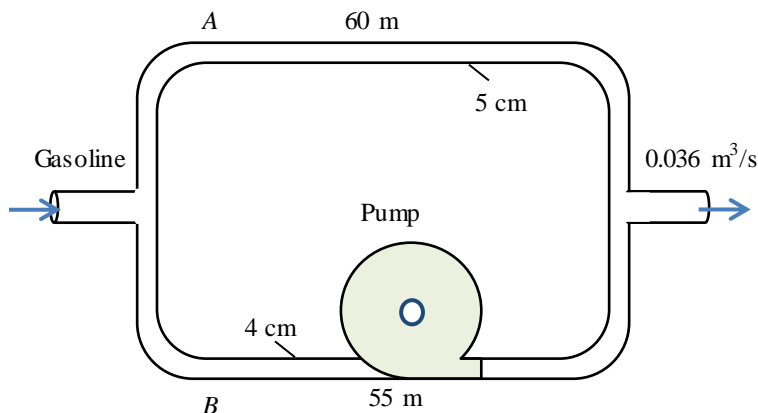


Figure 5.P4. Schematic for problem 5.4

This exercise is based on Problem 6-113 in White [1].

5. Solve Problem 5.4 with the following modification. Let the pump be running and delivering 45 kW to the flow in pipe 2. The fluid is gasoline at 20°C ( $\rho = 680 \text{ kg/m}^3$  and  $\mu = 2.9 \times 10^{-4} \text{ kg/m}\cdot\text{s}$ ). Determine (a) the flow rate in each pipe and (b) the overall pressure drop. This exercise is based on Problem 6-114 in White [1].
6. For the piping system shown in Figure 5.P6, all pipes are made of concrete with a roughness of 0.1 cm. Neglecting minor losses, compute the overall pressure drop  $p_1 - p_2$  in kPa if  $Q = 0.54 \text{ m}^3/\text{s}$ . The fluid is water at 20°C ( $\rho = 998 \text{ kg/m}^3$  and  $\mu = 1.002 \times 10^{-3} \text{ kg/m}\cdot\text{s}$ ). This exercise is based on Problem 6-118 in White [1].

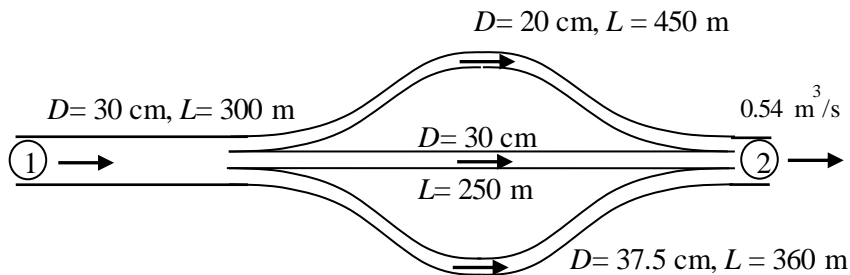


Figure 5.P6. Schematic for problem 5.6

7. Modify Problem 5.6 as follows: Let the pressure drop  $p_1 - p_2$  be 650 kPa. Neglecting minor losses, determine the flow rate in  $\text{m}^3/\text{h}$ .
8. Figure 5.P8 shows two commercial-steel pipes connected in parallel at points A and B. The pipe system transports water at 15°C at a flow rate ( $Q$ ) of  $1.2 \text{ m}^3/\text{s}$ . The length and diameter of pipe 1 are 1000 m and 50 cm, respectively. The length of pipe 2 is 1500 m. It is required to determine the diameter of pipe 2 such that the total pumping power ( $\dot{W}_p$ ) does not exceed 5 kW.

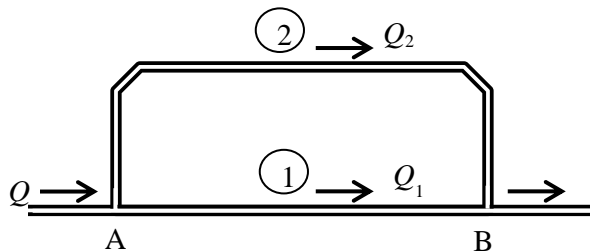


Figure 5.P8. Two pipes connected in parallel

Solve the problem by determining the friction factor ( $f$ ) from the following options:

- (a) Using a constant value for  $f = 0.015$  (Answer:  $D_2 \approx 33 \text{ cm}$ ).
- (b) Using the Swamee-Jain formula for the friction factor.
- (c) Using the Colebrook-White formula for the friction factor.



9. Using the pump characteristic curve given by Equation (5.12) and the Colebrook-White formula, develop an Excel sheet to determine the operating point for the pump-pipe system described in Example 5-1.
10. Figure 5.P10 shows three pumps connected in parallel to a horizontal 100-m-long commercial-steel pipe that carries water at 25°C. The three pumps are identical and their characteristic curve is given by Equation (5.12). For economic reasons it is desired to keep the water velocity in the common pipe below 2.8 m/s by selecting a suitable diameter for the pipe. Minor losses can be neglected. Use Excel and Solver to determine the operating point of the system, the diameter of the common pipe, and the power requirement of the three pumps.

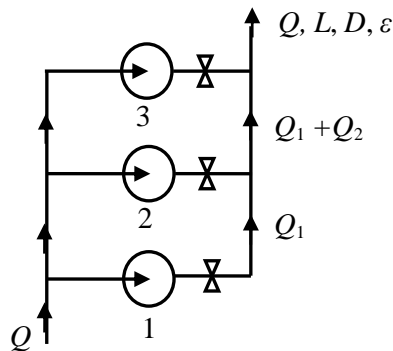


Figure 5.P10. Three centrifugal pumps connected in parallel

11. Figure 5.P11 shows three pumps connected in series to a horizontal commercial-steel pipe that has a diameter of 22 cm and carries water at 25°C. The characteristic curve for the three identical pumps is expressed by Equation (5.12). For economic reasons, it is desired to keep the velocity in the common pipe below 2.8 m/s. Minor losses can be neglected. Determine length of the common pipe, the operating point of the system, and the power requirement of the three pumps.

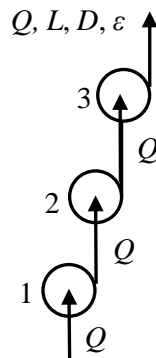


Figure 5.P11. Three centrifugal pumps connected in series

# 6

## **Hydraulic analyses of pipe networks**

Hydraulic analyses of pipe-network are based on the same principles applied in the previous chapter for analysing multi-pipe systems; which are the two principles of mass and energy conservation coupled with auxiliary formulae for determining the pipe friction. However, pipe-network analyses are more challenging because they involve more continuity equations and energy constraints to be simultaneously satisfied. Therefore, the analyses of practical pipe-networks require computer-aided numerical methods such as the Hardy-Cross method. Before introducing the Excel-aided method for pipe-network analyses, this chapter illustrates the limitation of mathematical analysis of looped pipe-networks by considering a simple network with three pipes. The chapter then presents the Excel-aided methodology that uses Solver to deal with the analyses of looped, branched, and mixed pipe networks.

### 6.1. The methodology of looped pipe-network analysis

Figure 6.1 shows two types of pipe network arrangements: (a) looped networks and (b) branched networks. The flow in the pipe network can be driven by the effect of gravity or by a motor-pump system. The connection points, called nodes, can be sources (supply points), sinks (demand or load points), or just junctions. The looped network in Figure 6.1.a has two sources, which are the reservoirs A and B, and six load points. The branched network in Figure 6.1.b has a single source, which is the pump A, and six load points. According to the notation scheme used in Figure 6.1, a single letter refers to a location or a pipe junction, e.g., A, B, etc., two letters refer to a pipe, e.g., AB, BC, etc., whereas numbers refer to pipe loops, e.g. loop 1, loop 2, etc.

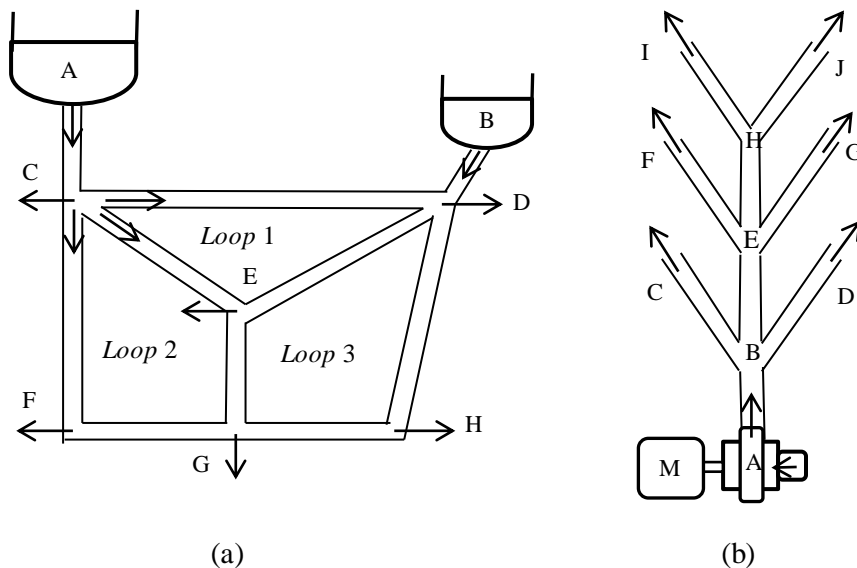


Figure 6.1. Pipe network arrangements: (a) looped and (b) branches networks

In a typical hydraulic analysis, the flow rates at the sources and outlets are given together with the lengths, diameters, and roughness of the pipes and the requirement is to determine the flow rates and pressure levels at the different nodes.

**The analytical model for a looped network**

In order to analyse the looped pipe network shown in Figure 6.1.a that has eight pipes, eight independent equations have to be formed from mass and energy balances. The continuity equation can be applied at two levels; (i) to the whole pipe network, and (ii) to any junction (node) in the network. Applied to the whole network shown in Figure 6.1.a for a steady flow of an incompressible fluid, the continuity equation leads to:

$$Q_A + Q_B = Q_C + Q_D + Q_E + Q_F + Q_G + Q_H \quad (6.1)$$

Applied to any junction in the network, the continuity equation requires the algebraic sum of all the flow rates meeting at the junction to be zero. For example, at junction C the equation becomes:

$$Q_C = Q_{AC} - Q_{CD} - Q_{CE} - Q_{CF} \quad (6.2)$$

Application of the continuity equation at the six nodes in the network shown in Figure 6.1.a leads to five (number of nodes minus 1) independent linear equations. The remaining three equations have to be obtained from the energy equation.

The general form of the energy equation, Equation (1.20), does not only account for the friction losses in the pipes, but also for the differences in elevations between the end points. However, for simplicity we will assume here that all pipes of the network under consideration are on the same horizontal plane. A special form of the energy equation can be written for a closed loop in which point B in the equation coincides with point A. In this case, the algebraic sum of the head losses in all the pipes forming a closed loop is balanced by any heads generated by inline booster pumps in the loop, i.e.,

$$\sum_1^M h_f = \sum_1^N h_p \quad (6.3)$$

Where  $M$  is the number of pipes forming the closed loop,  $N$  is the number of booster pumps in the loop,  $h_f$  is the head loss in each pipe (including the minor losses), and  $h_p$  is the head produced by a booster pump. When there is no booster pump within the loop, Equation (6.3) reduces to:

$$\sum_1^M h_f = 0 \quad (6.4)$$

Friction loss in a pipe ( $h_f$ ) can be determined by using the Darcy-Weisbach equation or the Hazen-Williams equation for pipes carrying water. Since we cannot be certain about the flow directions in the network pipes in advance, we have to assume them. The flow

directions of pipes CD, CE and CF in Figure 6.1.a are assumed directions. The true directions can only be confirmed after the analysis is done.

Applying Equation (6.4) to the three loops in the network provides the three (equal to the number of loops) additional equations needed to solve the problem. The solution of the eight equations should give the unknown values and directions of the flow rates in the eight pipes of the network. A positive flow value means that the assumed direction is correct and a negative value means that it has to be reversed. The following example illustrates the limitation of mathematical pipe-network analyses by considering a simple network that consists of only three pipes forming a single loop.

**Example 6-1. Mathematical analysis of a simple looped pipe network**

Figure 6.2 shows a pipe network that distributes water from a single source to two consumption points as shown in the figure. The friction factor for all three pipes can be taken as 0.025. Find the flow rates in the three pipes.

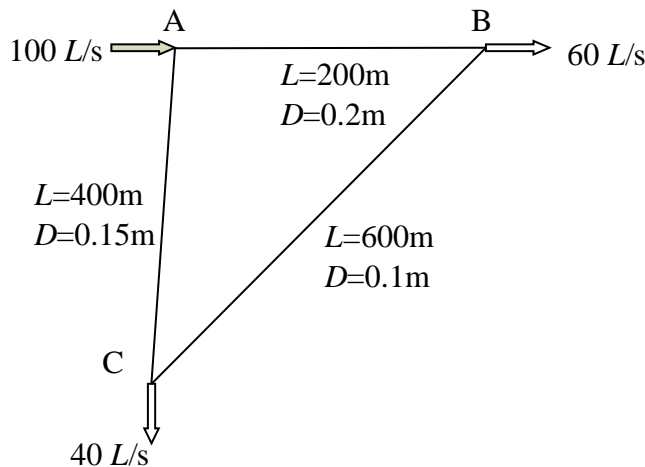


Figure 6.2. Pipe network in Example 6-1

**Solution**

For this simple network, there are only two possible flow arrangements depending on the flow direction in pipe BC as shown in Figures 6.3.a and 6.3.b. Since there are only three flow rates that have to be determined, three independent equations are needed to solve the problem. For this simple network, let us refer to pipe AB by pipe 1, pipe BC by pipe 2, and pipe AC by pipe 3. Starting with the arrangement shown in Figure 6.3.a, mass conservation leads to the following two equations:

$$Q_2 = Q_1 - 60 \tag{6.5}$$

$$Q_3 = 100 - Q_1 \tag{6.6}$$

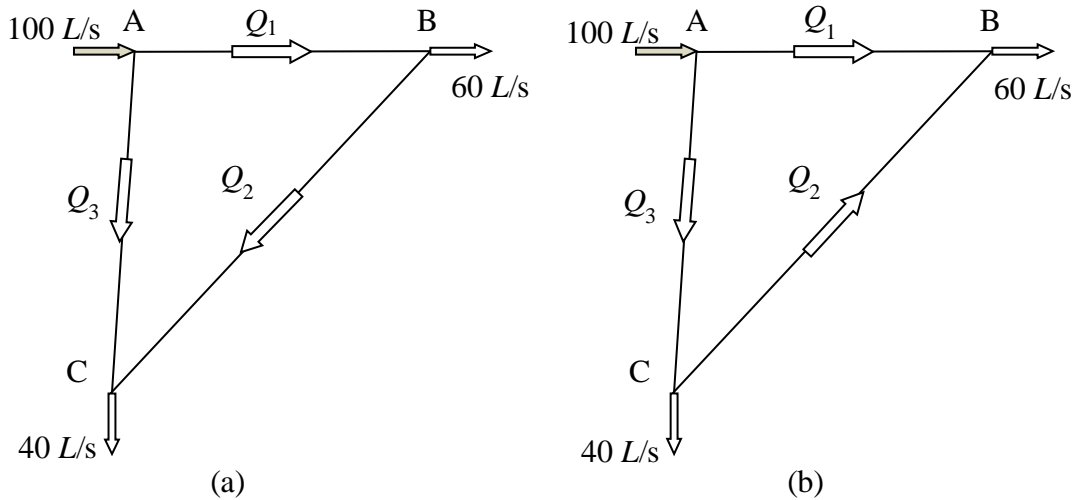


Figure 6.3. The two possible flow arrangements in the simple network

The third equation can be obtained by applying the energy equation (Equation (6.4)).

$$h_{f,1} + h_{f,2} - h_{f,3} = 0 \quad (6.7)$$

Equation (6.7) applies the sign convention that the two clockwise flows in pipes 1 and 2 are positive, while the counter clockwise flow in pipe 3 is negative. Using Equation (1.21) and substituting for  $V$  by  $Q/A$ , the equation becomes:

$$f_1 \frac{L_1}{D_1} \frac{Q_1^2}{2gA_1^2} + f_2 \frac{L_2}{D_2} \frac{Q_2^2}{2gA_2^2} - f_3 \frac{L_3}{D_3} \frac{Q_3^2}{2gA_3^2} = 0 \quad (6.8)$$

This equation can be put in the following simpler form:

$$K_1 Q_1^2 + K_2 Q_2^2 - K_3 Q_3^2 = 0 \quad (6.9)$$

Where,

$$K_1 = f_1 \frac{L_1}{D_1} \frac{1}{2gA_1^2} \quad (6.10)$$

$$K_2 = f_2 \frac{L_2}{D_2} \frac{1}{2gA_2^2} \quad (6.11)$$

$$K_3 = f_3 \frac{L_3}{D_3} \frac{1}{2gA_3^2} \quad (6.12)$$

Now, substituting for  $Q_2$  and  $Q_3$  from Equations (6.5) and (6.6), Equation (6.9) becomes:

$$K_1 Q_1^2 + K_2 (Q_1 - 60)^2 - K_3 (100 - Q_1)^2 = 0 \quad (6.13)$$

Expanding and rearranging Equation (6.13) leads to:

$$a Q_1^2 + b Q_1 + c = 0 \quad (6.14)$$

Where:

$$a = (K_1 + K_2 - K_3) \quad (6.15)$$

$$b = -(120K_1 - 200K_2) \quad (6.16)$$

$$c = 60^2 K_2 - 100^2 K_3 \quad (6.17)$$

Equation (6.14) is a quadratic equation that can be solved for  $Q_1$  once the numeric values of  $K_1$ ,  $K_2$ , and  $K_3$  are provided. There are two solutions for the quadratic equation, which are given by:

$$Q_1 = \frac{-b \pm \sqrt{b^2 - 4ac}}{2a} \quad (6.18)$$

Where  $a = 114350.4$ ,  $b = -1.3 \times 10^7$ , and  $c = 3.37 \times 10^8$ . Substituting for  $a$ ,  $b$ , and  $c$  in Equation (6.18) gives the following solutions:

*First solution:*  $Q_1 = 66.99$  l/s,  $Q_2 = 6.99$  l/s, and  $Q_3 = 33.0$  l/s

*Second solution:*  $Q_1 = 44.04$  l/s,  $Q_2 = -15.96$  l/s and  $Q_3 = 55.96$  l/s

The second solution, which leads to a negative value for  $Q_2$ , cannot be accepted because it either means that the magnitude of  $Q_2$  is negative, which is physically meaningless, or its direction is reversed, which goes against our initial assumption embedded in the formation of Equation (6.7). Trying to solve the problem by adopting the flow arrangement shown in Figure 6.3.b, i.e., by assuming that the flow in pipe BC goes in the opposite direction, leads to values of the flow rates in the pipes as complex numbers, which is also a physically unacceptable solution. Therefore, the only acceptable solution is the first solution shown above.

The pipe-network considered in this example could be analysed mathematically because of its simplicity and because of using constant values for the friction factors in

Equations (6.10) – (6.12). In general, the friction factor depends on the Reynolds number and, therefore, on the unknown pipe flow rate. Therefore, the complex practical pipe networks have to be analysed by using computer-aided methods [1]. In this respect, the earliest and mostly used method for the analysis of looped pipe-networks is the Hardy-Cross (H-C) method described in Appendix C. The following section presents an Excel-aided method for pipe-network analyses that is more general than the H-C method because it can be used for both looped and branching networks [2, 3].

### 6.2. Analyses of looped pipe-networks with Excel-Solver

This method utilises the multi-variable iterative capability of Solver that can take into consideration multiple constraints on the iterative process. The following example, which is based on Example 5-2 in Nalluri and Feather [4], demonstrates the method.

#### Example 6-2. Analysis of a two-loop network by Excel-Solver

Figure 6.4 shows a network that consists of two pipe loops with one source and five discharge (load) junctions. The valve in pipe BC is partially closed, which produces a local head loss of  $10.0 V^2/2g$ . Table 6.1. gives the lengths and diameters of each pipes. The roughness of all pipes is 0.06 mm. Determine the water flows in the network pipes.

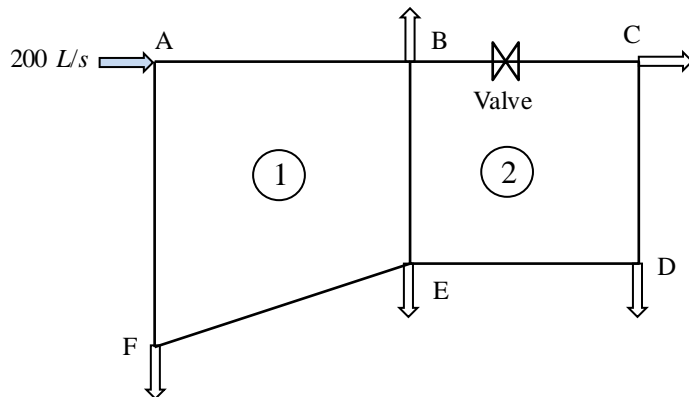


Figure 6.4. The two-loop pipe network of Example 6-2

Table 6.1. Pipes' lengths and diameters

Pipe	AB	BC	CD	DE	EF	AF	BE
Length (m)	500	400	200	400	600	300	200
Diameter (mm)	250	150	100	150	200	250	150

#### The analytical model

The Excel-aided solution procedure starts with guessed values for selected pipe flows. The remaining pipe flows are then calculated by Excel such that they satisfy the continuity equation. Since these initial flows are unlikely to satisfy the energy equation, Solver is used to adjust the guessed pipe flow rates so that the energy equations are satisfied for all the network loops while Excel recalculates the remaining pipe flows to



ensure that the nodal continuity equations are simultaneously satisfied. We need to guess the flow rate in only one pipe in each loop since the flows in the other pipes can be determined from the continuity equations. Let us guess the magnitude and direction of flow rate in pipe AB (loop 1) and pipe BC (loop 2) and calculate the flow rates in the other pipes in the network by applying mass conservation at the nodes (junctions). Accordingly, the flow rates in the other pipes are determined as follows:

Loop 1:

$$Q_{BE} = (Q_{AB} - Q_B - Q_{BC}) \quad (6.19)$$

$$Q_{AF} = -(Q_A - Q_{AB}) \quad (6.20)$$

$$Q_{EF} = -(Q_{AF} - Q_F) \quad (6.21)$$

Loop 2:

$$Q_{CD} = (Q_{BC} - Q_C) \quad (6.22)$$

$$Q_{BE} = -(Q_{AB} - Q_B - Q_{BC}) \quad (6.23)$$

$$Q_{DE} = -(Q_D - Q_{CD}) \quad (6.24)$$

Figure 6.5 shows the initial flows in the network for assumed values:  $Q_{AB}=120$  l/s and  $Q_{BC} = 50$  l/s. Your initial flows can be different from those shown in the figure provided that they satisfy the nodal continuity equations. The final solution may change the initial pipe flows in both magnitude and direction.

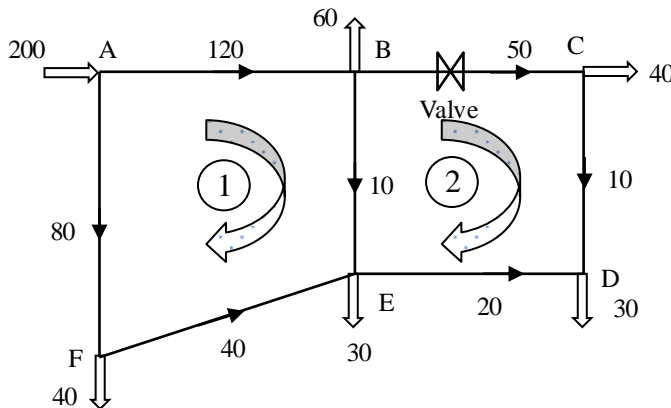


Figure 6.5. Initial flows and sign convention for the pipe network of Example 6-2

The second step in the procedure is to calculate the friction loss in each pipe of the network and calculate the net friction loss in each loop according to the assumed flow direction in the relevant pipes. In the present analyses, the friction losses in all the pipes are calculated using the Darcy-Weisbach equation, Equation (1.21). However, for pipe BC, the equation is modified to allow for the loss in the valve as follows:

$$h_{f,BC} = f \frac{L}{D} \frac{V^2}{2g} + 10 \frac{V^2}{2g} \quad (6.25)$$

More likely the energy equation, Equation (6.4), will not be satisfied by using the initially guessed flows. To satisfy the energy equation, Solver will be used to adjust the flow rates in pipes AB and BC so as to satisfy the following constraints on the iterative process:

$$\left| h_{f,AB} + h_{f,BE} - h_{f,EF} - h_{f,AF} \right| \leq \varepsilon \quad \text{Loop 1} \quad (6.26)$$

$$\left| h_{f,BC} + h_{f,CD} - h_{f,DE} - h_{f,BE} \right| \leq \varepsilon \quad \text{Loop 2} \quad (6.27)$$

Where  $| \quad |$  refers to the absolute value and  $\varepsilon$  is a prescribed positive tolerance that is acceptably small.

By using the absolute value of the error, the positive direction for friction doesn't have to be the same for all the loops, i.e., it can be clockwise or anti-clockwise for different loops. The absolute value also takes into consideration that the flow may not be in the suggested direction or may change its direction during the solution process. Also note that only the flow rates in pipes AB and BC need to be adjusted by Solver since the other pipe flow rates are adjusted automatically by applying Equations (6.19) to (6.24) in the main Excel sheet.

### Excel implementation

Figure 6.6 show the Excel sheet developed for applying the Excel-aided method for solving this example. The problems data (pipe lengths and diameters, roughness factor, and water viscosity) are shown at the left part of the sheet. The two values for the flow rates in pipe AB ( $Q_{AB}$ ) and pipe BC ( $Q_{BC}$ ) are guessed values while the flow rates in the other pipes ( $Q_{CD} - Q_{BE}$ ) are calculated according to Equations (6.19) to (6.24). The sheet then calculates the velocity ( $Q/A$ ) and Reynolds number ( $Re$ ) for each pipe. Based on these values, the sheet determines the friction factor ( $f$ ) and friction loss ( $hf$ ) in the pipes. Finally, the sheet calculates the balance of friction losses in the two loops as required by Equations (6.26) and (6.27). The formula bar shows how the balance of friction losses in loop 1 is calculated according to Equation (6.26).

O12															fx	
															=ABS(SIGN(Q_BC)*hf_BC+SIGN(Q_CD)*hf_CD-SIGN(Q_BE)*hf_BE-SIGN(Q_DE)*hf_D	
	A	B	C	D	E	F	G	H	I	J	K	L	M	N	O	P
1	Pipe	L(m)	D(m)		Q			V	Re		$\epsilon/d$	f		hf		
2	AB	500	0.25		Q_AB	0.12		2.44462	555595.4		0.00024	0.015747		hf_AB	9.59308	
3	BC	400	0.15		Q_BC	0.05		2.82942	385830.2		0.0004	0.017399		hf_BC	23.0119	
4	CD	200	0.1		Q_CD	0.01		1.27324	115749		0.0006	0.020489		hf_CD	3.38586	
5	DE	400	0.15		Q_DE	0.02		1.13177	154332.1		0.0004	0.018905		hf_DE	3.29122	
6	EF	600	0.2		Q_EF	0.04		1.27324	231498.1		0.0003	0.017506		hf_EF	4.33948	
7	AF	300	0.25		Q_AF	0.08		1.62975	370397		0.00024	0.016284		hf_AF	2.64539	
8	BE	200	0.15		Q_BE	0.01		0.56588	77166.03		0.0004	0.020739		hf_BE	0.45132	
9																
10	$\epsilon$	0.00006														$\Sigma hf$
11	visc	1.10E-06												Loop 1	3.05954	
12	gc	9.81												Loop 2	22.6553	
13																

Figure 6.6. Excel sheet developed for Example 6-2

Figure 6.6 shows that the imbalances in friction losses in the two loops with the initially guessed flows are not small. Solver can now be used to find the values of  $Q_{AB}$  and  $Q_{BC}$  that make the friction imbalances in the two loops become less than a specified value. Figure 6.7 shows the required set-up for this task.

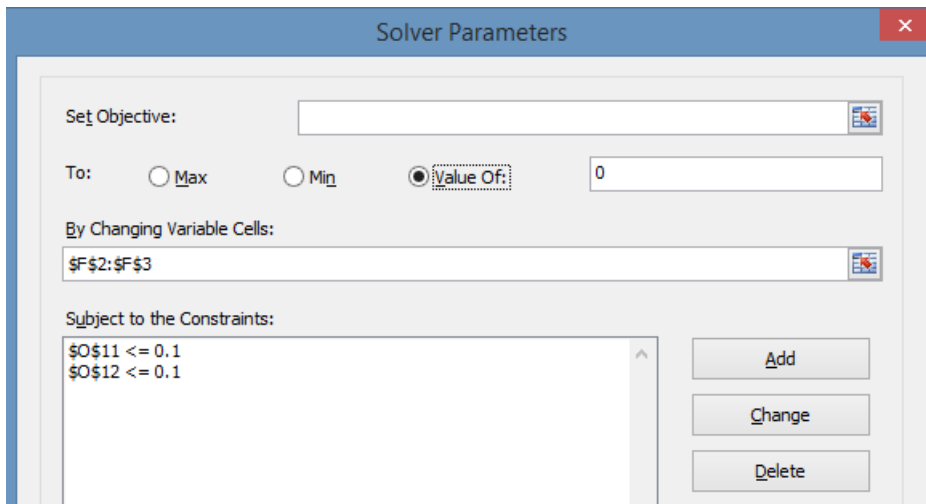


Figure 6.7. Solver set-up for Example 6-2

With this set-up the friction balances in the two loops should be below 0.1. The sheet automatically calculates the unknown flow rates by satisfying the continuity equations. Figure 6.8 shows the solution found by Solver. Note that the imbalances in friction losses in the two loops have been reduced to 0.1 or less. As shown in Table 6.2, Solver's solution shown in Figure 6.8 agrees closely with that given by Nalluri and Feather [4]. The following example applies the method to a pipe-network with three loops which was used by Benjamin [5] to illustrate the Hardy-Cross method. His solution will be used to verify the solution with Excel-Solver.

# Computer-Aided Thermofluid Analyses Using Excel

	A	B	C	D	E	F	G	H	I	J	K	L	M	N	O	P
1	Pipe	L(m)	D(m)		Q		V	Re		$\epsilon/d$	f		hf			
2	AB	500	0.25		Q_AB	0.1115	2.27212	516391.2		0.00024	0.015834		hf_AB	8.33265		
3	BC	400	0.15		Q_BC	0.035	1.97986	269980.7		0.0004	0.017882		hf_BC	11.5248		
4	CD	200	0.1		Q_CD	-0.005	-0.6383	58025.17		0.0006	0.022427		hf_CD	0.93137		
5	DE	400	0.15		Q_DE	0.035	1.98133	270181.5		0.0004	0.017881		hf_DE	9.54047		
6	EF	600	0.2		Q_EF	0.0485	1.54277	280503.4		0.0003	0.01717		hf_EF	6.2487		
7	AF	300	0.25		Q_AF	0.0885	1.80225	409601.2		0.00024	0.016138		hf_AF	3.2059		
8	BE	200	0.15		Q_BE	0.0165	0.93628	127675.1		0.0004	0.019338		hf_BE	1.15205		
9																
10	$\epsilon$	0.00006													$\Sigma$ hf	
11	visc	1.10E-06											Loop 1	0.0301		
12	gc	9.81											Loop 2	0.09912		
13																

Figure 6.8. Solver solution for Example 6-2

Table 6.2. Verification of the solution obtained by the Excel-Solver method

Pipe	Nalluri and Feather [4]	Excel-Solver
AB	0.11152	0.1115
BC	0.03505	0.0350
CD	0.00495	0.0050
DE	0.03495	0.0350
EF	0.04848	0.0485
AF	0.08848	0.0885
BE	0.01648	0.0165

### Example 6-3. Analysis of a three-loop network by Excel-Solver

Determine the flow rates in all the pipes in the network shown in Figure 6.9 according to the data given in Table 6.3. If the pressure head at point A is 40 m, find the pressure head at D (which might represent a fire-demand, for example).

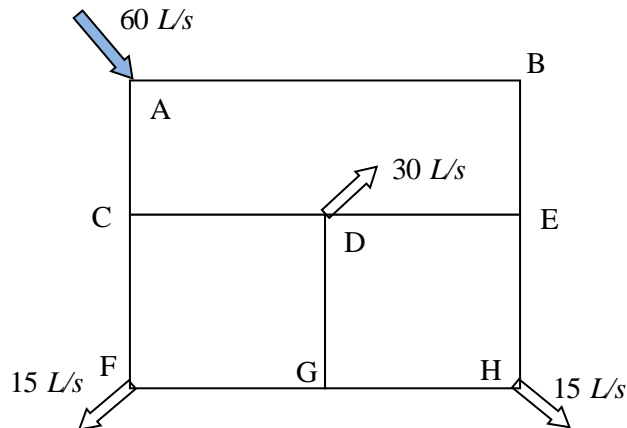


Figure 6.9. Pipe-network for Example 6-3

Table 6.3. Pipes' lengths and diameters

Pipe	Length (m)	Diameter (m)	Pipe	Length (m)	Diameter (m)
AB	250	0.3	DG	100	0.25
BE	100	0.2	FG	125	0.15
DE	125	0.2	CF	100	0.1
CD	125	0.2	EH	100	0.25
AC	100	0.15	GH	125	0.1

**The analytical model**

Following the procedure described above, the flow rate in one pipe in each loop is guessed and the flow rates in the other pipes are obtained from relevant mass balance equations. Figure 6.10 shows the initially assumed values and directions of the flows.

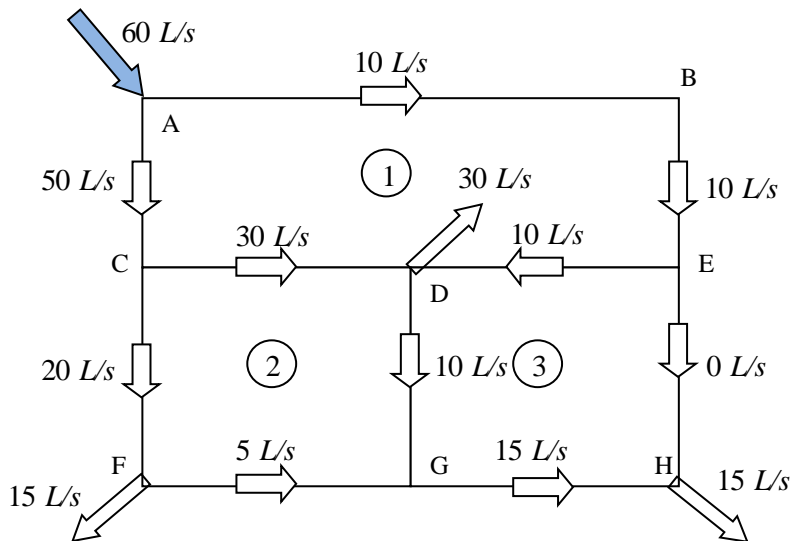


Figure 6.10. Pipe-network for Example 6-3 with initial flows

The flows in pipes *AB*, *CD*, and *DE* are guessed and those in the other seven pipes are determined as follows:

$$Q_{BE} = Q_{AB} \tag{6.28}$$

$$Q_{AC} = Q_A - Q_{AB} \tag{6.29}$$

$$Q_{DG} = Q_{DE} + Q_{CD} - Q_D \tag{6.30}$$

## Computer-Aided Thermofluid Analyses Using Excel

$$Q_{FG} = Q_{CF} - Q_F \quad (6.31)$$

$$Q_{CF} = Q_{AC} - Q_{CD} \quad (6.32)$$

$$Q_{EH} = Q_{BE} - Q_{DE} \quad (6.33)$$

$$Q_{GH} = Q_H - Q_{EH} \quad (6.34)$$

The three loops in the network provide the following energy constraints:

$$h_{f,AB} + h_{f,BE} + h_{f,DE} - h_{f,AC} - h_{f,CD} = 0 \quad \text{Loop 1} \quad (6.35)$$

$$h_{f,CD} + h_{f,DGg} - h_{f,CF} - h_{f,FG} = 0 \quad \text{Loop 2} \quad (6.36)$$

$$-h_{f,DE} + h_{f,EH} - h_{f,DG} - h_{f,GH} = 0 \quad \text{Loop 3} \quad (6.37)$$

### Excel implementation

Figure 6.11 shows the Excel sheet developed for this example. The (coloured) flow rates for pipes *AB*, *DE*, and *CD* are guessed flow rates. The flow rates for the other seven pipes are determined according to Equation (6.28) to (6.34). Based on the guessed flow rates, the sheet calculates the Reynolds number (*Re*), friction factor (*f*), and friction loss (*hf*) in each pipe. Figure 6.11 shows that the guessed flow rates do not satisfy the requirements of the energy equations, Equations (6.35), (6.36), and (6.37).

M13		fx =ABS(SIGN(Q_AB)*hf_AB+SIGN(Q_BE)*hf_BE+SIGN(Q_DE)*hf_DE-(SIGN(Q_AC)*hf_AC+SIGN(Q_CD)*hf_CD))													
	A	B	C	D	E	F	G	H	I	J	K	L	M	N	
1	Pipe	L(m)	D(m)		Q	V	Re	ks/d	f			hf			
2	L_AB	250	0.3		Q_AB	0.01	0.1414711	42441.318	0.0008333	0.0242748		hf_AB	0.0206353		
3	L_BE	100	0.2		Q_BE	0.01	1.2732395	127323.95	0.0025	0.0262635		hf_BE	2.1700691		
4	L_DE	125	0.2		Q_DE	0.01	0.3183099	63661.977	0.00125	0.0241957		hf_DE	0.0780944		
5	L_CD	125	0.2		Q_CD	0.03	0.9549297	190985.93	0.00125	0.0221798		hf_CD	0.6442906		
6	L_AC	100	0.15		Q_AC	0.05	1.5915494	318309.89	0.00125	0.0216783		hf_AC	1.3993801		
7	L_DG	100	0.25		Q_DG	0.01	0.5658842	84882.636	0.0016667	0.0247234		hf_DG	0.2690127		
8	L_FG	125	0.15		Q_FG	0.005	0.1018592	25464.791	0.001	0.0268805		hf_FG	0.0071074		
9	L_CF	100	0.1		Q_CF	0.02	1.1317685	169765.27	0.0016667	0.0236781		hf_CF	1.0305564		
10	L_EH	100	0.25		Q_EH	0	0	0	0.0025	0		hf_EH	0		
11	L_GH	125	0.1		Q_GH	0.015	0.3055775	76394.373	0.001	0.0229613		hf_GH	0.05464		
12													Σhf		
13	ε	0.00025										Loop 1	0.2251281		
14	visc	1.00E-06										Loop 2	0.1243605		
15	gc	9.81										Loop 3	0.4017471		
16															

Figure 6.11. Excel sheet for Example 6-3

Solver can now be used to adjust the three guessed flow rates in pipes *AB*, *DE*, and *CD* until Equations (6.35) to (6.37) are satisfied and Figure 6.12 shows Solver set-up for this problem.

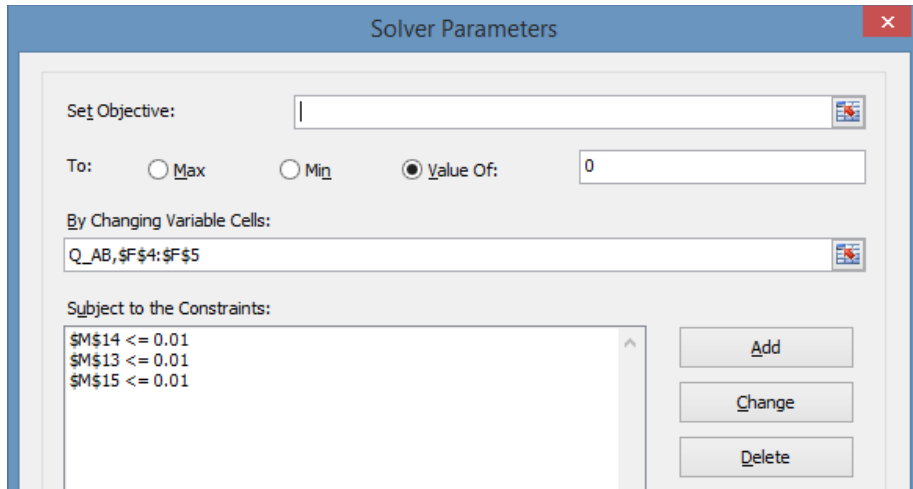


Figure 6.12. Solver set-up for Example 6-3

Note that Solver is only required to adjust the flow in the three pipes with the guessed flows to satisfy the constraints that represent the three energy equations. Figure 6.13 shows the final result obtained by Solver. Table 6.4 compares this result with that given by Benjamin [5] and proves their proximity to the Hardy-Cross solution.

fx =ABS(SIGN(Q_AB)*hf_AB+SIGN(Q_BE)*hf_BE+SIGN(Q_DE)*hf_DE-(SIGN(Q_AC)*hf_AC+SIGN(Q_CD)*hf_CD))														
	A	B	C	D	E	F	G	H	I	J	K	L	M	N
1	Pipe	L(m)	D(m)		Q	V	Re	ks/d	f			hf		
2	L_AB	250	0.3	Q_AB	0.0097835	0.1384078	41522.352	0.0008333	0.0243576			hf_AB	0.0198187	
3	L_BE	100	0.2	Q_BE	0.0097835	1.2456706	124567.06	0.0025	0.0262896			hf_BE	2.0791769	
4	L_DE	125	0.2	Q_DE	0.0064912	0.2066203	41324.051	0.00125	0.0255051			hf_DE	0.034686	
5	L_CD	125	0.2	Q_CD	0.0315883	1.0054882	201097.63	0.00125	0.0221195			hf_CD	0.7123784	
6	L_AC	100	0.15	Q_AC	0.0502165	1.5984417	319688.34	0.00125	0.0216748			hf_AC	1.4113032	
7	L_DG	100	0.25	Q_DG	0.0080795	0.4572067	68581	0.0016667	0.0251695			hf_DG	0.1787763	
8	L_FG	125	0.15	Q_FG	0.0036282	0.0739128	18478.191	0.001	0.0285602			hf_FG	0.0039762	
9	L_CF	100	0.1	Q_CF	0.0186282	1.0541396	158120.94	0.0016667	0.0237614			hf_CF	0.8971783	
10	L_EH	100	0.25	Q_EH	0.0032923	0.4191895	41918.954	0.0025	0.0283504			hf_EH	0.2539106	
11	L_GH	125	0.1	Q_GH	0.0117077	0.2385072	59626.791	0.001	0.0236349			hf_GH	0.0342632	
12													Σhf	
13	ε	0.00025										Loop 1	0.01	
14	visc	1.00E-06										Loop 2	0.0099998	
15	gc	9.81										Loop 3	0.0061851	
16														

Figure 6.13. Solver solution for Example 6-3

Table 6.4. Verification of Solver’s solution for the pipe-network of Example 6-3

Pipe	Benjamin [5]	Present solution	Pipe	Benjamin [5]	Present solution
AB	0.0098	0.00978	DG	0.0082	0.00808
BE	0.0098	0.00978	FG	0.0035	0.00363
ED	0.0065	0.00649	CF	0.0185	0.01863
DC	0.0317	0.03159	EH	0.0033	0.00329
AC	0.0502	0.05022	HG	0.0117	0.01171

### 6.3. Analyses of branched pipe-networks with Excel-Solver

The analysis of branched pipe-network with Excel and Solver basically follows the same procedure applied for the analysis of looped-networks. The basic equations for the analysis are the continuity and energy equations supplemented by an equation for determining the frictional losses. The following example, which is based on Example 5-4 in Nalluri and Feather [4], illustrates the procedure.

#### Example 6-4. Branched network connecting multi-reservoirs

Neglecting minor losses, determine the gravity-driven discharges in the pipes of the branched network shown in Figure 6.14 that carries water. The data of the pipes are given in Table 6.5 and the elevations of the three tanks A, B, C, and D are shown in the figure.

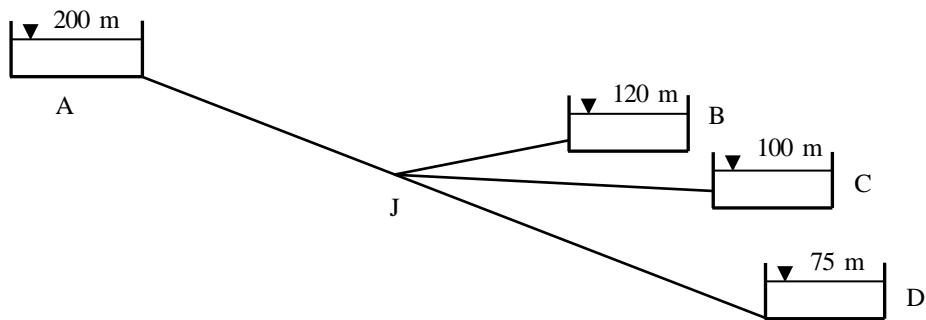


Figure 6.14. The branched pipe-network in Example 6-4

Table 6.5. Pipes' lengths and diameters

Pipe	Length (m)	Diameter (mm)
AJ	10,000	450
BJ	2,000	350
CJ	3,000	300
DJ	3,000	250

#### The analytical model

The energy equation requires that the friction loss between any two points (nodes)  $A$  and  $B$  in the network to be balanced by the difference in potential and kinetic heads between these two points in addition to the head produced by any booster pump along the line. Therefore, the energy equation takes the following form:

$$\sum_1^M h_f = h_p + (Z_A - Z_B) + \frac{V_A^2 - V_B^2}{2g} \quad (6.38)$$



Where  $M$  is the total number of pipes between the two points  $A$  and  $B$ . Without a booster pump along the line, the equation simplifies to:

$$\sum_1^M h_f = (Z_A - Z_B) + \frac{V_A^2 - V_B^2}{2g} \quad (6.39)$$

Nalluri and Feather [4] solved the problem by using the quantity balance method (the 'nodal' method). Their solution started with an assumed value for the head at joint  $J$  based on which the flow rate and head loss in each pipe were calculated. The guessed head at joint  $J$  was then adjusted successively in order to satisfy the energy equation. With the present method it is more convenient to follow the same procedure used in the previous section by assuming the flow rates in each pipe, determining the friction losses, and then using Solver to adjust the flow rates until the energy equation is satisfied within a specified tolerance. Figure 6.15 shows the magnitudes (litre/s) and directions of the flow rates initially assumed in each pipe.

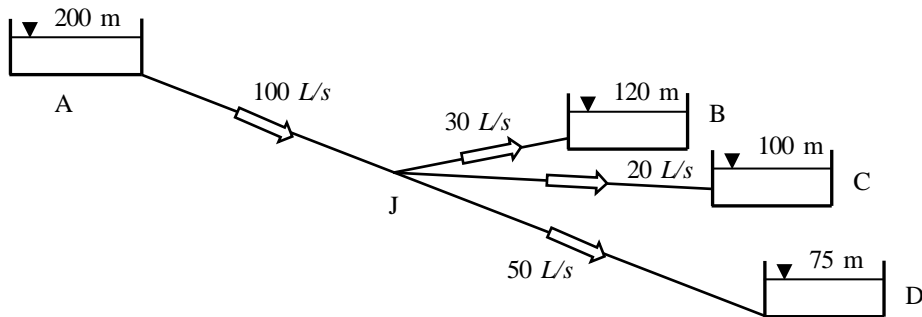


Figure 6.15. Assumed flows in the network

Three of the four flows at junction  $J$  have been assumed ( $AJ$ ,  $BJ$ , and  $CJ$ ), while the fourth ( $DJ$ ) is left to satisfy continuity:

$$Q_{DJ} = Q_{AJ} - Q_{BJ} - Q_{CJ} \quad (6.40)$$

Since there are no booster pumps in the network, Equation (6.39) applies. For pipes that have constant cross-sections, the velocities at both ends of the pipe are the same and, therefore, Equation (6.39) can be simplified to produce the following equations:

$$h_{f,AJ} + h_{f,BJ} - (Z_A - Z_B) = 0 \quad (6.41)$$

$$h_{f,AJ} + h_{f,CJ} - (Z_A - Z_C) = 0 \quad (6.42)$$

## Computer-Aided Thermofluid Analyses Using Excel

$$h_{f,AJ} + h_{f,DJ} - (Z_A - Z_D) = 0 \quad (6.43)$$

Equations (6.41) – (6.43) will be used as constraints for Solver solution. Once the friction losses in the different pipes are known, the elevation at the junction  $J$  can be determined from any of the following equations:

$$Z_J = Z_A - h_{f,AJ} \quad (6.44)$$

$$Z_J = Z_B + h_{f,BJ} \quad (6.45)$$

$$Z_J = Z_C + h_{f,CJ} \quad (6.46)$$

$$Z_J = Z_D + h_{f,DJ} \quad (6.47)$$

### The Excel sheet

Figure 6.16 shows the Excel sheet developed for this example. The flow rates in the three coloured or shaded cells are assumed, but the flow rate in pipe DJ is calculated from the continuity equation, Equation (6.40). Note that the formula bar shows the formula in cell **E19** that applies this equation. Based on the assumed pipe flow rates, the sheet calculates the relevant Reynolds numbers, friction factors, and friction losses.

E18		fx =E15-E16-E17									
	A	B	C	D	E	F	G	H	I	J	K
14		L	D	A	Q	V	Re	f	hf	HJ	
15	AJ	10000	0.45	0.159043	0.1	0.62876	282942.1	0.015864	7.103596	192.8964	
16	BJ	2000	0.35	0.096211	0.03	0.311814	109134.8	0.018568	0.525792	120.5258	
17	CJ	3000	0.3	0.070686	0.02	0.282942	84882.64	0.019531	0.796942	100.7969	
18	DJ	3000	0.25	0.049087	0.05	1.018592	254647.9	0.016917	10.73481	85.73481	
19											
20	ks	0.00006	m						Line AB	72.37061	
21	gc	9.81							Line AC	92.09946	
22	visc	1.00E-06							Line AD	107.1616	
23											

Figure 6.16. Excel sheet developed for Example 6-4

The top four cells in column J (i.e. **J15**, **J16**, **J17**, and **J18**) show the height at the junction J as calculated from Equations (6.44)-(6.47). These cells show different values because the assumed flow rates in the pipes are not correct. This is also indicated by the bottom three cells in column J that show the imbalances in the energy equations, Equations (6.41)-(6.43), which should be zeros. Since the assumed flow rates do not satisfy the energy equations, the values shown in the sheet are relatively large. Solver can now be used to find the correct flow rates (their magnitudes and directions) in the

three pipes AJ, BJ, and CJ that satisfy the energy equation. The required Solver set-up is shown in Figure 6.17.

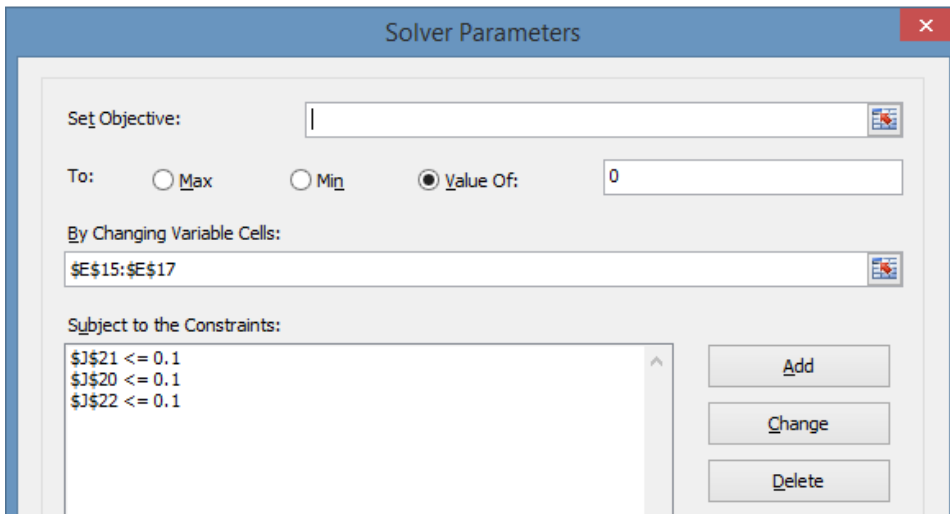


Figure 6.17. Solver set-up for Example 6-4

This set-up requires Solver to adjust the flow rates in the top three pipes such that the last three entries in column J, i.e. J20, J21, and J22, are close to zero. Note that the flow in pipe DJ is automatically determined by the continuity equation. Figure 6.18 shows the solution found by Solver that satisfies the energy equation as shown by the small values of the three entries in cell J20, J21, and J22. Also note that the resulting head losses in all four pipes now yield the same value for the elevation at joint J, which is 125.5 m. Table 6.6, which compares the present solution with that given by Nalluri and Feather [4], shows a close agreement between the two solutions.

	A	B	C	D	E	F	G	H	I	J	K
14		L	D	A	Q	V	Re	f	hf	HJ	
15	AJ	10000	0.45	0.159043	0.344796	2.167942	975573.8	0.013997	74.51151	125.4885	
16	BJ	2000	0.35	0.096211	0.104596	1.087151	380502.9	0.015654	5.388492	125.3885	
17	CJ	3000	0.3	0.070686	0.127594	1.805089	541526.7	0.015408	25.58849	125.5885	
18	DJ	3000	0.25	0.049087	0.112606	2.293987	573496.8	0.015711	50.56701	125.567	
19											
20	ks	0.00006	m						Line AB	0.1	
21	gc	9.81							Line AC	0.1	
22	visc	1.00E-06							Line AD	0.078516	
23											

Figure 6.18. Solver solution for Example 6-4

Table 6.6. Verification of the pipe flow rates in m<sup>3</sup>/s obtained by Solver with those given by Nalluri and Feather [4]

<i>Pipe</i>	<i>Nalluri and Feather [4]</i>	<i>Present solution</i>
AJ	0.344	0.344780
BJ	0.105	0.104696
CJ	0.127	0.127590
DJ	0.112	0.112606

#### 6.4. Analysis of mixed pipe networks

To illustrate the application of the Excel-Solver method for the analyses of a general pipe network that consists of branched pipes branches as well as looped pipes, consider the pipe network shown in Figure 6.19 that distributes water and has two sources and six discharge points. This network was analysed by Rivas *et al* [6] who also used Excel and Solver. Their solution will be used for verification.

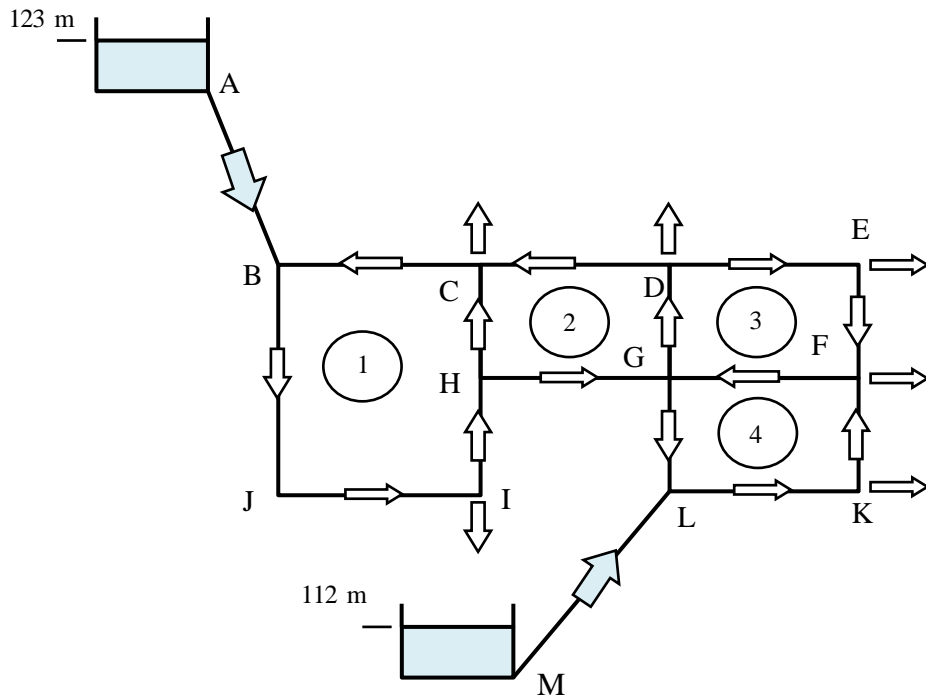


Figure 6.19. Pipe network (adapted from Rivas et al [6])

All the network pipes are made of steel with a roughness of 0.3 mm. The lengths and diameters of the 16 network-pipes are given in Table 6.7. The demand at the six nodes in litres per second is shown in Table 6.8.

Table 6.7. Pipe data

Pipe	Pipe size		Pipe	Pipe size	
	Diameter (mm)	Length (m)		Diameter (mm)	Length (m)
AB	250	200	CD	200	180
BJ	150	400	LM	250	140
IJ	200	300	KL	200	360
HI	300	190	FK	150	200
CH	80	210	FG	150	340
BC	200	300	GL	80	180
GH	150	160	EF	150	180
DG	300	200	DE	200	345

Table 6.8. Nodal demand

Node	C	D	E	I	F	K
Demand (l/s)	100	30	30	20	10	10

### The analytical model

Since the network has sixteen pipes, its analysis involves sixteen unknown flow rates. Applying the continuity equation at the eleven nodes in the network provides eleven linear equations. Four nonlinear equations can be formed by applying the energy equations over the four loops in the network. The fifth nonlinear equation can be formed by applying the energy equation between the two tanks A and M, for which the elevations are known. As for the analyses of looped and branched networks, the flows in some pipes are assumed and those in the other pipes are calculated by satisfying the continuity equation around each node. In this case, it is enough to assume the flow in five pipes, AB, BC, GH, KL and DE. The flows in the eleven remaining pipes are then calculated from the continuity equation as follows:

$$Q_{BJ} = Q_{AB} + Q_{BC} \quad (6.48)$$

$$Q_{IJ} = Q_{BJ} \quad (6.49)$$

$$Q_{HI} = Q_{IJ} - Q_I \quad (6.50)$$

$$Q_{CH} = Q_{HI} - Q_{GH} \quad (6.51)$$

$$Q_{DG} = Q_{CD} + Q_{DE} + Q_D \quad (6.52)$$

$$Q_{CD} = Q_{BC} + Q_C - Q_{CH} \quad (6.53)$$

$$Q_{LM} = Q_{KL} - Q_{GL} \quad (6.54)$$

$$Q_{FK} = Q_{KL} - Q_K \quad (6.55)$$

$$Q_{FG} = Q_{EF} + Q_{FK} - Q_F \quad (6.56)$$

$$Q_{GL} = Q_{GH} + Q_{FG} - Q_{DG} \quad (6.57)$$

$$Q_{EF} = Q_{DE} - Q_E \quad (6.58)$$

Applying the energy equation to the four loops provides four additional equations. Since there are no pumps in the system, the closed clockwise (or counter-clockwise) summation of the friction losses in each loop must be zero:

$$(-h_{f,HI} - h_{f,CH} - h_{f,BC}) - (h_{f,BJ} + h_{f,IJ}) = 0 \quad \text{Loop 1} \quad (6.59)$$

$$(-h_{f,DG} - h_{f,CD}) - (-h_{f,CH} + h_{f,GH}) = 0 \quad \text{Loop 2} \quad (6.60)$$

$$(h_{f,15} + h_{f,16}) - (-h_{f,8} - h_{f,13}) = 0 \quad \text{Loop 3} \quad (6.61)$$

$$(-h_{f,FK} - h_{f,FG}) - (h_{f,GL} + h_{f,KL}) = 0 \quad \text{Loop 4} \quad (6.62)$$

The 16<sup>th</sup> equation is formed by applying the energy equation along any route that connects points A and M. Selecting the route given by A-B-J-I-H-G-L-M:

$$(h_{f,AB} + h_{f,BJ} + h_{f,IJ} + h_{f,HI} + h_{f,GH} + h_{f,GL} - h_{f,LM}) - (z_A - z_M) = 0 \quad (6.63)$$

Since the initial pipe flows are unlikely to satisfy the energy equations, Solver will be used to adjust the five guessed pipe flows until the five energy equations are approximately satisfied.

### Excel implementation

The Excel sheet developed for this example is shown in Figure 6.20. The first columns on the left side of the sheet show the given network data that include the pipe roughness ( $\epsilon$ ), the kinematic viscosity of water (visc), the discharges at the six demand nodes, and the pipes diameters and lengths. Initial guesses are made for the flow rates of five pipes, one pipe in each loop. These are shown in the figure by the coloured or shaded cells. The flow rates in the other eleven pipes are then calculated from the continuity equations, Equations (6.48) to (6.58). The sheet then determines the velocity in each pipe followed by the Reynolds number, friction factor, and friction loss.

R2		=ABS(-SIGN(I7)*O7-SIGN(I6)*O6-SIGN(I5)*O5-SIGN(I4)*O4-SIGN(I3)*O3)																				
	A	B	C	D	E	F	G	H	I	J	K	L	M	N	O	P	Q	R	S	T	U	V
2	ε	0.0003		AB	0.25	200		0.0491	0.1		2.0372	5.1E+05		0.0212	3.5829		Loop1	1450.1		h E	-433.02	
3	Visc	1E-06		BJ	0.15	400		0.0177	0.2		11.318	1.7E+06		0.0236	410.56		Loop2	885.4		h B	119.42	
4	g	9.81		IJ	0.2	300		0.0314	0.2		6.3662	1.3E+06		0.022	68.092		Loop3	247.84		h J	-291.14	
5				HI	0.3	190		0.0707	0.18		2.5465	7.6E+05		0.0201	4.2144		Loop4	259.18		h I	-359.24	
6	Q C	0.1		CH	0.08	210		0.005	0.08		15.915	1.3E+06		0.028	950		LineA-M	514.24		h H	-363.45	
7	Q D	0.03		BC	0.2	300		0.0314	0.1		3.1831	6.4E+05		0.0222	17.186					h C	-1313.5	
8	Q E	0.03		GH	0.15	160		0.0177	0.1		5.6588	8.5E+05		0.0237	41.297					h D	-413.25	
9	Q F	0.01		DG	0.3	200		0.0707	0.25		3.5368	1.1E+06		0.02	8.5047					h G	-404.75	
10	Q I	0.02		CD	0.2	180		0.0314	0.12		3.8197	7.6E+05		0.0221	14.803					h L	109.49	
11	Q K	0.01		LM	0.25	140		0.0491	0.1		2.0372	5.1E+05		0.0212	2.508					h F	47.003	
12				KL	0.2	360		0.0314	0.1		3.1831	6.4E+05		0.0222	20.623					h K	88.869	
13	h A	123		FK	0.15	200		0.0177	0.09		5.093	7.6E+05		0.0238	41.865							
14	h M	112		FG	0.15	340		0.0177	0.15		8.4883	1.3E+06		0.0236	196.69							
15				GL	0.08	180		0.005	0		0	0.0E+00		0	0							
16				EF	0.15	180		0.0177	0.07		3.9612	5.9E+05		0.0238	22.872							
17				DE	0.2	345		0.0314	0.1		3.1831	6.4E+05		0.0222	19.764							
18																						

Figure 6.20. Excel sheet developed for the mixed pipe-network

Based on the calculated friction losses, the sheet determines the imbalance in the energy equation in the four loops (cells R2:R6) and along the route between points A and M. The last column shows the head obtained at each node (**U2:U12**). The specified and calculated pipe flows automatically satisfy continuity but, as the magnitudes of the friction imbalances show, they do not satisfy the energy constraint, Equations (6.59) – (6.63). Also, note that some nodes acquired negative elevations based on the assumed flow rates. Solver can now be used to search for the flows in the five pipes that satisfy the specified energy constraints, which will also give the correct elevations. Figure 6.21 shows the set-up for this analysis that requires Solver to perform the iteration with Equations (6.59) to (6.63) as constraints.

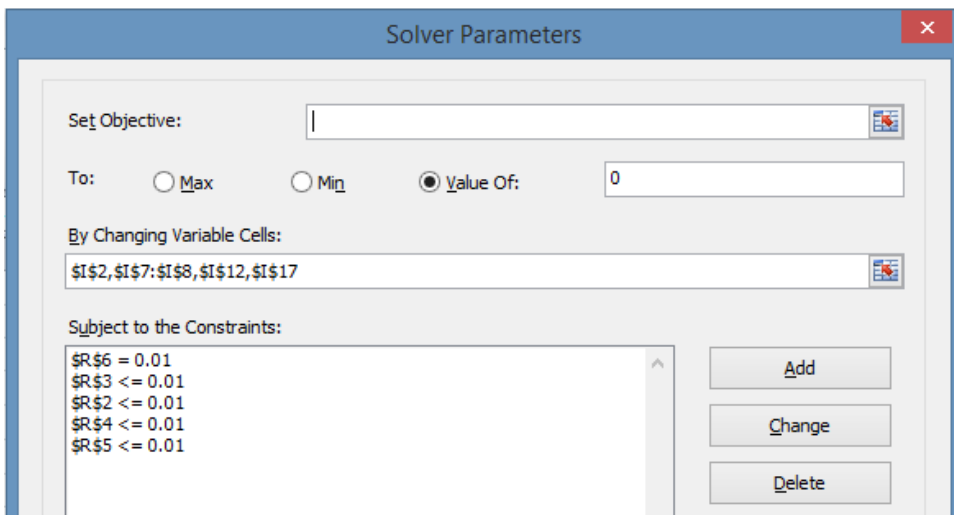


Figure 6.21. Solver set-up for analysing the mixed pipe-network

Figure 6.22 shows the solution determined by Solver that satisfied the five constraints with a specified tolerance of 0.01. The solutions obtained for the flow rates in the 16

pipes and for the heads at the eleven nodes are compared with those given by Rivas *et al* [6] in Figure 6.23. The figure shows close agreements with their results.

	A	B	C	D	E	F	G	H	I	J	K	L	M	N	O	P	Q	R	S	T	U	V
1				Pipe	D	L		A	Q		V	Re		f	hf		Loop1	0.0022		h E	96.989	
2	ks	0.0003		AB	0.25	200		0.0491	0.1415		2.8825	7.2E+05		0.021	7.1172		Loop2	0.01		h B	115.88	
3	Visc	1E-06		BJ	0.15	400		0.0177	0.0376		2.1287	3.2E+05		0.0241	14.862		Loop3	0.002		h J	101.02	
4	g	9.81		IJ	0.2	300		0.0314	0.0376		1.1974	2.4E+05		0.0228	2.499		Loop4	0.01		h I	98.522	
5				HI	0.3	190		0.0707	0.0176		0.2492	7.5E+04		0.023	0.0462		LineA-M	0.01		h H	98.475	
6	Q C	0.1		CH	0.08	210		0.005	0.0026		0.5223	4.2E+04		0.0308	1.1229					h C	97.352	
7	Q D	0.03		BC	0.2	300		0.0314	-0.1039		-3.3066	6.6E+05		0.0222	18.533					h D	97.311	
8	Q E	0.03		GH	0.15	160		0.0177	0.015		0.8484	1.3E+05		0.025	0.9777					h G	97.498	
9	Q F	0.01		DG	0.3	200		0.0707	0.0357		0.5045	1.5E+05		0.0216	0.1867					h L	111.13	
10	Q I	0.02		CD	0.2	180		0.0314	-0.0085		-0.207	4.1E+04		0.0261	0.0514					h F	98.531	
11	Q K	0.01		LM	0.25	140		0.0491	0.0585		1.1918	3.0E+05		0.0215	0.8735					h K	106.23	
12				KL	0.2	360		0.0314	0.0483		1.5373	3.1E+05		0.0226	4.8981							
13	h A	123		FK	0.15	200		0.0177	0.0383		2.1671	3.3E+05		0.0241	7.6978							
14	h M	112		FG	0.15	340		0.0177	0.0105		0.5918	8.9E+04		0.0255	1.0329							
15				GL	0.08	180		0.005	-0.0102		-2.0309	1.6E+05		0.0288	13.619							
16				EF	0.15	180		0.0177	-0.0178		-1.0094	1.5E+05		0.0248	1.5437							
17				DE	0.2	345		0.0314	0.0122		0.3871	7.7E+04		0.0244	0.3221							
18																						

Figure 6.22. Solver solution for the mixed pipe-network

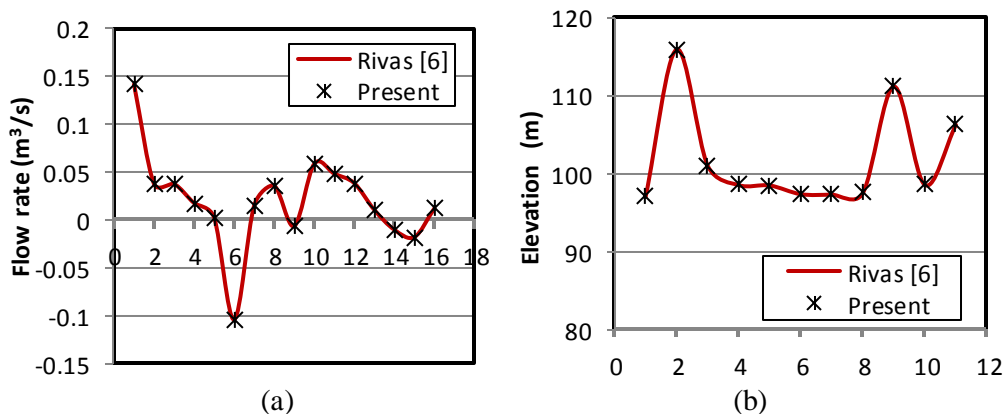


Figure 6.23. Comparison of the present results for the mixed pipe-network with those given by Rivas *et al* [6] for (a) the pipe flow rates and (b) nodal elevations

### 6.5. Closure

This chapter presented a method for using Excel and Solver for conducting hydraulic analyses of pipe networks. An important advantage of the Excel-Solver method for pipe-network analyses is that it can be applied to looped networks, branched networks, and mixed networks. The method can also be applied for pipe networks with specified heads as well as specified discharges. Apart from its generality, the method ensures that continuity is automatically satisfied as the iterative process approaches the correct solution. Appendix D illustrates the ability of the Excel-Solver method to deal with pipe-networks of practical complexity by considering a gravity-fed pipe network described by Brkic [8] that has two supply sources and 8 loops. The method can also be used for optimisation analyses of pipe-networks by adding an objective function for the economic optimisation.



All the analyses presented in this chapter were performed with the GRG Nonlinear method of Solver without using the automatic-scaling option. The number of iterations ranged from 5 for the two-loop network to 55 for the four-loop network.

## References

- [1] W.S. Janna, *Design of Fluid Thermal Systems*, third edition, CENGAGE Learning, 2011
- [2] A. N. El-Bahrawy, A spreadsheet teaching tool for analysis of pipe networks, *Engineering Journal of University of Qatar*, vol. 10, 1997, p. 33 – 50, the internet: [https://www.researchgate.net/profile/Aly\\_El-Bahrawy/contributions](https://www.researchgate.net/profile/Aly_El-Bahrawy/contributions), last accessed 24/1/2018.
- [3] A. M. Elfeki, Pipe network analysis example with Excel Solver, Researchgate, available at: [https://www.researchgate.net/publication/258051650\\_Pipe\\_Network\\_Analysis\\_Example\\_with\\_Excel\\_Solver](https://www.researchgate.net/publication/258051650_Pipe_Network_Analysis_Example_with_Excel_Solver), last accessed 20/6/2017.
- [4] C. Nalluri and R.E. Feather, *Civil Engineering Hydraulics*, Fourth Edition, Blackwell Publishing, 2008.
- [5] M.M. Benjamin, Analysis of complex pipe networks with multiple loops and inlets and outlets, the internet: <http://faculty.washington.edu/markbenj/CEE342/Abbreviated%20Hardy-Cross.pdf>, last accessed 20/6/2017.
- [6] A. Rivas, T. Gómez-Acebo, and J. C. Ramos. The application of spreadsheets to the analysis and optimization of systems and processes in the teaching of hydraulic and thermal engineering, *Computer Applications in Engineering Education*, Vol. 14, Issue 4, 2006, pp. 256-268.
- [7] White, *Fluid Mechanics*, Seventh Edition, McGraw-Hill, 2011.
- [8] D. Brkic, Spreadsheet-Based Pipe Networks Analysis for Teaching and Learning Purpose, *Spreadsheets in Education (eJSiE)*: Vol. 9: Iss. 2, Article 4, 2016. Available at: <http://epublications.bond.edu.au/ejsie/vol9/iss2/4>
- [9] Chemical Engineer Guide (CheGuide), [https://cheguide.com/pipe\\_network.html](https://cheguide.com/pipe_network.html), (Last accessed July 27, 2019).

## Exercise

1. All the five pipes in the network shown in Figure 6.P1 are horizontal and have a friction factor  $f = 0.025$ . For the given inlet and exit flow rate of  $0.054 \text{ m}^3/\text{s}$  of water at  $20^\circ\text{C}$  ( $\rho = 998 \text{ kg/m}^3$  and  $\mu = 1.002 \times 10^{-3} \text{ kg/m}\cdot\text{s}$ ), determine the flow rate and direction in all pipes. If  $p_A = 800 \text{ kPa}$  gage, determine the pressures at points  $B$ ,  $C$ , and  $D$ . This exercise is based on Problem 6.127 in White [7].
2. Analyse the gravity-driven pipe network shown in Figure 6.P2 that distributes water from one reservoir to five demand points via 19 cast iron pipes ( $\varepsilon = 0.00026 \text{ m}$ ). The accompanying table shows the lengths and internal diameters of the network pipes that are laid on a flat area with no variation in elevation.
3. Perform pipe network analysis and calculate water flow in all branches of the network shown in Figure 6.P3 that has two sources, 14 discharge points, and 22 pipes. Hazen-Williams coefficient for each pipe is provided in the accompanying table.

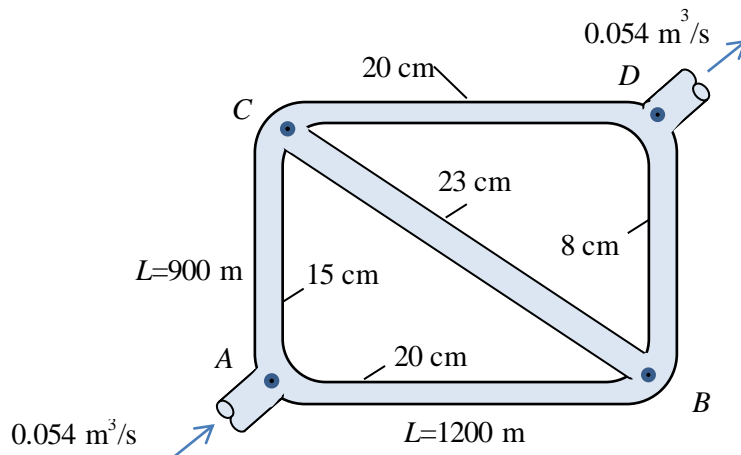


Figure 6.P1. A pipe-network with two loops (adapted from White [7])

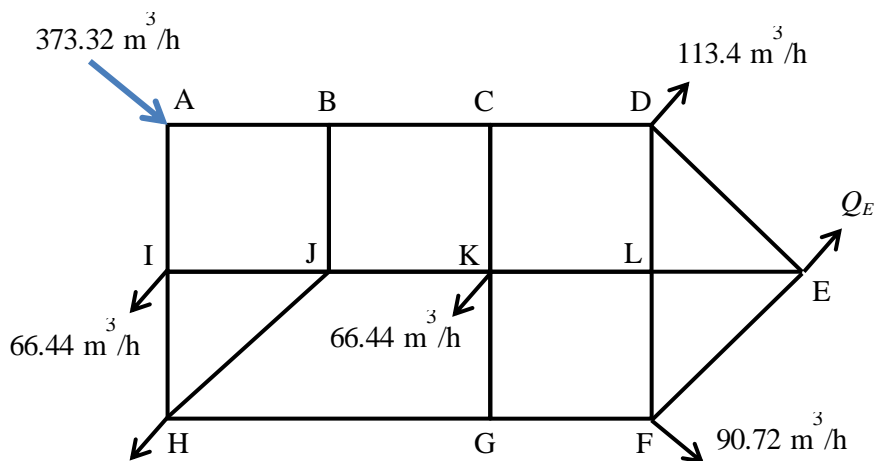


Figure 6.P2. A pipe-network with 8 loops (adapted from Brkic (8) with modifications)

Pipe	Length (m)	Diameter (m)	Pipe	Length (m)	Diameter (m)
AB	457.2	0.305	JK	304.8	0.152
BC	304.8	0.203	KL	335.3	0.254
CD	365.8	0.203	EL	304.8	0.254
DE	609.6	0.203	HJ	548.6	0.152
EF	853.4	0.203	BJ	335.3	0.152
FG	335.3	0.203	GK	548.6	0.152
GH	304.8	0.203	CK	365.9	0.254
HI	762.0	0.203	FL	548.6	0.152
AI	243.8	0.203	DL	396.2	0.152
IJ	396.2	0.152			

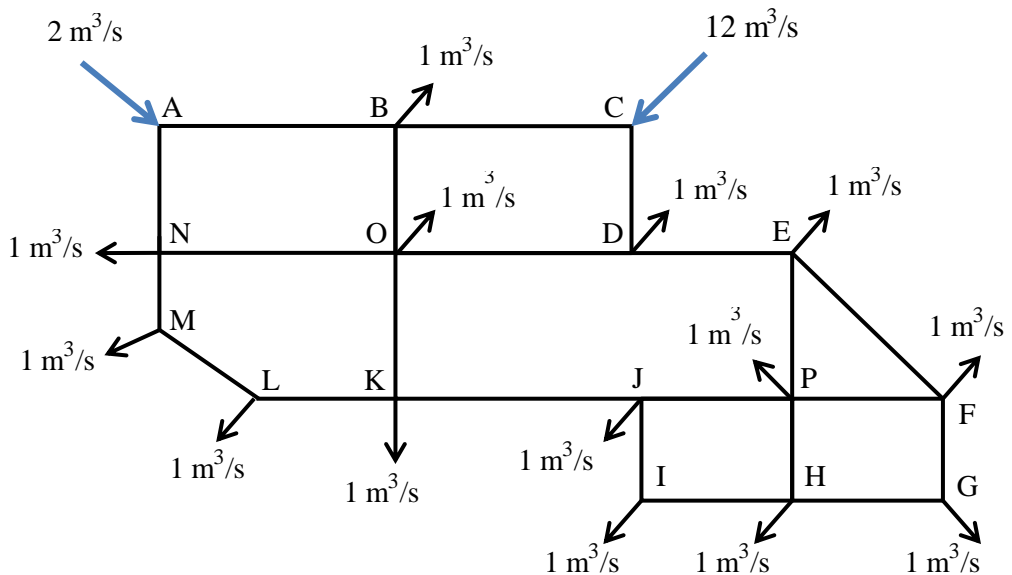


Figure 6.P3. A pipe-network with seven loops (Adapted from CheGuide.com [9])

Pipe No.	Pipe	Diameter (mm)	Length (m)	C
1	AB	1000	1000	100
2	BO	750	925	100
3	NO	750	1000	100
4	AN	750	925	100
5	MN	500	350	100
6	LM	500	671	100
7	KL	500	400	100
8	KO	500	650	100
9	DO	750	1000	120
10	BC	1000	1000	120
11	CD	1000	925	120
12	DE	1000	800	120
13	EF	750	763	120
14	EP	1000	650	120
15	FP	750	400	120
16	FG	750	125	120
17	GH	750	400	120
18	HP	500	125	120
19	HI	500	800	120
20	IJ	500	125	120
21	JP	500	800	120
22	JK	500	1000	120

# 7

## **Finite-difference solution of the steady heat-conduction equation**

Numerical solution methods, such as the finite-difference (FD) method and the finite-element (FE) method, enable us to deal with multi-dimensional heat-conduction in complex geometries. A common feature in these methods is that they replace the original conduction equation with a system of linear equations that can be solved using standard methods. Compared to the FE method, the FD method is easier to apply because it directly replaces the derivatives in the equation by finite differences. This chapter focuses on using the FD method for solving the steady heat-conduction equation. Before introducing the FD method, simple one-dimensional heat conduction problems are solved with the analytical solution method and then with the FD method so as to highlight the differences between the numerical and the analytical methods. The FD method is then applied to the heat-conduction equation with various boundary conditions. The chapter presents two approaches for applying the FD method with Excel. The first approach assembles the system of linear equations and uses Excel's matrix functions to solve it, while the second approach uses circular calculations and, therefore, does not require the system of linear equations to be assembled.

### 7.1. Analytical solution of the steady one-dimensional conduction equation

The general equation that governs the heat transfer by conduction in a medium with a constant thermal conductivity is the following partial differential equation [1]:

$$\frac{\partial^2 T}{\partial x^2} + \frac{\partial^2 T}{\partial y^2} + \frac{\partial^2 T}{\partial z^2} + \frac{\dot{e}_g}{k} = \frac{1}{\alpha} \frac{\partial T}{\partial t} \quad (7.1)$$

Where  $k$  is the thermal conductivity,  $\dot{e}_g$  the volumetric rate of heat-generation, and  $\alpha$  the thermal diffusivity of the medium ( $\alpha = k/\rho c_p$ ). For steady one-dimensional heat-transfer by conduction without heat generation, the equation reduces to:

$$\frac{d^2 T}{dx^2} = 0 \quad (7.2)$$

The analytical solution of Equation (7.2) can be obtained by integrating it twice, i.e.:

$$\frac{dT}{dx} = C_1 \quad (7.3)$$

$$T(x) = C_1 x + C_2 \quad (7.4)$$

Values of the two unknown constants  $C_1$  and  $C_2$  can then be determined if given two independent boundary conditions. The following two examples illustrate the application of the analytical solution method by using simple boundary conditions.

**Example 7-1. One-dimensional heat-conduction with prescribed-temperatures**

The inner and outer sides of a large plane wall of thickness  $L = 0.3$  m and thermal conductivity  $k = 0.8$  W/m<sup>2</sup>.°C are kept at constant temperatures of 20°C and 5°C, respectively. Determine the temperatures at  $x = 0.1$  m and  $x = 0.2$  m during a steady heat transfer by conduction.

**Solution**

In this case, the two constants in Equation (7.4) can be determined by applying the boundary conditions as follows:

$$T = T_0 \text{ at } x = 0; \quad \text{Which leads to } C_2 = T_0$$

$$T = T_L \text{ at } x = L; \quad \text{Which leads to } C_1 = (T_L - T_0)/L$$

Substituting the values obtained for  $C_1$  and  $C_2$  in Equation (7.4) yields:

$$T(x) = T_0 - \frac{x}{L}(T_L - T_0) \tag{7.5}$$

Substituting for  $x/L = 1/3$  and  $x/L = 2/3$  in Equation (7.5), gives the two temperatures:

$$T_{0.1} = 10^\circ\text{C}$$

$$T_{0.2} = 15^\circ\text{C}$$

This solution indicates that the temperature changes linearly between the two wall surfaces.

**Example 7-2. One-dimensional heat-conduction with a specified heat-flux**

Consider the steady heat conduction in a large plane wall of thickness  $L = 0.3$  m and thermal conductivity  $k = 0.8$  W/m<sup>2</sup>.°C. Suppose that the inner side of the wall is subjected to a constant heat flux  $\dot{q} = 50$  W/m<sup>2</sup> while the outer side of the wall is kept constant at 40°C. Determine the temperature at the inner side of the wall and at the centre of the wall.

**Solution**

Equation (7.4) also applies for this case and values of the constants  $C_1$  and  $C_2$  can be determined by applying the two boundary conditions:

$$\dot{q}_0 = 50 \text{ W/m}^2$$

$$T_L = 40^\circ\text{C}$$

From the first boundary condition:

$$\frac{dT}{dx} = C_1 = -\frac{\dot{q}_o}{k} \quad (7.6)$$

Substituting the given values for  $\dot{q}_o$  and  $k$  gives:

$$C_1 = -50/0.8 = -62.5 \text{ [}^\circ\text{C/m]}$$

Applying the second boundary condition:

$$T_L = C_1L + C_2 \quad (7.7)$$

Substituting the values given for  $T_L$  and  $L$  gives:

$$C_2 = T_L - C_1L = 40 + 62.5 \times 0.3 = 58.75 \text{ [}^\circ\text{C]}$$

Therefore, the equation that describes the temperature variation with  $x$  is:

$$T(x) = 58.75 - 62.5x \quad (7.8)$$

By substituting  $x = 0$  and  $x = 0.15$  in Equation (7.8) we get:

$$T_0 = 58.75^\circ\text{C}, \quad T_{L/2} = 49.375^\circ\text{C}$$

Generally speaking, the analytical method has an important advantage which is that it yields continuous solutions that can be used to determine the temperature at any desired value of  $x$  within the wall. However, its disadvantage is that these solutions are only applicable for simple one-dimensional (1D) and two-dimensional (2D) geometries. Although, analytical solutions of the heat-conduction equation could also be obtained for a number of unsteady 1D and 2D cases, these solutions usually involve complex equations that require using tables of special functions.

## 7.2. Application of the FD method to the steady 1D conduction equation

Unlike the analytical solution method, the FD method and other numerical solution methods for the heat-conduction equation do not provide continuous solutions like Equation (7.5) and Equation (7.8). Instead, they provide numerical values of the temperature at selected points (called nodes) in the physical (spatial or temporal) domain. These values are obtained by creating and then solving a system of algebraic equations that involve the unknown nodal temperatures and take care of the specified boundary conditions. The advantage of the numerical solution methods is that they can deal with three-dimensional (3D) geometries and complex boundary conditions easier than the analytical solution method.

Having identified the relevant form of the conduction equation and boundary conditions, the procedure for applying the FD method is as follows [1, 2]:

1. Lay a grid of nodal points over the solution domain.
2. Write the FD equation relevant to the differential equation and apply it at each internal node of the grid. This results in a difference equation for each node.
3. Assemble all the difference equations into a global system. This system will not have a unique solution before applying the boundary conditions.
4. Apply the boundary conditions by adding the relevant difference equation of the boundary nodes or by modifying the global system.
5. Solve the resulting algebraic system of equations to determine the nodal values of the temperature.

The method will be illustrated by considering the case in Example 7-1 for which the relevant form of the conduction equation is Equation (7.2) and the relevant boundary conditions are the two specified surface temperatures at  $x = 0$  and  $x = L$ .

**Step 1:** The first step in applying the FD method is to divide the wall into nodes as shown in Figure 7.1. This choice makes nodes 1 and 2 coincide with the points at which the temperatures are required, i.e.  $x = 0.1$  and  $0.2$  m.

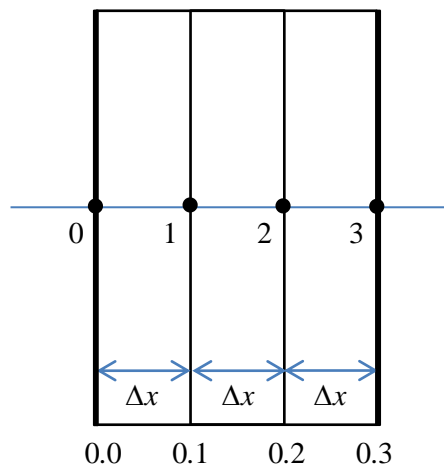


Figure 7.1. Node distribution for the wall in Example 7-1

**Step 2:** The second step is to replace the derivatives in the governing equation by finite differences. In general, the first derivative is approximated by:

$$\frac{dT}{dx} \approx \frac{\Delta T}{\Delta x} \quad (7.9)$$



Where  $\Delta x$  is the distance between two adjacent nodes. However, there are two ways to evaluate  $\Delta T$  in the above approximation given by:

$$\left. \frac{\Delta T}{\Delta x} \right|_{FW} = \frac{T_{m+1} - T_m}{x_{m+1} - x_m} \quad (7.10)$$

$$\left. \frac{\Delta T}{\Delta x} \right|_{BW} = \frac{T_m - T_{m-1}}{x_m - x_{m-1}} \quad (7.11)$$

Where  $m$  refers to the node number and can take the values 0, 1, 2, or 3. The first approximation is called *forward difference*, while the second approximation is called *backward difference*. Similarly, the second derivative is approximated by:

$$\frac{d^2 T}{dx^2} = \frac{d}{dx} \left( \frac{dT}{dx} \right) \approx \frac{T_{m-1} - 2T_m + T_{m+1}}{\Delta x^2} \quad (7.12)$$

The above approximation of the second derivative is called *central difference*. With this approximation, the FD equivalent of Equation (7.2) is the following algebraic equation:

$$\frac{T_{m-1} - 2T_m + T_{m+1}}{\Delta x^2} = 0 \quad (7.13)$$

**Step 3:** Applying Equation (7.13) at the two interior nodes 1 and 2 gives the following equations:

$$\frac{T_0 - 2T_1 + T_2}{\Delta x^2} = 0 \quad (\text{node 1}) \quad (7.14)$$

$$\frac{T_1 - 2T_2 + T_3}{\Delta x^2} = 0 \quad (\text{node 2}) \quad (7.15)$$

**Step 4:** Multiplying both sides of Equations (7.14) and (7.15) by  $\Delta x^2$  and substituting the numerical values for  $T_0$ ,  $T_3$ , and  $\Delta x$  leads to the following linear equations:

$$20 - 2T_1 + T_2 = 0 \quad (7.16)$$

$$T_1 - 2T_2 + 5 = 0 \quad (7.17)$$

**Step 5:** Simultaneous solution of Equations (7.16) and (7.17) for  $T_1$  and  $T_2$  gives  $T_1 = 15^\circ\text{C}$  and  $T_2 = 10^\circ\text{C}$ , which is the same solution obtained earlier by using the analytical method.

The formulation of the FD method described above is limited to:

1. One-dimensional heat-conduction
2. A simple boundary condition (specified-temperature on both sides of the wall)
3. Absence of heat generation in the medium

While the specified-temperature boundary conditions made the FD easy to apply, the lack of heat generation resulted in a linear temperature variation through the wall that enabled it to give exact values. However, the following points have to be borne in mind when dealing with more general cases:

1. The FD method only gives approximate solutions to the conduction equation which may not be exact, e.g., when there is heat generation or a variable  $k$ .
2. The accuracy of the FD results can be improved by increasing the number of nodes that divide the physical domain.
3.  $\Delta x$  does not always have to be uniform as shown in Figure 7.1, but can be varied so as to make a better use of the computer time and memory.
4. The boundary conditions need not be specified values since the FD method can deal with specified heat flux, convective, or other boundary conditions.
5. In multi-dimensional heat-conduction analyses the FD equations involve  $\Delta y$  and  $\Delta z$  and in unsteady conduction analyses they also involve  $\Delta t$ .

The following sections show how the FD method can be used to solve the conduction equation with heat-generation and different boundary conditions and how to deal with two-dimensional heat conduction. As the number of nodes increase, the size of the resulting algebraic system also increases and has to be solved by using a computer-based numerical method. In this respect, the following sections illustrate two methods offered by Excel for solving the algebraic system by using its matrix functions or its iterative-calculation option. More information about the FD method and its approximations is given by Recktenwald [2].

### **7.3. Dealing with various boundary conditions**

Like the analytical solution method, the FD method can deal with boundary conditions other than specified temperature such as:

1. Specified heat flux
2. Convection boundary condition
3. Radiation boundary condition
4. Insulated surface, symmetry surface, and mixed boundary condition

The FD equations for boundary nodes are obtained from energy balance around the node in question. For example, consider the wall shown in Figure 7.2 that experiences uniform heat generation at the rate  $\dot{e}_g$  per unit volume.

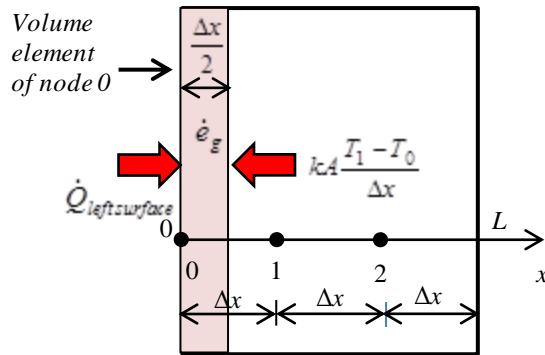


Figure 7.2. Treatment of boundary nodes with specified heat-flux (adapted from Cengel and Ghajar [1])

For steady heat conduction, energy balance around any node gives:

$$\dot{Q}_{left} + \dot{Q}_{right} + \dot{E}_{g, element} = 0 \quad (7.18)$$

For node 0, the FD representation of Equation (7.18) is:

$$\dot{Q}_{left} + kA \frac{T_1 - T_0}{\Delta x} + \dot{e}_g (A\Delta x / 2) = 0 \quad (7.19)$$

The first term in Equation (7.19) that accounts for the rate of heat transfer at the left side of the element volume depends on the particular boundary condition being considered, which can be convection, radiation, flux, or other boundary condition. For illustration, reconsider Example 7-2 that involves a boundary surface with a specified heat flux. By dividing the thickness of the wall  $L$  into two equal sections,  $\Delta x = L/2 = 0.15$  m, the positions of the three nodes involved are as shown in Figure 7.3.

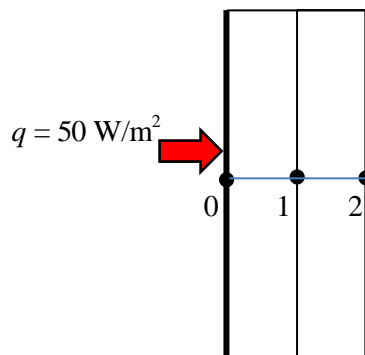


Figure 7.3. Node distribution for Example 7-2

Being an interior node, the FD equation for node 1 is obtained from Equation (7.13) as:

$$\frac{T_0 - 2T_1 + T_2}{\Delta x^2} = 0 \quad (7.20)$$

Multiplying Equation (7.20) by  $\Delta x^2$  and substituting the value of  $T_2$  gives:

$$T_0 = 2T_1 - 40 \quad (7.21)$$

The FD equation for node 0 is obtained by applying Equation (7.19) with  $\dot{e}_g = 0$ :

$$\dot{q}_o + k \frac{T_1 - T_0}{\Delta x} = 0 \quad (7.22)$$

Multiplying Equation (7.22) by  $\Delta x$  and rearranging gives:

$$T_1 = T_0 - \dot{q}_o \frac{\Delta x}{k} \quad (7.23)$$

Substituting for  $T_1$  from Equation (7.23) in Equation (7.22) and rearranging gives:

$$T_0 = 2 \left( \dot{q}_o \frac{\Delta x}{k} \right) + 40 \quad (7.24)$$

Substituting the values of  $\dot{q}_o$ ,  $k$ , and  $\Delta x$  in Equation (7.24) gives:

$$T_0 = 58.75^\circ\text{C}$$

Substituting for  $T_0$  in Equation (7.23) gives:

$$T_1 = 49.375^\circ\text{C}$$

Note that the temperature values obtained by the FD method in this example are also the same as the exact values obtained analytically.

#### 7.4. Conduction with heat generation

For steady one-dimensional conduction heat-transfer in a medium with heat generation, the conduction equation becomes:

$$\frac{d^2 T}{dx^2} + \frac{\dot{e}_g}{k} = 0 \quad (7.25)$$

The FD representation of Equation (7.25) for any interior node  $m$  is [1]:

$$\frac{T_{m-1} - 2T_m + T_{m+1}}{\Delta x^2} + \frac{\dot{e}_g}{k} = 0 \quad (7.26)$$

Multiplying by  $\Delta x^2$ ,

$$T_{m-1} - 2T_m + T_{m+1} = -\frac{\dot{e}_g}{k} \Delta x^2 \quad (7.27)$$

The following example illustrates the application of the FD method for heat-conduction with heat generation and prescribed-temperature boundary conditions. The example is based on Example 2-20 in Cengel and Ghajar [1].

**Example 7-3. FD solution of the steady 1D heat-conduction with heat generation**

A plane wall of thickness  $2L$  that is made of a material having a uniform thermal conductivity  $k$  experiences a uniform heat generation at the rate  $\dot{e}_g$  where:

$$\begin{aligned} 2L &= 0.01 \text{ m;} \\ k &= 18.0 \text{ W/(m}\cdot\text{°C);} \\ \dot{e}_g &= 7.2 \times 10^7 \text{ W/m}^3; \end{aligned}$$

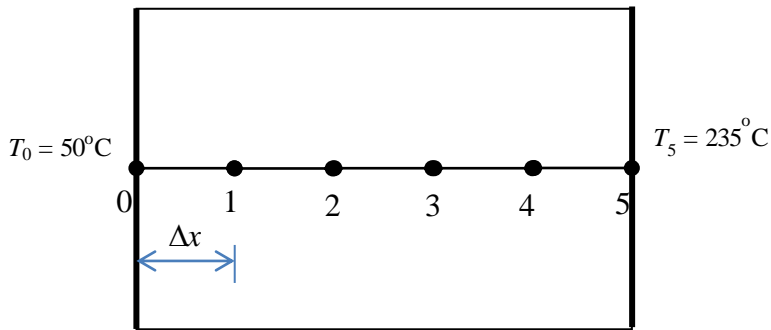


Figure 7.4. Nodal network for Example 7-3

Using the FD method with 6 equally-spaced nodes as shown in Figure 7.4,

- (a) Determine the temperature profile for the boundary conditions:  $T_{-L} = 50^\circ\text{C}$  and  $T_{+L} = 235^\circ\text{C}$ ,
- (b) Compare the FD results with the exact analytical solution.

**Solution**

**Step 1:** Figure 7.4 shows the solution domain divided into 5 equal portions. In this case,  $\Delta x = 0.01/5 = 0.002$  m.

**Step 2:** Applications of Equation (7.27) at the four interior nodes give:

$$T_0 - 2T_1 + T_2 = -R \tag{7.28}$$

$$T_1 - 2T_2 + T_3 = -R \tag{7.29}$$

$$T_2 - 2T_3 + T_4 = -R \tag{7.30}$$

$$T_3 - 2T_4 + T_5 = -R \tag{7.31}$$

Where,

$$R = \dot{e}_g \Delta x^2 / k \tag{7.32}$$

**Steps 3 and 4:** Since the temperatures at node 0 ( $T_0$ ) and node 5 ( $T_5$ ) are known, the above system of linear equations can be put in the following matrix form:

$$\begin{bmatrix} -2 & 1 & 0 & 0 \\ 1 & -2 & 1 & 0 \\ 0 & 1 & -2 & 1 \\ 0 & 0 & 1 & -2 \end{bmatrix} \begin{bmatrix} T_1 \\ T_2 \\ T_3 \\ T_4 \end{bmatrix} = \begin{bmatrix} -R - T_0 \\ -R \\ -R \\ -R - T_5 \end{bmatrix} \tag{7.33}$$

**Step 5:** The above algebraic system can be solved by using the matrix inverse method with Excel's matrix functions as described in Chapter 2. Figure 7.5 shows the Excel sheet developed for this example.

	A	B	C	D	E	F	G	H	I	J	K	L	M	N	O
1	FD 6 nodes														
2	T_0	50	oC		Δx	0.002									
3	T_L	235	oC												
4					R	16									
5	L	0.005	m												
6					-2	1	0	0		T1	-66				
7	k	18	W/(m.oC)		1	-2	1	0		T2	-16				
8					0	1	-2	1		T3	-16				
9	e_gen	7.20E+07	W/m3		0	0	1	-2		T4	-251				
10															
11					-0.8	-0.6	-0.4	-0.2			119				
12					-0.6	-1.2	-0.8	-0.4			172				
13					-0.4	-0.8	-1.2	-0.6			209				
14					-0.2	-0.4	-0.6	-0.8			230				
15															

Figure 7.5. Excel sheet developed for Example 7-3

The left hand side of the sheet stores the given data of the wall based on which the values of  $\Delta x$  and  $R$  are calculated and stored in cell **F2** and **F4**, respectively. The coefficient matrix is stored in cells **E6:H9**, while the right-hand side (r.h.s.) vector is stored in cell **K6: K9**. The formula bar reveals the formula that calculates the first element of the r.h.s. vector. The inverse matrix is calculated using the “**MINVERSE**” function in cells **E11:H14**. The inverse matrix is then multiplied by the r.h.s. vector and the result is stored in cells **J11:J14**.

- (a) According to the solution shown in Figure 7.5, the values of the four temperatures are:  $T_1 = 119^\circ\text{C}$ ,  $T_2 = 172^\circ\text{C}$ ,  $T_3 = 209^\circ\text{C}$ , and  $T_4 = 230^\circ\text{C}$ .
- (b) The analytical solution for this example problem is given by [1]:

$$T = \frac{\dot{e}_g}{2k} (L^2 - \theta^2) + \frac{T_{s2} - T_{s1}}{2L} \theta + \frac{T_{s2} + T_{s1}}{2}, \quad (7.34)$$

Where  $\theta$  is related to  $x$  by:

$$\theta = x - L/2 \quad (7.35)$$

Note that the two surfaces at  $x = 0$  and  $x = L$  correspond to  $\theta = -L/2$  and  $+L/2$ , respectively. Figure 7.6 compares the FD solution to the exact analytical solution obtained by substituting the different values of  $\theta$  in Equation (7.34). As the figure shows, the FD solution agrees well with the analytical solution.

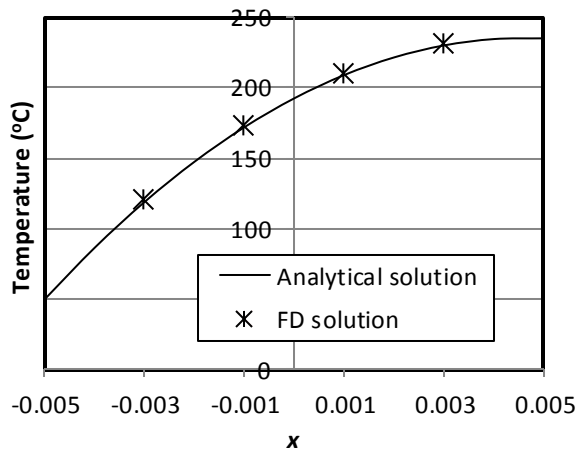


Figure 7.6. Comparison of the analytical and FD solutions of Example 7-3

### 7.5. Two-dimensional steady heat conduction

For a steady-state, two-dimensional heat conduction in a medium with uniform thermal properties and without heat generation, Equation (7.1) reduces to:

$$\frac{\partial^2 T}{\partial x^2} + \frac{\partial^2 T}{\partial y^2} = 0 \quad (7.36)$$

The application of the FD method to Equation (7.36) basically follows the same steps described above for the 1D equation. The following example that demonstrates the 2D application was given by Karimi [3].

**Example 7-4. FD solution of the steady two-dimensional heat conduction**

The 30x30 cm<sup>2</sup> solid section illustrated in Figure 7.7 has its right and bottom surfaces maintained at 100°C and 150°C, respectively. The left surface is insulated, while the top surface is exposed to a convective environment at  $T_\infty = 20^\circ\text{C}$  and heat transfer coefficient  $h = 30 \text{ W}/(\text{m}^2 \cdot ^\circ\text{C})$ . The thermal conductivity of the solid  $k = 5.0 \text{ W}/(\text{m} \cdot ^\circ\text{C})$  and there is no heat generation. By dividing the solid into a nodal network in which  $\Delta x = \Delta y = 10 \text{ cm}$ , use the FD method to find the temperatures at nodal points 1 through 9.

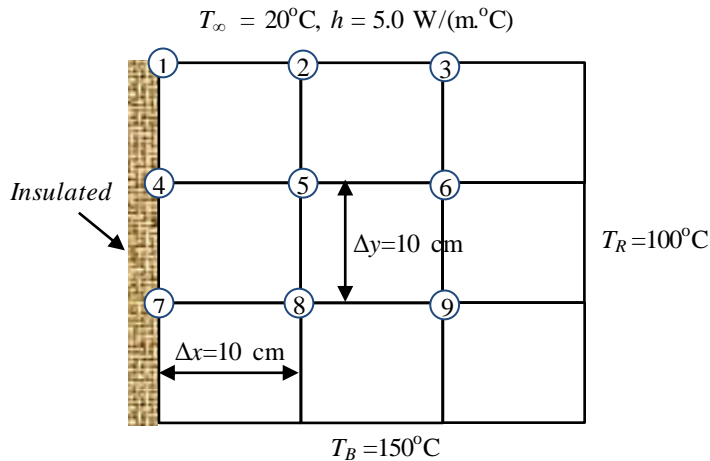


Figure 7.7. The solution domain and nodal network for Example 7-4

**Solution**

For the internal nodes, the FD representation of Equation (7.36) is [1]:

$$\frac{T_{m-1,n} - 2T_{m,n} + T_{m+1,n}}{\Delta x^2} + \frac{T_{m,n-1} - 2T_{m,n} + T_{m,n+1}}{\Delta y^2} = 0 \quad (7.37)$$

Where  $m$  and  $n$  refer to the node's locations in the  $x$  and  $y$ -directions, respectively. Since for the present case  $\Delta x = \Delta y$ , Equation (7.37) can be simplified to:

$$T_{m-1,n} + T_{m+1,n} + T_{m,n-1} + T_{m,n+1} - 4T_{m,n} = 0 \quad (7.38)$$



Applying Equation (7.38) to the four internal nodes, 5, 6, 8, and 9, we get the following four algebraic equations:

$$T_4 + T_2 + T_6 + T_8 - 4 T_5 = 0 \quad (7.39)$$

$$T_5 + T_3 + T_R + T_9 - 4 T_6 = 0 \quad (7.40)$$

$$T_7 + T_5 + T_9 + T_B - 4 T_8 = 0 \quad (7.41)$$

$$T_8 + T_6 + T_R + T_B - 4 T_9 = 0 \quad (7.42)$$

For nodes 4 and 7 that lie on the insulated surface, where  $\dot{q} = 0$ , energy balance gives:

$$T_1 + 2T_5 + T_7 - 4T_4 = 0 \quad (7.43)$$

$$T_4 + 2T_8 + T_B - 4T_7 = 0 \quad (7.44)$$

For nodes 1, 2, and 3 that lie on the top surface, energy balance that takes into account the convection boundary condition gives [3]:

$$T_2 + T_4 + \beta T_\infty - (2+\beta) T_1 = 0 \quad (7.45)$$

$$T_1 + T_3 + 2T_5 + 2\beta T_\infty - 2(2+\beta)T_2 = 0 \quad (7.46)$$

$$T_2 + 2T_6 + T_R + 2\beta T_\infty - 2(2+\beta)T_3 = 0 \quad (7.47)$$

Where  $\beta = h\Delta x/k$ .

The nine linear equations, Equations (7.39) to (7.47), can be put in matrix form as:

$$\begin{bmatrix} -(2+\beta) & 1 & 0 & 1 & 0 & 0 & 0 & 0 & 0 \\ 1 & -2(2+\beta) & 1 & 0 & 2 & 0 & 0 & 0 & 0 \\ 0 & 1 & -2(2+\beta) & 0 & 0 & 2 & 0 & 0 & 0 \\ 1 & 0 & 0 & -4 & 2 & 0 & 1 & 0 & 0 \\ 0 & 1 & 0 & 1 & -4 & 1 & 0 & 1 & 0 \\ 0 & 0 & 1 & 0 & 1 & -4 & 0 & 0 & 1 \\ 0 & 0 & 0 & 1 & 0 & 0 & -4 & 2 & 0 \\ 0 & 0 & 0 & 0 & 1 & 0 & 1 & -4 & 1 \\ 0 & 0 & 0 & 0 & 0 & 1 & 0 & 1 & -4 \end{bmatrix} \begin{Bmatrix} T_1 \\ T_2 \\ T_3 \\ T_4 \\ T_5 \\ T_6 \\ T_7 \\ T_8 \\ T_9 \end{Bmatrix} = \begin{Bmatrix} -\beta T_\infty \\ -2\beta T_\infty \\ -2\beta T_\infty - T_R \\ 0 \\ 0 \\ -T_R \\ -T_B \\ -T_B \\ -T_R - T_B \end{Bmatrix} \quad (7.48)$$

This system of algebraic equations can be solved by using Excel's matrix inversion function and Figure 7.8 shows the Excel sheet prepared for this purpose. The figure

## Computer-Aided Thermofluid Analyses Using Excel

shows the given data at the left hand side of the sheet based on which the sheet calculates the coefficients and right-hand side vector of the linear system.

D3		f <sub>c</sub> = -(2+β)													
	A	B	C	D	E	F	G	H	I	J	K	L	M	N	O
1															
2	T <sub>R</sub>	100		T1	T2	T3	T4	T5	T6	T7	T8	T9			
3	T <sub>B</sub>	150		-2.6	1	0	1	0	0	0	0	0		R1	-12
4	T <sub>∞</sub>	20		1	-5.2	1	0	2	0	0	0	0		R2	-24
5				0	1	-5.2	0	0	2	0	0	0		R3	-124
6	Δx	0.1		1	0	0	-4	2	0	1	0	0		R4	0
7	Δy	0.1		0	1	0	1	-4	1	0	1	0		R5	0
8				0	0	1	0	1	-4	0	0	1		R6	-100
9	h	30		0	0	0	1	0	0	-4	2	0		R7	-150
10	k	5		0	0	0	0	1	0	1	-4	1		R8	-150
11				0	0	0	0	0	1	0	1	-4		R9	-250
12	β	0.6													
13															

Figure 7.8. Excel sheet developed for Example 7-4

Figure 7.9 shows the inverse matrix and the solution obtained by multiplying the inverse matrix with the right-hand side vector. Table 7.1 compares the present solution with that given by Karimi [3] who solved the algebraic system by using Solver as shown in Chapter 3. The table shows that the two solutions are identical.

13																
14				-0.5252	-0.15542	-0.04831	-0.2101	-0.23469	-0.09581	-0.0805	-0.11191	-0.05193		T1	67.4482	
15				-0.15542	-0.28676	-0.07771	-0.11735	-0.258	-0.11735	-0.05595	-0.10647	-0.05595		T2	68.46907	
16				-0.04831	-0.07771	-0.23844	-0.04791	-0.11735	-0.16219	-0.02596	-0.05595	-0.05454		T3	74.15267	
17				-0.2101	-0.11735	-0.04791	-0.42891	-0.35219	-0.13177	-0.15335	-0.18449	-0.07906		T4	94.89625	
18				-0.11735	-0.129	-0.05867	-0.1761	-0.49479	-0.1761	-0.09224	-0.19288	-0.09224		T5	95.21915	
19				-0.04791	-0.05867	-0.0811	-0.06588	-0.1761	-0.36303	-0.03953	-0.09224	-0.11382		T6	96.56241	
20				-0.0805	-0.05595	-0.02596	-0.15335	-0.18449	-0.07906	-0.34841	-0.24029	-0.07984		T7	121.6985	
21				-0.05595	-0.05323	-0.02798	-0.09224	-0.19288	-0.09224	-0.12014	-0.38833	-0.12014		T8	120.9489	
22				-0.02596	-0.02798	-0.02727	-0.03953	-0.09224	-0.11382	-0.03992	-0.12014	-0.30849		T9	116.8778	
23																

Figure 7.9. FD solution of Example 7-4

Table 7.1. Comparison of the present solution with that given by Karimi [3]

°C	Karimi [3]	Present solution
$T_1$	67.44	67.448
$T_2$	68.46	68.469
$T_3$	74.15	74.153
$T_4$	94.89	94.896
$T_5$	95.21	95.219
$T_6$	96.56	96.562
$T_7$	121.69	121.69
$T_8$	120.95	120.949
$T_9$	116.88	116.878

**7.6. Application of the FD method using Excel ‘s iterative calculation option**

In the two previous sections the FD method was applied by assembling the nodal equations into a global system of linear equations that could be solved by using Excel’s matrix functions (or Solver). Although this approach of applying the FD method with Excel is straight-forward and simple to implement, Excel enables an alternative approach for applying the method by using its iterative calculation option that doesn’t require the algebraic system to be assembled explicitly. Instead, the Excel sheet is developed in the shape of the heat-transfer medium and each node in the solution domain is represented by a cell that stores the corresponding FD equation. The stored FD equations are then solved simultaneously by activating Excel’s iterative calculation option. Apart from eliminating the need to assemble the algebraic system, this approach makes the FD model look more like a physical model than a mathematical one [4,5].

Example 7-4 will be used to illustrate this method and Figure 7.10 shows the Excel sheet prepared for this purpose. A 3x3 block of cells is reserved for the 9 nodes with unknown temperatures, while the cells in the block boundaries store the values of the ambient temperature (20°C) and the two surface temperatures (100°C and 150°C).

	A	B	C	D	E	F	G	H
1								
2	T_R	100						
3	T_B	150		20	20	20	20	
4	T_∞	20						100
5					0.00			100
6	Δx	0.1						100
7	Δy	0.1		150	150	150	150	
8								
9	h	30						
10	k	5						
11								
12	β	0.6						
13								

Figure 7.10. Excel sheet for Example 7-4 showing the 3x3 grid of nodes and the boundary temperatures

Each cell of the 3x3 block stores the relevant nodal FD formula that determines its temperature from those of the surrounding cells as given by the FD equations. When entered into the coloured Excel cells, the interdependence between the different nodal equations will create circular references. By allowing iterative-calculations, Excel will find the solution that satisfies all the inter-related nodal equations without having to assemble the global system of equations.

Equation (7.38) for the four internal nodes 5,6,8,9 can be written as:

$$T_{\text{node}} = (T_{\text{left}} + T_{\text{top}} + T_{\text{right}} + T_{\text{bottom}})/4 \tag{7.49}$$

## Computer-Aided Thermofluid Analyses Using Excel

The formula bar in Figure 7.10 shows the formula typed in cell **E5** that stores the FD equation for node 5 based on Equation (7.49), which is:

$$\mathbf{E5} = (\mathbf{D5} + \mathbf{E4} + \mathbf{F5} + \mathbf{E6})/4$$

Note that the usual reference by cell-location is used. For the other three internal nodes, the above formula can be simply copied and pasted in the cells **F5**, **E6**, and **F6**, respectively. However, pasting the formula in cells **F5** that correspond to node 6 will cause a circular reference as shown in Figure 7.11. When this occurs, press the “**OK**” button and proceed to paste the formula in cells **E6** and **F6** that correspond to nodes 8 and 9, respectively.

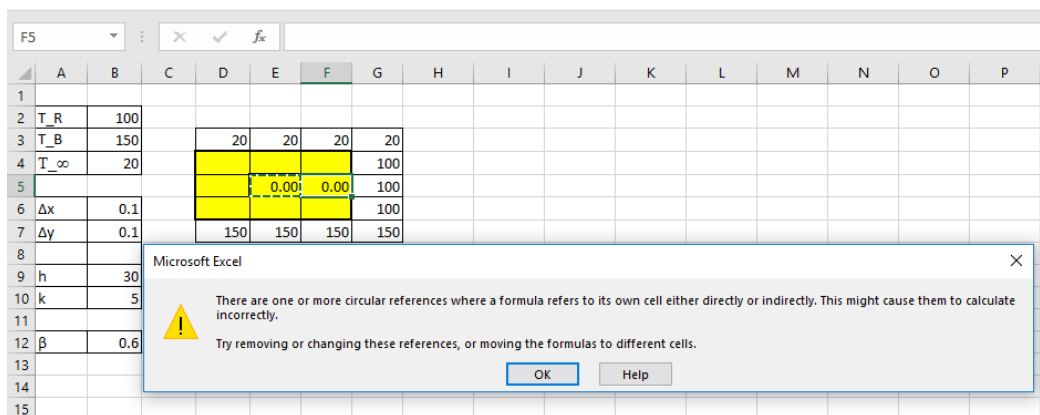


Figure 7.11. The circular-calculation warning message given by Excel when its iterative-solution option is not active

We also have to enter the relevant FD equations for the boundary nodes 1, 2, and 3 that lie on the top convection boundary in the respective cells. Taking node 1 as an example, the relevant FD equation is obtained by re-arranging Equation (7.45) as follows:

$$T_1 = (T_2 + T_4 + \beta T_\infty)/(2 + \beta) \quad (7.50)$$

Using cell-location referencing, the above formula is entered in cell **D4** as follows:

$$\mathbf{D4} = (\mathbf{E4} + \mathbf{D5} + \beta \times \mathbf{D3})/(2 + \beta)$$

Similarly, the following formulae are entered in cells **E4** and **F4** for nodes 2 and 3, respectively, based on Equations (7.46) and (7.47):

$$\mathbf{E4} = (\mathbf{D4} + \mathbf{F4} + \mathbf{D5} + \beta \times \mathbf{E3})/(2 + (2 + \beta))$$

$$\mathbf{F4} = (\mathbf{E4} + \mathbf{G4} + \mathbf{E5} + \beta \times \mathbf{F3})/(2 + (2 + \beta))$$

The FD equations for node 4 and node 7 that lie on the insulated left side of the solid are to be obtained by rearranging Equations (7.43) and (7.44) following the same procedure and typed in cells **D5** and **D6**, respectively. Figure 7.12 reveals the complete set of formulae for the nine cells. The simultaneous solution of the equations can now be found by using Excel’s iterative calculation option. To do that, go to “**File**”→ “**Options**”→ “**Formulas**” and then select “**Enable iterative calculation**”.

D	E	F	G
=T_∞	=T_∞	=T_∞	=T_∞
=(E4+D5+β*D3)/(2+β)	=(D4+F4+2*E5+2*β*E3)/(2*(2+β))	=(E4+G4+2*F5+2*β*F3)/(2*(2+β))	=T_R
=(D4+2*E5+D6)/4	=(D5+E4+F5+E6)/4	=(E5+F4+G5+F6)/4	=T_R
=(D5+2*E6+D7)/4	=(D6+E5+F6+E7)/4	=(E6+F5+G6+F7)/4	=T_R
=T_B	=T_B	=T_B	=T_B

Figure 7.12. The nine nodal FD equations entered in the corresponding cells

Figure 7.13 shows the solution determined by Excel for Example 7-4 with this method. Comparison with the temperature values obtained earlier, confirms the solution’s accuracy.

20	20	20	20
67.45	68.47	74.15	100
94.90	95.22	96.56	100
121.70	120.95	116.88	100
150	150	150	150

Figure 7.13. The temperature distribution in the solid of Example 7-4

The solution was obtained with the default settings of 100 as the maximum number of iterations and 0.001 as the maximum change. In certain situations, these default values may have to be adjusted so as to save computer time or to avoid solution divergence [4]. Although  $\Delta x$  and  $\Delta y$  do not have to be equal for the application of this approach, it makes the application of the method easier. Also note that this approach suits 1D and 2D heat-conduction problems, but not 3D conduction problems unless the cells in the third direction are stored in separate sheets of the workbook.

### 7.7. Closure

This chapter demonstrated the usefulness of Excel for applying the finite-difference method to solve the steady heat-conduction equation. The basic technique of the numerical method was explained by considering the simple 1D steady conduction in a plane wall with specified-temperature boundary conductions and did not involve heat

generation before showing how the method can deal with different boundary conditions, heat-generation, and 2D conduction.

As an educational tool, Excel has an important advantage compared to other computer software by offering two methods for applying the FD method. The first approach, which is more conventional, explicitly forms the global system of linear equations and uses the matrix-inversion method to solve the system with Excel's matrix functions. This approach, which suits the simple cases of steady 1D conduction equations, has been used to introduce the FD method. The second approach avoids the explicit formation of the algebraic systems by utilising Excel's iterative-calculations capability. The advantage of this approach is that it makes the FD model look like a physical model of the conduction problem. As shown in the following chapter, this approach is also useful for solving the transient 2D conduction equation with the FD method.

For the purpose of simplification, all the examples considered in the chapter solved the heat conduction equation in simple 1D or 2D geometries. Appendix E describes a FD analysis of the steady conduction heat-transfer in a triangular fin. This case shows how the method can be used to deal with a more complex geometry.

### References

- [1] Y. A. Cengel and A. J. Ghajar, *Heat and Mass Transfer: Fundamentals and Applications*. 4<sup>th</sup> edition, McGraw-Hill, 2011
- [2] G. W. Recktenwald, Finite-Difference Approximations to the Heat Equation, *Mechanical Engineering*, 10, 1-27, 2004
- [3] A. Karimi, A compilation of examples for using Excel in solving heat transfer problems, American Society for Engineering Education Conference, AC 2009-2284, University of Texas, San Antonio, 2009
- [4] E. M. A. Mokheimer and M. A. Antar, On the use of spreadsheets in heat conduction analysis, *International Journal of Mechanical Engineering Education* Vol 28 No 2, April 2000
- [5] R. Edwards and M. Lobaugh, Using Excel to Implement the Finite Difference Method for 2-D Heat Transfer in a Mechanical Engineering Technology Course, 121<sup>st</sup> ASEE Annual Conference and Exposition, Indianapolis, June 15-18, 2014

### Exercises

1. Figure 7.P1 shows a large uranium plate of thickness  $L = 4$  cm and thermal conductivity  $k = 28$  W/m·K in which heat is generated uniformly at a constant rate of  $\dot{e}_g = 5 \times 10^6$  W/m<sup>3</sup>. One side of the plate is maintained at 0°C by iced water while the other side is subjected to convection to an environment at  $T_\infty = 30^\circ\text{C}$  with a heat transfer coefficient  $h = 45$  W/m<sup>2</sup>·K. Considering a total of five equally spaced nodes in the medium, two at the boundaries and three at the middle, develop three Excel sheets to estimate the exposed surface temperature of the plate under steady conditions using the finite difference method with the following options:

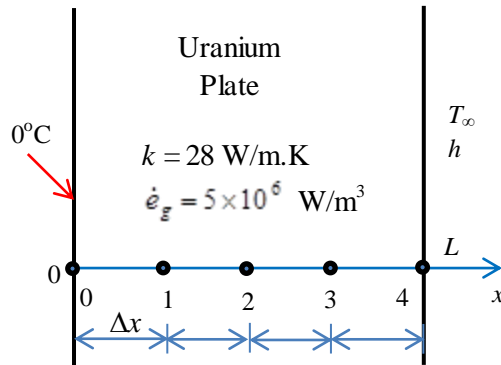


Figure 7.P1 Schematic for Problem 7.1 (adapted from Cengel and Ghajar [1])

- (a) Using the explicit method
- (b) Using the implicit method that assembles and solves the linear system
- (c) Using the implicit method with the iterative-calculation option

This exercise is based on Example 5-1 in Cengel and Ghajar [1].

2. Develop an Excel sheet to Solve Example 7-3 with 10 equally-spaced nodes and compare the FD solutions with 5 and 10 nodes with the exact analytical solution given by Equation (7.34).
3. Consider the fin with an insulated tip shown in Figure 7.P3. The fin is of thermal conductivity  $k$ , length  $L$ , constant cross-sectional area  $A$ , perimeter  $P$ , and specified base temperature  $T_w$ . The heat transfer coefficient to ambient at  $T_\infty$  is  $h$ .

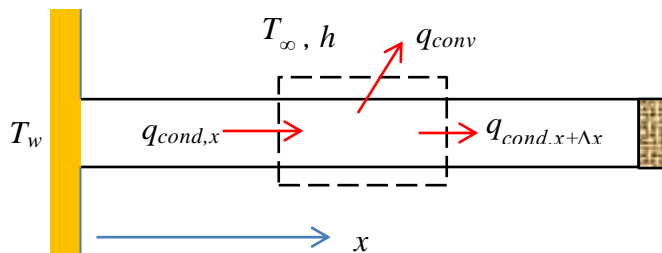


Figure 7.P3 Schematic for Problem 7.3 (adopted from Recktenwald [2])

Neglecting the temperature variation over the cross-sectional area, for small Biot numbers ( $Bi = hL_c/k$ ), the governing equation in a dimensionless form is:

$$\frac{d^2\theta}{dX^2} - m^2\theta = 0$$

Where,

## Computer-Aided Thermofluid Analyses Using Excel

$$X = x / L, \quad \theta = \frac{T - T_{\infty}}{T_w - T_{\infty}}, \quad m = \sqrt{PhL^2 / Ak}$$

Develop an Excel sheet for analysing the steady one dimensional heat conduction in the fin subjected to the following boundary conditions:

$$\theta(0) = 1,$$

$$\left. \frac{d\theta}{dX} \right|_{X=1} = 0$$

Compare your FD solution at the 5 nodes with the following analytical solution:

$$\theta(x) = \frac{\text{Cosh}[m(1 - X)]}{\text{Cosh}(m)}$$



# 8

## **Finite-difference solution of the transient heat-conduction equation**

This chapter extends the methodology presented in the previous chapter so as to solve the transient heat-conduction equation with the finite-difference (FD) method. The chapter initially considers the 1D conduction-equation to demonstrate the application of the method by using both the explicit forward-in-time central difference in space (FTCS) scheme and the implicit backward-in-time central difference in space (BTCS) scheme. For the implicit scheme that requires a system of linear equations to be solved, the chapter presents two methods for using Excel. The first method explicitly forms and solves the linear system using the tri-diagonal matrix algorithm (TDMA), while the second method does not form the linear system but uses Excel's iterative-calculation option to solve the nodal equations. For solving the 2D conduction equation that requires a large system of linear equations to be solved with the first method, only the second method for applying the implicit FD scheme is used.

### 8.1. Transient 1D conduction: the explicit FTCS formulation

The transient one-dimensional heat-transfer by conduction is governed by:

$$\frac{\partial T}{\partial t} = \alpha \frac{\partial^2 T}{\partial x^2} \quad (8.1)$$

As shown in the previous chapter, the FD method replaces the spatial derivative ( $\partial^2 T / \partial x^2$ ) by the central difference defined by Equation (7.13). For the temporal term ( $\partial T / \partial t$ ) either forward or backward differences can be used, i.e.:

$$\left. \frac{\partial T}{\partial t} \right|_{FW} \approx \frac{T_m^{i+1} - T_m^i}{\Delta t} \quad (8.2)$$

$$\left. \frac{\partial T}{\partial t} \right|_{BW} \approx \frac{T_m^i - T_m^{i-1}}{\Delta t} \quad (8.3)$$

Depending on whether Equation (8.2) or (8.3) is selected, two FD formulations for Equation (8.1) are possible: a forward-in-time central-difference in space (FTCS) scheme and a backward-in-time central-difference in space (BTCS) scheme. This section focuses on the first scheme.

By using Equation (8.2), the FD approximation of Equation (8.1) becomes:

$$\frac{T_m^{i+1} - T_m^i}{\Delta t} = \alpha \frac{T_{m+1}^i - 2T_m^i + T_{m-1}^i}{\Delta x^2} \quad (8.4)$$

Note that the temperatures at the two neighbouring nodes are evaluated at time level  $i$ . Equation (8.4) can be rearranged as follows:

$$T_m^{i+1} = T_m^i + \tau(T_{m+1}^i - 2T_m^i + T_{m-1}^i) \quad (8.5)$$

Where,  $\tau$  is the dimensionless mesh Fourier number defined as:

$$\tau = \frac{\alpha \Delta t}{\Delta x^2} \quad (8.6)$$

Equation (8.5) calculates the temperature at the current time step ( $i$ ) from the known values at the previous time step. Starting with a known temperature field, it can be used directly to compute the new temperature field because all the values of  $T_m^{i+1}$  can be updated independently. The FTCS scheme is easy to implement, but it is only conditionally stable by requiring the time step  $\Delta t$  to be chosen such that [1]:

$$\tau < \frac{1}{2} \quad (8.7)$$

The following example shows how the scheme is applied.

**Example 8-1. Solving the transient 1D conduction equation with the FTCS scheme**

Transient heat-conduction occurs in a plate with length  $L = 0.1$  m and diffusivity  $\alpha = 0.1$ . The boundary conditions are  $T(0,t) = T(L,t) = 0$  and the initial temperature distribution is given by:

$$T(x) = \sin(\pi x/L) \quad (8.8)$$

The exact temperature variation is given by [1]:

$$T(x,t) = \sin\left(\frac{\pi x}{L}\right) \exp\left(-\frac{\alpha \pi^2 t}{L^2}\right) \quad (8.9)$$

Use the FD method with a grid of 21 equally-spaced nodes and a suitable time step to determine the temperature variation at  $t = 0.2$  s.

**Solution**

By dividing the length of the plate into 21 equally-spaced nodes,  $\Delta x = 0.1/20 = 0.05$  m. According to Equation (8.7), the maximum allowable time step  $\Delta t$  is given by:

$$\Delta t = 0.5 \times 0.05^2 / 0.1 = 0.0125 \text{ s}$$

Therefore, we can use a time step of 0.01 s. The following procedure for implementing the FD solution with Excel follows that described by Anthony [2]. Figure 8.1 shows the

## Computer-Aided Thermofluid Analyses Using Excel

sheet into which the specified values of  $\alpha$ ,  $\Delta x$ , and  $\Delta t$  are entered at the top part of the sheet.

	A	B	C	D	E	F	G	H	I	J	K	L	M	N	O	P	Q	R	S	T	U	V
1		$\Delta x$	0.05		$\Delta t$	0.01		$\alpha$	0.1													
2		$x \rightarrow$																				
3		$t \downarrow$																				
4	0	0	0.05	0.1	0.15	0.2	0.25	0.3	0.35	0.4	0.45	0.5	0.55	0.6	0.65	0.7	0.75	0.8	0.85	0.9	0.95	1
5	0	0	0.156	0.309	0.454	0.588	0.707	0.809	0.891	0.951	0.988	1.000	0.988	0.951	0.891	0.809	0.707	0.588	0.454	0.309	0.156	0

Figure 8.1. The Excel sheet with the nodal coordinates and initial temperatures for Example 8-1

The  $x$ -values of the 21 nodes are entered in cells **B4** to **V4**. The following row of cells, i.e., cells **B5** to **V5** store the initial temperature profile as obtained from Equation (8.8). The formula bar reveals the formula that calculated the initial temperature at  $x=0.5$  cm. Cells **B6** and **V6** store the specified boundary conditions at  $x=0$  and  $x=L$ . Next, we aim to determine the temporal temperature variation by dividing the required time span (0.2 s) into equal time levels  $\Delta t$  long. Enter the first 10 time-levels in column A in the Excel sheet, as shown in Figure 8.2.

	A	B	C	D	E	F	G	H	I	J	K	L	M	N	O	P	Q	R	S	T	U	V
1		$\Delta x$	0.05		$\Delta t$	0.01		$\alpha$	0.1													
2		$x \rightarrow$																				
3		$t \downarrow$																				
4	0	0	0.05	0.1	0.15	0.2	0.25	0.3	0.35	0.4	0.45	0.5	0.55	0.6	0.65	0.7	0.75	0.8	0.85	0.9	0.95	1
5	0	0	0.156	0.309	0.454	0.588	0.707	0.809	0.891	0.951	0.988	1.000	0.988	0.951	0.891	0.809	0.707	0.588	0.454	0.309	0.156	0
6	0.01	0																				
7	0.02	0																				
8	0.03	0																				
9	0.04	0																				
10	0.05	0																				
11	0.06	0																				
12	0.07	0																				
13	0.08	0																				
14	0.09	0																				
15	0.1	0																				

Figure 8.2. Calculating the time levels and inserting the two boundary conditions

Each time level is calculated by adding  $\Delta t$  to the previous time level. In Figure 8.2, the expression in the formula bar in cell **A6** shows the specific Excel formula used to compute the new time level,  $t_2$ , by adding the fixed time increment ( $\Delta t$ ) to the previous time level,  $t_1$ , stored in the cell immediately above it, i.e., cell **A5**. The time levels at other periods are obtained by simply copying the formula in cell **A6** and pasting it in cells **A7** to **A25** as shown in Figure 8.3. The boundary conditions at  $x=0$  and  $x=L$  are then inserted in columns **B6:B25** and **V6:V25**. For clarification, these two columns are given a blue colour. Equation (8.5) is then applied in cell **C6** to calculate the temperatures at time level 2 ( $t=\Delta t$ ) and  $x=\Delta x$  as shown in the formula bar of Figure 8.3. This formula is then copied and pasted in all other cells in the same row (**D6:U6**) and the following rows (**C7:U25**).

C6     $=C5+\alpha*\Delta t/\Delta x^2*(D5-2*C5+B5)$

	A	B	C	D	E	F	G	H	I	J	K	L	M	N	O	P	Q	R	S	T	U	V
1		$\Delta x$	0.05		$\Delta t$	0.01		$\alpha$	0.1													
2																						
3		$x \rightarrow$																				
4	$t \downarrow$	0	0.05	0.1	0.15	0.2	0.25	0.3	0.35	0.4	0.45	0.5	0.55	0.6	0.65	0.7	0.75	0.8	0.85	0.9	0.95	1
5	0	0	0.156	0.309	0.454	0.588	0.707	0.809	0.891	0.951	0.988	1.000	0.988	0.951	0.891	0.809	0.707	0.588	0.454	0.309	0.156	0
6	0.01	0	0.155	0.306	0.450	0.582	0.700	0.801	0.882	0.942	0.978	0.990	0.978	0.942	0.882	0.801	0.700	0.582	0.450	0.306	0.155	0
7	0.02	0	0.153	0.303	0.445	0.576	0.693	0.793	0.874	0.932	0.968	0.980	0.968	0.932	0.874	0.793	0.693	0.576	0.445	0.303	0.153	0
8	0.03	0	0.152	0.300	0.441	0.571	0.686	0.785	0.865	0.923	0.959	0.971	0.959	0.923	0.865	0.785	0.686	0.571	0.441	0.300	0.152	0
9	0.04	0	0.150	0.297	0.436	0.565	0.680	0.778	0.856	0.914	0.949	0.961	0.949	0.914	0.856	0.778	0.680	0.565	0.436	0.297	0.150	0
10	0.05	0	0.149	0.294	0.432	0.559	0.673	0.770	0.848	0.905	0.940	0.952	0.940	0.905	0.848	0.770	0.673	0.559	0.432	0.294	0.149	0
11	0.06	0	0.147	0.291	0.428	0.554	0.666	0.762	0.840	0.896	0.931	0.942	0.931	0.896	0.840	0.762	0.666	0.554	0.428	0.291	0.147	0
12	0.07	0	0.146	0.288	0.424	0.548	0.660	0.755	0.831	0.887	0.922	0.933	0.922	0.887	0.831	0.755	0.660	0.548	0.424	0.288	0.146	0
13	0.08	0	0.145	0.285	0.419	0.543	0.653	0.747	0.823	0.879	0.912	0.924	0.912	0.879	0.823	0.747	0.653	0.543	0.419	0.285	0.145	0
14	0.09	0	0.143	0.283	0.415	0.538	0.647	0.740	0.815	0.870	0.904	0.915	0.904	0.870	0.815	0.740	0.647	0.538	0.415	0.283	0.143	0
15	0.1	0	0.142	0.280	0.411	0.532	0.640	0.733	0.807	0.861	0.895	0.906	0.895	0.861	0.807	0.733	0.640	0.532	0.411	0.280	0.142	0
16	0.11	0	0.140	0.277	0.407	0.527	0.634	0.726	0.799	0.853	0.886	0.897	0.886	0.853	0.799	0.726	0.634	0.527	0.407	0.277	0.140	0
17	0.12	0	0.139	0.274	0.403	0.522	0.628	0.718	0.791	0.845	0.877	0.888	0.877	0.845	0.791	0.718	0.628	0.522	0.403	0.274	0.139	0
18	0.13	0	0.138	0.272	0.399	0.517	0.622	0.711	0.783	0.836	0.868	0.879	0.868	0.836	0.783	0.711	0.622	0.517	0.399	0.272	0.138	0
19	0.14	0	0.136	0.269	0.395	0.512	0.616	0.704	0.776	0.828	0.860	0.871	0.860	0.828	0.776	0.704	0.616	0.512	0.395	0.269	0.136	0
20	0.15	0	0.135	0.266	0.391	0.507	0.610	0.697	0.768	0.820	0.851	0.862	0.851	0.820	0.768	0.697	0.610	0.507	0.391	0.266	0.135	0
21	0.16	0	0.134	0.264	0.387	0.502	0.604	0.691	0.761	0.812	0.843	0.854	0.843	0.812	0.761	0.691	0.604	0.502	0.387	0.264	0.134	0
22	0.17	0	0.132	0.261	0.384	0.497	0.598	0.684	0.753	0.804	0.835	0.845	0.835	0.804	0.753	0.684	0.598	0.497	0.384	0.261	0.132	0
23	0.18	0	0.131	0.259	0.380	0.492	0.592	0.677	0.746	0.796	0.827	0.837	0.827	0.796	0.746	0.677	0.592	0.492	0.380	0.259	0.131	0
24	0.19	0	0.130	0.256	0.376	0.487	0.586	0.670	0.738	0.788	0.818	0.829	0.818	0.788	0.738	0.670	0.586	0.487	0.376	0.256	0.130	0
25	0.2	0	0.128	0.254	0.372	0.482	0.580	0.664	0.731	0.780	0.810	0.820	0.810	0.780	0.731	0.664	0.580	0.482	0.372	0.254	0.128	0

Figure 8.3. Excel sheet prepared for solving Example 8-1 with the FTCS scheme

Figure 8.3 shows the temperatures determined by the FD formula at different nodes and time levels. Figure 8.4 shows the initial temperature profile and the temperature profiles at time  $t=0.2$  s as determined by the FTCS scheme and by the exact analytical solution given by Equation (8.9). A close agreement is achieved between the two solutions because the time step used is sufficiently small. Figure 8.5 shows the solution at  $t = 1.0$  s with a larger time step  $\Delta t = 0.05$ . In this case,  $\tau = 2$  and as the figure show the FTCS scheme becomes unstable.

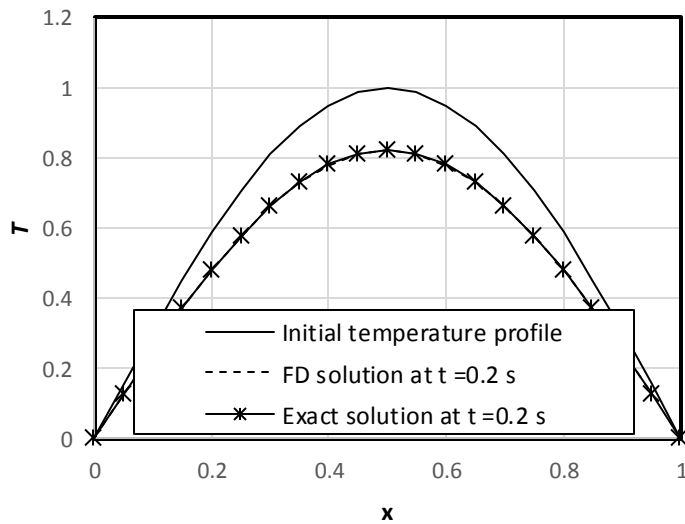


Figure 8.4. Comparison of the FTCS solution with the exact analytical solution ( $t = 0.2$  s,  $\Delta t = 0.01$ s)

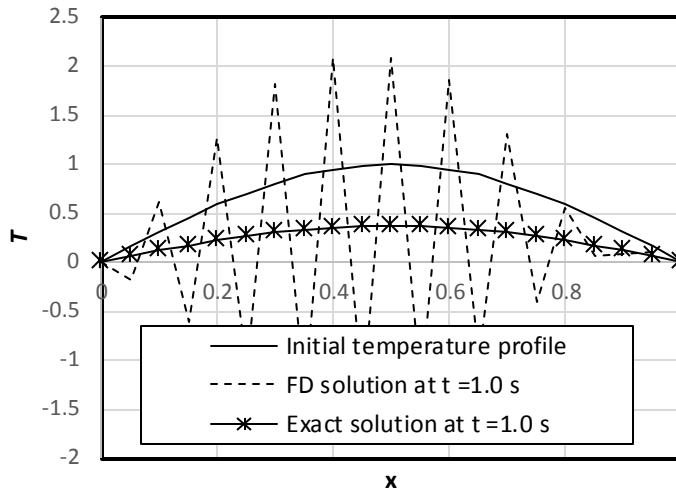


Figure 8.5. Comparison of the FTCS solution with the exact analytical solution  
( $t = 1.0$  s,  $\Delta t = 0.05$  s)

### 8.2. Transient 1D conduction: the implicit BTCS formulation

Substituting Equation (8.3) into the left-hand side of Equation (8.1) and substituting Equation (7.13) into the right-hand side of the equation gives;

$$\frac{T_m^i - T_m^{i-1}}{\Delta t} = \alpha \frac{T_{m-1}^i - 2T_m^i + T_{m+1}^i}{\Delta x^2} \quad (8.10)$$

Here also, the temperatures at the two neighbouring nodes are evaluated at time level  $i$ . Equation (8.10) can be rearranged as follows:

$$aT_{m-1}^i + bT_m^i - cT_{m+1}^i = d \quad (8.11)$$

Where,  $a = -\alpha / \Delta x^2$

$$b = \left(1 / \Delta t + 2\alpha / \Delta x^2\right)$$

$$c = -\alpha / \Delta x^2$$

$$d = (1 / \Delta t)T_m^{i-1}$$

Unlike Equation (8.5), Equation (8.11) is not a simple algebraic formula for computing  $T_m^i$  from its value at the previous time level,  $T_m^{i-1}$  because  $T_m^i$  and its neighbours,  $T_{m+1}^i$

and  $T_{m-1}^i$ , are at the same time level. Thus, Equation (8.11) is one equation in a system of equations for the values of  $T$  at the internal nodes of the spatial mesh. Equations similar to Equation (8.11) can be written for each node, thus, forming a system of algebraic equations that can be written as [1]:

$$\begin{bmatrix} b_1 & c_1 & 0 & 0 & 0 & 0 \\ a_2 & b_2 & c_2 & 0 & 0 & 0 \\ 0 & a_3 & b_3 & c_3 & 0 & 0 \\ 0 & 0 & \ddots & \ddots & \ddots & 0 \\ 0 & 0 & 0 & a_{N-1} & b_{N-1} & c_{N-1} \\ 0 & 0 & 0 & 0 & a_N & b_N \end{bmatrix} \begin{bmatrix} T_1^i \\ T_2^i \\ T_3^i \\ \vdots \\ T_{N-1}^i \\ T_N^i \end{bmatrix} = \begin{bmatrix} d_1 \\ d_2 \\ d_3 \\ \vdots \\ d_{N-1} \\ d_N \end{bmatrix} \quad (8.12)$$

The above system of linear equations has to be solved at every time level in order to determine the temperatures at that time level. Note that the coefficient matrix does not change with time, but the r.h.s. vector does. Also note that the algebraic system of equations has only three non-zero diagonals and, therefore, can be solved by using the tri-diagonal matrix algorithm (TDMA) which is more efficient than the matrix inversion method [3].

Although the BTCS scheme requires solving the system of linear equations in Equation (8.12) at each time step, the additional development effort and computer time are compensated for by the improved stability of the scheme that allows larger time steps to be used compared to the explicit FTCS scheme. As shown in the previous chapter, Excel offers two options for solving the system of linear equations one of which explicitly assembles and then solves the system, while the other uses the iterative-calculation option of Excel to solve the systems without assembling it. The two methods are presented below.

### 8.2.1. Application of the BTCS scheme by assembling the linear system

Figure 8.6 shows the Excel sheet prepared for solving Example 8-1 by using the BTCS scheme. To make the sheet look like that used for applying the FTCS scheme, the linear system of Equation (8.12) has to be solved externally for the temperature values shown at each time level. This has been achieved by writing a custom VBA function called “**FDimplicit**” that determines the coefficient matrix given by Equation (8.12) and solves the resulting system by calling a TDMA solver, called “**TDMA**”. Both the “**FDimplicit**” function and the “**TDMA**” solver are listed in Appendix F. Figure 8.7 compares the FD solution obtained with  $\Delta t = 0.01$  s with the exact solution at  $t = 0.2$  s. The figure shows a close agreement between the two solutions. Figure 8.8, that compares the temperature values obtained at  $t = 1.0$  s with  $\Delta t = 0.05$  s with the exact solution, does not show any sign of solution instability with this scheme for which the time step is limited by the required accuracy rather than the scheme’s stability.

# Computer-Aided Thermofluid Analyses Using Excel

		[=FdimPLICIT( $\Delta x, \Delta t, \alpha, N, M, L, B4:V4$ )]																				
A	B	C	D	E	F	G	H	I	J	K	L	M	N	O	P	Q	R	S	T	U	V	
1	$\Delta x$	0.05		$\Delta t$	0.05		$\alpha$	0.1		N	21											
2	$x \rightarrow$																					
3	$t \downarrow$	0	0.05	0.1	0.15	0.2	0.25	0.3	0.35	0.4	0.45	0.5	0.55	0.6	0.65	0.7	0.75	0.8	0.85	0.9	0.95	
4	0	0	0.156	0.309	0.454	0.588	0.707	0.809	0.891	0.951	0.988	1.000	0.988	0.951	0.891	0.809	0.707	0.588	0.454	0.309	0.156	0
5	0.05	0	0.149	0.295	0.433	0.560	0.674	0.771	0.849	0.906	0.941	0.953	0.941	0.906	0.849	0.771	0.674	0.560	0.433	0.295	0.149	0
6	0.1	0	0.142	0.281	0.412	0.534	0.642	0.735	0.809	0.864	0.897	0.908	0.897	0.864	0.809	0.735	0.642	0.534	0.412	0.281	0.142	0
7	0.15	0	0.135	0.268	0.393	0.509	0.612	0.700	0.771	0.823	0.855	0.866	0.855	0.823	0.771	0.700	0.612	0.509	0.393	0.268	0.135	0
8	0.2	0	0.129	0.255	0.375	0.485	0.583	0.667	0.735	0.785	0.815	0.825	0.815	0.785	0.735	0.667	0.583	0.485	0.375	0.255	0.129	0
9		0	0.128	0.254	0.373	0.482	0.580	0.664	0.731	0.781	0.811	0.821	0.811	0.781	0.731	0.664	0.580	0.482	0.373	0.254	0.128	0
10																						

Figure 8.6. Excel sheet prepared for solving Example 8-1 with the BTCS scheme

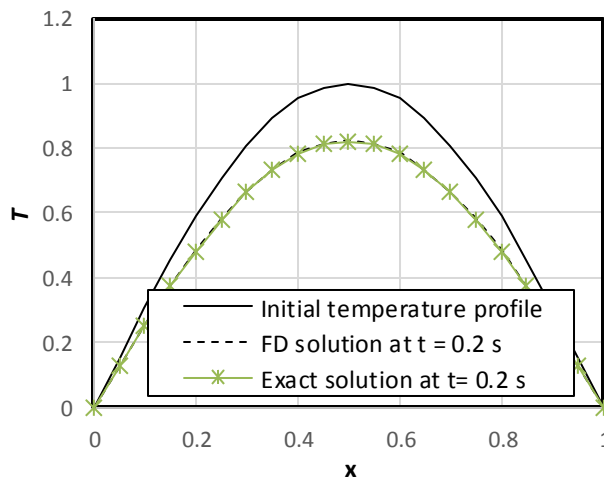


Figure 8.7. Comparison of the BTCS solution with the exact analytical solution ( $t = 0.2$  s,  $\Delta t = 0.01$  s)

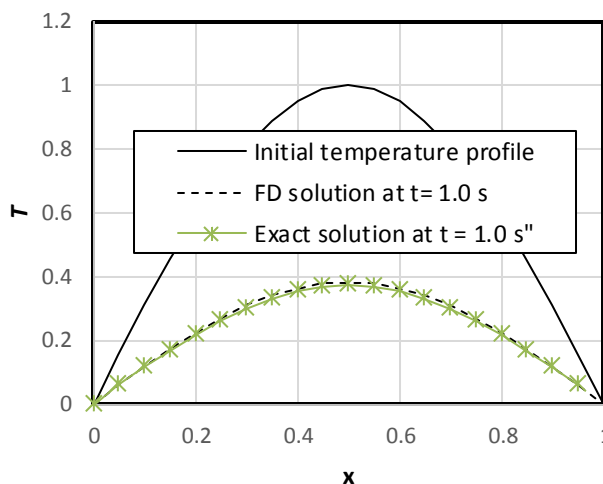


Figure 8.8. Comparison of the FTCS solution with the exact analytical solution ( $t = 1.0$  s,  $\Delta t = 0.05$  s)



**8.2.2. Application of the BTCS scheme by using iterative calculations**

Mokheimer and Antar [4] applied the BTSC scheme with the alternative method that does not require the algebraic system to be formed, i.e., by allowing the iterative-solution option of Excel to solve the nodal equations. To use their method, Equation (8.10) is rearranged as follows:

$$T_m^i = \frac{T_m^{i-1} + \tau(T_{m-1}^i + T_{m+1}^i)}{(1 + 2\tau)} \tag{8.13}$$

Where,  $\tau$  is defined by Equation (8.6). Figure 8.9 shows the Excel sheet developed for this method. The data part at the top of the sheet adds the calculation of the Fourier number  $\tau$  from Equation (8.6) in cell **O1**. The formula bar reveals the formula in cell **C5** that uses Equation (8.13) to determine the temperature at  $x = \Delta x$ :

$$C5 = (C4 + \tau * (B6 + D5))/(1 + 2 * \tau)$$

This formula is copied and pasted in cell **D5:U5** at the same row. Figure 8.9 shows the nodal temperatures calculated by this method when the iterative calculation option of Excel is active. The figure shows that the calculated temperatures are the same as their corresponding values shown in Figure 8.6.

	A	B	C	D	E	F	G	H	I	J	K	L	M	N	O	P	Q	R	S	T	U	V	
1		Δx	0.05		Δt	0.05		α	0.1		N	21		τ	2								
2		x →																					
3	t ↓	0	0.05	0.1	0.15	0.2	0.25	0.3	0.35	0.4	0.45	0.5	0.55	0.6	0.65	0.7	0.75	0.8	0.85	0.9	0.95	1	
4	0	0	0.156	0.309	0.454	0.588	0.707	0.809	0.891	0.951	0.988	1.000	0.988	0.951	0.891	0.809	0.707	0.588	0.454	0.309	0.156	0	
5	0.05	0	0.149	0.294	0.432	0.56	0.674	0.771	0.849	0.906	0.941	0.953	0.941	0.906	0.849	0.771	0.674	0.56	0.433	0.295	0.149	0	
6	0.1	0																				0	

Figure 8.9. Application of the BTCS scheme by allowing Excel’s circular calculations

**8.3. Transient 2D heat-conduction: A general formulation**

The transient 2D heat-conduction with heat generation and a constant thermal conductivity is governed by the following equation:

$$\frac{\partial^2 T}{\partial x^2} + \frac{\partial^2 T}{\partial y^2} + \frac{\dot{e}_g}{k} = \frac{1}{\alpha} \frac{\partial T}{\partial t} \tag{8.14}$$

The FD equations for solving the equation can be developed by following one of the two schemes described in the previous section for the transient 1D conduction. While the two special derivatives are approximated by central-differences, either the forward-difference or the backward-difference can be used for the temporal derivative. This section presents the formulation part that is common to both schemes.

Consider the two-dimensional metal plate shown in Figure 8.10 that is initially at a uniform temperature of 90°C, while its top and right sides are exposed to heat-transfer by convection and the left side is insulated. Heat is then generated in the plate at a rate of  $\dot{e}_g$ , but the temperature at the bottom side of the plate is held constant at 90°C.

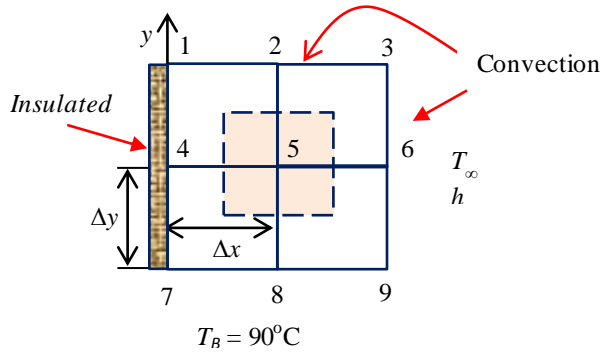


Figure 8.10. Geometry and boundary conditions

For the internal node, node 5, energy balance in the surrounding element gives:

$$\dot{Q}_{cond, left} + \dot{Q}_{cond, above} + \dot{Q}_{cond, right} + \dot{Q}_{cond, below} + \dot{E}_{gen, element} = \frac{\Delta E_{element}}{\Delta t} \quad (8.15)$$

Substituting for the six terms in Equation (8.15) by relevant expressions:

$$k\Delta y \frac{T_{left} - T_{node}}{\Delta x} + k\Delta x \frac{T_{above} - T_{node}}{\Delta y} + k\Delta y \frac{T_{right} - T_{node}}{\Delta x} + k\Delta x \frac{T_{below} - T_{node}}{\Delta y} + \Delta x \Delta y \dot{e}_g = \rho \cdot c_p \frac{T_{node}^{i+1} - T_{node}^i}{\Delta t} \quad (8.16)$$

Since  $\Delta x = \Delta y$ , dividing by  $k$  and substituting for  $\Delta x$  and  $\Delta y$  with  $l$ :

$$T_{left} + T_{above} + T_{right} + T_{below} - 4T_{node} + \frac{l^2}{k} \dot{e}_g = \frac{T_{node}^{i+1} - T_{node}^i}{\tau} \quad (8.17)$$

Substituting the numbers of the nodes surrounding node 5, the equation becomes:

$$T_4 + T_2 + T_6 + T_B - 4T_5 + \frac{l^2}{k} \dot{e}_g = \frac{T_5^{i+1} - T_5^i}{\tau} \quad (8.18)$$

From Figure 8.11 that shows the energy transfer in the zone surrounding node 2 energy balance gives:

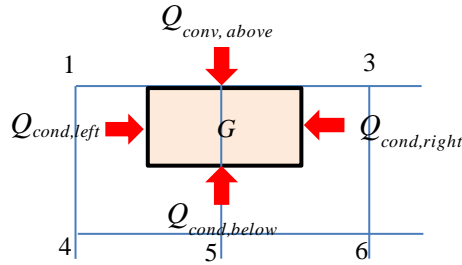


Figure 8.11. The energy-balance zone for node 2

$$\dot{Q}_{cond, left} + \dot{Q}_{conv, above} + \dot{Q}_{cond, right} + \dot{Q}_{cond, below} + \dot{E}_{gen, element} = \Delta E_{element} / \Delta t \quad (8.19)$$

Evaluating the six terms in Equation (8.19) from relevant expressions, we get:

$$k\Delta y \frac{T_{left} - T_{node}}{\Delta x} + h\Delta x(T_{\infty} - T_{node}) + k\Delta y \frac{T_{right} - T_{node}}{\Delta x} + k\Delta x \frac{T_{below} - T_{node}}{\Delta y} + \Delta x \Delta y \dot{e}_g = \rho \cdot c_p \frac{T_{node}^{i+1} - T_{node}^i}{\Delta t} \quad (8.20)$$

Specifying the relevant temperatures around node 2, the equation becomes:

$$k(T_1 - T_2) + hl(T_{\infty} - T_2) + k(T_3 - T_2) + k(T_5 - T_2) + l^2 \dot{e}_g = \rho \cdot c_p \frac{T_2^{t+1} - T_2^i}{\Delta t} \quad (8.21)$$

Following the same procedure, the FD equations for the other boundary nodes can be obtained from energy balance around each node. Note that no time level has been assigned to the temperatures on the left side of Equations (8.18) and (8.21). The appropriate time level depends on whether the scheme to be used is explicit or implicit as explained in the following two sections

#### 8.4. The explicit FTCS scheme for 2D conduction

With this scheme, the temperatures in the left side of the nodal equations represented by Equation (8.20) are taken at the old time-level ( $i$ ). The example that illustrates application of the scheme is based on one given by Cengel and Ghajar [5] who also solved the problem by using the explicit scheme.

#### Example 8-2. Transient 2D heat-conduction with heat-generation

Two-dimensional transient heat transfer takes place in an L-shaped solid body as shown in Figure 8.12. The thermal conductivity and diffusivity of the body are  $k = 15 \text{ W/m}\cdot\text{°C}$  and  $\alpha = 3.2 \times 10^{-6} \text{ m}^2/\text{s}$ , respectively. The left surface of the body is insulated, while the

right surface is subjected to heat flux at a uniform rate of  $\dot{q}_R = 5000 \text{ W/m}^2$  and the entire top surface is subjected to convection to ambient air at  $T_\infty = 25^\circ\text{C}$  with a convection coefficient of  $h = 80 \text{ W/m}^2 \cdot ^\circ\text{C}$ . Heat is generated in the body at a rate of  $\dot{e}_g = 2 \times 10^6 \text{ W/m}^3$ . The body is initially at a uniform temperature of  $90^\circ\text{C}$ , which is then maintained at the bottom surface at all times.

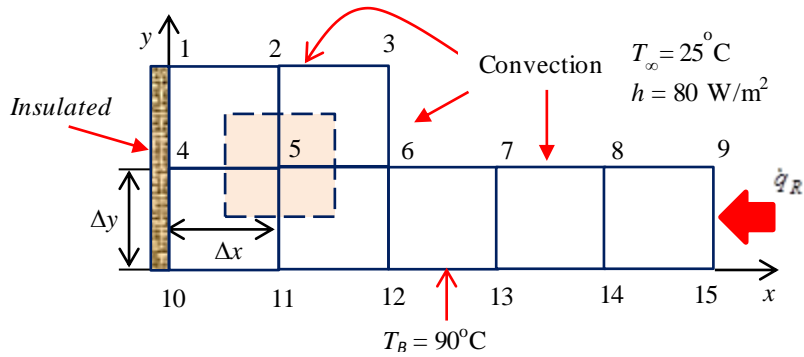


Figure 8.12. Geometry and boundary conditions of Example 8-2

Using the FD method with a nodal network consisting of 15 equally spaced nodes, determine the temperature at the top corner (node 3) of the body after 1, 3, 5, and 10 minutes.

### The analytical model

Noting the similarity between Figures 8.10 and 8.12, Equation (8.18) gives:

$$T_4^i + T_2^i + T_6^i + T_B - 4T_5^i + \frac{l^2}{k} \dot{e}_g = \frac{T_5^{i+1} - T_5^i}{\tau} \quad (8.22)$$

Rearranging:

$$T_5^{i+1} = (1 - 4\tau)T_5^i + \tau \left( T_2^i + T_4^i + T_6^i + T_B + \frac{\dot{e}_g l^2}{k} \right) \quad (8.23)$$

Similarly, for node 2 Equation (8.21) takes the following form:

$$T_2^{i+1} = \left( 1 - 4\tau - 2\tau \frac{hl}{k} \right) T_2^i + \tau \left( T_1^i + T_3^i + 2T_5^i + \frac{2hl}{k} T_\infty + \frac{\dot{e}_g l^2}{k} \right) \quad (8.24)$$

With appropriate modifications, Equation (8.24) can be applied to nodes 7 and 8:

$$T_7^{i+1} = \left(1 - 4\tau - 2\tau \frac{hl}{k}\right) T_7^i + \tau \left(T_6^i + T_8^i + 2T_B + \frac{2hl}{k} T_\infty + \frac{\dot{e}_g l^2}{k}\right) \quad (8.25)$$

$$T_8^{i+1} = \left(1 - 4\tau - 2\tau \frac{hl}{k}\right) T_8^i + \tau \left(T_7^i + T_9^i + 2T_B + \frac{2hl}{k} T_\infty + \frac{\dot{e}_g l^2}{k}\right) \quad (8.26)$$

The FD equations for the remaining 5 nodes as obtained by energy balance around the respective node are as follows [5]:

$$T_1^{i+1} = \left(1 - 4\tau - 2\tau \frac{hl}{k}\right) T_1^i + 2\tau \left(T_2^i + T_4^i + \frac{hl}{k} T_\infty + \frac{\dot{e}_g l^2}{2k}\right) \quad (8.27)$$

$$T_3^{i+1} = \left(1 - 4\tau - 4\tau \frac{hl}{k}\right) T_3^i + 2\tau \left(T_2^i + T_6^i + \frac{2hl}{k} T_\infty + \frac{\dot{e}_g l^2}{2k}\right) \quad (8.28)$$

$$T_4^{i+1} = (1 - 4\tau) T_4^i + \tau \left(T_1^i + 2T_5^i + T_B + \frac{\dot{e}_g l^2}{k}\right) \quad (8.29)$$

$$T_6^{i+1} = \left(1 - 4\tau - 4\tau \frac{hl}{3k}\right) T_6^i + \frac{\tau}{3} \left(2T_3^i + 4T_5^i + 2T_7^i + 4T_B + \frac{4hl}{k} T_\infty + \frac{3\dot{e}_g l^2}{k}\right) \quad (8.30)$$

$$T_9^{i+1} = \left(1 - 4\tau - 2\tau \frac{hl}{k}\right) T_9^i + 2\tau \left(T_8^i + T_B + \frac{\dot{q}_R l}{k} + \frac{hl}{k} T_\infty + \frac{\dot{e}_g l^2}{2k}\right) \quad (8.31)$$

Stability considerations limit the time step for the explicit FTCS scheme by requiring that the primary coefficient, i.e., the coefficient of  $T_m^i$  in the respective nodal equation, to be greater than or equal to zero for all nodes. Since the smallest coefficient is that of Equation (8.28) for node 3, this requirement leads to [5]:

$$\Delta t \leq \frac{l^2}{4\alpha(1 + hl/k)} \quad (8.32)$$

According to Equation (8.32), the maximum time step for  $l = 1.2$  cm is given by:

$$\Delta t \leq (0.012)^2 / 4 \times 3.12 \times 10^{-6} (1 + 80 \times 0.012/15) = 10.6 \text{ s}$$

Cengel and Ghajar [5] used  $\Delta t = 10$  s, which will also be used in the present analysis.

**Excel implementation**

The approach adopted for applying the explicit scheme for the 2D transient heat conduction equation closely follows that described by Mokheimer and Antar [4]. Figure 8.13 that shows the Excel sheet developed for applying the scheme. The data part on the left side of the sheet stores the given information about the thermal conductivity and diffusivity of the solid, the rate of heat-generation, the specified boundary temperatures, etc. The temperatures at nodes 10, 11, 12, 13, 14, and 15 that lie at the bottom surface are fixed to 90°C. Based on these data, the formula in cell G2 determines the Fourier number  $\tau$  that appears in the FD equations of the different nodes.

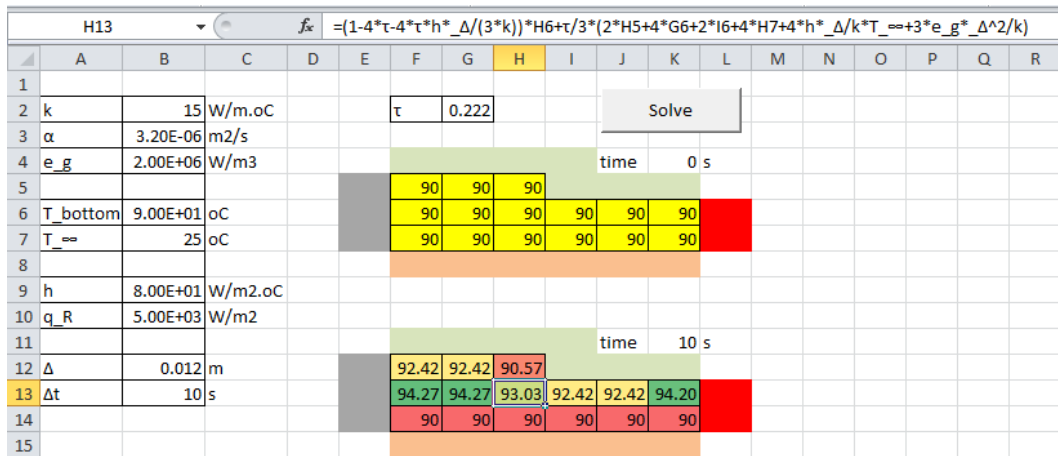


Figure 8.13. Excel sheet developed for Example 8-2 by the explicit scheme

Figure 8.13 shows two L-shaped cell configurations that represent the 15 nodes in the FD grid at two consecutive time levels. The top configuration stores the initial solution (e.g.,  $t = 0$ ), while the bottom configuration stores the solution at the new time level (e.g.,  $t = \Delta t$ ) as obtained by applying Equations (8.23) to (8.31) to the values stored in the top configuration. The formula bar shows the formula that calculates the temperature at node 6 using Equation (8.30). To obtain the temperatures at the next time level, i.e.,  $t = 2\Delta t$ , the values of the temperature in the bottom block are copied and pasted in the corresponding cells of the top block (use the special “paste-values” feature). This procedure needs to be repeated until the required time level is reached.

The repetitive copy-and-paste action can be automated by recording a macro for these two steps as explained in Appendix F. Figure 8.13 shows a “Solve” button that is linked to the recorded macro to activate it. Pressing the “Solve” button once will advance the time by  $\Delta t$ . In order to keep record of the time, the following formula was entered in cell K11:

$$K11 = K4 + \Delta t$$

The initial value of cell **K4** was set to zero as shown in Figure 8.13. Therefore, the corresponding value calculated in cell **K11** is equal to  $\Delta t$ , which is 10 s. The values in cells **K4** and **K11** will be automatically updated after every paste-values step to become 10 and 20 s, respectively. The FD solutions determined by the Excel sheet at time = 1, 3, 5, and 10 minutes are shown in Figure 8.14. The calculated temperature values at node 3 shown in the figure, which are 100.2, 105.9, 106.5, and 106.6°C, agree with the corresponding values obtained by Cengel and Ghajar [5].

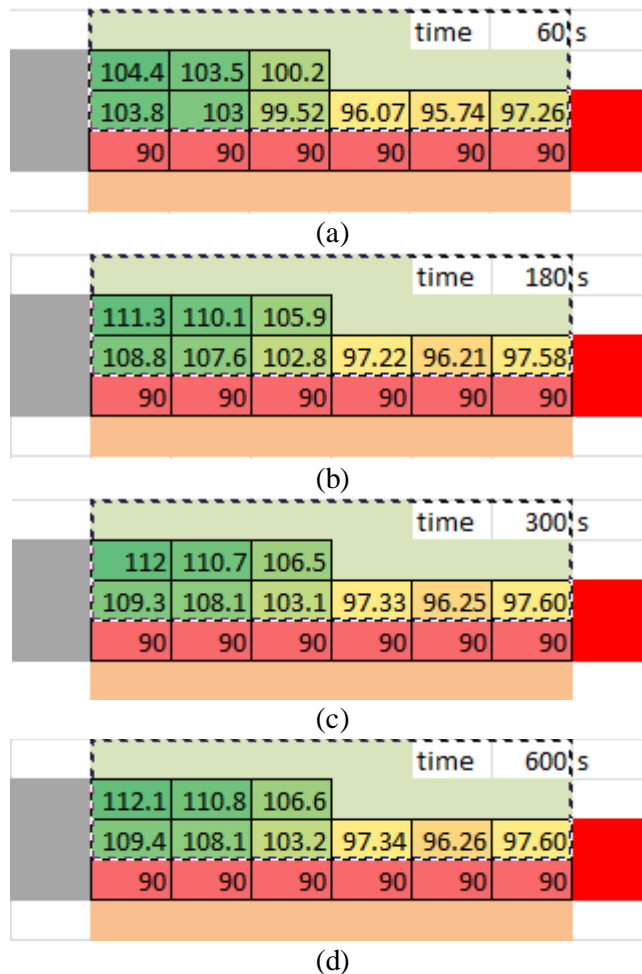


Figure 8.14. FD solutions by the explicit scheme after time 1, 3, 5, and 10 minutes

### 8.5. The implicit BTCS scheme for 2D conduction

In the implicit scheme, the temperatures in the left side of the nodal FD equations are evaluated at the new time level ( $i+1$ ). As for 1D conduction, the BTCS scheme can either be applied by assembling and then solving the linear system of equations or by using iterative calculations to directly solve the equations. Since the first option leads to

a large system of linear equations to be solved, only the second option will be used in following analysis. Accordingly, Equation (8.18) for node 5 becomes:

$$T_4^{i+1} + T_2^{i+1} + T_6^{i+1} + T_B - 4T_5^{i+1} + \frac{l^2}{k} \dot{e}_g = \frac{T_5^{i+1} - T_5^i}{\tau} \quad (8.33)$$

Rearranging the equation:

$$T_5^{i+1} = \left[ T_5^i + \tau \left( T_4^{i+1} + T_2^{i+1} + T_6^{i+1} + T_B + \frac{\dot{e}_g l^2}{k} \right) \right] / (1 + 4\tau) \quad (8.34)$$

The FD equations for the other nodes can also be obtained by rearranging those of the explicit scheme as follows:

$$T_1^{i+1} = \left[ T_1^i + 2\tau \left( T_2^{i+1} + T_4^{i+1} + \frac{hl}{k} T_\infty + \frac{\dot{e}_g l^2}{2k} \right) \right] / \left( 1 + 4\tau + 2\tau \frac{hl}{k} \right) \quad (8.35)$$

$$T_2^{i+1} = \left[ T_2^i + \tau \left( T_1^{i+1} + T_3^{i+1} + 2T_5^{i+1} + \frac{2hl}{k} T_\infty + \frac{\dot{e}_g l^2}{k} \right) \right] / \left( 1 + 4\tau + 2\tau \frac{hl}{k} \right) \quad (8.36)$$

$$T_3^{i+1} = \left[ T_3^i + 2\tau \left( T_2^{i+1} + T_6^{i+1} + \frac{2hl}{k} T_\infty + \frac{\dot{e}_g l^2}{2k} \right) \right] / \left( 1 + 4\tau + 4\tau \frac{hl}{k} \right) \quad (8.37)$$

$$T_4^{i+1} = \left[ T_4^i + \tau \left( T_1^{i+1} + 2T_5^{i+1} + T_B + \frac{\dot{e}_g l^2}{k} \right) \right] / (1 + 4\tau) \quad (8.38)$$

$$T_6^{i+1} = \left[ T_6^i + \frac{\tau}{3} \left( 2T_3^i + 4T_5^i + 2T_7^i + 4T_B + \frac{4hl}{k} T_\infty + \frac{3\dot{e}_g l^2}{k} \right) \right] / \left( 1 + 4\tau + 4\tau \frac{hl}{3k} \right) \quad (8.39)$$

$$T_7^{i+1} = \left[ T_7^i + \tau \left( T_6^{i+1} + T_8^{i+1} + 2T_B + \frac{2hl}{k} T_\infty + \frac{\dot{e}_g l^2}{k} \right) \right] / \left( 1 + 4\tau + 2\tau \frac{hl}{k} \right) \quad (8.40)$$

$$T_8^{i+1} = \left[ T_8^i + \tau \left( T_7^i + T_9^i + 2T_B + \frac{2hl}{k} T_\infty + \frac{\dot{e}_g l^2}{k} \right) \right] / \left( 1 + 4\tau + 2\tau \frac{hl}{k} \right) \quad (8.41)$$

$$T_9^{i+1} = \left[ T_9^i + 2\tau \left( T_8^{i+1} + T_B + \frac{\dot{q}_R l}{k} + \frac{hl}{k} T_\infty + \frac{\dot{e}_g l^2}{2k} \right) \right] / \left( 1 + 4\tau + 2\tau \frac{hl}{k} \right) \quad (8.42)$$



**Excel implementation**

The Excel sheet for the implicit scheme can be developed from that of the explicit scheme by modifying the nodal FD equations written in bottom block of cells with those given by Equations (8.34) to (8.42). Since the right-hand sides of these equations involve temperatures at the new time level  $i+1$ , the iterative-calculations option of Excel must be active. Figure 8.15 shows the resulting sheet using the same spacial and time steps  $l = 0.012$  m and  $\Delta t = 10$  s. The formula bar reveals that for node 6 based on Equation (8.39). The figure shows slightly different temperature values from those obtained with the explicit scheme as shown in Figure 8.13. As for the explicit scheme, pressing the “Solve” button once will advance the time by  $\Delta t$ .

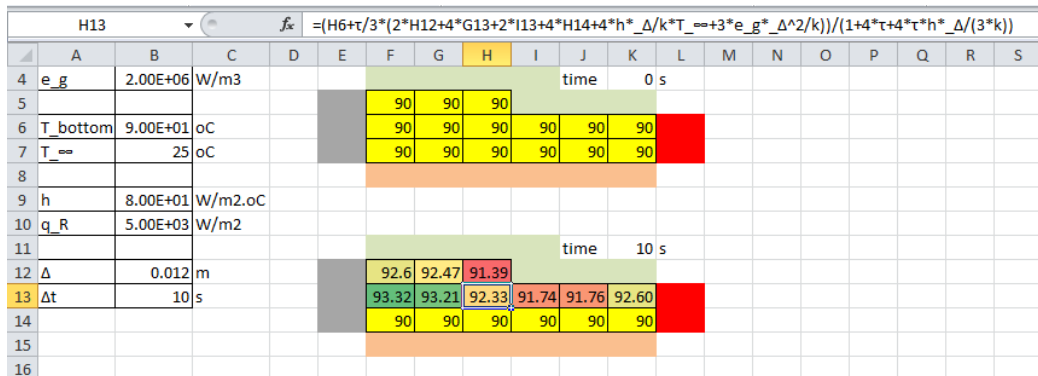


Figure 8.15. Excel sheet developed for Example 8-2 by the implicit scheme

Table 8.2 compares the temperature values at node 3 as determined by the explicit and the implicit schemes after ½, 1, 3, 5, and 10 minutes. As the figures show, the percentage deviation between the values obtained with the two schemes just after ½ minute is more than 4.3%, but decrease with time and diminishes after 10 minutes.

Table 8.2. Comparison of the solutions obtained with the explicit and the implicit schemes for the temperature at node 3

Time (s)	FTCS (°C)	BTCS (°C)	Deviation (%)
30	97.2	93.1	4.304
60	100.2	99.02	1.178
180	105.9	105.3	0.567
300	106.5	106.4	0.094
600	106.6	106.6	0.000

Figure 8.16 compares the solution obtained with the implicit scheme for the temperature at node 3 at different times with those obtained with the explicit scheme using three values of the time step; 2, 5, and 10 s. The figure shows that the temperature approaches a steady-state value of about 106.6°C after 6 minutes. Figure 8.16 also indicates that the solution obtained with explicit scheme depends on the time step and

approaches that obtained with implicit scheme as the time step is reduced. The effect of the spatial step  $l=\Delta x=\Delta y$  can also be investigated.

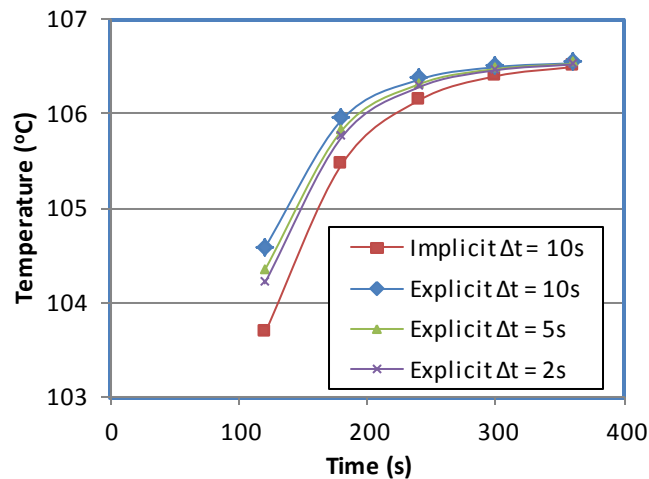


Figure 8.16. Values of the temperature at node 3 obtained with the explicit scheme using three time-steps compared to those obtained with the implicit scheme

## 8.6. Closure

The chapter showed how Excel can be used to solve the transient 1D and 2D heat-conduction equations with the FD method. Both explicit and implicit FD formulations of the method were considered. For the explicit formulations of the FD method, the chapter highlighted the need for selecting reasonably small time steps in order to ensure the solution's stability. For the implicit scheme, the chapter illustrated the usefulness of Excel's iterative-calculation option for solving the transient 1D and 2D conduction equations. Although the schemes discussed in the chapter can be applied to solve the full 3D conduction equation, application of the FD method for solving 3D heat-conduction problems with complex geometries and boundary conditions is better done with dedicated computer programs [6].

## References

- [1] G. W. Recktenwald, Finite-Difference Approximations to the Heat Equation, Mechanical Engineering, 10, 1-27, 2004
- [2] P. Anthony, Solutions of One Dimensional Heat Equation Using Excel Worksheet , Imperial Journal of Interdisciplinary Research (IJIR) Vol-2, Issue-8, 2016 ISSN: 2454-1362, available at: <http://www.onlinejournal.in>, Last access 21/9/2019
- [3] Wikipedia, [http://en.wikipedia.org/wiki/Tridiagonal\\_matrix\\_algorithm](http://en.wikipedia.org/wiki/Tridiagonal_matrix_algorithm). Last access 21/9/2019
- [4] E. M. A. Mokheimer and M. A. Antar, On the use of spreadsheets in heat conduction analysis, International Journal of Mechanical Engineering Education Vol 28 No 2, April 2000

- [5] Y. A. Cengel and A. J. Ghajar, *Heat and Mass Transfer: Fundamentals and Applications*. 4<sup>th</sup> edition, McGraw-Hill, 2011
- [6] G. W. Recktenwald, *Introduction to Numerical Methods and MATLAB: Implementations and Applications*, Pearson Higher Ed, 2000

**Exercises**

1. Figure 8.P1 shows a large uranium plate of thickness  $L = 4$  cm, thermal conductivity  $k = 28$  W/m·°C, and thermal diffusivity  $\alpha = 12.5 \times 10^{-6}$  m<sup>2</sup>/s that is initially at a uniform temperature of 200°C. Heat is generated uniformly in the plate at a constant rate of  $\dot{e}_g = 5 \times 10^6$  W/m<sup>3</sup>. At time  $t = 0$ , one side of the plate is brought into contact with iced water and is maintained at 0°C at all times, while the other side is subjected to convection to an environment at  $T_\infty = 30^\circ\text{C}$  with a heat transfer coefficient of  $h = 45$  W/m<sup>2</sup>·°C.

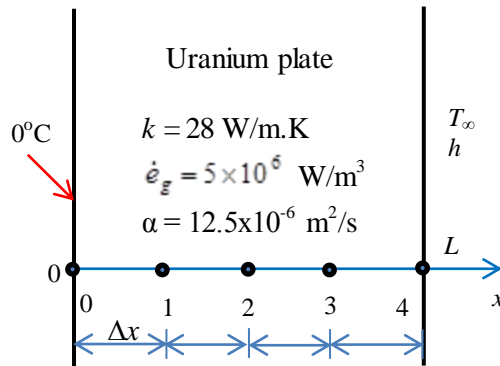


Figure 8.P1 Schematic for Problem 8.1 (adapted from Cengel and Ghajar [1])

Considering a total of five equally spaced nodes in the medium, two at the boundaries and three at the middle, develop three Excel sheets to estimate the exposed surface temperature of the plate 2.5 min after the start of cooling using:

- (a) the explicit method,
- (b) the implicit method that uses the iterative-calculation option,
- (c) the implicit method that assembles and solves the linear system.

This exercise is based on Example 5-5 in Cengel and Ghajar [1].

2. When time-accurate solutions of the conduction equation are important, the Crank-Nicolson (C-N) scheme has significant advantages over the FTCS and BTCS schemes. The C-N scheme is implicit like BTCS and also unconditionally stable. The scheme is not significantly more difficult to implement than the BTCS scheme. Develop an Excel sheet for solving Example 8-1 by using the C-N scheme. For more information about the C-N scheme refer to Recktenwald [1].
3. Develop the general FD equations for node 3 and node 6 in Figure 8.10.

4. Solve the two-dimensional transient heat transfer in an L-shaped solid body given in Example 8-2 by using a finer nodal network that consists of equally spaced nodes with  $\Delta x = \Delta y = 0.6$  cm, as shown in Figure 8.P4. Using the explicit FD method, determine the temperature at the top corner (node 5) of the body after 1, 3, 5, and 10 min. Compare your solution with that obtained with the original grid.

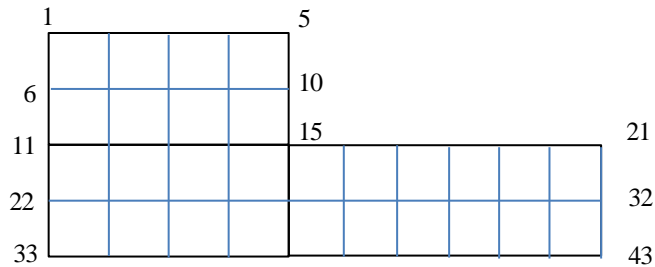


Figure 8.P4. FD grid for problem 8.4

Hint: You do not have to develop new equations except for nodes 10 and 32. The equations developed in Example 8-2 can be used for the other nodes, but you have to use a smaller time step.

5. Repeat the above exercise by using the implicit BTCS scheme. Use either the iterative-calculation option of Excel or the matrix-inversion method to solve the resulting system of algebraic equations. Compare your solution with  $\Delta t = 10, 15,$  and  $20$  s with that obtained with the coarser grid for the temperature at node 3.
6. A hot surface is to be cooled by attaching aluminium fins ( $k = 237$  W/m $\cdot$ °C and  $\alpha = 97.1 \times 10^{-6}$  m $^2$ /s) that have triangular cross sections as shown in Figure 9P.6. Each fin has length  $L = 5$  cm, base thickness  $t = 1$  cm, and very large width  $w$ . The temperature of the surrounding medium is  $15^\circ\text{C}$ , and the heat transfer coefficient on the surfaces is  $35$  W/m $^2$ ·°C. Initially, the fins are at a uniform temperature of  $30^\circ\text{C}$ , and at time  $t = 0$ , the temperature of the hot surface is suddenly raised to  $120^\circ\text{C}$ . Assuming one-dimensional heat conduction along the fin, use the finite difference method with six equally spaced nodes to determine the nodal temperatures after 2 min by using:
- The explicit finite-difference formulation
  - The implicit finite-difference formulation

Also, determine how long it will take for steady conditions to be reached.

Hint. Refer to Appendix E for the solution of the steady heat conduction equation on the triangular fin with similar boundary conditions.

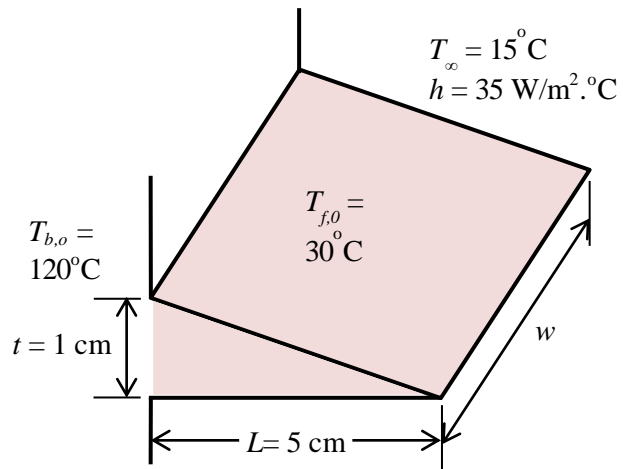


Figure 8.P6. The dimensions and initial and boundary conditions of the triangular fin

# 9

## **Thermodynamic analyses of gas power cycles**

Energy-conversion cycles that involve phase changes of the working fluid, like the Rankine cycle, require the determination of fluid properties at different phases of the fluid. For the analyses of these cycles, computer-aided methods that use property functions are more convenient than traditional methods that use property tables and charts. For gas cycles that do not involve phase changes computer-aided methods are also more accurate because they allow the application of the variable specific-heat method of analysis instead of the approximate constant specific-heat method. This chapter shows how Thermax functions can be used to analyse two important gas power-generation cycles which are the Brayton cycle and the Otto cycle. The results obtained for the Brayton cycle by using the ideal-gas property functions provided by Thermax are compared to those obtained by using the Ideal-Gas add-in developed at the University of Alabama [1]. For the Otto cycle, energy as well as exergy analyses are presented. The values obtained for the key parameters of the cycles are also verified against the relevant values given in standard thermodynamics textbooks.

### 9.1. The ideal Brayton cycle

The Brayton cycle is the ideal cycle for gas-turbines. Unlike real gas-turbine cycle, it is a closed cycle with a constant mass of the working fluid going through the system's components as shown in Figure 9.1. The cycle consists of four processes; compression in an ideal gas compressor, heat-addition from a high-temperature source, expansion in an ideal gas turbine, and heat-rejection to a low-temperature sink. Figure 9.2 shows the cycle on a  $T$ - $s$  diagram. Although the working fluid can be any suitable gas, in the following analysis it is assumed to be air.

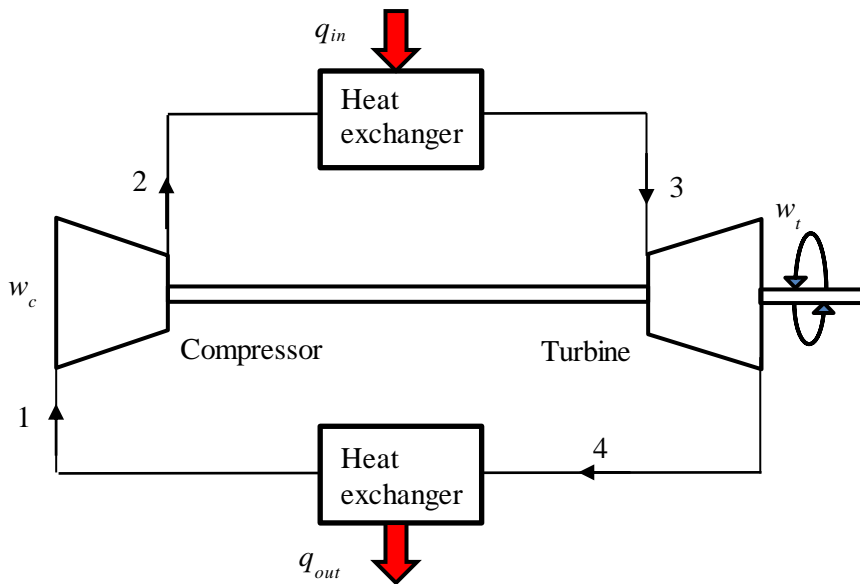


Figure 9.1. Schematic diagram of the closed-cycle gas-turbine

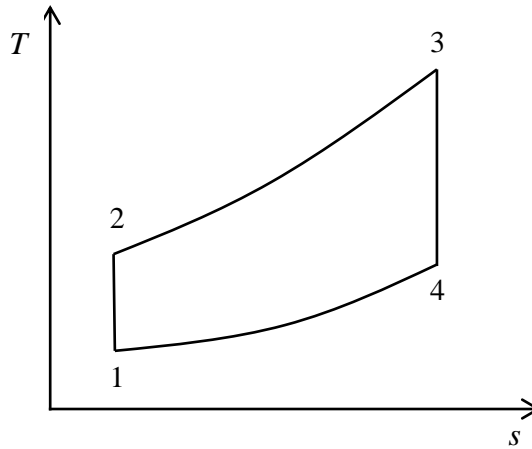


Figure 9.2.  $T$ - $s$  diagram for the ideal Brayton cycle

Referring to Figure 9.2, the compressor work ( $w_c$ ) and turbine work ( $w_t$ ), per unit mass flow rate of the air, are determined from:

$$w_c = (h_2 - h_1) \quad (9.1)$$

$$w_t = (h_3 - h_4) \quad (9.2)$$

Where  $h_1$ ,  $h_2$ ,  $h_3$ , and  $h_4$  are values of the enthalpy at states, 1, 2, 3, and 4, respectively. The amount of heat addition ( $q_{in}$ ) per unit mass flow of the air is given by:

$$q_{in} = (h_3 - h_2) \quad (9.3)$$

Therefore, the net work ( $w_{net}$ ), back-work ratio ( $BWR$ ), and thermal efficiency ( $\eta$ ) of the cycle are determined from:

$$w_{net} = w_t - w_c \quad (9.4)$$

$$BWR = w_c / w_t \quad (9.5)$$

$$\eta = w_{net} / q_{in} \quad (9.6)$$

Given the compressor's inlet temperature,  $T_1$ , and the turbine's inlet temperature,  $T_3$ , the discharge temperature from the compressor ( $T_2$ ) and the discharge temperature from the turbine ( $T_4$ ) are determined by using the variable specific-heat method of analysis from the corresponding relative pressures  $P_{r2}$  and  $P_{r4}$  given by:



$$P_{r2} = P_{r1} \times \frac{P_2}{P_1} \tag{9.7}$$

$$P_{r4} = P_{r3} \times \frac{P_4}{P_3} \tag{9.8}$$

Where  $P_{r1}$  and  $P_{r2}$  are the relative pressures at states 1 and 2, respectively. For the ideal cycle without pressure losses,  $P_3 = P_2$  and  $P_4 = P_1$ . The following example, which is based on Example 9.5 in Cengel and Boles [2], illustrates the procedure of using Thermo property functions for analysing the cycle with Excel.

**Example 9-1. Analysis of the simple ideal Brayton cycle**

A gas-turbine power plant that operates on an ideal Brayton cycle with air as the working fluid has a pressure ratio of 8. The gas temperature at the compressor inlet is 300 K and at the turbine inlet is 1300 K. Determine (a) the net work per unit mass flow rate of the working fluid, (b) the back work ratio, and (c) the thermal efficiency.

**Solution**

Figure 9.3 shows the Excel sheet developed for this example using Thermo property functions. The figure shows the general layout adopted in this book for sheet arrangement according to which the sheet is divided from left to right into three main parts: (i) Input data, (ii) Intermediate calculations, and (iii) Final results. In the present case, the input data include the given values of the two temperature values at states 1 and 3 ( $T_1$  and  $T_3$ ) and the pressure ratio ( $rp$ ). The middle part of the sheet, which is reserved for the calculation of intermediate results, shows the calculated values of the two unknown temperatures  $T_2$  and  $T_4$  and the enthalpy values at the four states in the cycle. The final results are the compressor work ( $w_c$ ), the turbine work ( $w_t$ ), the heat input ( $Q_{in}$ ), the back work ratio (BWR), and thermal efficiency ( $\eta$ ) as shown on the right side of the sheet.

η		fx =(w_t-w_c)/q_in										
	A	B	C	D	E	F	G	H	I	J	K	L
1	<b>Input Data</b>			<b>Intermediate calculations</b>				<b>Final results</b>				
2	T_1	300	K	Pr_2	11.06829198		h_1	299.8455		w_c	243.6869	
3												
4	rp	8		T_2	538.1465495		h_2	543.5324		w_t	606.014	
5												
6	T_3	1300	K	Pr_4	41.69167583		h_3	1396.057		q_in	852.5248	
7												
8				T_4	769.2393498		h_4	790.0433		BWR	0.402114	
9												
10										η	0.425005	
11												

Figure 9.3. The Excel sheet developed for Example 9-1

## Computer-Aided Thermofluid Analyses Using Excel

Table 9.1 shows the formula entered in each cell of the calculations part using Thermax functions. Only three Thermax functions from the Gas-group have been used in the Excel model with air as the gas which are: **GasPr\_TK**, **GasTK\_Pr**, and **Gash\_TK**. For the purpose of comparison, a similar Excel sheet was developed by using the IdealGas add-in developed at the University of Alabama [1]. Figure 9.4 shows the Excel sheet and Figure 9.5 reveals the function used in it.

Table 9.1. Usage of Thermax functions in the analysis

Cell	Parameter	Excel formulae and Thermax functions
E2	Pr_2	=GasPr_TK("Air";T_1) * rp
E4	T_2	=GasTK_Pr("Air";Pr_2)
E6	Pr_4	=GasPr_TK("Air";T_3)/rp
E8	T_4	=GasTK_Pr("Air";Pr_4)
H2	h_1	=Gash_TK("Air";T_1)
H4	h_2	=Gash_TK("Air";T_2)
H6	h_3	=Gash_TK("Air";T_3)
H8	h_4	=Gash_TK("Air";T_4)

The screenshot shows an Excel spreadsheet with the following data:

	A	B	C	D	E	F	G	H	I	J	K
1	<b>Input Data</b>			<b>Intermediate calculations</b>					<b>Final results</b>		
2	T_1	300 K		Pr_2	11.01667122		h_1	299.6384		w_c	243.6869
3											
4	rp	8		T_2	538.1465495		h_2	543.3253		w_t	606.014
5											
6	T_3	1300 K		Pr_4	41.49723248		h_3	1395.85		q_in	852.5248
7											
8				T_4	769.2393498		h_4	789.8362		BWR	0.402114
9											
10										η	0.425005
11											

Figure 9.4. Excel sheet for Example 9-1 using the IdealGas add-in

The screenshot shows the following IdealGas functions used in the calculations:

	D	E	F	G	H
	<b>Intermediate calculations</b>				
	Pr_2	=Prel_air(T_1,"si")*rp		h_1	= h_air(T_1,"si")
	T_2	= T_Prel_air(Pr_2,"si")		h_2	= h_air(T_2,"si")
	Pr_4	= Prel_air(T_3,"si")/rp		h_3	= h_air(T_3,"si")
	T_4	= T_Prel_air(Pr_4,"si")		h_4	= h_air(T_4,"si")

Figure 9.5. IdealGas functions used in the Excel sheet of Example 9-1

Table 9.2 shows the values determined by the two property add-ins for the key cycle parameters and their corresponding values given by Cengel and Boles [2]. The figure of the table show only minor differences between the values obtained by the two property add-ins and those given by Cengel and Boles [2].

Table 9.2. Verification of the two add-ins' results with those of Cengel and Boles [2]

Parameter	Cengel and Boles [2]	Thermax	IdealGas
$w_c$	244.16	243.69	243.69
$w_t$	606.60	606.01	606.01
$q_{in}$	851.62	852.52	852.52
BWR	0.403	0.402	0.402
$\eta$	0.426	0.425	0.425

### 9.2. The regenerative Brayton Cycle

Gas turbines can sustain higher combustion temperatures than those typically met in internal-combustion engines, but the high combustion temperatures lead to high exhaust temperatures as well. By adding a regenerator to the simple gas-turbine system as shown in Figure 9.6, the energy in the hot exhaust gases that can reach more than 500°C is utilised to preheat the compressed air before it goes to the combustion chamber; a process called *regeneration*. Regeneration reduces the fuel combustion and improves the plant's thermal efficiency, but the cost of the heat-exchanger increases that of the modified system. The economic benefit due to regeneration depends not only on the cost of the heat-exchanger, but also on the system's pressure ratio. While the cost of the heat-exchanger depends on its size and effectiveness, there is a certain value for the pressure ratio that maximises the system's thermal efficiency.

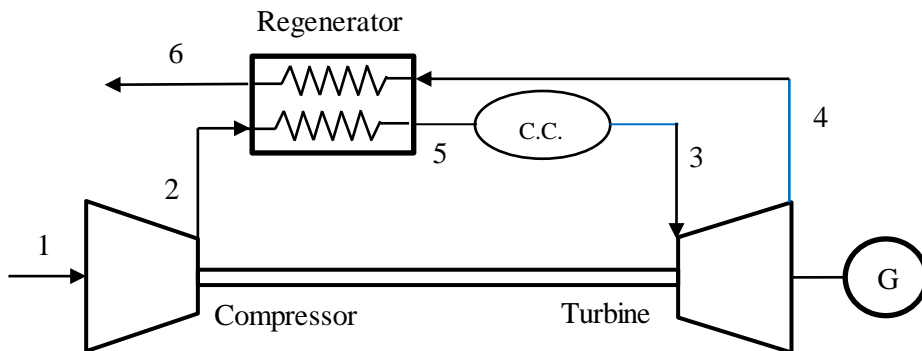


Figure 9.6. Schematic diagram of the regenerative gas-turbine

Figure 9.7 shows the  $T$ - $s$  diagram for the regenerative Brayton cycle assuming zero pressure losses in the combustion chamber and heat-exchanger. Due to friction losses in both compressor and turbine, the actual exit temperatures from these devices (i.e.,  $T_2$

and  $T_4$ ) are different from the ideal values obtainable by the isentropic compression and expansion processes ( $T_{2s}$  and  $T_{4s}$ ).

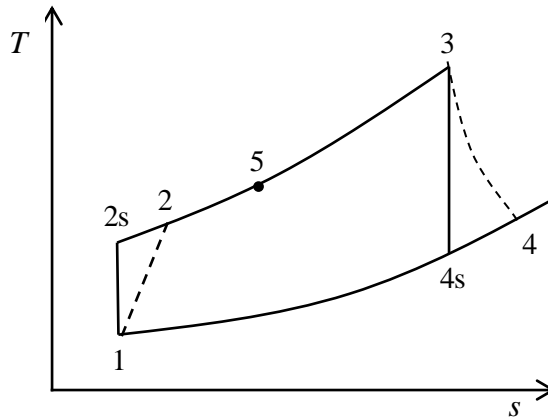


Figure 9.7.  $T$ - $s$  diagram for the regenerative Brayton cycle

As for the simple Brayton cycle considered earlier, the thermal efficiency ( $\eta$ ) is given by:

$$\eta = w_{net} / q_{in} \quad (9.9)$$

Where,  $w_{net}$  is the net output work from the plant and  $q_{in}$  is its heat input. The net output work for the gas-turbine power plant is the difference between the turbine work output ( $w_t$ ) and the compressor work input ( $w_c$ ). Using the numbering scheme of Figures 9.6 and 9.7 to indicate the state of the working fluid entering and leaving the compressor and turbine, the net output work in terms of fluid enthalpies is given by:

$$w_{net} = (h_3 - h_4) - (h_2 - h_1) \quad (9.10)$$

The heat input to the power plant is given by the difference in enthalpies of the combustion gases and the preheated air entering the combustion chamber, i.e.:

$$q_{in} = (h_3 - h_5) \quad (9.11)$$

Given the temperature and pressure of air at the compressor inlet, the ideal relative pressure after the compressor ( $P_{r,2s}$ ) is determined from [2]:

$$P_{r,2s} = P_{r1} \frac{P_2}{P_1} = P_{r1} \cdot r_p \quad (9.12)$$

Where,  $r_p$  stands for the pressure ratio.  $P_{r2s}$  is then used to find  $T_{2s}$ , which is the temperature after an ideal isentropic compression process. Once  $T_{2s}$  is found,  $h_{2s}$  can be determined by using the property function. The actual enthalpy ( $h_2$ ) is then found from:

$$h_2 = h_1 + (h_{2s} - h_1) / \eta_c \quad (9.13)$$

Where,  $\eta_c$  is the compressor's isentropic efficiency. Similarly, the relative pressure after the expansion process ( $P_{r4s}$ ) is determined from:

$$P_{r4s} = P_{r3} \frac{P_4}{P_3} = P_{r3} / r_p \quad (9.14)$$

$P_{r4s}$  is then used to find the temperature after an ideal expansion process  $T_{4s}$ , from which  $h_{4s}$  can be determined. The actual enthalpy ( $h_4$ ) is then found from:

$$h_4 = h_3 - (h_3 - h_{4s}) \times \eta_t \quad (9.15)$$

Where,  $\eta_t$  is the turbine's isentropic efficiency. The temperature of the compressed air entering the combustion chamber ( $T_5$ ) and, therefore, the saving in fuel consumption, depends on the effectiveness of the regenerator ( $\varepsilon$ ) which is defined as:

$$\varepsilon = (T_5 - T_2) / (T_4 - T_2) \quad (9.16)$$

Given an estimate for  $\varepsilon$ , Equation (9.16) can be rearranged to get:

$$T_5 = T_2 + \varepsilon(T_4 - T_2) \quad (9.17)$$

### Example 9-2. Analysis of the regenerative Brayton cycle

A gas-turbine power plant operates on a regenerative Brayton cycle with air entering the compressor at 100 kPa, 300 K. Combustion gases leave the combustion chamber at 1400 K. The regenerator effectiveness is 80% and the isentropic efficiency of both the compressor and the turbine is 80%. Determine the pressure ratio that yields the maximum net work output and the maximum thermal efficiency of the plant.

#### Solution

Figure 9.8 shows the Excel sheet prepared for this example using Thermax functions. The input data shown in the left-side of the sheet includes the air intake temperature ( $T_1$ ) and pressure ( $P_1$ ), the pressure ratio ( $P_{ratio}$ ), and the combustion temperature ( $T_3$ ). The data part also includes the isentropic efficiency of the compressor ( $Eff_c$ ), the isentropic efficiency of the turbine ( $Eff_t$ ), and the regenerator effectiveness ( $Eff_{regen}$ ). The middle part of the sheet shows the calculated values of  $T_2$  and  $T_4$ . The figure shows the enthalpy values as obtained by using Thermax functions. The formula

## Computer-Aided Thermofluid Analyses Using Excel

used in each cell is inserted next to it. The right-side of the sheet shows the main results, which include values of the input compression work, the output expansion work, the net work output, the heat input, and the thermal efficiency.

η		fx = (w_t-w_c)/Q_in									
	B	C	D	E	F	G	H	I	J	K	L
1											
2	T_1	300		h_1	299.8455	=Gash_TK("air",T_1)		h_5	890.2033	=h_2+Eff_regen*(h_4-h_2)	
3	P_1	100		Pr_1	1.383536	=GasPr_TK("air",T_1)					
4	Pratio	10		Pr_2s	13.83536	=Pr_1*Pratio		w_c	349.0347	=h_2-h_1	
5	T_3	1400		T_2s	572.0764	=GasTK_Pr("air",Pr_2s)		w_t	565.2241	=h_3-h_4	
6	Eff_c	0.8		h_2s	579.0732	=Gash_TK("air",T_2s)		w_net	216.1894	=w_t-w_c	
7	Eff_t	0.8		h_2	648.8802	=h_1+(h_2s-h_1)/Eff_c		Q_in	625.5549	=h_3-h_5	
8	Eff_regen	0.8		T_2	638.1146	=GasTK_h("air",h_2)		η	0.345596	=(w_t-w_c)/Q_in	
9											
10				h_3	1515.758	=Gash_TK("air",T_3)					
11				Pr_3	454.3223	=GasPr_TK("air",T_3)					
12				Pr_4s	45.43223	=Pr_3/Pratio					
13				T_4s	786.8156	=GasTK_Pr("air",Pr_4s)					
14				h_4s	809.2281	=Gash_TK("air",T_4s)					
15				h_4	950.5341	=h_3-(h_3-h_4s)*Eff_t					
16				T_4	914.5512	=GasTK_h("air",h_4)					
17											

Figure 9.8. The Excel sheet developed for the regenerative Brayton cycle

The sheet shows the results at a pressure ratio of 10 at which the corresponding values of the net output work and thermal efficiency are 216.19 kJ/kg and 0.346, respectively. The value of the pressure-ratio (Pratio) in cell C4 was changed from 2 to 16 and Figure 9.9 shows the calculated values for the net specific work and thermal efficiency plotted against the pressure ratio. The figure shows that the net output work and thermal efficiency reach their maximum values at different pressure ratios. While the maximum net work output occurs at a pressure ratio of about 8, the maximum thermal efficiency occurs much earlier at a pressure ratio of about 5 or less.

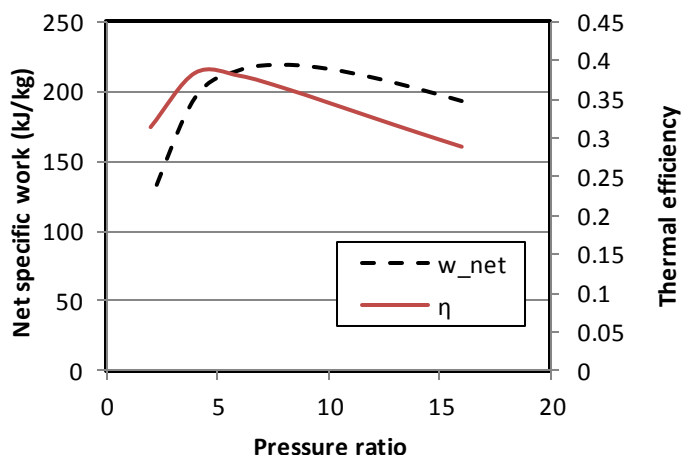


Figure 9.9. Variation of the net specific work and thermal efficiency of the regenerative Brayton cycle with the turbine's pressure ratio

### 9.3. Energy analysis of the Otto cycle

The Otto cycle and the Diesel cycle are two ideal cycles used for modelling the cycles in internal combustion (I.C.) engines. While the Otto cycle is used for modelling spark-ignition I.C. engines, the Diesel cycle is used for modelling compression-ignition I.C. engines. Figure 9.10 shows the four processes that constitute the Otto cycle, which are:

Process 1-2: Adiabatic and reversible compression of air

Process 2-3: Constant-volume heat addition

Process 3-4: Adiabatic and reversible expansion of air

Process 4-1: Constant-volume heat rejection

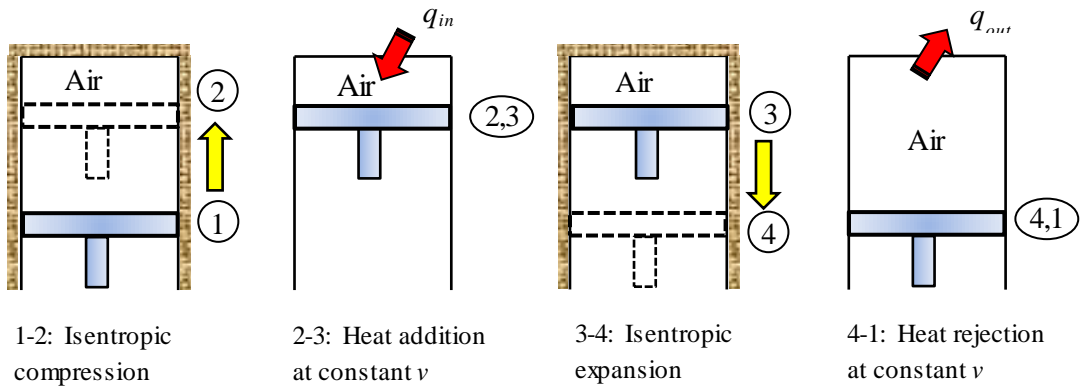


Figure 9.10. The Otto cycle (Adapted from Cengel and Boles [2])

The  $P$ - $v$  diagram of the Otto cycle is shown in Figure 9.11. Processes 1-2 and 3-4 are isentropic processes because they are both adiabatic and reversible. The following analysis of the Otto cycle, which is based on the first law of thermodynamics, is called an “energy analysis” of the cycle.

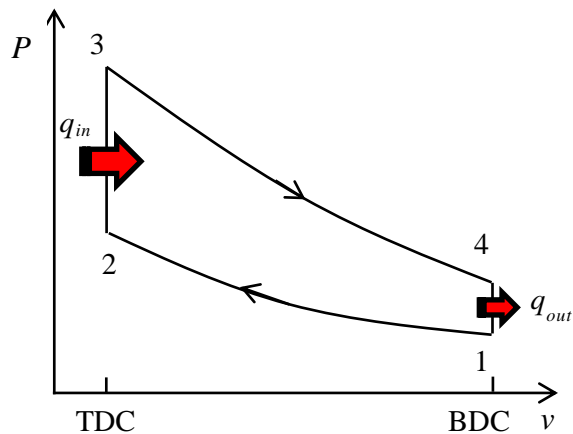


Figure 9.11.  $P$ - $v$  diagram of the Otto cycle (Adapted from Cengel and Boles [2])

**The analytical model**

For the ideal Otto-cycle shown in Figures 9.10 and 9.11 with air as an ideal-gas [3]:

$$v_1 = RT_1 / P_1 \quad (9.18)$$

$$v_2 = v_1 / r \quad (9.19)$$

$$v_3 = v_2 \quad (9.20)$$

$$v_4 = v_1 \quad (9.21)$$

Where,  $R$  is the gas constant (for air  $R= 0.287$  kJ/kg.K) and  $r$  is the compression ratio of the cycle (for modern spark-ignition engines  $8 \leq r \leq 11$ ). For or the isentropic compression and expansion processes:

$$\frac{v_{r2}}{v_{r1}} = \frac{v_2}{v_1} = 1/r \quad (9.22)$$

$$\frac{v_{r4}}{v_{r3}} = \frac{v_4}{v_3} = r \quad (9.23)$$

Where,  $v_r$  is the relative specific volume. The last two relationships can be used to determine the two temperatures after the compression and expansion processes. The amount of heat added in process 2-3 per kg of the working fluid ( $q_{in}$ ) is calculated from:

$$q_{in} = (u_3 - u_2) \quad (9.24)$$

The amount of heat removed per kg of the working fluid ( $q_{in}$ ) is calculated from:

$$q_{out} = (u_4 - u_1) \quad (9.25)$$

Applying the first-law of thermodynamics, the net work from the cycle is given by:

$$w_{net} = q_{in} - q_{out} \quad (9.26)$$

Therefore, the thermal efficiency of the Ott cycle ( $\eta_{Otto}$ ) is given by:

$$\eta_{Otto} = \frac{w_{net}}{q_{in}} \quad (9.27)$$



The cycle's mean-effective pressure (MEP) is defined as:

$$MEP = \frac{W_{net}}{v_{max} - v_{min}} = \frac{W_{net}}{v_1 - v_2} \quad (9.28)$$

Although the above model uses the usual air-standard assumptions, Equations (9.22) and (9.23) take into consideration the variation of the specific heat with temperature. Therefore, the model yields more realistic results than those obtained by using the approximate constant specific heat method which is more convenient for hand calculations.

**Example 9-3. Energy analysis of the Otto cycle**

An ideal Otto cycle has a compression ratio of 8. At the beginning of the compression process, air is at 100 kPa and 17°C. During the constant-volume heat-addition process, 800 kJ/kg of heat is transferred to air. Accounting for the variation of specific heats of air with temperature, conduct an energy analysis of the cycle to determine:

- (i) the net work output and thermal efficiency,
- (ii) the mean effective pressure for the cycle.

This example is based on Examples 9-2 in Cengel and Boles [2].

**Solution**

Figures 9.12 and 9.13 show the Excel sheets developed for the analysis of the Otto cycle using property functions for ideal gases provided by Thermax and IdealGAs, respectively. The sheets show the formulae used in the calculation parts and the formula window in each sheet reveals the formula used for the calculation of the mean effective pressure according to Equation (9.28). Since the IdealGas add-in does not provide a function for determining the gas temperature from its internal energy, the temperature T\_3 in Figure 9.13 has been found by using the Goal-Seek command. Table 9.3 compares the values obtained by the two add-ins to those given by Cengel and Boles [2]. The figures in the table show good agreement between the three solutions.

	B	C	D	E	F	G	H	I	J	K	L
15	Energy analysis										
16	rc	8		v_1	0.8323	=R_air*T_1/P_1	u_3	1273.924	=u_2+Q_in	q_out	381.9115
17	T_1	290	K	u_1	206.5157	=gasu_1TK("air",T_1)	T_3	1572.592	=gasTK_1u("air",u_3)		
18	P_1	100	kPa	vr_1	676.0638	=gasvr_1TK("air",T_1)	P_3	4338.186	=(T_3/T_2)*P_2	w_net	418.0885
19	Q_in	800	kJ/kg	vr_2	84.50797	=vr_1/rc	vr_3	6.064618	=gasvr_1TK("air",T_3)		
20				T_2	648.7274	=GasTK_1vr("air",vr_2)	vr_4	48.51694	=vr_3*rc	η_l	0.522611
21	R_air	0.287		u_2	473.9238	=gasu_1TK("air",T_2)	T_4	793.1169	=GasTK_1vr("air",vr_4)		
22				P_2	1789.593	=(T_2/T_1)*rc*P_1	u_4	588.4273	=gasu_1TK("air",T_4)	MEP	574.0903
23				v_2	0.104038	=R_air*T_2/P_2	v_4	0.8323	=v_1		
24											

Figure 9.12. Excel sheet developed for Example 9-3

	B	C	D	E	F	G	H	I	J	K	L	
15	Energy analysis											
16	rc	8		v_1	0.8323	=R_air*T_1/P_1		u_3	1273.784	=u_2+Q_in	q_out	381.9112
17	T_1	290	K	u_1	206.3773	=u_air(T_1,"si")		T_3	1572.595	1572.595		
18	P_1	100	kPa	vr_1	680.7629	=Vrel_air(T_1,"si")		P_3	4338.192	=(T_3/T_2)*P_2	w_net	418.0888
19	Q_in	800	kJ/kg	vr_2	85.09536	=vr_1/rc_		vr_3	6.106743	=Vrel_air(T_3,"si")		
20				T_2	648.7274	=T_vrel_air(vr_2,"si")		vr_4	48.85395	=vr_3*rc_	η_I	0.522611
21	R_air	0.287		u_2	473.7844	=u_air(T_2,"si")		T_4	793.1182	=T_vrel_air(vr_4,"si")		
22				P_2	1789.593	=(T_2/T_1)*rc_*P_1		u_4	588.2885	=u_air(T_4,"si")	MEP	574.0909
23				v_2	0.104038	=R_air*T_2/P_2		v_4	0.8323	=v_1		
24												

Figure 9.13. Excel sheet developed for Example 9-3 using the IdealGas add-in

Table 9.3. Key parameters in the energy analysis

Parameter	Cengel and Boles [2]	Thermax	IdealGas
$T_2$	652.4	648.7	648.7
$T_3$	1575.1	1572.6	1572.6
$T_4$	795.6	793.1	793.1
$P_2$	1799.7	1789.6	1789.6
$P_3$	4345.0	4338.2	4338.2
$q_{out}$	381.83	381.91	381.91
$w_{net}$	418.17	418.09	418.09
$\eta_{Otto}$	0.523	0.523	0.523
MEP	574.0	574.1	574.1

Using the approximate method of analysis with fixed values of the specific heat, it can be shown that the thermal efficiency of the Otto cycle is given by [3]:

$$\eta_{otto} = 1 - (1/r_c)^{k-1} \tag{9.29}$$

Where,  $k$  is the ratio of specific heats  $c_p/c_v$  for air. Substituting  $r_c = 8$  and  $k = 1.4$  in Equation (9.29), the calculated thermal efficiency is 0.565. Although values of the thermal efficiency obtained by both the exact and the approximate methods are exaggerated compared to that of actual engines that of the variable specific heat method, which is 0.523, is more realistic.

#### 9.4. Exergy analysis of the Otto cycle

Energy analyses, such as that presented in the previous section, evaluate the general performance of energy-conversion systems using overall performance indicators such as the thermal efficiency for power-producing systems and the coefficient of performance (COP) for refrigeration systems. By comparison, the analyses based on the second-law of thermodynamics, which are called *exergy* analyses, enable the locations, types, and true magnitudes of waste and loss to be determined. Therefore, exergy analyses can be used in design analyses of thermofluid systems to further the goal of achieving more efficient use of resources [4].

### The analytical model

Exergy ( $\phi$ ) is a thermodynamic property that measures the ability of the working fluid to do useful work. Per unit mass in a closed system like that of the engine shown in Figure 9.10, exergy is given by [2]:

$$\phi = (u - u_0) - T_0(s - s_0) + P_0(v - v_0) + \frac{V^2}{2} + gz \quad (9.30)$$

Where  $u$  is the internal energy and  $u_0$ ,  $s_0$ , and  $P_0$ , respectively, refer to the values of the internal energy, entropy and pressure at the dead state which is the surroundings. Neglecting changes in the kinetic and potential energies, and taking into consideration that  $v_3 = v_2$  in this case, the exergy input in process 2-3 is determined from:

$$\phi_{input} = (\phi_3 - \phi_2) = (u_3 - u_2) - T_0(s_3 - s_2) \quad (9.31)$$

Exergy of the working fluid can be destroyed in a process because of irreversibilities such as friction losses and heat-transfer over a finite-temperature difference. In general, the exergy destruction ( $x_{dest}$ ) in a process is determined from:

$$\begin{aligned} x_{dest} &= T_0 s_{gen} = T_0 (\Delta s_{sys} - s_{in} + s_{out}) \\ &= T_0 \left( (s_2 - s_1)_{sys} - \frac{q_{in}}{T_{b,in}} + \frac{q_{out}}{T_{b,out}} \right) \end{aligned} \quad (9.32)$$

Where,  $s_{gen}$  refers to the entropy generated in the process. In the Otto cycle, processes 1-2 and 3-4 are both adiabatic and reversible. Therefore, for these two processes:

$$x_{dest} = 0 \quad (9.33)$$

However, processes 2-3 and 4-1 both involve heat transfer with the surroundings and that makes them externally irreversible processes. While process 2-3 involves heat addition only, process 4-1 involves heat rejection only. For these two processes, exergy destructions are obtained from:

$$x_{dest} = T_0 \left( (s_3 - s_2) - \frac{q_{in}}{T_H} \right) \quad \text{Process 2-3} \quad (9.34)$$

$$x_{dest} = T_0 \left( (s_1 - s_4) + \frac{q_{out}}{T_L} \right) \quad \text{Process 4-1} \quad (9.35)$$

The exergy destruction of the whole Otto cycle is the sum of the exergy destructions in the heat-addition and heat-rejection processes. Since  $s_2 = s_1$  and  $s_4 = s_3$ , the exergy destruction in the Otto cycle becomes:

$$x_{dest} = T_0 \left( \frac{q_{out}}{T_L} - \frac{q_{in}}{T_H} \right) \tag{9.36}$$

**Example 9-4. Exergy analyses of the Otto cycle**

Accounting for the variation of specific heats of air with temperature, conduct an exergy analysis for the Otto cycle considered in Example 9-3 to determine:

- (i) the exergy destruction associated with the Otto cycle (all four processes as well as the cycle), assuming that heat is transferred to the working fluid from a source at 1700 K and heat is rejected to the surroundings at 290 K, and
- (ii) the exergy of the exhaust gases when they are purged.

This example is based on Example 9-10 in Cengel and Boles [2] and therefore, the present results can be compared with their calculations for verification of the relevant Thermax functions.

**Solution**

The two sheets developed for Example 9-3 were extended for this exergy analysis and Figure 9.14 shows the extension that is needed in the lower part of the one using Thermax functions. Table 9.4 shows the functions used in this extension. The sheet using the IdealGas add-in was extended in a similar way. The additional data needed for exergy analysis include the temperature and pressure of the surroundings, temperature of the heat source, and the sink temperature. By obtaining the required entropy values at the different states from the energy part, the two sheets determine the exergy destructions in the four processes of the cycle, the total exergy destruction, and the exergy lost in the heat-rejection process. Table 9.5 compares the calculated values to those given by Cengel and Boles [2]. The figures in the table show a good agreement between the results of the two add-ins and those given by Cengel and Boles [2].

25						
26	<b>Exergy analysis</b>					
27	T_0	290	Ed_12	0	Ed_cycle	245.441 kJ/kg
28	P_0	100	Ed_34	0		
29					v_0	0.8323
30	T_source	1700	Dels23	-0.75607	u_0	206.5157
31	T_sink	290	Ed_23	82.78839 kJ/kg	Dels40	0.756065
32						
33			Dels14	-0.75607	E_4	162.6526 kJ/kg
34			Ed_41	162.6526 kJ/kg		
35						

Figure 9.14. Excel sheet developed for Example 9-4 using Thermax

Table 9.4. Thermax functions used in exergy analysis of the Otto cycle

Cell	Formula
F30	=gass0_1TK("air",T_2)-gass0_1TK("air",T_3)-R_air*LN(P_2/P_3)
F31	=T_0*(-Dels23-Q_in/T_source)
F33	=Dels23
F34	=T_0*(Dels14+q_out/T_sink)
I27	=Ed_23+Ed_41
I29	=v_1
I30	=gasu_1TK("air",T_0)
I31	=-Dels14
I33	=(u_4-u_0)-T_0*Dels40-P_0*(v_4-v_0)

Table 9.5. Results of the Otto cycle exergy analysis

	Cengel and Boles [2]	Thermax	IdealGas
$x_{dest,2-3}$	82.2	82.8	82.79
$x_{dest,4-1}$	163.2	162.7	162.65
$x_{dest,Otto}$	245.4	245.4	245.44
$\phi_4$	163.2	162.6	162.65

The figures in Table 9.5 show that two thirds of the total exergy supplied to the engine is lost during the heat-rejection process. Therefore, any design efforts that aim to minimise the loss of exergy in the heat-rejection process can effectively improve the performance of the Otto cycle. For example, the lost exergy can be used in a cogeneration system that utilises the heat for producing steam for industrial applications or for air-conditioning purposes. The figures in Table 9.5 also show that the exergy destruction in the heat-addition process are about one third of the total exergy destruction. While increasing the heat-addition temperature improves the thermal efficiency of the cycle, it increases the rate of exergy destruction in this process. Therefore, the selection of this temperature requires a careful consideration of the two factors among other practical considerations.

### 9.5. Closure

This chapter illustrated the use of the two property add-ins, Thermax and IdealGas [1], for the analyses of two basic power-generation cycles which are the Brayton cycle and the Otto cycle. With respect to such gas cycles, property functions enable the exact variable specific-heat method to be used; which gives more realistic estimations than the approximate constant-specific heat method. The analyses show that the functions provided by Thermax and IdealGas give identical results. While the IdealGas functions have the advantage of allowing the two systems of units to be used, Thermax functions are more general because the same function can be used for different gases. Thermax

also provides additional functions not provided by IdealGas such as the **GasTK\_1u** and **GasTK\_1h** functions that determine the temperature from a given value of internal energy or enthalpy, respectively.

Although not demonstrated in this chapter, the automation of property calculations by using property functions also enables Excel to be used for iterative solutions and optimisation analyses of various types of energy-conversion systems using its two “What-if analysis” tools; Goal-Seek and Solver. The scope of thermodynamic analyses with the Excel-based platform can be widened by using a number of other educational and research-oriented Excel add-ins that have been developed by academic institutions and individuals [5-7].

### References

- [1] The University of Alabama, Mechanical Engineering, Excel for Mechanical Engineering project, Internet: <http://www.me.ua.edu/excelinme/index.htm> (Last accessed July 19, 2018)
- [2] Y. A. Cengel and M. A. Boles. *Thermodynamics an Engineering Approach*, McGraw-Hill, 8<sup>th</sup> Edition, 2015
- [3] W.W. Pulkrabek, *Engineering Fundamentals of the Internal Combustion Engine*, Second Edition, Pearson Prentice Hall, 2004.
- [4] A. Bejan, G. Tsatsaronis, M. Moran, *Thermal Design & Optimization*, John Wiley & Sons, 1996.
- [5] D. G. Goodwin, "TPX: thermodynamic properties for Excel", [http://termodinamicaparaiaq.blogspot.com/p/tpx\\_12.html](http://termodinamicaparaiaq.blogspot.com/p/tpx_12.html) (Last accessed July 11, 2019)
- [6] The University of Virginia, Free Excel/VBA Spreadsheets for Thermodynamics: Rankine, Brayton, Otto and Diesel Cycles, Internet: <http://www.faculty.virginia.edu/ribando/modules/xls/Thermodynamics/> (Last accessed July 1, 2019)
- [7] I. Bell, CoolProp. Available at <https://sourceforge.net/projects/coolprop/files/CoolProp/> (Last accessed July 11, 2019)
- [8] M.J. Moran and H.N. Shapiro, *Fundamentals of Engineering Thermodynamics*, 5<sup>th</sup> edition, John Wiley, & Sons. Inc. 2006

### Excercises

1. Figure 9.9 shows that the net output work and thermal efficiency of the regenerative Brayton cycle reach their maximum values at different pressure ratios; which is about 8 for the maximum net work output and about 5 or less for the maximum thermal efficiency. Use Solver to determine the exact values of the pressure ratios.
2. A regenerative gas turbine with intercooling and reheat operates at steady state. Air enters the compressor at 100 kPa, 300 K with a mass flow rate of 5.8 kg/s. The pressure ratio across the two-stage compressor is 10. The pressure ratio across the two-stage turbine is also 10. The intercooler and reheater each operate at 300 kPa. At the inlets to the turbine stages, the temperature is 1400 K. The temperature at the

inlet to the second compressor stage is 300 K. The isentropic efficiency of each compressor and turbine stage is 80%. The regenerator effectiveness is 80%. Figure 9.P2 shows the  $T$ - $s$  diagram of the regenerative gas turbine cycle.

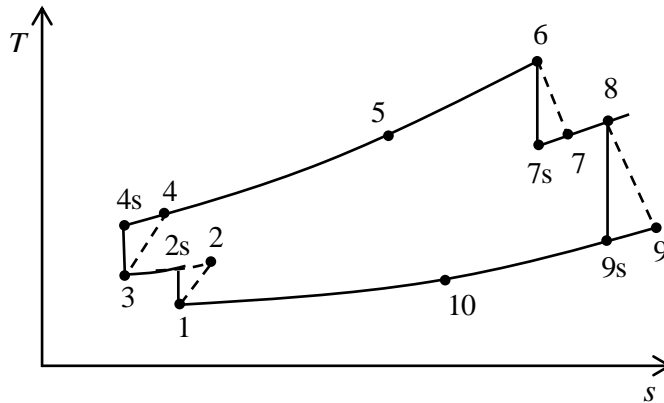


Figure 9.P2.  $T$ - $s$  diagram for the regenerative gas turbine with intercooling

Develop an Excel sheet to determine: (a) the thermal efficiency, (b) the back work ratio, (c) the net power developed, in kW. Compare your solution with that of Example 9-11 in Moran and Shapiro [8].

- The air-standard Diesel cycle shown in Figure 9.P3 operates with a compression ratio of 18. At the beginning of the compression process the temperature is 300 K and the pressure is 0.1 MPa. The cutoff ratio for the cycle is 2. Using Thermo or any other property add-in, develop an Excel sheet to determine (a) the temperature and pressure at the end of each process of the cycle, (b) the thermal efficiency, (c) the mean effective pressure, in MPa. Compare your solution with that of Example 9-2 in Moran and Shapiro [8].

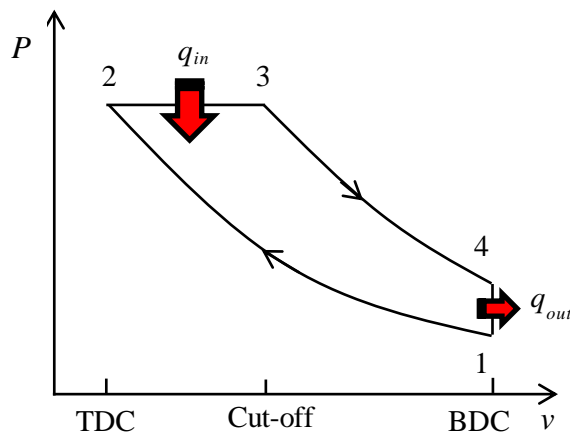


Figure 9.P3.  $P$ - $v$  diagram of the Diesel cycle

# 10

## **Analyses of simple and multi-stage compression VCR cycles**



The vapour-compression refrigeration (VCR) refrigeration systems used in various residential, commercial, and industrial applications are the main contributor to the ozone-layer depletion problem and a major contributor to the global-warming problem. Therefore, improving the performance of these systems is a critical matter. The performance of the simple single-stage VCR system deteriorates when there is a large difference between the evaporator and condenser temperatures. In this case, multi-stage compression VCR systems that split the refrigeration cycle into low-pressure and high-pressure stages become more attractive. However, these systems are more expensive and, in order to get their best performance, their stages have to be optimised. The chapter presents optimisation analyses of two-stage and three-stage compression cycles using refrigerant R134a. The results obtained by the property functions provided by Thermax and by the add-in developed for R134a at the University of Alabama (UA) [1] are verified against the relevant values given by Moran and Shapiro [2] and Cengel and Boles [3].

### 10.1. The ideal vapour-compression refrigeration cycle

Figure 10.1 shows a schematic diagram of the basic VCR system and Figure 10.2 shows the  $T$ - $s$  diagram for the ideal VCR cycle that consists of the following four processes:

1. Process 1-2: reversible adiabatic compression process
2. Process 2-3: constant-pressure heat-rejection process in the condenser
3. Process 3-4: expansion in an expansion valve or a capillary tube
4. Process 4-1: constant-pressure heat-addition process in the evaporator

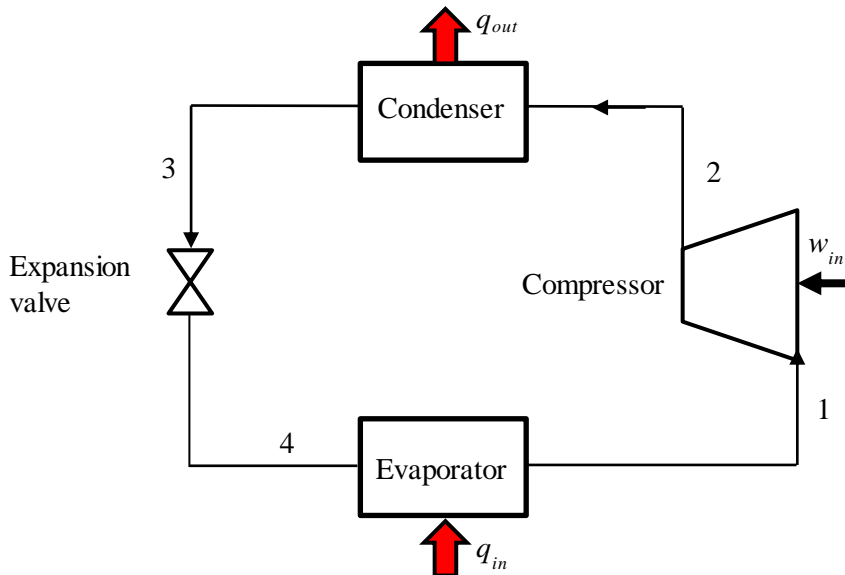


Figure 10.1. Schematic diagram of the single-stage vapour-compression refrigeration system

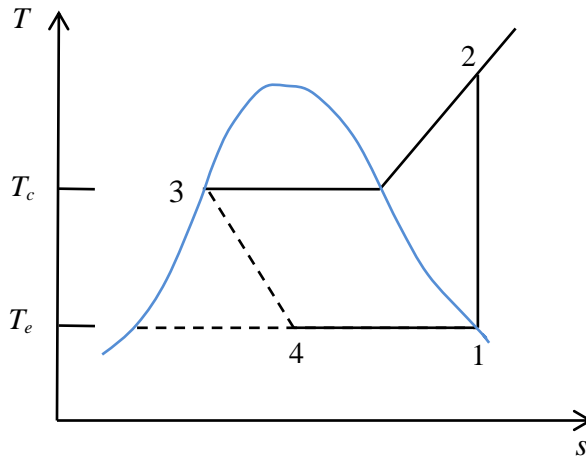


Figure 10.2.  $T$ - $s$  diagram for the ideal vapour-compression refrigeration cycle

The ideal cycle does not account for the irreversibility and pressure losses in the system components and the compressor is assumed to be adiabatic and reversible. Therefore, the compression process is isentropic as shown in Figure 10.2. Assuming steady operation of all the system components and neglecting changes in kinetic and potential energy across each component, the energy interactions with the surroundings in the different components per unit mass flow rate of the refrigerant in the system are described by the following relationships.

Compressor input work:

$$w_c = (h_2 - h_1) \quad (10.1)$$

Heat rejection in the condenser:

$$q_{out} = (h_2 - h_3) \quad (10.2)$$

Heat input in the evaporator:

$$q_{in} = (h_1 - h_4) \quad (10.3)$$

Adiabatic process in the expansion valve or capillary tube:

$$h_4 = h_3 \quad (10.4)$$

Three parameters measure the performance of the VCR systems; which are its coefficient of performance ( $COP$ ), cooling capacity ( $CC$ ) in ton of refrigeration, and the compressor power ( $\dot{W}_c$ ):

$$COP = \frac{q_{in}}{w_c} \quad (10.5)$$

$$CC = \frac{60\dot{m}q_{in}}{211} \quad (10.6)$$

$$\dot{W}_c = \dot{m}(h_2 - h_1) \quad (10.7)$$

Where  $\dot{m}$  is the mass flow rate of the refrigerant in the system in kg/s. The following example, which is based on Example 10-1 in Moran and Shapiro [2], illustrates the use of Thermax and the UA add-in “R134a” for analysing the cycle.

### Example 10-1. Analysis of the ideal vapour-compression refrigeration cycle

An ideal VCR cycle thermally connected to a cold region at 0°C and a warm region at 26°C uses refrigerant R134a as the working fluid. The refrigerant enters the compressor as saturated vapour at 0°C and leaves the condenser as saturated liquid at 26°C. The mass flow rate of the refrigerant is 0.08 kg/s. Determine (a) the compressor power, in kW, (b) the refrigeration capacity, in tons, and (c) the coefficient of performance.

### Solution

Figure 10.3 shows the Excel sheet developed for this example using Thermax. The given data for the evaporator and condenser temperatures and refrigerant mass flow rate are shown on the left side of the sheet as  $T_e$ ,  $T_c$ , and  $m_{ref}$ , respectively. The middle part of the sheet shows the formulae used for determining the different enthalpy values using functions from Thermax. The enthalpy at state 1,  $h_1$ , is determined by using the function **Refh\_Tx** that returns the enthalpy of saturated vapour ( $h_v$ ) at a given temperature. The entropy at this point ( $s_1$ ) is found by using another function, **Rehs\_Tx**, that determines the entropy of saturated vapour at a given temperature ( $T$ ) and quality ( $x$ ).

The right-hand side of the sheet calculates the compressor power,  $w_c$ , according to Equation (10.7), the cooling capacity,  $CC$ , according to Equation (10.6), and the coefficient of performance ( $COP$ ) according to Equation (10.5). A similar sheet was developed by using property functions from the R134a add-in provided by the University of Alabama [1]. Table 10.1 that compares the calculated values for the key cycle parameters by the two add-ins shows a good agreement between the add-in results with their corresponding values given by Moran and Shapiro [2].

COP		=q_in/w_c							
A	B	C	D	E	F	G	H	I	
1									
2	T_e	0	oc	h_1	398.600	=Refh_Tx("R134a",T_e,1)	w_c	1.409	kW
3				s_1	1.727	=Refs_Tx("R134a",T_e,1)			
4	T_c	26	oc				q_in	13.010	kW
5				P_c	685.430	=RefPsat_T("R134a",T_c)	CC	3.700	Ton
6	m_ref	0.08	kg/s						
7				h_2	416.207	=Refh_Ps("R134a",P_c,s_1)			
8							COP	9.237	
9				h_3	235.970	=Refh_Tx("R134a",T_c,0)			
10									
11				h_4	235.970	=h_3			
12									

Figure 10.3. Excel sheet developed for the ideal VCR cycle of Example 10-1

Table 10.1. Comparison of the ideal VCR cycle key parameters given by the two add-ins with their values given by Moran and Shapiro [2]

Parameter	Moran & Shapiro [2]	Thermax	UA Add-in R134a
Compressor work [kW]	1.40	1.409	1.409
Refrigeration capacity (ton)	3.67	3.700	3.700
COP	9.24	9.237	9.235

### 10.2. The actual vapour-compression refrigeration cycle

In actual VCR cycles, all four processes are irreversible because of friction losses in the compressor and heat-transfer with finite temperature differences in the evaporator and condenser. Some degree of subcooling also occurs at the condenser discharge. These modifications to the ideal cycle affect both the cooling capacity and COP of the VCR system. Figure 10.4 shows the  $T$ - $s$  diagram for the actual VCR cycle.

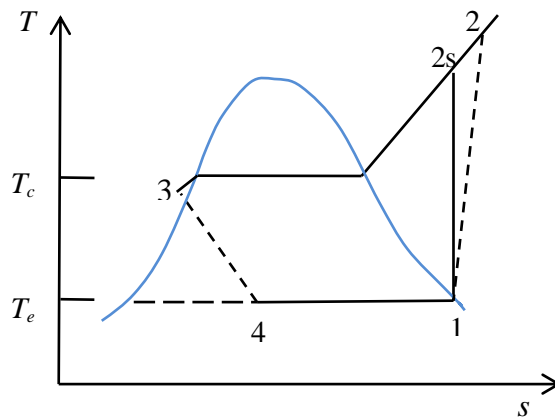


Figure 10.4.  $T$ - $s$  diagram for the actual VCR cycle

For simplification, it is assumed that saturated vapour refrigerant enters the compressor where it is compressed to a pressure that matches the required condenser temperature. The actual exit temperature at state 2 is higher than the corresponding temperature in the ideal cycle at state 2s, while the actual exit temperature from the condenser at state 3 is lower than the corresponding temperature in the ideal cycle, which is  $T_c$ . Referring to Figure 10.4, the relationships that determine the specific compressor work and heat-rejection in the condenser become:

$$w_c = (h_2 - h_1) \quad (10.8)$$

$$q_{out} = (h_2 - h_3) \quad (10.9)$$

The enthalpy at state 2 can be determined from:

$$h_2 = h_1 + (h_{2s} - h_1) / \eta_c \quad (10.10)$$

Where  $\eta_c$  is the isentropic efficiency of the compressor. The enthalpy at state 3 is approximately taken as the enthalpy of the saturated refrigerant at the given temperature. The following example, which illustrates the use of the Thermax and R134a add-ins for analysing the actual VCR cycle, is based on Example 10-3 in Moran and Shapiro [2].

### Example 10-2. Analysis of the actual vapour-compression refrigeration cycle

A VCR system thermally connected to a cold region at 0°C and a warm region at 26°C uses refrigerant R134a as the working fluid. The refrigerant temperature in the evaporator is -10°C, while the condenser pressure is 9 bars, which corresponds to a saturation temperature of 36°C for R134a. The refrigerant exits the condenser as subcooled liquid at 30°C. Analyse the cycle to determine its COP and cooling capacity taking the isentropic efficiency of the compressor as 80%.

### Solution

Figure 10.5 shows the Excel sheet developed for analysing the cycle with Thermax. Note the additional entries in the data and calculations parts. In the data part, the condenser pressure is entered instead of the condenser temperature. The data part also added the subcooled fluid temperature, T\_3, and the compressor efficiency ( $\eta_c$ ). The calculations part adds a new formula for determining the compressor discharge enthalpy, h\_2. Also, note that the enthalpy at state 3 is now evaluated at 30°C and not at the saturation temperature corresponding to the condenser pressure, which is 36°C.

A similar Excel sheet was developed using the UA add-in for R134a. Table 10.2 compares values of the three cycle parameters  $w_c$ , CC, and COP as determined by the two add-ins with their corresponding values given by Moran and Shapiro [2]. The figures in the table show that the results obtained by the two add-ins are slightly

different from those given by Moran and Shapiro [2]. It should be noted that the work input in the actual cycle is more than that of the ideal cycle of Example 10-1, while the cooling capacity is lower. Therefore, the COP dropped from 9.235 in the ideal cycle to 3.83 in the actual cycle, which is more realistic.

	A	B	C	D	E	F	G	H	I
1									
2	T_e	-10	oc	h_1	392.660	=Refh_Tx("R134a",T_e,1)	w_c	3.154	kW
3				s_1	1.733	=Refs_Tx("R134a",T_e,1)			
4	P_c	911.88	kPa				Q_in	12.075	kW
5				T_c	36.001	=RefTsatsat_P("R134a",P_c)			
6	m_ref	0.08	kg/s				CC	3.434	Ton
7				T_3	30.001	=T_c-6			
8	η_comp	0.8		h_2s	424.201	=Refh_Ps("R134a",P_c,s_1)	COP	3.828	
9				h_2	432.087	=h_1+(h_2s-h_1)/η_comp			
10				h_3	241.722	=Refh_Tx("R134a",T_3,0)			
11				h_4	241.722	=h_3			
12									

Figure 10.5. Excel sheet developed for the actual VCR cycle of Example 10-2

Table 10.2. Comparison of the actual VCR cycle key parameters with their values given by Moran and Shapiro [2]

Parameter	Moran & Shapiro [2]	Thermax	UA add-in R134a
Compressor work [kW]	3.10	3.154	3.153
Refrigeration capacity (ton)	3.41	3.434	3.433
COP	3.86	3.828	3.830

### 10.3. Optimisation analysis of the ideal two-stage compression cycle

A number of industrial refrigeration applications have very low evaporator temperatures. In such cases, the two-stage cascade refrigeration system shown in Figure 10.6 becomes more feasible. In this system, a flash-chamber is added at an intermediate pressure. Part of the refrigerant evaporates during the flashing process and mixed with the refrigerant leaving the low-pressure compressor. The mixture is then compressed to the condenser pressure by the high-pressure compressor. The liquid in the flash chamber is throttled to the evaporator pressure to cool the refrigerated space as it vaporizes in the evaporator. Figure 10.7 shows the  $T$ - $s$  diagram for the ideal cycle.

#### 10.3.1. The analytical model

The refrigerant is assumed to leave the evaporator as a saturated vapour and both compression processes are assumed to be isentropic. The refrigerant leaves the condenser as a saturated liquid and is throttled to a flash chamber pressure.

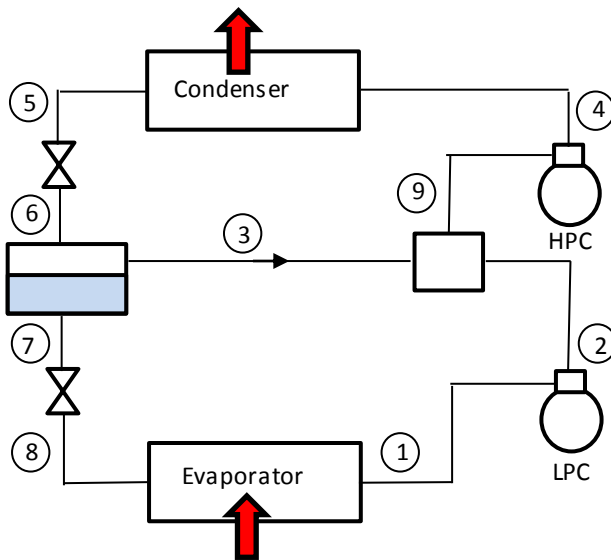


Figure 10.6. Schematic diagram for a two-stage compression VCR system

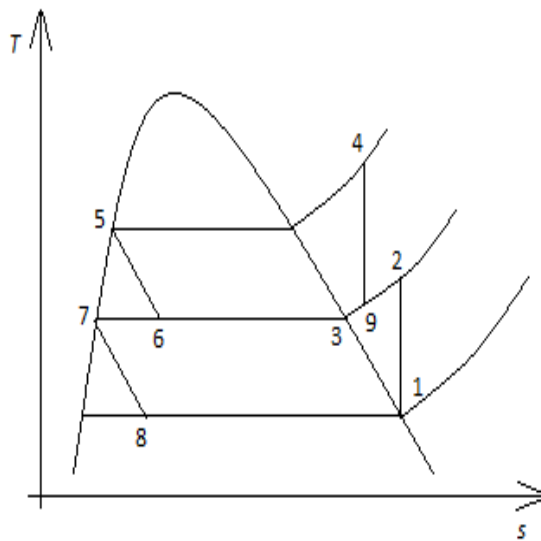


Figure 10.7.  $T$ - $s$  diagram for a two-stage compression VCR system

Taking the mass flow rate of the refrigerant in the condenser as  $\dot{m}$ , the fractions of this flow rate that are separated after the flash chamber as saturated vapour  $\dot{m}_v$  and saturated liquid  $\dot{m}_l$  are given by:

$$\dot{m}_v = x_6 \dot{m} \quad (10.11)$$

$$\dot{m}_l = (1 - x_6)\dot{m} \quad (10.12)$$

Where  $x_6$  is the quality at state 6. Therefore, the rates of heat removal in the evaporator  $\dot{Q}_e$  and heat rejection in the condenser  $\dot{Q}_c$  are given by:

$$\dot{Q}_e = \dot{m}_l(h_1 - h_8) \quad (10.13)$$

$$\dot{Q}_c = \dot{m}(h_4 - h_5) \quad (10.14)$$

The compression work  $\dot{W}_c$  which has two parts one in the low-temperature cycle and another in the high-temperature cycle, is given by.

$$\dot{W}_c = \dot{m}_l(h_2 - h_1) + \dot{m}(h_4 - h_3) \quad (10.15)$$

The COP of the system is then given by:

$$COP = \frac{\dot{Q}_e}{\dot{W}_c} = \frac{(1 - x_6)(h_1 - h_8)}{(1 - x_6)(h_2 - h_1) + (h_4 - h_3)} \quad (10.16)$$

### 10.3.2. The optimisation analysis

Cengel and Boles [3] considered a two-stage VCR system with refrigerant R134a as the working fluid. In what follows, their data and analysis results will be used to verify the results obtained by using Excel and property functions provided by Thermax and the add-in developed at the University of Alabama (UA) for refrigerant R134a [1].

#### Example 10-3. Optimisation of the ideal two-stage compression cycle

An ideal two-stage compression VCR system operates between evaporator and condenser pressures of 0.14 and 0.8 MPa, respectively, and its flash chamber has a pressure of 0.32 MPa.

#### Solution

Figure 10.8 shows the Excel sheet developed for analysing the two-stage compression cycle using property functions. The three values of the evaporator, condenser, and flash-chamber pressures are stored in the data part that occupies the left side of the sheet. Calculations of the enthalpy values and the quality at state 6 are done in the two central columns using Thermax functions. Based on the calculated values of state enthalpies, the sheet determines the amount of heat absorbed in the evaporator ( $q_E$ ), the heat rejected in the condenser ( $q_C$ ), the total compression work ( $w_{comp}$ ), and the cycle's COP (COP). Figure 10.9 shows the formulae entered in the three columns that calculate the intermediate and final results and Thermax functions they use. In addition



to the three Thermax functions shown in Table 10.1, this analysis requires the function “Refs\_Ph(“R134a”,P\_flash,h\_9)” to determine the entropy  $s_9$  from the known pressure and enthalpy values at state 9.

	A	B	C	D	E	F	G	H	I	J	K
1											
2	P_evap	140	kPa	h_1	387.3095		s_2	1.740259		q_E	146.287
3				s_1	1.740259		h_2	404.0627			
4	P_cond	800	kPa							q_C	178.9803
5				h_5	243.6307		h_3	400.0385			
6	P_flash	320	kPa							w_comp	32.69327
7				h_6	243.6307		h_9	403.2381			
8				x_6	0.204904		s_9	1.737308		COP	4.47453
9											
10				h_7	203.3228		s_4	1.737308			
11							h_4	422.611			
12				h_8	203.3228						
13											

Figure 10.8. The Excel sheet developed for the two-stage compression VCR system

	D	E	F	G	H	I	J	K
h_1	=Refh_Px("R134a",P_evap,1)			s_2	=s_1		q_E	=(1-x_6)*(h_1-h_8)
s_1	=Refs_Px("R134a",P_evap,1)			h_2	=Refh_Ps("R134a",P_flash,s_2)		q_C	=h_4-h_5
h_5	=Refh_Px("R134a",P_cond,0)			h_3	=Refh_Px("R134a",P_flash,1)		w_comp	=(1-x_6)*(h_2-h_1)+1*(h_4-h_9)
h_6	=h_5			h_9	=x_6*h_3+(1-x_6)*h_2		COP	=q_E/w_comp
x_6	=(h_6-h_7)/(h_3-h_7)			s_9	=Refs_Ph("R134a",P_flash,h_9)			
h_7	=Refh_Px("R134a",P_flash,0)			s_4	=s_9			
h_8	=h_7			h_4	=Refh_Ps("R134a",P_cond,s_4)			

Figure 10.9. Excel formulae and Thermax functions used in the Excel sheet

A similar Excel sheet was also developed using the relevant property functions provided by the add-in developed at the University of Alabama for refrigerant R134a [1]. Table 10.4 compares the values of various cycle parameters obtained by the two Excel sheets with their corresponding values given by Cengel and Boles [3]. The figures in the table show that the values of  $\dot{Q}_e$ ,  $\dot{W}_c$ , and COP given by both add-ins are very close to those given by Cengel and Boles [3]. The COP of the two-stage compression cycle can be improved by suitably adjusting the pressure at the flash-chamber. The results obtained by changing the value of this pressure are shown in Figure 10.10. The figure shows that the cycle’s COP can reach 5.49 at a flash-chamber pressure of around 400 kPa.

Table 10.4. Analysis results for the two-stage compression cycle

	Cengel and Boles [3]	Thermax	UA add-in R134a	Error (%)
$h_1$	239.16	387.3095	387.3244	-0.0038
$s_1$		1.740259	1.740194	0.0037
$h_2$	255.93	404.0627	404.0133	0.0122
$h_3$	251.88	400.0385	400.0513	-0.0032
$h_4$	274.48	422.611	422.6194	-0.0020
$h_5$	95.47	243.6307	243.6611	-0.0125
$h_6$	95.47	243.6307	243.6611	-0.0125
$x_6$	0.2049	0.204904	0.204879	0.0122
$h_7$	55.16	203.3228	203.364	-0.0203
$h_8$	55.16	203.3228	203.364	-0.0203
$h_9$	255.10	403.2381	403.2016	0.0091
$s_9$		1.737308	1.737218	0.0052
$\dot{Q}_e$	146.3	146.287	146.2708	0.0111
$\dot{W}_c$	32.71	32.69327	32.68758	0.0174
COP	4.47	4.47453	4.474811	-0.0063

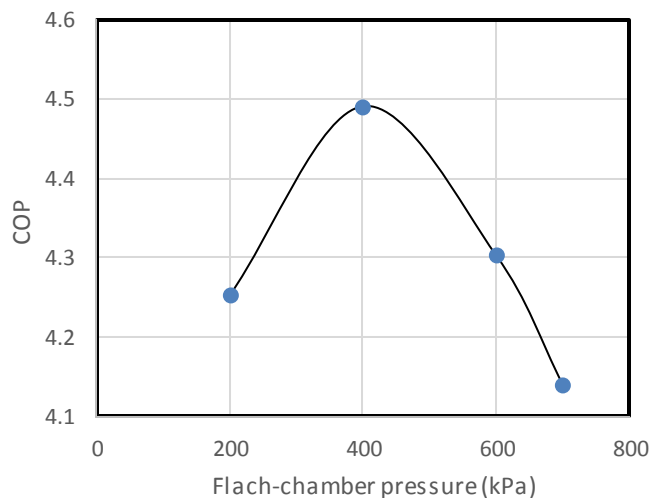


Figure 10.10. Variation of the COP with the flash-chamber pressure in the two-stage compression VCR system

The maximum COP and corresponding flash-chamber pressure can be determined more precisely by using Solver and Figure 10.11 shows the completed Solver Parameters dialog box for this task.

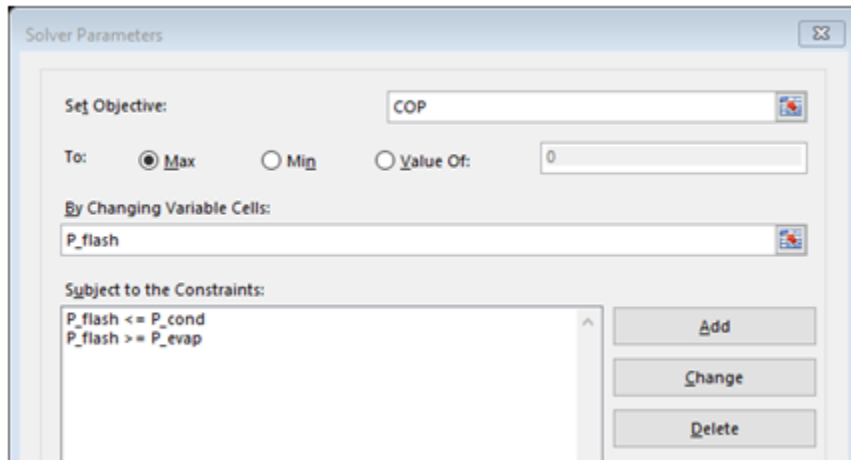


Figure 10.11. Solver Parameters dialog box for optimisation of the two-stage compression cycle

Two constraints have been imposed so as to keep the value of the flash-chamber pressure,  $P_{flash}$ , between the specified values of the evaporator and condenser pressures. Figure 10.12 shows that the solution reached by Solver by using the GRG Nonlinear method. According to this solution the maximum COP is 4.49 and occurs at a flash-chamber pressure of 375.45 kPa. Further improvement of the system's COP is still possible by using more than one flash chamber at different pressure levels as show in the following section.

	A	B	C	D	E	F	G	H	I	J	K
1											
2	P_evap	140	kPa	h_1	387.3095		s_2	1.740259		q_E	146.3881
3				s_1	1.740259		h_2	407.4025			
4	P_cond	800	kPa							q_C	178.9833
5				h_5	243.6307		h_3	402.6593			
6	P_flash	375.4545	kPa							w_comp	32.59521
7				h_6	243.6307		h_9	406.5653			
8				x_6	0.176504		s_9	1.737318		COP	4.491092
9											
10				h_7	209.5452		s_4	1.737318			
11							h_4	422.614			
12				h_8	209.5452						
13											

Figure 10.12. Solver solution for optimisation of the two-stage compression cycle

#### 10.4. Optimisation analysis of the three-stage compression cycle

By using two flash chambers instead of one chamber, three-stage compression VCR systems can be more cost-effective than two-stage compression systems if the temperature lift is sufficiently high. Figure 10.13 shows a schematic diagram for such a system and Figure 10.14 shows its ideal  $T$ - $s$  diagram.

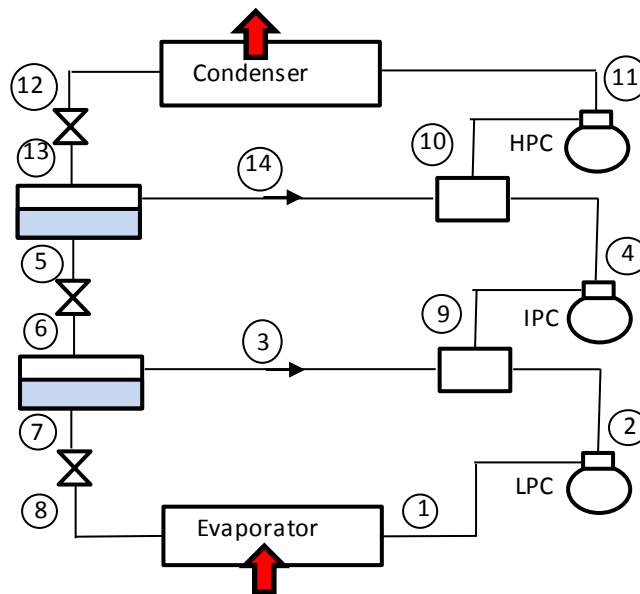


Figure 10.13. Schematic of the three-stage compression VCR system

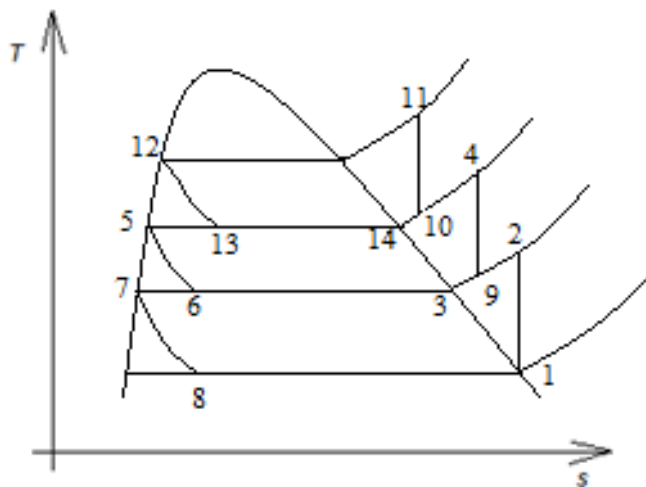


Figure 10.14.  $T-s$  diagram for the ideal three-stage compression VCR cycle

Depending on the refrigerant used in the system, there are certain values of the two flash-chamber pressures that maximise the system's COP. However, unlike the two-stage compression system, the determination of these pressures requires the use of an optimisation software since it is not as easy to find them by varying the flash-chamber pressures as in the case of a single flash chamber. In what follows, the optimum flash-chamber pressures will be determined by using Solver.

#### 10.4.1. The analytical model

Taking the mass flow rate of the refrigerant in the condenser to be  $\dot{m}$ , the mass flow rates of the vapour and liquid fractions after the high-pressure flash chamber are given by:

$$\dot{m}_{14} = x_{13}\dot{m} \quad (10.17)$$

$$\dot{m}_5 = (1 - x_{13})\dot{m} \quad (10.18)$$

Accordingly, the mass flow rates of the vapour and liquid fractions after the low-pressure flash chamber are given by:

$$\dot{m}_3 = x_6(1 - x_{13})\dot{m} \quad (10.19)$$

$$\dot{m}_7 = (1 - x_6)(1 - x_{13})\dot{m} \quad (10.20)$$

The total compression work and the rate of heat rejection in the condenser are now given by:

$$\dot{W}_{ct} = \dot{m}_7(h_2 - h_1) + (\dot{m}_3 + \dot{m}_7)(h_4 - h_9) + \dot{m}(h_{11} - h_{10}) \quad (10.21)$$

$$\dot{Q}_c = \dot{m}(h_{11} - h_{12}) \quad (10.22)$$

Therefore, the system's COP is given by:

$$COP = \dot{Q}_c / \dot{W}_{ct} \quad (10.23)$$

#### 10.4.2. The optimisation analysis

The advantage of the three-stage compression cycle over the simple and the two-stage compression cycles is illustrated by the following example in which the evaporator and condenser pressures in the three systems are identical.

#### Example 10-4. Optimisation of the ideal three-stage compression cycle

The system to be analysed has the same evaporator and condenser pressures as in the two-stage cycle considered earlier, i.e., 0.14 and 0.8 MPa, respectively. It is required to determine values of the two flash-chamber pressures that maximise the system's COP.

#### Solution

Figure 10.15 shows the Excel sheet prepared for this example by extending that of the two-stage compression cycle shown in Figure 10.6. The data part now includes two

## Computer-Aided Thermofluid Analyses Using Excel

flash-chamber pressures,  $P_{fc1}$  and  $P_{fc2}$  instead of one. The two flash-chamber pressures are initially assigned values of 320 kPa and 520 kPa. A third column has also been added to the calculations part to determine the enthalpy and entropy values in the high-pressure stage.

	A	B	C	D	E	F	G	H	I	J	K	L	M	N
1														
2	P_evap	140	kPa	h_1	387.3095	s_2	1.740259	h_14	408.1266	q_E	147.1226			
3				s_1	1.740259	h_2	404.0627							
4	P_cond	800	kPa					h_12	243.6307	q_C	178.7782			
5				h_5	223.2044	h_3	400.0385							
6	P_fc1	320	kPa					h_13	243.6307	w_comp	31.6556			
7				h_6	223.2044	h_9	403.656	x_13	0.110459					
8	P_fc2	520	kPa	x_6	0.101068	s_9	1.738802					COP	4.647602	
9								h_10	413.2285					
10				h_7	203.3228	s_4	1.738802	s_10	1.736658					
11						h_4	413.8621							
12				h_8	203.3228			s_11	1.736658					
13								h_11	422.4089					
14														

Figure 10.15. Excel sheet for analysing the three-stage compression VCR cycle

Figure 10.15 shows that at the specified values of the pressures at the two flash chambers, the COP is 4.65. Although this COP is higher than the optimum pressure obtained earlier for the two-stage compression cycle, which is 4.49, it is still not the maximum possible value for the COP of the three-stage cycle. The maximum COP can be determined by optimising the two flash-chamber pressures by using Solver. Solver Parameters dialog box is shown in Figure 10.16.

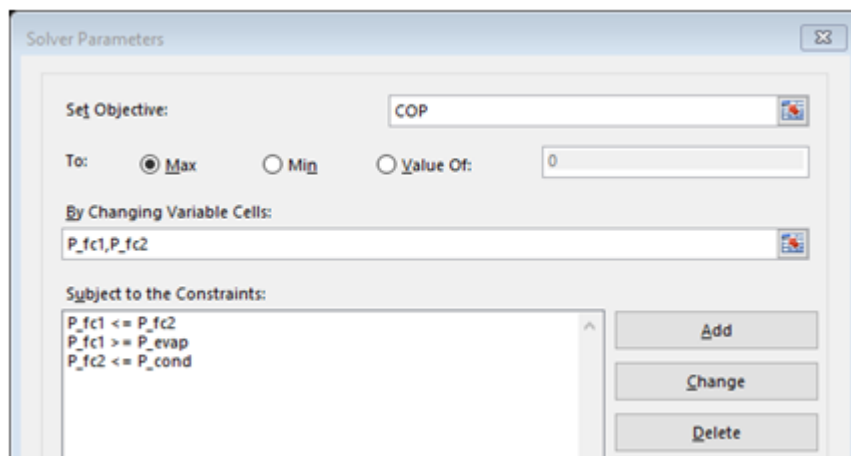


Figure 10.16. Solver Parameters box for the optimisation of the three-stage cycle

As Figure 10.16 shows, three constraints have been imposed so as to keep the value of the two flash-chamber pressures,  $P_{fc1}$  and  $P_{fc2}$ , between the specified values of the evaporator pressure  $P_{evap}$ , and the condenser pressure,  $P_{cond}$ , i.e.:

$$P_{evap} < P_{fc1}$$

$$P_{fc1} < P_{fc2}$$

$$P_{fc2} < P_{cond}$$

Figure 10.17 shows the solution determined by Solver according to which the maximum COP is reached when the flash-chamber pressures are 283.465 kPa and 498.434 kPa. Comparison of the cycle's overall parameters shown in Figure 10.17 with those shown in Figure 10.12 indicates that the cooling rate per unit flow rate of the refrigerant ( $q_E$ ) has increased from 146.388 kJ for the two-stage system to 147.158 kJ for the three-stage system, while the corresponding compressors work decreased from 32.595 kJ to 31.579 kJ. As a result, the COP of the three-stage system reached 4.66; which is higher than that of the two-stage compression cycle (COP=4.49) by about 3.23% and higher than that of the simple VCR cycle (COP=3.97) by about 14.44%. The advantage of the three-stage system over the simple and the two-stage compression systems becomes more profound as the temperature lift increases.

	A	B	C	D	E	F	G	H	I	J	K	L	M	N
1														
2	P_evap	140	kPa	h_1	387.3095		s_2	1.740259		h_14	407.4098		q_E	147.1581
3				s_1	1.740259		h_2	401.5401						
4	P_cond	800	kPa							h_12	243.6307		q_C	178.7373
5				h_5	221.3546		h_3	398.0706						
6	P_fc1	283.465	kPa							h_13	243.6307		w_comp	31.57926
7				h_6	221.3546		h_9	401.1472		x_13	0.119729			
8	P_fc2	498.434	kPa	x_6	0.113242		s_9	1.738787					COP	4.659959
9										h_10	412.2944			
10				h_7	198.7873		s_4	1.738787		s_10	1.736527			
11							h_4	412.9587						
12				h_8	198.7873					s_11	1.736527			
13										h_11	422.368			
14														

Figure 10.17. Solution determined by Solver for the three-stage compression VCR cycle

### 10.5. Closure

This chapter illustrated the use of Thermax functions for the analyses of basic refrigeration cycles including the ideal VCR cycle and the actual VCR cycle. The results obtained by using Thermax functions for refrigerant R134a were verified with those given in standard textbooks or determined by another property add-in developed at the

Mechanical Engineering Department at the University of Alabama [1]. The chapter also showed how the Excel-based modelling platform can be used for analysing and optimising two-stage cascade and multi-stage compression VCR systems.

Most of the fluid states in the analysed VCR analyses lie in the compressed liquid or saturated mixture regions and, therefore, the accuracy of Thermax functions for these states is not questionable because they calculate the refrigerants properties using the data provided by ASHRAE. Regarding the accuracy of estimating the fluid properties in the superheated region by the relevant Thermax functions, the analyses presented in this chapter showed that the accuracy of these functions has a minor effect on the accuracy of estimating the overall cycle parameters determined by Thermax. Therefore, Thermax function can be used to analyse the effects of other improvements to the simple VCR cycle such as adding a suction-line heat exchanger to the system [4].

A number of Excel add-ins have been developed by academic and research institutions that can be used to widen the scope of analyses of VCR systems by using the Excel-based platform. A good example of these add-ins is the REFPROP add-in developed by the National Institute of Standards and Technology (NIST). REFPROP provides properties of a large number of conventional and alternative refrigerants including refrigerants mixtures [5]. A free-source alternative to REFPROP is the CoolProp software developed by Bell [6].

### References

- [1] The University of Alabama, Website of Excel in Mechanical Engineering, <https://www.me.ua.edu/ExcelinME/>
- [2] M.J. Moran and H.N. Shapiro, Fundamentals of Engineering Thermodynamics, 5<sup>th</sup> edition, John Wiley & Sons, Inc, 2006.
- [3] A. Cengel, and M.A. Boles, Thermodynamics an Engineering Approach, McGraw-Hill, 8<sup>th</sup> Edition, 2015
- [4] M.M. El-Awad, Effect of Suction-Line Heat Exchangers on the Performance of Alternative Refrigerants to R-22, IOSR Journal of Mechanical and Civil Engineering (IOSR-JMCE), Volume 13, Issue 3 Ver. IV (May- Jun. 2016), PP 109-117
- [5] E.W. Lemmon, M.L. Huber, M.O. McLinden, *NIST Reference Fluid Thermodynamic and Transport Properties— REFPROP* Version 8.0, User's Guide, National Institute of Standards and Technology, Physical and Chemical Properties Division, Boulder, Colorado 80305, 2007.
- [6] I. Bell, CoolProp. Available at <https://sourceforge.net/projects/coolprop/files/CoolProp/> (Last accessed July 11, 2019)

### Exercises

1. It is required to compare the performance of refrigerant R134a as an alternative fluid to refrigerant R22 for air-conditioning (air-cooling) applications. By suitably modifying the Excel sheet developed for Example 10-1, compare the compressor



- power (kW), refrigeration capacity (ton), and coefficient of performance of the vapour-compression refrigeration cycle with both refrigerants for an evaporator temperature of  $10^{\circ}\text{C}$  and various condenser temperatures typical to your environment.
2. It is required to compare the performance of refrigerant R134a as an alternative fluid to refrigerant R22 for air-conditioning (air-heating) applications. By suitably modifying the Excel sheet developed for Example 10-1, compare the compressor power (kW), heating capacity (kW), and coefficient of performance of the vapour-compression refrigeration cycle with both refrigerants for a condenser temperature of  $40^{\circ}\text{C}$  and various evaporator temperatures typical to your environment.
  3. Modify the Excel sheet developed for Example 10-2 to model the performance of the actual VCR cycle with R22 as refrigerant. Take the evaporator temperature as  $-10^{\circ}\text{C}$ , the condenser pressure as 1390 kPa (at which the saturation temperature is  $36^{\circ}\text{C}$ ), the compressor exit temperature as  $30^{\circ}\text{C}$ , and the compressor isentropic efficiency as 80%.
  4. Repeat Exercise 10.3 with R410A or R717 as the refrigerant.
  5. By making suitable extensions to the Excel sheet developed for Example 10-2, determine the rates of exergy destruction within the compressor and expansion valve, in kW, for  $T_0 = 299\text{K}$  ( $26^{\circ}\text{C}$ ). (Answer: 0.58 kW and 0.39 kW).

# Appendices

**Appendix A: Properties of air and water at atmospheric pressure**

**Table A.1. Properties of air at various temperatures<sup>†</sup>**

$T$ °C	$\rho$ kg/m <sup>3</sup>	$c_p$ kJ/kg.K	$\mu$ kg/m.s	$\nu$ m <sup>2</sup> /s	$k$ W/m.°C	$\alpha$ m <sup>2</sup> /s	Pr
-150	2.866	0.983	8.636x10 <sup>-6</sup>	3.013x10 <sup>-6</sup>	0.01171	4.158x10 <sup>-6</sup>	0.7246
-100	2.038	0.966	1.189x10 <sup>-5</sup>	5.837x10 <sup>-6</sup>	0.01582	8.036x10 <sup>-6</sup>	0.7263
-50	1.582	0.999	1.474x10 <sup>-5</sup>	9.319x10 <sup>-6</sup>	0.01979	1.252x10 <sup>-5</sup>	0.7440
-40	1.514	1.002	1.527x10 <sup>-5</sup>	1.008x10 <sup>-5</sup>	0.02057	1.356x10 <sup>-5</sup>	0.7436
-30	1.451	1.004	1.579x10 <sup>-5</sup>	1.087x10 <sup>-5</sup>	0.02134	1.465x10 <sup>-5</sup>	0.7425
-20	1.394	1.005	1.630x10 <sup>-5</sup>	1.169x10 <sup>-5</sup>	0.02211	1.578x10 <sup>-5</sup>	0.7408
-10	1.341	1.006	1.680x10 <sup>-5</sup>	1.252x10 <sup>-5</sup>	0.02288	1.696x10 <sup>-5</sup>	0.7387
0	1.292	1.006	1.729x10 <sup>-5</sup>	1.338x10 <sup>-5</sup>	0.02364	1.818x10 <sup>-5</sup>	0.7362
5	1.269	1.006	1.754x10 <sup>-5</sup>	1.382x10 <sup>-5</sup>	0.02401	1.880x10 <sup>-5</sup>	0.7350
10	1.246	1.006	1.778x10 <sup>-5</sup>	1.426x10 <sup>-5</sup>	0.02439	1.944x10 <sup>-5</sup>	0.7336
15	1.225	1.007	1.802x10 <sup>-5</sup>	1.470x10 <sup>-5</sup>	0.02476	2.009x10 <sup>-5</sup>	0.7323
20	1.204	1.007	1.825x10 <sup>-5</sup>	1.516x10 <sup>-5</sup>	0.02514	2.074x10 <sup>-5</sup>	0.7309
25	1.184	1.007	1.849x10 <sup>-5</sup>	1.562x10 <sup>-5</sup>	0.02551	2.141x10 <sup>-5</sup>	0.7296
30	1.164	1.007	1.872x10 <sup>-5</sup>	1.608x10 <sup>-5</sup>	0.02588	2.208x10 <sup>-5</sup>	0.7282
35	1.145	1.007	1.895x10 <sup>-5</sup>	1.655x10 <sup>-5</sup>	0.02625	2.277x10 <sup>-5</sup>	0.7268
40	1.127	1.007	1.918x10 <sup>-5</sup>	1.702x10 <sup>-5</sup>	0.02662	2.346x10 <sup>-5</sup>	0.7255
45	1.109	1.007	1.941x10 <sup>-5</sup>	1.750x10 <sup>-5</sup>	0.02699	2.416x10 <sup>-5</sup>	0.7241
50	1.092	1.007	1.963x10 <sup>-5</sup>	1.798x10 <sup>-5</sup>	0.02735	2.487x10 <sup>-5</sup>	0.7228
60	1.059	1.007	2.008x10 <sup>-5</sup>	1.896x10 <sup>-5</sup>	0.02808	2.632x10 <sup>-5</sup>	0.7202
70	1.028	1.007	2.052x10 <sup>-5</sup>	1.995x10 <sup>-5</sup>	0.02881	2.780x10 <sup>-5</sup>	0.7177
80	0.9994	1.008	2.096x10 <sup>-5</sup>	2.097x10 <sup>-5</sup>	0.02953	2.931x10 <sup>-5</sup>	0.7154
90	0.9718	1.008	2.139x10 <sup>-5</sup>	2.201x10 <sup>-5</sup>	0.03024	3.086x10 <sup>-5</sup>	0.7132
100	0.9458	1.009	2.181x10 <sup>-5</sup>	2.306x10 <sup>-5</sup>	0.03095	3.243x10 <sup>-5</sup>	0.7111
120	0.8977	1.011	2.264x10 <sup>-5</sup>	2.522x10 <sup>-5</sup>	0.03235	3.565x10 <sup>-5</sup>	0.7073
140	0.8542	1.013	2.345x10 <sup>-5</sup>	2.745x10 <sup>-5</sup>	0.03374	3.898x10 <sup>-5</sup>	0.7041
160	0.8148	1.016	2.420x10 <sup>-5</sup>	2.975x10 <sup>-5</sup>	0.03511	4.241x10 <sup>-5</sup>	0.7014
180	0.7788	1.019	2.504x10 <sup>-5</sup>	3.212x10 <sup>-5</sup>	0.03646	4.593x10 <sup>-5</sup>	0.6992
200	0.7459	1.023	2.577x10 <sup>-5</sup>	3.455x10 <sup>-5</sup>	0.03779	4.954x10 <sup>-5</sup>	0.6974
250	0.6746	1.033	2.760x10 <sup>-5</sup>	4.091x10 <sup>-5</sup>	0.04104	5.890x10 <sup>-5</sup>	0.6946
300	0.6158	1.044	2.934x10 <sup>-5</sup>	4.765x10 <sup>-5</sup>	0.04418	6.871x10 <sup>-5</sup>	0.6935
350	0.5664	1.056	3.101x10 <sup>-5</sup>	5.475x10 <sup>-5</sup>	0.04721	7.892x10 <sup>-5</sup>	0.6937
400	0.5243	1.069	3.261x10 <sup>-5</sup>	6.219x10 <sup>-5</sup>	0.05015	8.951x10 <sup>-5</sup>	0.6948
450	0.4880	1.081	3.415x10 <sup>-5</sup>	6.997x10 <sup>-5</sup>	0.05298	1.004x10 <sup>-4</sup>	0.6965
500	0.4565	1.093	3.563x10 <sup>-5</sup>	7.806x10 <sup>-5</sup>	0.05572	1.117x10 <sup>-4</sup>	0.6986
600	0.4042	1.115	3.846x10 <sup>-5</sup>	9.515x10 <sup>-5</sup>	0.06093	1.352x10 <sup>-4</sup>	0.7037
700	0.3627	1.135	4.111x10 <sup>-5</sup>	1.133x10 <sup>-4</sup>	0.06581	1.598x10 <sup>-4</sup>	0.7092
800	0.3289	1.153	4.362x10 <sup>-5</sup>	1.326x10 <sup>-4</sup>	0.07037	1.855x10 <sup>-4</sup>	0.7149
900	0.3008	1.169	4.600x10 <sup>-5</sup>	1.529x10 <sup>-4</sup>	0.07465	2.122x10 <sup>-4</sup>	0.7206
1000	0.2772	1.184	4.826x10 <sup>-5</sup>	1.741x10 <sup>-4</sup>	0.07868	2.398x10 <sup>-4</sup>	0.7260
1500	0.1990	1.234	5.817x10 <sup>-5</sup>	2.922x10 <sup>-4</sup>	0.09599	3.908x10 <sup>-4</sup>	0.7478
2000	0.1553	1.264	6.630x10 <sup>-5</sup>	4.270x10 <sup>-4</sup>	0.11113	5.664x10 <sup>-4</sup>	0.7539

<sup>†</sup> Adopted from Y. A. Cengel and A. J. Ghajar, *Heat and Mass Transfer: Fundamentals and Applications*. 5<sup>th</sup> edition, McGraw-Hill, 2015.

**Table A.2: Properties of water (saturated liquid) at various temperatures**

$^{\circ}\text{C}$	$c_p$ kJ/kg. $^{\circ}\text{C}$	$\rho$ kg/m <sup>3</sup>	$\mu \times 10^4$ kg/m.s	$k$ W/m. $^{\circ}\text{C}$	Pr
0	4.225	999.8	17.90	0.566	13.25
5	4.207	999.7	15.26	0.576	11.15
10	4.195	999.2	13.10	0.585	9.40
15	4.187	998.7	11.39	0.594	8.03
20	4.180	997.6	10.08	0.602	7.00
25	4.179	996.3	8.96	0.611	6.13
30	4.176	995.3	8.03	0.619	5.41
35	4.174	994.0	7.24	0.627	4.83
40	4.174	992.0	6.56	0.633	4.33
45	4.174	990.1	6.00	0.639	3.92
50	4.175	988.2	5.52	0.645	3.57
55	4.179	985.5	5.09	0.650	3.27
60	4.179	983.3	4.71	0.654	3.01
65	4.183	980.6	4.34	0.659	2.76
70	4.185	977.9	4.07	0.664	2.57
75	4.189	974.8	3.81	0.667	2.39
80	4.193	971.6	3.57	0.671	2.23
90	4.201	965.3	3.19	0.676	1.98
100	4.211	958.3	2.83	0.682	1.76
110	4.223	950.9	2.56	0.685	1.59
120	4.237	942.9	2.34	0.685	1.45
140	4.276	926.1	1.96	0.685	1.23
160	4.326	907.0	1.74	0.681	1.11
180	4.382	886.7	1.54	0.676	1.02
200	4.452	864.3	1.39	0.667	1.00
230	4.576	828.4	1.21	0.648	0.86
260	4.731	785.2	1.07	0.616	0.83

## Appendix B: The numerical tools provided by Thermax

The Thermax add-in provides, in addition to its functions for fluid properties, a Newton-Raphson solver for non-linear equations and two interpolation functions for tabulated data. This appendix shows why these numerical tools are needed in thermofluid analyses and how they are used with the help of relevant examples.

### B.1. The Newton-Raphson solver “NRM”

Excel’s cell formulae become too restrictive and inconvenient to use when dealing with iterative solutions and optimisation analyses that involve implicit equations. This occurs, for example, when dealing with type-2 or type-3 pipe-flow problems, which themselves require iterative solutions, by using the following Colebrook-White (C-W) equation that determines the Darcy friction factor ( $f$ ) in a turbulent pipe flow:

$$\sqrt{\frac{1}{f}} = -2.0 \log_{10} \left( \frac{\varepsilon/D}{3.7} + \frac{2.51}{\text{Re} \sqrt{f}} \right) \quad (1.25)$$

In this case, Excel has to deal with two nested iterations; an inner iteration to determine  $f$  and an outer iteration to determine the pipe’s diameter or the flow rate.

Another nonlinear equation in thermofluid analyses is the following Benedict-Webb-Rubin (BWR) equation of state [1]:

$$P = \frac{R_u T}{\tilde{v}} + \left( B_0 R_u T - A_0 - \frac{C_0}{T^2} \right) \frac{1}{\tilde{v}^2} + \frac{b R_u T - a}{\tilde{v}^3} + \frac{a \alpha}{\tilde{v}^6} + \frac{c}{\tilde{v}^3 T^2} \left( 1 + \frac{\gamma}{\tilde{v}^2} \right) e^{-\gamma/\tilde{v}^2} \quad (B.1)$$

Where  $R_u$  is the universal gas constant,  $P$  is the absolute pressure,  $T$  is the absolute temperature, and  $\tilde{v}$  is the molar specific volume. The BWR equation is one of the most accurate equations of state, but it is implicit in  $\tilde{v}$  and requires an iterative solution to determine the molar specific volume. Therefore, its use in thermodynamic optimisation analyses faces a similar problem to that of the C-W equation in type-2 or type-3 flow problems.

The Newton-Raphson solver provided by Thermax is a custom function developed with VBA for solving nonlinear equations such as the C-W equation and the BWR equation. To illustrate the use of this “NRM” solver, let us use it to determine the error of the ideal-gas law compared to the BWR equation of state by calculating the specific volume of carbon dioxide (CO<sub>2</sub>) at 0.2 MPa and temperatures in the range 273 – 373K. Figure B.1 shows the Excel sheet developed for this purpose and Table B.1 reveals the formulae used in the sheet.

## Computer-Aided Thermofluid Analyses Using Excel

F3		f <sub>x</sub>		=NRM("BWR",E3,P,D3)				
	A	B	C	D	E	F	G	H
1								
2				<i>T</i>	<i>v<sub>ideal</sub></i>	<i>v<sub>BWR</sub></i>	<i>error_v<sub>ideal</sub></i>	
3	P_	200000	Pa	273	11.34861	11.29804143	0.44759	
4				283	11.76431	11.71375945	0.43155	
5	Ru	8314	J/kmol-K	293	12.18001	12.12947677	0.41662	
6				303	12.59571	12.54519338	0.40268	
7				313	13.01141	12.96090929	0.38964	
8				323	13.42711	13.37662453	0.37742	
9				333	13.84281	13.79233913	0.36593	
10				343	14.25851	14.2080531	0.35513	
11				353	14.67421	14.62376648	0.34494	
12				363	15.08991	15.0394793	0.33532	
13				373	15.50561	15.45519157	0.32622	
14								

Figure B.1. Excel sheet for determining the specific volume by the ideal-gas law compared to the BWR equation of state

Table B.1. The formulae used in the Excel sheet using the NRM solver

<i>T</i>	<i>v<sub>ideal</sub></i>	<i>v<sub>BWR</sub></i>	<i>error_v<sub>ideal</sub></i>
273	=Ru*D3/P	=NRM("BWR",E3,P,D3)	=ABS(F3-E3)/F3*100
283	=Ru*D4/P	=NRM("BWR",E4,P,D4)	=ABS(F4-E4)/F4*100
293	=Ru*D5/P	=NRM("BWR",E5,P,D5)	=ABS(F5-E5)/F5*100
303	=Ru*D6/P	=NRM("BWR",E6,P,D6)	=ABS(F6-E6)/F6*100
313	=Ru*D7/P	=NRM("BWR",E7,P,D7)	=ABS(F7-E7)/F7*100
323	=Ru*D8/P	=NRM("BWR",E8,P,D8)	=ABS(F8-E8)/F8*100
333	=Ru*D9/P	=NRM("BWR",E9,P,D9)	=ABS(F9-E9)/F9*100
343	=Ru*D10/P	=NRM("BWR",E10,P,D10)	=ABS(F10-E10)/F10*100
353	=Ru*D11/P	=NRM("BWR",E11,P,D11)	=ABS(F11-E11)/F11*100
363	=Ru*D12/P	=NRM("BWR",E12,P,D12)	=ABS(F12-E12)/F12*100
373	=Ru*D13/P	=NRM("BWR",E13,P,D13)	=ABS(F13-E13)/F13*100

The formula bar in Figure B.1 reveals the following Excel formula in cell **F3** that uses the NRM solver to calculate  $\tilde{v}$  at 273K:

$$=NRM("BWR",E3,P,D3)$$

Note that the function NRM requires four input arguments: "BWR", E3, P, and D3. The first argument, "BWR", is the name of another user-defined VBA function for the particular nonlinear equation to be solved; which in this case is the BWR equation. The second argument, E3, is an initial guess for the dependent variable in the nonlinear

equation; i.e.,  $\tilde{v}$  in Equation (B.1). The third and fourth arguments,  $P$  and  $D3$ , are values of two independent variables in the nonlinear equation; which are  $P$  and  $T$  in Equation (B.1). For the C-W equation, they are the values of  $\varepsilon/D$  and  $Re$ . The function “BWR” that applies the BWR equation is listed below:

```

Function BWR(x, P, T)
Dim Ru, a, A0, b, B0, c, C0, alfa, gama
'Carbon dioxide, CO2
Ru = 8314
a = 13.86
A0 = 277.3
b = 0.00721
B0 = 0.04991
c = 1511000.0
C0 = 14040000.0
alfa = 0.0000847
gama = 0.00539
BWR = P - Ru * T / x + (B0 * Ru * T - A0 - C0 / T ^ 2) / (x ^ 2) + (b * Ru * T
- a) / x ^ 3 + a * alfa / x ^ 6 + c / (x ^ 3 * T ^ 2) * (1 + gama / x ^ 2) * Exp(-
gama / x ^ 2)
End Function
    
```

The different constants given in the BWR function are those of carbon dioxide ( $\text{CO}_2$ ). Note that the value determined by the ideal-gas law in cell **E3** is used as an initial guess for the BWR equation. Figure B.2 shows the deviation of the ideal-gas law from the BWR equation in estimating the specific volume.

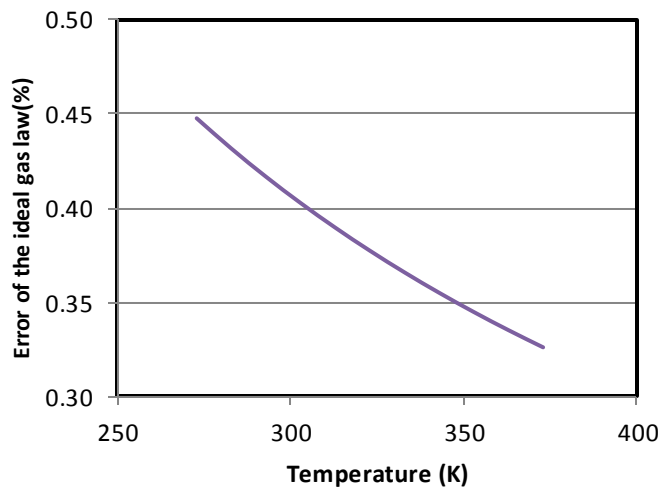


Figure B.2. Errors in the specific volume estimations by the ideal-gas law compared to the BWR equation of state for carbon-dioxide

### B.2. The interpolation functions “Interpol1” and “Interpol2”

The two functions provided by Thermax for the interpolation of tabulated data, called **Interpol1** and **Interpol2**, use linear and quadratic equations, respectively. These functions enable tabulated fluid properties to be used in parametric studies and optimisation analyses. For example, Figure B.3 shows an Excel sheet in which three properties of engine oil are given at various temperatures: the density ( $\rho$ ), specific heat ( $c_p$ ), and kinematic viscosity ( $\nu$ ).

H7											
fx =Interpol1(T_,B5:B13,C5:C13,9)											
	A	B	C	D	E	F	G	H	I	J	
1		Engine oil (unused)		From Holman p 657							
2											
3		ToC	$\rho$ [kg/m <sup>3</sup> ]	$c_p$ [kJ/kg.oC]	$\nu$ [m <sup>2</sup> /s]						
4							T_	90	oC		
5		0	899.12	1.796	0.00428						
6		20	888.23	1.88	0.0009			Interpol1	Interpol2		
7		40	876.05	1.964	0.00024		Density	846.015	846.465		
8		60	864.04	2.047	8.39E-05		Sp. Heat	2.175	2.172		
9		80	852.02	2.131	3.75E-05		Viscosity	2.89E-05	2.92E-05		
10		100	840.01	2.219	2.03E-05						
11		120	828.96	2.307	1.24E-05						
12		140	816.94	2.395	8.00E-06						
13		160	805.89	2.483	5.60E-06						
14											

Figure B.3. Using the interpolation functions for tabulated data

The interpolation functions can be used to calculate the three oil properties at any temperature within the range of tabulated data. Both **Interpol1** and **Interpol2** require four input arguments referred to as: X, XX, YY, and Ndata. Their meanings are as follows:

- X passes the value of the independent property (i.e. temperature) at which the value of the dependent property (i.e. viscosity) is to be determined.
- XX and YY are vectors that store the tabulated data (in this case, the temperature, **B5:B13**, and viscosity values, **E5:E13**).
- Ndata passes the number of entries in the tabulated data. For the oil properties shown in Figure B.3, Ndata = 9.

The formula bar in Figure B.3 reveals the formula in which the linear interpolation function **Interpol1** is used to determine the viscosity at 90°C. The following example shows how the interpolation functions can be used in a typical analysis.



**Example B-1. Effect of oil temperature on the drag force over a flat plate**

Engine oil at 20°C flows over the upper surface of a 5-m-long flat plate as shown in Figure B.4. If the oil velocity is 2 m/s, plot the variation of the total drag force ( $F_D$ ) per unit width of the entire plate  $F_D$  with oil temperatures in the range 40 - 150°C.

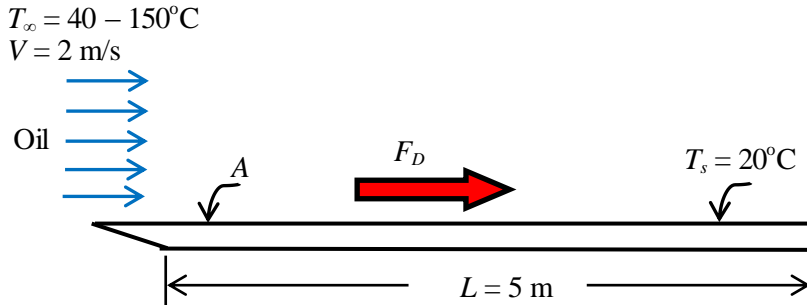


Figure B.4. Flow of oil over a flat plate (adapted from Cengel and Ghajar [2])

**The analytical model**

The drag force ( $F_D$ ) over a flat plate is due to friction, which is given by [2]:

$$F_D = C_f A \rho V^2 / 2 \quad (\text{B.2})$$

Where  $C_f$  is the friction coefficient (not to be confused with the friction factor  $f$ ),  $A$  is the surface area of the plate, and  $\rho$  and  $V$  are the density and velocity of oil, respectively.

The value of the friction coefficient depends on whether the flow is laminar or turbulent as indicated by the Reynolds number ( $Re_L$ ). For the flow over a flat plate, the critical Reynolds number above which the flow becomes turbulent is about  $5 \times 10^5$ . For laminar flows, the friction coefficient is given by:

$$C_f = 1.328 Re_L^{-0.5} \quad Re_L < 5 \times 10^5 \quad (\text{B.3})$$

For turbulent flows, it is given by:

$$C_f = 0.074 Re_L^{-0.2} \quad 5 \times 10^5 \leq Re_L \leq 10^7 \quad (\text{B.4})$$

Note that fluid properties are evaluated at the average temperature  $(T_s + T_\infty)/2$ , e.g., if the oil temperature is 60°C, the oil viscosity and density are evaluated at 40°C.

### Solution with Excel

Figure B.5 shows the Excel sheet developed for this example. The data part shows the given information concerning the oil temperature ( $T_{oil}$ ), plate temperature ( $T_{plate}$ ), oil velocity (Velocity), and plate length (Length). Based on the specified oil temperature, the sheet calculates the average temperature ( $T_{average}$ ) and the corresponding oil density ( $\rho_{oil}$ ) and kinematic viscosity ( $\nu_{oil}$ ). The sheet then calculates the Reynolds number ( $Re$ ) and friction coefficient ( $C_f$ ). The single final result, which is the drag force ( $F_D$ ), is shown on the right-side of the sheet. The figure reveals the formulae entered in each cell in the calculations part and the formula bar reveals that used for determining the drag force in cell **I2**.

F_D		fx		=Cf*(Length*1)*p_oil*(Velocity^2)/2				
	B	C	D	E	F	G	H	I
1								
2	T_oil	40	oC	T_average	30	=(T_oil+T_plate)/2	F_D	88.445 N
3	T_plate	20	oC	p_oil	882.14	=Interpl1(T_average,Data!\$5:\$13,Data!\$5:\$13,9)		
4	Velocity	2	m/s	v_oil	0.00057	=Interpl1(T_average,Data!\$5:\$13,Data!\$5:\$13,9)		
5	Length	5	m					
6				Re	17543.86	=Velocity*Length/v_oil		
7				Cf	0.010026	=IF(Re<500000,1.328*Re^-0.5,0.074*Re^-0.2)		
8								

Figure B.5. The Excel sheet developed for Example B-1

The friction coefficient is calculated depending on the value of the Reynolds number by using the following nested-If formula in cell **F7**:

$$C_f = \text{IF}(Re < 500000, 1.328 * Re^{-0.5}, 0.074 * Re^{-0.2})$$

The above formula determines whether to use Equation (B.3) or Equation (B.4) to calculate the friction coefficient depending on the value of the Reynolds number.

Figure B.5 shows the calculations at an oil temperature of 40°C, which is the initial oil temperature in the required range. At the average temperature, which is 30°C, the sheet uses the linear interpolation function **Interpl1** to determine the values of the oil density and viscosity. At this temperature the calculated drag force,  $F_D$ , is 88.445 N. By inserting a different value for the oil temperature, say 50°C, the sheet automatically updates its calculations. Figure B.6 shows a plot of the drag force determined at different oil temperatures in the range 40°C to 150°C.

The linear and quadratic interpolation functions are useful in thermofluid analyses not only for determining fluid properties, but also for the interpolation of other types of tabulated data that is required by such analyses. Table B.2 shows the cost per metre of galvanised-steel air-conditioning ducts for different diameters of the duct. By permitting automatic determination of the duct diameter from the tabulated data, the

interpolation functions are useful for optimisation analyses that aim to determine the optimum duct diameter.

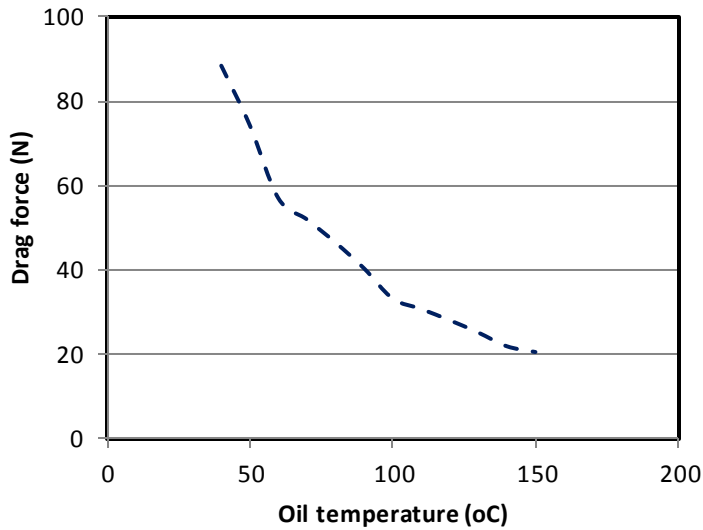


Figure B.6. Variation of the drag force with oil temperature

Table B.2. Cost of galvanised-steel air-conditioning ducts

Duct diameter (m)	Cost per linear metre (\$)
0.10	9.0
0.15	11.5
0.20	14.5
0.25	17.0
0.30	22.5
0.35	29.0
0.40	34.0
0.45	40.0
0.50	50.0

### References

- [1] Y.A. Cengel, and M.A. Boles, *Thermodynamics an Engineering Approach*, McGraw-Hill, 7<sup>th</sup> Edition, 2007
- [2] Y.A. Cengel and A.J. Ghajar. *Heat and Mass Transfer: Fundamentals and Applications*. McGraw Hill, 2011

**Exercises**

10. Using the data for properties of air at atmospheric pressure given in Appendix A, develop an Excel sheet that can be used to determine the kinematic viscosity of air at any given temperature in the range 200 – 1000K by using:
  - a. The trendline feature of Excel
  - b. The linear-interpolation function (**Interpl**) provided by Thermax.
  
11. Develop a VBA function to determine the friction factor from the Colebrook-White equation and use it with the NRM solver to determine the frictional losses ( $h_f$ ) in a circular pipe that carries air at 20°C with the following data:

$$D = 25 \text{ cm}, L = 150 \text{ m}, V = 7 \text{ m/s}, k_s = 0.045 \text{ mm}.$$

### Appendix C: Application of the Hardy-Cross method with Excel

This appendix supplements Chapter 6 by presenting the Hardy Cross (H-C) method for the analyses of looped pipe-networks. The appendix shows how the method can be applied by using Excel. To illustrate the method, consider the single-loop network shown in Figure C.1. There is one source at node *A* and three discharge points at the other three nodes *B*, *C*, and *D*. It is required to determine the magnitudes and directions of the four pipe flows that satisfy both the conservation of mass and the conservation of energy.

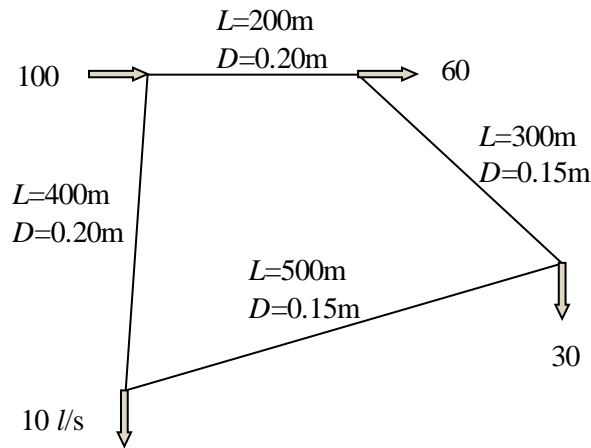


Figure C.1. A pipe network with a single-loop

#### The Hardy-Cross method

For steady, incompressible flow in a looped pipe-network, the two principles can be expressed by the following equations:

$$\sum_1^{NPipes} Q_i = 0 \tag{C.1}$$

$$\sum_1^{MPipes} h_{f,j} = 0 \tag{C.2}$$

Where *NPipes* is the number of pipes connected to the particular node (2 in the present case) and *MPipes* is the number of pipes in each loop (4 in the present case).

The solution procedure starts by assuming the flow rates and directions in the pipes such that they satisfy the continuity equation, Equation (C.1), at all the pipe-junctions. Suppose that we assume the flow directions to be as shown in Figure C.2 and we assume that the flow rate in pipe AB to be 50 litre/s. Then the flow rates in the other pipes can be determined by the continuity equation as shown in the figure.

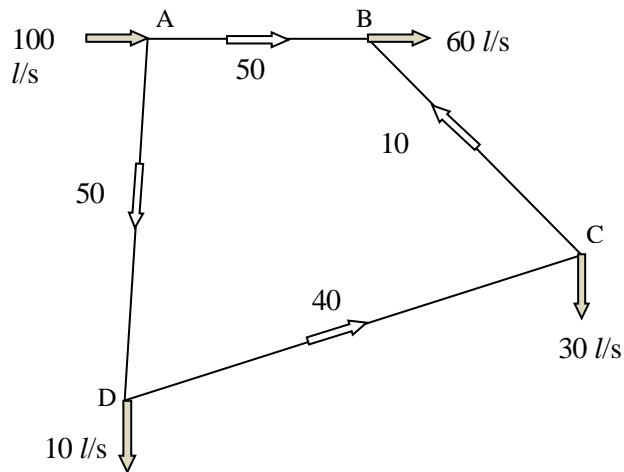


Figure C.2. Assumed flow rates in the network

The assumed pipe flows are unlikely to satisfy the energy equation. Therefore, they are corrected in steps until they practically satisfy the energy equation as follows:

$$Q_{new} = Q_{old} + \Delta Q \quad (C.3)$$

Where  $Q_{new}$  and  $Q_{old}$ , refer to the initial and the adjusted flow rates, respectively, and  $\Delta Q$  is a correction term that depends on the energy equation. The correction procedure has to be repeated a number of times until the energy equation is satisfied. It remains to show how the correction term  $\Delta Q$  is determined.

The Darcy-Weisbach equation for the friction head, Equation (1.21), can be written as:

$$h_f = KQ^2 \quad (C.4)$$

Where  $K$  is given by:

$$K = \frac{Lf}{2gDA^2} = \frac{2Lf}{g\pi^2 D^3} \quad (C.5)$$

Applying Equation (C.4) to the corrected flow rate given by Equation (C.3), we get:

$$h_f = K(Q + \Delta Q)^2 \quad (C.6)$$

Expanding the right-hand side of Equation (C.6):

$$h_f = K(Q^2 + 2Q.\Delta Q + \Delta Q^2) \quad (C.7)$$

Neglecting the term ( $\Delta Q^2$ ), the equation becomes:

$$h_f = K(Q^2 + 2Q.\Delta Q) \quad (C.8)$$

Applied to all four pipes in the loop, Equation (C.2) leads to:

$$\sum K(Q^2 + 2Q.\Delta Q) = 0 \quad (C.9)$$

Rearranging the equation, it becomes:

$$\sum KQ^2 + \Delta Q \sum 2KQ = 0 \quad (C.10)$$

Or,

$$\Delta Q = -\frac{\sum KQ^2}{\sum 2KQ} = -\sum h_f / \left( 2\sum \frac{h_f}{Q} \right) \quad (C.11)$$

When applying Equation (C.11), a sign convention must be adopted to take into consideration the flow direction in the particular pipe. In the following discussion, the friction losses in the clockwise direction are taken as positive while those in the counter-clockwise direction are taken as negative. In general, this sign convention means that the friction loss in a pipe that is common to two loops (or more) will be given a negative sign with one loop but a positive sign with the other loop(s).

The steps of applying the H-C method are as follows:

1. Make a guess for the flow rate (magnitude and direction) in one pipe of each loop and calculate the flow rates in the other pipes in the network by applying the continuity equation at the respective nodes.
2. Calculate the friction loss  $h_f$  in each pipe of the network and determine the net friction loss in each loop according to the flow direction in the relevant pipes (clockwise positive and counter-clockwise negative). Most likely, these will not be zeros at the initially guessed pipe flows.
3. Calculate a correction increment  $\Delta Q_i$  for the flows in loop  $i$  from Equation (C.11). The summations in Equation (C.11) are performed over the number of pipes in each loop.
4. Obtain new pipe flows in each loop by modifying the old ones according to Equation (C.3).

- Repeat steps 2, 3, and 4 until the correction increments become small and the variations in the flow rates become negligible.

A number of articles and videos in the internet explain how the H-C method can be implemented in Excel [1,2]. The following example demonstrates its application to analyse the single-loop pipe-network shown in Figure C.1.

**Example C-1. Analysis of a simple pipe-network by the H-C method**

Figure C.1 shows a pipe network that distributes water to three consumption points as shown in the figure. Determine the flow rates in the four pipes if a friction factor for all pipes can be taken as 0.025.

**Solution**

**Step 1:** The first step is to assume flow rates in the four pipes that satisfy continuity. It is enough to assume the value of the flow rate in one pipe since the other flow rates must follow the continuity equation. Let us assume that the flow in pipe AB is 50 l/s in the direction shown in Figure C.2. The magnitudes and directions of other flow rates are automatically determined by applying the continuity equation at the four nodes. Figure C.2 shows the magnitudes and directions of the flow rates in the network that satisfy the continuity equation at all the nodes based on the assumed flow in pipe AB.

**Step 2:** The second step is to determine the resulting velocities and friction head losses in the different pipes. Figure C.3 shows the sheet developed for these calculations. The given information about the network pipes, i.e., their lengths and diameters, are entered on the left side of the sheet. Values of the gravity acceleration (gc) and friction factor (f) are entered at the top left-side of the sheet. These two parameters are labelled.

	A	B	C	D	E	F	G	H	I	J	K
1	gc	9.81									
2	f	0.025									
3											
4	Pipe	L(m)	d(m)	A	Q	V	hf	hf/Q	ΔQ	Qnew	
5	AB	200	0.2	0.031416	0.050	1.591549	3.2276116	64.55223	0.015748	0.066	
6	BC	300	0.15	0.017671	-0.010	-0.56588	-0.816068	81.60677		0.006	
7	CD	500	0.15	0.017671	-0.040	-2.26354	-21.76181	544.0452		-0.024	
8	AD	400	0.2	0.031416	-0.050	-1.59155	-6.455223	129.1045		-0.034	
9											

Figure C.3. Excel sheet developed for Example C-1

The cross-sectional areas of the different pipes are calculated in column E so as to determine the fluid velocities in column G. Based on these velocities the friction losses are determined in column G. Table C.1 shows the formulae in columns G and H that calculate the pipe velocities and friction head losses. Note that in the formula for the friction head loss (hf), the head loss is multiplied by SIGN(Q) so as to account for the direction of the flow in the pipe – which can change during the iteration process.



Table C.1. Formulae in columns G to K

V	Hf	hf/Q	$\Delta Q$	Q <sub>new</sub>
=F5/E5	=f*(B5/C5)*G5^2/(2*gc)*SIGN(F5)	=H5/F5	=-SUM(H5:H8)/SUM(I5:I8)/2	=F5+\$J\$5
=F6/E6	=f*(B6/C6)*G6^2/(2*gc)*SIGN(F6)	=H6/F6		=F6+\$J\$5
=F7/E7	=f*(B7/C7)*G7^2/(2*gc)*SIGN(F7)	=H7/F7		=F7+\$J\$5
=F8/E8	=f*(B8/C8)*G8^2/(2*gc)*SIGN(F8)	=H8/F8		=F8+\$J\$5

**Step 3:** The third step is to determine  $\Delta Q$  according to Equation (C.11) which requires the determination of hf/Q. Table C.1 also reveals the formulae that calculate hf/Q in column I and  $\Delta Q$  in column J. Since  $\Delta Q$  is the same for all pipes, it is calculated for pipe AB only but used for the other pipes as well as shown in the last column of Table C.1. As shown in Figure C.3, the value obtained for this first iteration is  $\Delta Q = 0.0157$ .

**Step 4:** New values for the flow rates in the four pipes according to Equation (C.3). Column K in the sheet shown in Figure C.3 shows the new values of the flow rates.

**Step 5:** The adjusted flow rates obtained in step 4 can now be used as initial values for the second iteration. Table C.2 shows the calculations in the second iteration which are based on the new values of the flow rates following the same steps described for the first iteration. Note that the  $\Delta Q$  has dropped to 0.0047. Table C.2 also shows the new values of the flow rates after the second iteration. These new values of the flow rates can now be used as initial values for the third iteration. As shown in Table C.3, calculations of the third iteration yield a very small value for  $\Delta Q$  of 0.0001.

Table C.2. Results of the second iteration

Pipe	Q	V	hf	hf/Q	$\Delta Q$	Q <sub>new</sub>
AB	0.066	2.092834	5.5809832	84.88403	0.004707	0.070
BC	0.006	0.325289	0.2696557	46.91027		0.010
CD	-0.024	-1.37236	-7.999415	329.8501		-0.020
AD	-0.034	-1.09026	-3.029247	88.44087		-0.030

Table C.3. Results of the third iteration

Pipe	Q	V	hf	hf/Q	$\Delta Q$	Q <sub>new</sub>
AB	0.070	2.242649	6.4086065	90.96041	0.000144	0.071
BC	0.010	0.591626	0.8920015	85.31902		0.011
CD	-0.020	-1.10603	-5.195783	265.8355		-0.019
AD	-0.030	-0.94045	-2.25394	76.2881		-0.029

Figure C.4 shows the variation of  $\Delta Q$  with the iteration number. The figure indicates that the change in the flow rates after the third iteration is small and, therefore, the flow rates obtained after the third iteration can be taken as the final solution. The plus sign

with the flows in AB and BC means that their direction is clockwise, while the minus sign with the flows in CD and AD means that their direction is counter-clockwise. Note that the flow in pipe BC was initially assumed to be in the counter-clockwise direction, but the final solution showed that it is clockwise.

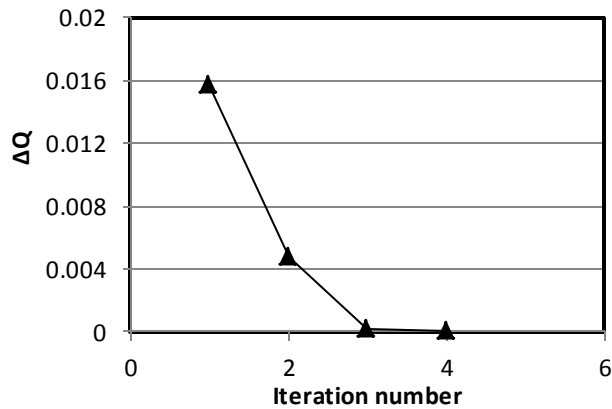


Figure C.4. Variation of  $\Delta Q$  with iteration number

**Example C-2. Application of the H-C method to pipe-networks with multiple loops**

Determine the flow rates in the pipe-network shown in Figure C.5. The valve in pipe BC is partially closed, which produces a local head loss of  $10.0 V^2/2g$ . The roughness of all pipes is 0.06 mm.

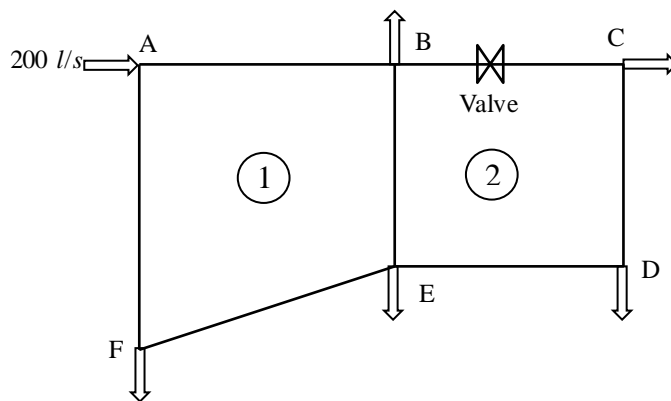


Figure C.5. The two-loop pipe network of Example C-2

This case is based on Example 5-2 in Nalluri and Feather [3].

**Solution**

Pipe networks with multiple loops will have pipes that are common to two or more loops such as Pipe BE in Figure C.5. In this case, the pipe will have a different  $\Delta Q$  in each loop. Suppose that the two values of  $\Delta Q$  are  $\Delta Q_1$  for loop 1 and  $\Delta Q_2$  for loop 2. The effective  $\Delta Q$  for pipe BE is calculated from [1]:

$$\Delta Q_{BE,1} = \Delta Q_1 - \Delta Q_2 \quad \text{Loop 1} \quad (C.12.a)$$

$$\Delta Q_{BE,2} = \Delta Q_2 - \Delta Q_1 \quad \text{Loop 2} \quad (C.12.b)$$

Note that the two values of  $\Delta Q$  have the same magnitude but opposite signs.

Figure C.6 shows the Excel sheet developed for this example. As usual, the left side of the sheet shows the problem data that consist of the pipes lengths (L) and diameters (D), the roughness factor of the pipe material ( $\epsilon$ ), and the viscosity of the fluid (visc). Column E shows the flow rates in the pipes; two of which are guessed ( $Q_{AB}$  and  $Q_{BC}$ ) and the rest are calculated by applying the continuity equation at the different nodes.

I7		fx =SIGN(E7)*(H7*(B7/C7)*F7^2/(2*gc)+10*F7^2/2/gc)												
A	B	C	D	E	F	G	H	I	J	K	L	M	N	
Loop 1	L	D		Q	Q/A	Re	f	hf	$\Sigma(hf/Q)$	$\Delta Q$	$\Delta Q$ other	$\Delta Q$ effective	New Q	
2	AB	500	0.25	0.12	2.4446	540845.1	0.015779	9.612204	80.101703	-0.005725		-0.0057251	0.114275	
3	BE	200	0.15	0.01	0.5659	75117.38	0.020825	0.453191	45.319088	-0.005725	-0.011222	0.0054965	0.015497	
4	EF	600	0.2	-0.04	-1.2732	225352.1	0.017557	-4.35196	108.79894	-0.005725		-0.0057251	-0.045725	
5	AF	300	0.25	-0.08	-1.6297	360563.4	0.016325	-2.65202	33.150193	-0.005725		-0.0057251	-0.085725	
6	Loop 2							3.061422	267.36993	-0.005725				
7	BC	400	0.15	0.05	2.8294	375586.9	0.017431	23.0472	460.94399	-0.011222		-0.0112216	0.038778	
8	CD	200	0.1	0.01	1.2732	112676.1	0.02055	3.396039	339.60388	-0.011222		-0.0112216	-0.001222	
9	DE	400	0.15	-0.02	-1.1318	150234.8	0.018963	-3.30142	165.07109	-0.011222		-0.0112216	-0.031222	
10	BE	200	0.15	-0.01	-0.5659	75117.38	0.020825	-0.45319	45.319088	-0.011222	-0.005725	-0.0054965	-0.015497	
11								22.68863	1010.938	-0.011222				
12	$\epsilon$	0.00006												
13	visc	1.13E-06												
14	gc	9.81												
15														

Figure C.6. Excel sheet developed for solving Example C-2 by the Hardy Cross method

Based on these initial flow rates, the sheet determines the Reynolds numbers, friction factors, and friction losses. The friction factors are determined by using the Swamee-Jain formula (Equation (1.25)). The formula bar reveals the formula that applies Equation (1.25). The flow rate adjustment ( $\Delta Q$ ) in each loop is determined according to Equation (C.11). For loop 1,  $\Delta Q = -0.0057251$  and for loop 2,  $\Delta Q = -0.011222$ . For pipe BE, which is common to both loops, the effective values of  $\Delta Q$  have the same magnitude for both loops, which is 0.0054965. The new flow rates in the different pipes are obtained according to Equation (C.3).

To avoid repetition of the whole procedure for the following iterations, the new  $Q$  values in column (N) can be copied and pasted (using the "Paste Values" option) in column (E) that stores the old values. This is to be repeated until  $\Delta Q$  became reasonably small so that there was no significant change in  $Q$  in all the network pipes. Figure C.7 shows the result after 5 iterations when  $\Delta Q$  dropped to small values in both loops. The minus sign before the flow rates in pipes EF, AF, CD, DE, and BE means that their directions are counter-clockwise relative to the respective loop. Note that, the flow in pipe BE, which is common to the two loops, has the same magnitude ( $0.01645 \text{ m}^3/\text{s}$ )

## Computer-Aided Thermofluid Analyses Using Excel

but opposite directions. While its direction is clockwise (+) in loop 1, it becomes counter-clockwise (-) in loop 2.

	A	B	C	D	E	F	G	H	I	J	K	L	M	N
1	Loop 1	L	D		Q	Q/A	Re	f	hf	$z(hf/Q)$	$\Delta Q$	$\Delta Q$ other	$\Delta Q$ effective	New Q
2	AB	500	0.25		0.111503	2.2715	502547.4	0.015867	8.345708	74.847586	-2.27E-06		-0.0000023	0.111500
3	BE	200	0.15		0.016451	0.9309	123575.5	0.019418	1.143608	69.516101	-2.27E-06	-1.58E-06	-0.0000007	0.016450
4	EF	600	0.2		-0.0485	-1.5437	273224.2	0.017214	-6.27233	129.33363	-2.27E-06		-0.0000023	-0.048500
5	AF	300	0.25		-0.0885	-1.8029	398861.1	0.016175	-3.21558	36.335332	-2.27E-06		-0.0000023	-0.088500
6	Loop 2								0.001407	310.03265	-2.27E-06			
7	BC	400	0.15		0.035052	1.9835	263299.3	0.01792	11.58803	330.59789	-1.58E-06		-0.0000016	0.035050
8	CD	200	0.1		-0.00495	-0.63	55755.26	0.022564	-0.91301	184.51087	-1.58E-06		-0.0000016	-0.004950
9	DE	400	0.15		-0.03495	-1.9777	262522.3	0.017925	-9.5287	272.65157	-1.58E-06		-0.0000016	-0.034950
10	BE	200	0.15		-0.01645	-0.9309	123575.5	0.019418	-1.14361	69.516101	-1.58E-06	-2.27E-06	0.0000007	-0.016450
11									0.002702	857.27643	-1.58E-06			
12	$\epsilon$	0.00006												
13	visc	1.13E-06												
14	gc	9.81												
15														

Figure C.7. The Excel sheet for Example C-2 with the adjusted flows after five iterations

Table C.4 compares the present pipe flows, in  $\text{m}^3/\text{s}$ , with those given by Nalluri and Feather [3]. The table shows a good agreement between the two solutions. The same problem was solved in Example 6.2 by using the Excel-Solver method and the solution obtained is also shown in the table.

Table C.4. Comparison of the pipe flow rates obtained by the H-C method with those obtained by Nalluri and Feather [3]

Pipe	Nalluri and Feather [3]	H-C solution	Excel-Solver
AB	0.11152	0.11150	0.1115
BC	0.03505	0.03505	0.0350
CD	0.00495	0.00495	0.0050
DE	0.03495	0.03495	0.0350
EF	0.04848	0.04850	0.0485
AF	0.08848	0.08850	0.0885
BE	0.01648	0.01645	0.0165

## References

- [1] TM's Channel, Pipe network analysis in Excel using Hardy Cross method, Video, available at: <https://www.youtube.com/watch?v=M8f1FNgeq7o>, last accessed 20/6/2017.
- [2] A. M. Elfeki, Pipe network analysis example with Excel Solver, Researchgate, available at: [https://www.researchgate.net/publication/258051650\\_Pipe\\_Network\\_Analysis\\_Example\\_with\\_Excel\\_Solver](https://www.researchgate.net/publication/258051650_Pipe_Network_Analysis_Example_with_Excel_Solver), last accessed 20/6/2017.
- [3] C. Nalluri and R.E. Feather, *Civil Engineering Hydraulics*, Fourth Edition.

### Appendix D: Analyses of a gravity-driven network with eight loops

This appendix applies the Excel-Solver method presented in Chapter 6 for hydraulic analyses of pipe-networks to a network of practical complexity. The case considered is the gravity-driven network presented by Brkic [1] shown in Figure D.1. The network distributes water from two reservoirs to four demand points via 19 cast iron pipes ( $\varepsilon = 0.00026$  m) that are laid on a flat area with no variation in elevation. Table D.1 shows the lengths of the 19 network pipes.

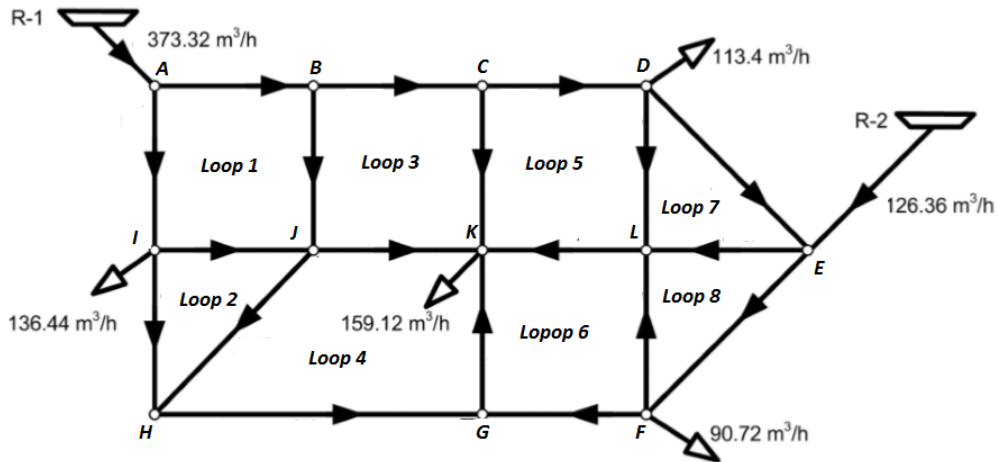


Figure D.1. A pipe-network with eight loops (adopted from Brkic [1])

This network will be analysed by using the same initial pipe diameters used by Brkic [1] so that comparison can be made with his solution for the pipe flow rates shown in Table D.1. In the present analysis the effect of the method used to evaluate friction factor on the results obtained by Solver is assessed by using both the Swamee-Jain formula and the Colebrook-White formula.

#### D.1. The analytical model

Following the procedure described in Chapter 6 for the analysis of pipe networks using Excel and Solver, the flow rates in 8 selected pipes were specified and those in the remaining 11 pipes were determined by applying the continuity equation at each junction. Solver is then used to adjust the initial flow rates in order to satisfy the energy equation. The assumed flow-directions for all the pipes are shown in Figure D.1. The initially assumed flow rates are those for pipes AB, BC, CD, DE, EF, HI, JK, and KL. The flow rates in the remaining 11 pipes are calculated from continuity as follows:

$$Q_{FG} = Q_{GK} - Q_{GH} \quad (D.1)$$

$$Q_{GH} = Q_{HI} + Q_{HJ} \quad (D.2)$$

Table D.1. Pipe data and initial flow rates in the 8-loop network [1]

Brkic [1] notation	Pipe	Length (m)	Initial diameter (m)	Initial flow rate (m <sup>3</sup> /h)
/1/	AB	457.2	0.305	173.32
/2/	BC	304.8	0.203	150
/3/	CD	365.8	0.203	130
/4/	DE	609.6	0.203	6.6
/5/	EF	853.4	0.203	100
/6/	FG	335.3	0.203	0.28
/7/	GH	304.8	0.203	16.88
/8/	HI	762.0	0.203	13.56
/9/	AI	243.8	0.203	200
/10/	IJ	396.2	0.152	50
/11/	JK	304.8	0.152	70
/12/	KL	335.3	0.254	51.96
/13/	EL	304.8	0.254	32.96
/14/	HJ	548.6	0.152	3.32
/15/	BJ	335.3	0.152	23.32
/16/	GK	548.6	0.152	17.16
/17/	CK	365.9	0.254	20
/18/	FL	548.6	0.152	9
/19/	DL	396.2	0.152	10

$$Q_{IA} = 373.32 - Q_{AB} \quad (D.3)$$

$$Q_{IJ} = Q_{AI} - 136.44 - Q_{HI} \quad (D.4)$$

$$Q_{LE} = 126.36 + Q_{DE} - Q_{EF} \quad (D.5)$$

$$Q_{JH} = Q_{IJ} + Q_{BJ} - Q_{JK} \quad (D.6)$$

$$Q_{BJ} = Q_{AB} - Q_{BC} \quad (D.7)$$

$$Q_{GK} = 159.12 - Q_{JK} - Q_{KL} - Q_{CK} \quad (D.8)$$

$$Q_{CK} = Q_{BC} - Q_{CD} \quad (D.9)$$

$$Q_{FL} = Q_{EF} - 90.72 - Q_{FG} \quad (D.10)$$

$$Q_{DL} = Q_{CD} - 113.4 - Q_{DE} \quad (D.11)$$

The energy equation imposes 8 constraints on the iterative solution, one for each loop. Taking the clockwise flow direction as positive, the constraints are:

$$h_{f,AB} + h_{f,BJ} - h_{f,AI} - h_{f,IJ} = 0 \quad \text{Loop 1} \quad (D.12)$$

$$h_{f,II} + h_{f,HJ} - h_{f,HI} = 0 \quad \text{Loop 2} \quad (D.13)$$

$$h_{f,BC} + h_{f,CK} - h_{f,BJ} - h_{f,JK} = 0 \quad \text{Loop 3} \quad (D.14)$$

$$h_{f,JK} - h_{f,GK} - h_{f,GH} - h_{f,HJ} = 0 \quad \text{Loop 4} \quad (D.15)$$

$$h_{f,CD} + h_{f,DL} + h_{f,KL} - h_{f,CK} = 0 \quad \text{Loop 5} \quad (D.16)$$

$$h_{f,FG} + h_{f,GK} - h_{f,KL} - h_{f,FL} = 0 \quad \text{Loop 6} \quad (D.17)$$

$$h_{f,DE} + h_{f,EL} - h_{f,DL} = 0 \quad \text{Loop 7} \quad (D.18)$$

$$h_{f,EF} + h_{f,FL} - h_{f,EL} = 0 \quad \text{Loop 8} \quad (D.19)$$

### D.2. The hydraulic analysis

To investigate the effect of the formula for the friction-factor on the analysis results, two Excel sheets were developed for the hydraulic analyses of this network one of which applies Darcy-Weisbach equation with the Swamee-Jain (S-J) formula, while the other applies the Colebrook-White (C-W) formulae. Figure D.2 shows the sheet that uses the S-J formula.

O2															
=ABS(SIGN(H2)*L2+SIGN(H16)*L16-SIGN(H10)*L10-SIGN(H11)*L11)															
A	B	C	D	E	F	G	H	I	J	K	L	M	N	O	P
			pipe	L (m)	D (m)	A	Q (m3/h)	V (m/s)	Re	f	hf		Errors		
2	ρ	1000	pipe1	457.2	0.305	0.073062	173.32	0.658956	1.78E+05	2.08E-02	0.6886		Loop 1	4.777856	
3	visc	1.13E-06	pipe2	304.8	0.203	0.032365	150	1.28738	2.31E+05	2.21E-02	2.8003		Loop 2	1.850565	
4	g	9.81	pipe3	365.8	0.203	0.032365	130	1.115729	2.00E+05	2.22E-02	2.5418		Loop 3	0.368482	
5	ε	0.00026	pipe4	609.6	0.203	0.032365	6.6	0.056645	1.02E+04	3.30E-02	0.0162		Loop 4	2.411048	
6			pipe5	853.4	0.203	0.032365	100	0.858253	1.54E+05	2.26E-02	3.5610		Loop 5	2.737789	
7			pipe6	335.3	0.203	0.032365	0.28	0.002403	4.32E+02	9.69E-02	0.0000		Loop 6	0.111988	
8			pipe7	304.8	0.203	0.032365	16.88	0.144873	2.60E+04	2.74E-02	0.0440		Loop 7	0.025513	
9			pipe8	762	0.203	0.032365	13.56	0.116379	2.09E+04	2.85E-02	0.0738		Loop 8	3.615675	
10			pipe9	243.8	0.203	0.032365	200	1.716507	3.08E+05	2.18E-02	3.9349				
11			pipe10	396.2	0.152	0.018146	50	0.765404	1.03E+05	2.45E-02	1.9068		Maxerror	0.001	
12			pipe11	304.8	0.152	0.018146	70	1.071565	1.44E+05	2.40E-02	2.8174				
13			pipe12	335.3	0.254	0.050671	51.96	0.284845	6.40E+04	2.35E-02	0.1283				
14			pipe13	304.8	0.254	0.050671	32.96	0.180687	4.06E+04	2.50E-02	0.0499				
15			pipe14	548.6	0.152	0.018146	3.32	0.050823	6.84E+03	3.69E-02	0.0175				
16			pipe15	335.3	0.152	0.018146	23.32	0.356984	4.80E+04	2.62E-02	0.3753				
17			pipe16	548.6	0.152	0.018146	17.16	0.262686	3.53E+04	2.72E-02	0.3448				
18			pipe17	365.9	0.254	0.050671	20	0.10964	2.46E+04	2.71E-02	0.0239				
19			pipe18	548.6	0.152	0.018146	9.00	0.137773	1.85E+04	2.99E-02	0.1046				
20			pipe19	396.2	0.152	0.018146	10	0.153081	2.06E+04	2.94E-02	0.0916				
21															

Figure D.2. The Excel sheet developed for analysing the pipe-network with eight loops by using the Swamee-Jain formula

The data part stores the water density (ρ) and viscosity (visc), the gravity constant (g), and the pipe roughness (ε). The length and diameter for the 19 pipes are stored in columns E and F, respectively. The sheet calculates the cross-sectional area for each pipe in column G. Column H stores the initial flow rates in the pipes. The 8 coloured (shaded) cells in this column store the assumed flow rates while those determined according to Equation (D.1) – (D.11) are not coloured. Note that the calculated pipe

flow rates are the same as those given by Brkic [1] and Table D.1. The calculated pipe friction losses are stored in column L. The formula bar in Figure D.2 reveals the formula for determining the error in satisfying the energy equation in loop 1 according to Equation (D.12).

Since the initially assumed flow rates in the pipes satisfy only the continuity equation but not the energy equation, most of the errors calculated by Equations (D.12) – (D.19) in column O are not close to zero. The flow rates that minimise the errors in the energy equations to sufficiently small values can be found by Solver and the set-up for the task is shown in Figure D.3.

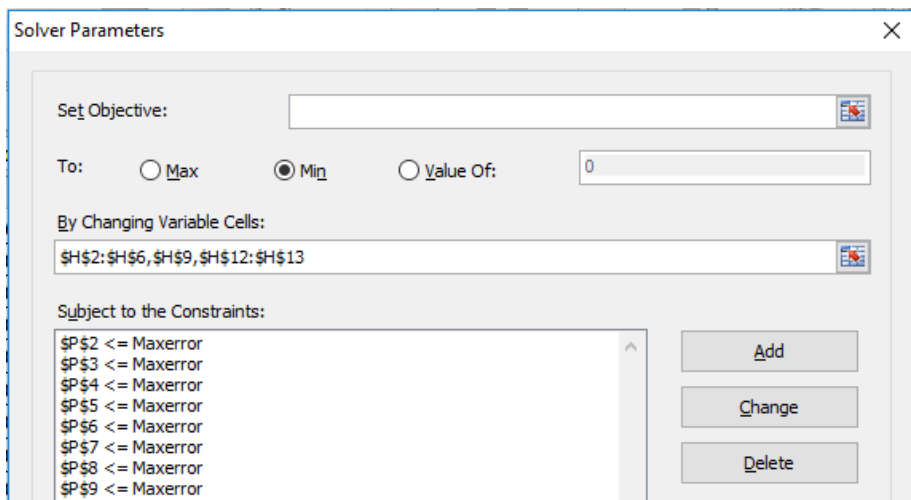


Figure D.3. Solver set-up for the analysis of the pipe-network with eight loops

Note that the “**Set Objective**” slot is left blank and the variables to be changed are the flow rates in the 8 selected pipes. There are 8 constraints which require the absolute values of the errors in satisfying Equations (D.12) – (D.19) to be reduced to a maximum tolerance (Maxerror) of 0.001. Attempts were made to use the **Evolutionary** method of Solver for the present analyses, but the method failed to converge to a solution even with the different numerical options offered by Solver. The **GRG Nonlinear** method also failed to converge to a solution with automatic-scaling. Figure D.4 shows the solution found with **GRG Nonlinear** method but without automatic-scaling. Note that all the 8 constraints are now satisfied. Figure D.5 compares the flow rates with Solver with those obtained by Brkic [1]. The figure shows that the values calculated by the S-J formula agree well with those obtained by Brkic [1] who used the node-loop method and solved the resulting linear system with Excel matrix functions.



=ABS(SIGN(H2)*L2+SIGN(H16)*L16-SIGN(H10)*L10-SIGN(H11)*L11																		
	A	B	C	D	E	F	G	H	I	J	K	L	M	N	O	P		
1				pipe	L (m)	D (m)	A	Q (m <sup>3</sup> /h)	V (m/s)	Re	f	hf				Errors		
2	p	1000		pipe1	457.2	0.305	0.073062	200.62176	0.762757	2.06E+05	2.06E-02	0.9135				Loop 1	0.001	
3	visc	1.13E-06		pipe2	304.8	0.203	0.032365	144.16286	1.237283	2.22E+05	2.21E-02	2.5914				Loop 2	0.001	
4	g	9.81		pipe3	365.8	0.203	0.032365	59.347935	0.509356	9.15E+04	2.34E-02	0.5587				Loop 3	0.001	
5	ε	0.00026		pipe4	609.6	0.203	0.032365	-37.20648	-0.31933	5.74E+04	2.46E-02	0.3834				Loop 4	0.001	
6				pipe5	853.4	0.203	0.032365	31.289558	0.268544	4.82E+04	2.51E-02	0.3875				Loop 5	0.001	
7				pipe6	335.3	0.203	0.032365	-45.19	-0.38781	6.97E+04	2.41E-02	0.3046				Loop 6	0.001	
8				pipe7	304.8	0.203	0.032365	53.84	0.462086	8.30E+04	2.37E-02	0.3865				Loop 7	2.3E-05	
9				pipe8	762	0.203	0.032365	34.808201	0.298743	5.37E+04	2.48E-02	0.4227				Loop 8	0.001	
10				pipe9	243.8	0.203	0.032365	172.69824	1.482189	2.66E+05	2.19E-02	2.9508						
11				pipe10	396.2	0.152	0.018146	1.4500347	0.022197	2.99E+03	4.63E-02	0.0030				Maxerror	0.001	
12				pipe11	304.8	0.152	0.018146	38.876822	0.595129	8.01E+04	2.50E-02	0.9035						
13				pipe12	335.3	0.254	0.050671	26.774444	0.146778	3.30E+04	2.58E-02	0.0374						
14				pipe13	304.8	0.254	0.050671	57.86	0.317211	7.13E+04	2.32E-02	0.1429						
15				pipe14	548.6	0.152	0.018146	19.03	0.291345	3.92E+04	2.68E-02	0.4187						
16				pipe15	335.3	0.152	0.018146	56.458906	0.864277	1.16E+05	2.43E-02	2.0414						
17				pipe16	548.6	0.152	0.018146	8.6538103	0.132473	1.78E+04	3.01E-02	0.0973						
18				pipe17	365.9	0.254	0.050671	84.814923	0.464957	1.05E+05	2.23E-02	0.3545						
19				pipe18	548.6	0.152	0.018146	-14.24	-0.21805	2.93E+04	2.79E-02	0.2436						
20				pipe19	396.2	0.152	0.018146	-16.84559	-0.25787	3.47E+04	2.72E-02	0.2406						
21																		

Figure D.4. Solver solution for the pipe-network using the Swamee-Jain formula

The second sheet that uses the Colebrook-White formula was developed following a similar procedure and Solver was used to determine the flow rates that satisfy the energy equations. Figure D.6 shows the solution obtained with the **GRG Nonlinear** method of Solver with this formula. Figure D.5 that also shows the flow rates calculated by this formula shows that their values are close to those obtained with the Swamee-Jain formula and agree well with those obtained by Brkic [1].

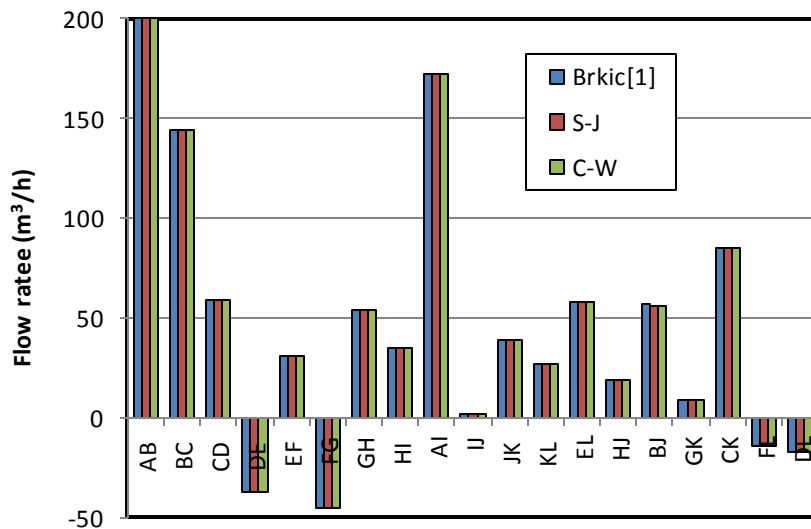


Figure D.5. Comparison of the flow rates obtained by the present analyses for the eight-loop pipe-network with those given by Brkic [1]

# Computer-Aided Thermofluid Analyses Using Excel

fx =IF(I2=0,0,IF(J2<2000,64/J2,NRM("colebrook",0.01,K2,J2)))

	A	B	C	D	E	F	G	H	I	J	K	L	M	N	O	P	Q
1				pipe	L (m)	D (m)	A	Q (m <sup>3</sup> /h)	V (m/s)	Re	ε/D	f	hf		Errors		
2	p	1000		pipe1	457.2	0.305	0.073062	200.62382	0.762764	2.06E+05	8.52E-04	2.04E-02	0.9068		Loop 1	0.001	
3	visc	1.13E-06		pipe2	304.8	0.203	0.032365	144.11712	1.23689	2.22E+05	1.28E-03	2.20E-02	2.5707		Loop 2	0.001	
4	g	9.81		pipe3	365.8	0.203	0.032365	59.340834	0.509295	9.15E+04	1.28E-03	2.33E-02	0.5539		Loop 3	0.001	
5	ε	0.00026		pipe4	609.6	0.203	0.032365	-37.20728	-0.31933	5.74E+04	1.28E-03	2.44E-02	0.3803		Loop 4	0.001	
6				pipe5	853.4	0.203	0.032365	31.303839	0.268666	4.83E+04	1.28E-03	2.49E-02	0.3847		Loop 5	0.001	
7				pipe6	335.3	0.203	0.032365	-45.15	-0.38752	6.96E+04	1.28E-03	2.39E-02	0.3017		Loop 6	0.001	
8				pipe7	304.8	0.203	0.032365	53.87	0.462343	8.31E+04	1.28E-03	2.35E-02	0.3837		Loop 7	7.79E-05	
9				pipe8	762	0.203	0.032365	34.817515	0.298823	5.37E+04	1.28E-03	2.46E-02	0.4195		Loop 8	0.001	
10				pipe9	243.8	0.203	0.032365	172.69618	1.482171	2.66E+05	1.28E-03	2.18E-02	2.9302				
11				pipe10	396.2	0.152	0.018146	1.438666	0.022023	2.96E+03	1.71E-03	4.52E-02	0.0029		Maxerror	0.001	
12				pipe11	304.8	0.152	0.018146	38.892649	0.595371	8.01E+04	1.71E-03	2.47E-02	0.8960				
13				pipe12	335.3	0.254	0.050671	26.732946	0.14655	3.29E+04	1.02E-03	2.56E-02	0.0370				
14				pipe13	304.8	0.254	0.050671	57.85	0.317128	7.13E+04	1.02E-03	2.30E-02	0.1418				
15				pipe14	548.6	0.152	0.018146	19.05	0.29166	3.92E+04	1.71E-03	2.66E-02	0.4156				
16				pipe15	335.3	0.152	0.018146	56.506696	0.865008	1.16E+05	1.71E-03	2.41E-02	0.2073				
17				pipe16	548.6	0.152	0.018146	8.7181161	0.133458	1.80E+04	1.71E-03	2.98E-02	0.0977				
18				pipe17	365.9	0.254	0.050671	84.776288	0.464745	1.04E+05	1.02E-03	2.22E-02	0.3515				
19				pipe18	548.6	0.152	0.018146	-14.26	-0.21836	2.94E+04	1.71E-03	2.76E-02	0.2420				
20				pipe19	396.2	0.152	0.018146	-16.85189	-0.25797	3.47E+04	1.71E-03	2.70E-02	0.2385				
21																	

Figure D.6. Hydraulic solution found with Solver using the Colebrook-White formula

## References

- [1] D. Brkic, Spreadsheet-Based Pipe Networks Analysis for Teaching and Learning Purpose, *Spreadsheets in Education (eJSIE)*: Vol. 9: Iss. 2, Article 4, 2016. Available at: <http://epublications.bond.edu.au/ejsie/vol9/iss2/4>

### Appendix E: Finite-difference analysis of the heat transfer from a triangular fin

This appendix supplements Chapter 7 that deals with the numerical solution of the steady conduction equation using the finite-difference (FD) method. The appendix demonstrates the application of the FD method for solving the conduction equation in complex geometries by considering the case of the heat-conduction in a triangular fin given by Cengel and Ghajar [1] in Example 5-2.

#### Case description

An aluminium alloy fin ( $k=180 \text{ W/m.K}$ ) has a triangular cross section as shown in Figure E.1. The fin has length  $L=5 \text{ cm}$ , base thickness  $t = 1 \text{ cm}$ , and very large width  $w$ . The base of the fin is maintained at a temperature of  $T_b=200^\circ\text{C}$ . The fin losses heat to the surrounding medium at  $T_\infty = 25^\circ\text{C}$  with a heat transfer coefficient of  $h = 15 \text{ W/m}^2.\text{K}$ . Using the finite difference method with six equally spaced nodes along the fin in the  $x$ -direction, determine the temperature variation in the fin along its length.

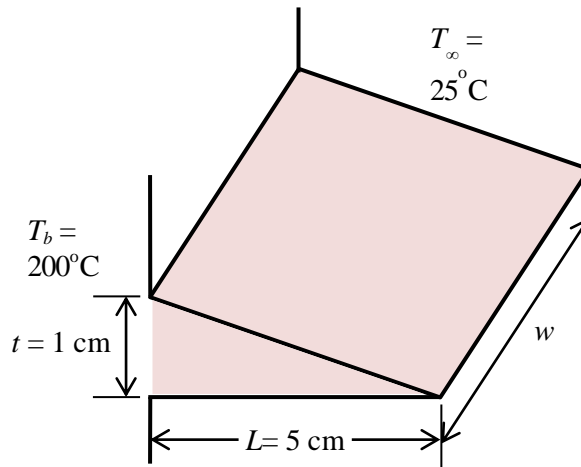


Figure E.1. The dimensions and boundary conditions of the triangular fin

#### Developing the FD equations

As discussed in Chapter 7, for steady one-dimensional conduction heat-transfer in a medium without heat generation, the conduction equation reduces to:

$$\frac{d^2T}{dx^2} = 0 \quad (\text{E.1})$$

Two boundary conditions are given, which are: (i) specified temperature at the base and (ii) convection boundary condition at the top and bottom surfaces as shown in Figure E.1. To develop the relevant FD equations, the fin is divided into five segments of equal length ( $\Delta x$ ) as shown in Figure E.2.

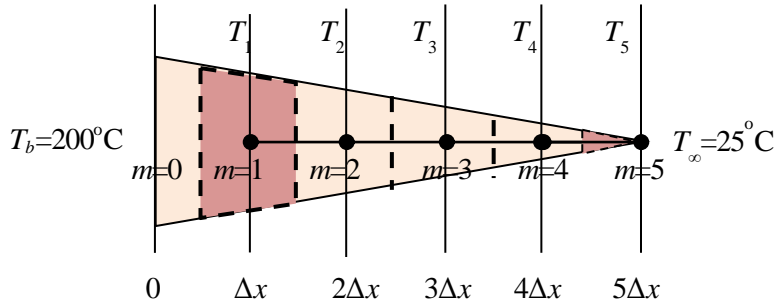


Figure E.2. Numerical mesh of nodes for the triangular fin

At steady state, the rate of heat transfer by conduction entering each segment from its left side is balanced by the rate of heat transfer leaving the segment by conduction through its right side and by convection through the top and bottom surface areas, i.e.

$$\dot{Q}_{cond,L} = \dot{Q}_{cond,R} + \dot{Q}_{conv} \quad (E.2)$$

Where,  $\dot{Q}_{cond,L}$  and  $\dot{Q}_{cond,R}$  refer to the heat transfer by conduction through left and right sides of the fin segment, respectively, while  $\dot{Q}_{conv}$  refers to the heat transfer by convection from the top and bottom sides of the segment. Applying Fourier law for conduction for  $\dot{Q}_{cond,L}$  and  $\dot{Q}_{cond,R}$  and Newton's law of cooling for  $\dot{Q}_{conv}$ , the following equation is obtained based on Equation (E.2):

$$-A_L k \left. \frac{dT}{dx} \right|_{xL} = -A_R k \left. \frac{dT}{dx} \right|_{xR} + hA_{conv}(T - T_\infty) \quad (E.3)$$

The temperature derivatives in Equation (E.3) are now replaced by the respective finite temperature differences across the segment. For node 1, these are given by:

$$\left. \frac{dT}{dx} \right|_{xL} \approx \frac{(T_1 - T_0)}{\Delta x} \quad (E.4)$$

$$\left. \frac{dT}{dx} \right|_{xR} \approx \frac{(T_2 - T_1)}{\Delta x} \quad (E.5)$$

Substituting in Equation (E.3), the resulting FD equation for node 1 is:

$$-A_L k \frac{(T_1 - T_0)}{\Delta x} = -A_R k \frac{(T_2 - T_1)}{\Delta x} + hA_{conv}(T_1 - T_\infty) \quad (E.6)$$

Where the three areas  $A_L$ ,  $A_R$  and  $A_{conv}$  are calculated from:

$$A_L = \frac{(L - \Delta x / 2)wt}{L} \quad (E.7)$$

$$A_R = \frac{(L - 3\Delta x / 2)wt}{L} \quad (E.8)$$

$$A_{conv} = 2 \frac{w\Delta x}{\cos(\theta)} \quad (E.9)$$

Where  $L$ ,  $w$ , and  $t$  are the three dimensions of the fin shown in Figure E.1 and  $\theta$  is the fin's angle ( $\theta = \tan^{-1}(t/2L)$ ).

Equations similar to Equation (E.6) can be obtained for nodes 2, 3, and 4 by replacing the temperature derivatives and side areas with the respective values for each node. However, node 5 requires a slightly different treatment because there is no heat transfer by conduction from its right side and also because its convection area is half the value at the other segments. Table E.1 shows the corresponding terms in Equation (E.6) for the five nodes as described in more details by Cengel and Ghajar [1].

Table E.1. Terms in Equation (E.3) corresponding to each node

	Node 1	Node 2	Node 3	Node 4	Node 5
$\left. \frac{dT}{dx} \right _{xL}$	$\frac{(T_1 - T_0)}{\Delta x}$	$\frac{(T_2 - T_1)}{\Delta x}$	$\frac{(T_3 - T_2)}{\Delta x}$	$\frac{(T_4 - T_3)}{\Delta x}$	$\frac{(T_5 - T_4)}{\Delta x}$
$\left. \frac{dT}{dx} \right _{xR}$	$\frac{(T_2 - T_1)}{\Delta x}$	$\frac{(T_3 - T_2)}{\Delta x}$	$\frac{(T_4 - T_3)}{\Delta x}$	$\frac{(T_5 - T_4)}{\Delta x}$	0
$A_L$	$\frac{(L - \Delta x / 2)wt}{L}$	$\frac{(L - 3\Delta x / 2)wt}{L}$	$\frac{(L - 5\Delta x / 2)wt}{L}$	$\frac{(L - 7\Delta x / 2)wt}{L}$	$\frac{(L - 9\Delta x / 2)wt}{L}$
$A_R$	$\frac{(L - 3\Delta x / 2)wt}{L}$	$\frac{(L - 5\Delta x / 2)wt}{L}$	$\frac{(L - 7\Delta x / 2)wt}{L}$	$\frac{(L - 9\Delta x / 2)wt}{L}$	0
$A_{conv}$	$2w \frac{\Delta x}{\cos(\theta)}$	$2w \frac{\Delta x}{\cos(\theta)}$	$2w \frac{\Delta x}{\cos(\theta)}$	$2w \frac{\Delta x}{\cos(\theta)}$	$2w \frac{\Delta x / 2}{\cos(\theta)}$

The FD equations for the five nodes can be written as:

$$C_{1,m}(T_{m-1} - T_m) + C_{2,m}(T_{m+1} - T_m) + C_{3,m}(T_\infty - T_m) = 0 \quad (E.10)$$

Where,  $m = 1, 2, 3, 4$ , or  $5$ . For nodes 1 to 4 the constants  $C_{1,m}$ ,  $C_{2,m}$  and  $C_{3,m}$  are obtained from:

$$C_{1,m} = \left[ 1 - \left( m - \frac{1}{2} \right) \frac{\Delta x}{L} \right] \quad (\text{E.11})$$

$$C_{2,m} = \left[ 1 - \left( m + \frac{1}{2} \right) \frac{\Delta x}{L} \right] \quad (\text{E.12})$$

$$C_{3,m} = \frac{h(\Delta x)^2}{kL \sin \theta} \quad (\text{E.13})$$

For node 5, the three constants are obtained from:

$$C_{1,5} = \tan \theta \quad (\text{E.14})$$

$$C_{2,5} = 0 \quad (\text{E.15})$$

$$C_{3,5} = \frac{h\Delta x}{k \cos \theta} \quad (\text{E.16})$$

Substituting for each node the respective values in Equation (E.10) leads to the following system of linear equations that can be solved to determine the five unknown temperatures:

$$C_{1,1}(T_0 - T_1) + C_{2,1}(T_2 - T_1) + C_{3,1}(T_\infty - T_1) = 0 \quad (\text{E.17})$$

$$C_{1,2}(T_1 - T_2) + C_{2,2}(T_3 - T_2) + C_{3,2}(T_\infty - T_2) = 0 \quad (\text{E.18})$$

$$C_{1,3}(T_2 - T_3) + C_{2,3}(T_4 - T_3) + C_{3,3}(T_\infty - T_3) = 0 \quad (\text{E.19})$$

$$C_{1,4}(T_3 - T_4) + C_{2,4}(T_5 - T_4) + C_{3,4}(T_\infty - T_4) = 0 \quad (\text{E.20})$$

$$C_{1,5}(T_4 - T_5) + 0 + C_{3,5}(T_\infty - T_5) = 0 \quad (\text{E.21})$$

### Excel implementation

The algebraic system of Equations (E.17) – (E.21) can be rearranged in a matrix form and then solved by using the matrix-inversion method as shown in Chapter 2. Alternatively, the system can be solved by using Solver and Figure E.3 shows the Excel sheet developed for this method. The left part of the sheet shows the given data for the fin. Cells **C5** stores the base temperature ( $T_b=200^\circ\text{C}$ ), while cell **C6** stores the ambient temperature ( $T_\infty=25^\circ\text{C}$ ). Cells **H3** to **L3** contain guessed values of the temperatures  $T_1$  to  $T_5$ .

	A	B	C	D	E	F	G	H	I	J	K	L	M
1													
2	L	0.05	m	$\theta$	0.0997		T0	T1	T2	T3	T4	T5	T $\infty$
3	t	0.01	m	sin $\theta$	0.0995		200	150	100	50	40	30	25
4													
5	Tb	200	$^{\circ}$ C				m	1	2	3	4	5	
6	T $\infty$	25	$^{\circ}$ C				C1	0.9	0.7	0.5	0.3	0.1	0.1
7	k	180					C2	0.7	0.5	0.3	0.1	0	
8	h	15					C3	0.001675	0.001675	0.001675	0.001675	0.000837	0.000837
9													
10	$\Delta x$	0.01	m				R	9.790628	9.874377	21.95813	1.974875	0.995813	
11													

Figure E.3. Excel sheet prepared for FD solution of the triangular fin

Cells **H5** to **L5** store the values of  $m$  corresponding to each node. The following three rows store values of the three constant  $C_{1,m}$ ,  $C_{2,m}$  and  $C_{3,m}$  that correspond to each node. The bottom row (cells **H10** to **L10**) stores values of the residuals in the right-hand-sides of the algebraic equations resulting from the substitution of the guessed values of the temperatures in Equations (E.17) – (E.21). The formula bar reveals the formula used for the calculation of  $R_4$ . Note that, since the guessed temperatures are not correct, the residuals are not zeros.

Solver can now be used to adjust values of the five temperatures until the five corresponding residuals become approximately zeros. Figure E.4 shows the set-up of Solver for this task.

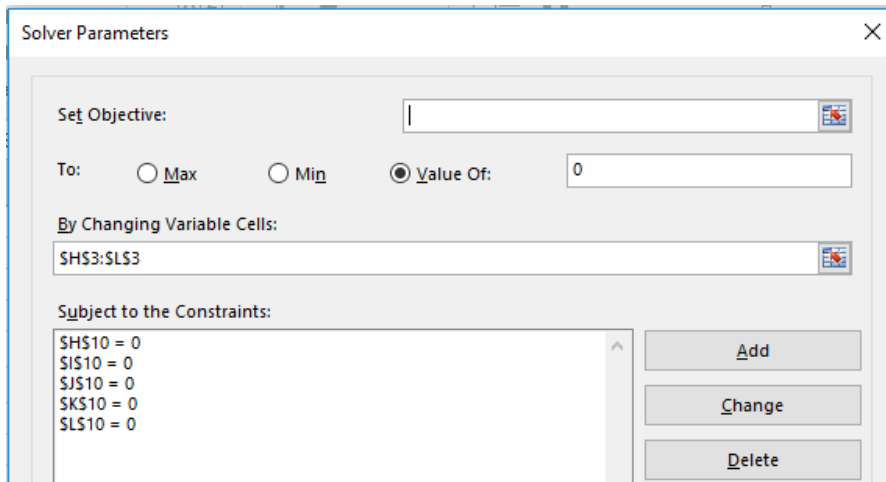


Figure E.4. Solver set-up for FD solution of the triangular fin

Note that the target cell is left blank. The adjustable cells are the guessed temperature stored in cells **H3** to **L3**. The constraints added require that values of the residuals stored in cells **H10** to **L10** become approximately zeros. In this case, Solver will iterate

## Computer-Aided Thermofluid Analyses Using Excel

until all the constraints are satisfied. Figure E.5 shows the sheet with Solver solution which is:  $T_1 = 198.6^\circ\text{C}$ ,  $T_2 = 197.1^\circ\text{C}$ ,  $T_3 = 195.7^\circ\text{C}$ ,  $T_4 = 194.3^\circ\text{C}$ , and  $T_5 = 192.9^\circ\text{C}$ . The same solution was given by Cengel and Ghajar [1].

	A	B	C	D	E	F	G	H	I	J	K	L	M
1													
2	L	0.05	m	$\theta$	0.0997		T0	T1	T2	T3	T4	T5	$T_\infty$
3	t	0.01	m	$\sin\theta$	0.0995		200	198.5676	197.1412	195.7209	194.3069	192.9008	25
4													
5	Tb	200	$^\circ\text{C}$				m	1	2	3	4	5	
6	$T_\infty$	25	$^\circ\text{C}$				C1	0.9	0.7	0.5	0.3	0.1	0.1
7	k	180					C2	0.7	0.5	0.3	0.1	0	
8	h	15					C3	0.001675	0.001675	0.001675	0.001675	0.000837	0.000837
9													
10	$\Delta x$	0.01	m				R	1.48E-06	-2.1E-06	-2.2E-05	8.79E-07	-2.8E-07	
11													

Figure E.5. Solver solution of the FD equations of the triangular fin

## References

- [1] Y. A. Cengel and A. J. Ghajar, *Heat and Mass Transfer: Fundamentals and Applications*. 4<sup>th</sup> edition, McGraw-Hill, 2011



## Appendix F: Macros and VBA functions for applying the finite-difference method with Excel

This appendix supplements Chapter 8 that deals with the numerical solution of the transient heat-conduction equation with the finite-difference (FD) method. It describes the procedure of recording the macro needed for implementing the explicit FTCS scheme in Example 8-2 and provides the two VBA functions, **Fdimplicit** and **TDMA**, needed for implementing the implicit BTCS scheme in Example 8-1. A macro is a useful feature for performing parametric analyses and repetitive calculations. It allows Excel to record the sequence of actions for the initial value of the targetted parameter and then repeat them for other values by a push of a button. The **TDMA** solver is also useful for solving systems of linear equations that arise in other types of thermofluid analyses.

### F.1. Recording a macro

The procedure of creating the macro can be demonstrated by describing that needed for applying the explicit finite-difference scheme (FTCS) in Example 8-2. Figure F.1 shows the Excel sheet developed for this example.

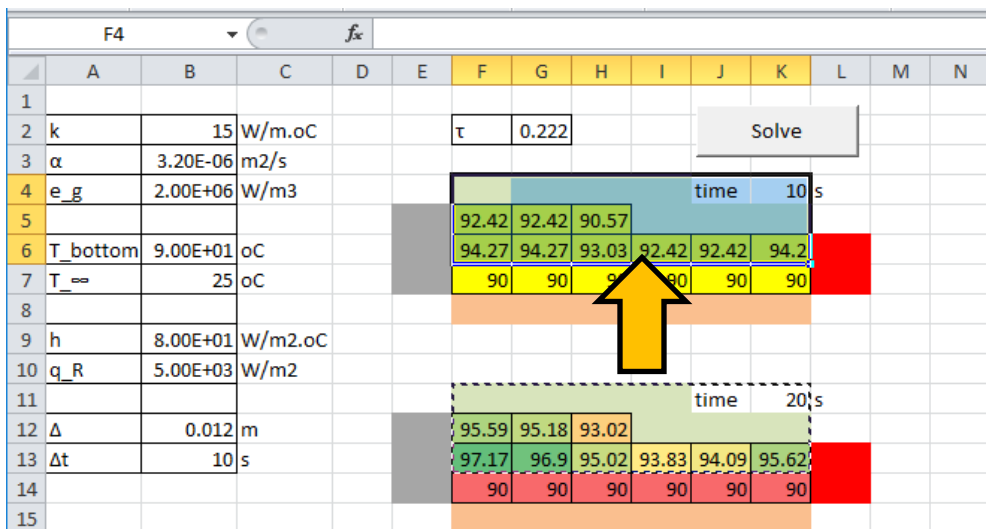


Figure F.1. Advancing the FD solution by copying the temperature values after one time-step from the bottom cells and pasting them in the coressponding top cells

Figure F.1 shows the FD solution at two consecutive time levels. The cells in the bottom block store the temperature values at the current time level  $i$ , while those in the top block calculate the temperatures at the new time level  $i+1$  after one time-step ( $\Delta t$ ). To update the temperature values in the top block, the values in the bottom cells are copied and pasted in the coressponding top cells. This procedure is repeated until the targetted time level is reached. To create the macro for this repetitive procedure:

## Computer-Aided Thermofluid Analyses Using Excel

1. Go to the **Developer** tab and select “**Record Macro**” as shown in Figure F.2. The form shown in Figure F.3 will appear to you. The first macro will automatically be given the name “**Macro 1**”. You can change this name and give it a description if you like. Press “**OK**”.
2. Copy the values in the bottom block of cells, i.e. cells **F11:K13**
3. Use **Paste-special** to paste the values in the top cells; **F4:K6** (Figure F.1)
4. Go back to the **Developer** tab and select “**Stop Recording**” (Figure F.4)

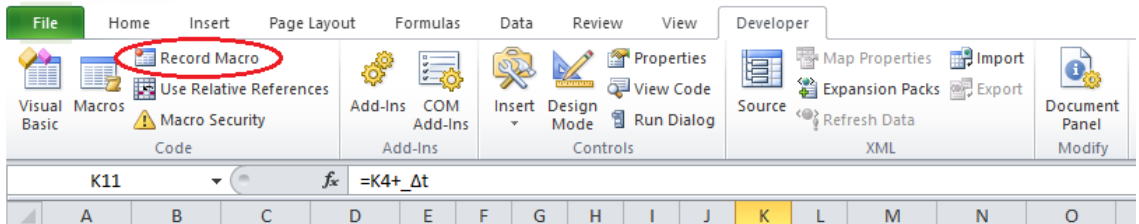


Figure F.2. Initiating the macro by selecting “Record Macro” from the Developer tab

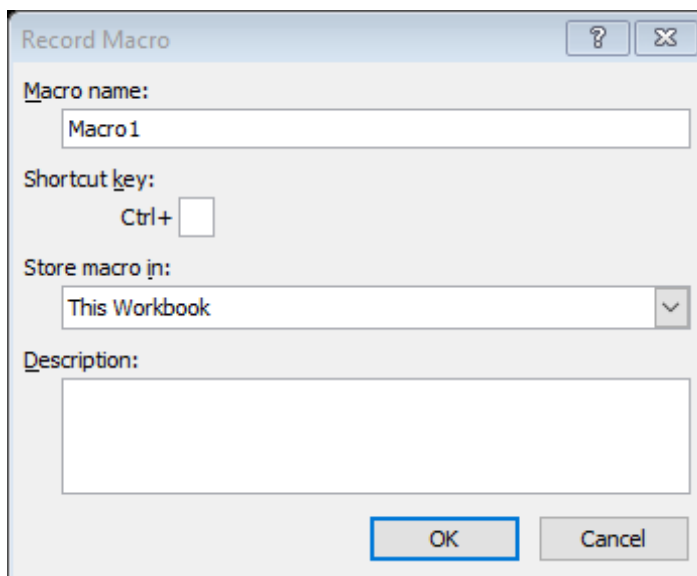
The image shows the 'Record Macro' dialog box. It has a title bar with a question mark and a close button. The 'Macro name:' field contains 'Macro1'. The 'Shortcut key:' field shows 'Ctrl+' followed by an empty box. The 'Store macro in:' dropdown menu is set to 'This Workbook'. The 'Description:' field is empty. At the bottom, there are 'OK' and 'Cancel' buttons.

Figure F.3. Form for selecting the macro, adding a description to the macro, and changing its name if needed

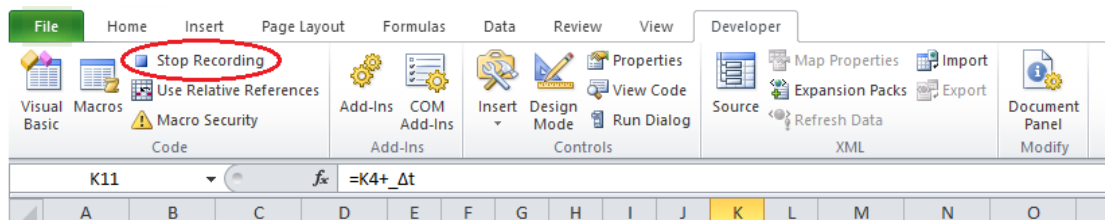


Figure F.4. Ending the micro recording by selecting the “Stop Recording” function

To create a button for the new macro, go to the **Developer** tab and insert a “**button form control**” as shown in Figure F.5. Place the button in a suitable location in the sheet and the form shown in Figure F.6 will appear to you. As the figure shows, the button will automatically be given the name “**Button1\_Click**”.

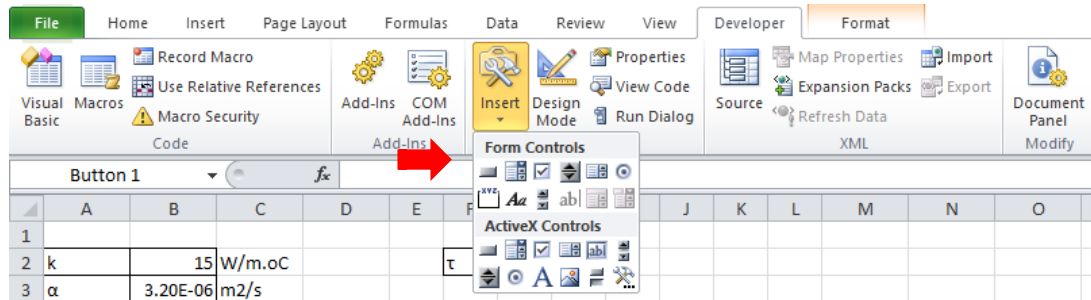


Figure F.5. Creating a button for the new macro

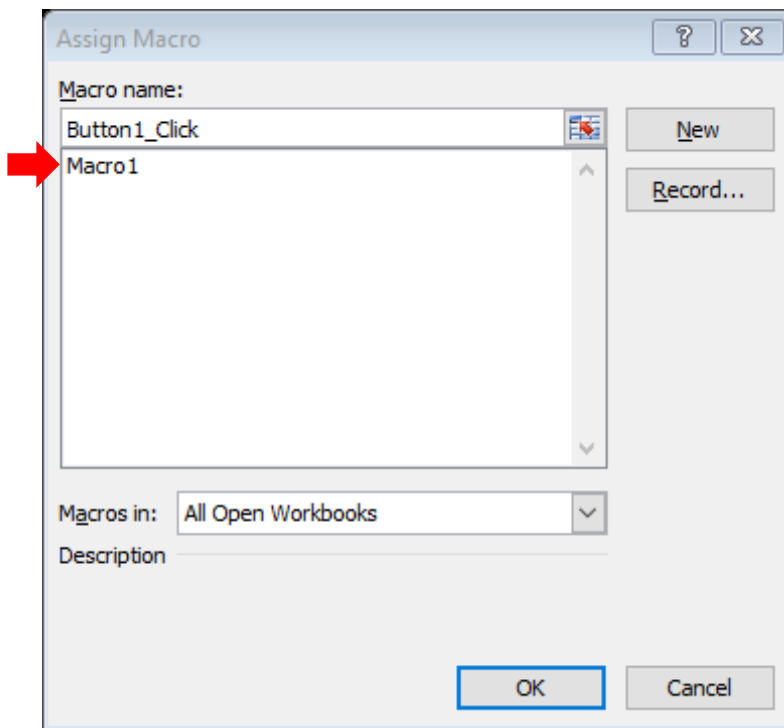


Figure F.6. Assigning “Button 1” to “Macro 1”

This button should now be linked to the macro and the form shown in Figure F.6 gives you a list of the available macros to select from. Since Macro1 is the only macro we have created so far, the list only includes it. Select “**Macro1**” and press “**OK**”. The new button will then appear in the Excel sheet with the name “**Button 1**” as shown in Figure F.7. Your macro is now ready to use and you by pressing the button once, Excel will automatically advance the explicit solution by one time step.

## Computer-Aided Thermofluid Analyses Using Excel

	A	B	C	D	E	F	G	H	I	J	K	L	M	N
1														
2	k	15	W/m.oC			$\tau$	0.222					Button 1		
3	$\alpha$	3.20E-06	m2/s											
4	e_g	2.00E+06	W/m3							time	10 s			
5						92.42	92.42	90.57						
6	T_bottom	9.00E+01	oC			94.27	94.27	93.03	92.42	92.42	94.2			
7	T_∞	25	oC			90	90	90	90	90	90			
8														

Figure F.7. The Excel sheet with the new button “Button 1”

To change the button’s name to a more meaningful one like “Solve”, “Run”, “Advance solution”, etc, place the cursor on the button and click the right side of your mouse. The form shown in Figure F.8 will then appear to you. Select “Edit Text” and change the name as desired. For more information about this feature, the reader can refer to specialised references or the internet [1,2].

D	E	F	G	H	I	J	K	L	M	N	O	P
		$\tau$	0.222					Button 1				
								time	1			
		92.42	92.42	90.57								
		94.27	94.27	93.03	92.42	92.42	94					
		90	90	90	90	90	90					
								time	2			
		95.59	95.18	93.02								

Figure F.8. Changing the name “Button 1” to a more indicative one

### F.2. The VBA functions

The function **Fdimplicit** determines the coefficient matrix given by Equation (9.12), while the **TDMA** function applies the tri-diagonal matrix algorithm for solving the resulting system of linear-equations. The two functions are listed below.

#### The function Fdimplicit

Function Fdimplicit(Dx, Dt, alfa, N, M, L, Temp)

Dim A As Variant

Dim B As Variant

Dim C As Variant

Dim D As Variant

Dim Sol As Variant

ReDim A(150), B(150), C(150), D(150), Sol(1 To 150)

```
Ai = -alfa / (Dx * Dx)
Bi = (1 / Dt) + (2 * alfa / Dx / Dx)
Ci = -alfa / Dx / Dx
```

```
For ic = 1 To N
A(ic) = Ai
B(ic) = Bi
C(ic) = Ci
D(ic) = (1 / Dt) * Temp(ic)
Next ic
```

```
B(1) = 1#
C(1) = 0#
D(1) = 0#
A(N) = 0#
B(N) = 1#
D(N) = 0#
```

```
Temp = tdma(A, B, C, D, N, Sol)
FdimPLICIT = Sol
End Function
```

### **The function TDMA**

```
Function tdma(A, B, C, X, N, XX) As Variant
With Worksheets("Sheet1")
Dim AA, BB, CC, DD As Variant
```

```
Dim ic As Integer
ReDim AA(1 To N)
ReDim BB(1 To N)
ReDim CC(1 To N)
ReDim DD(1 To N)
ReDim XX(1 To N)
```

```
For ic = 1 To N
AA(ic) = A(ic)
BB(ic) = B(ic)
CC(ic) = C(ic)
XX(ic) = X(ic)
Next ic
```

```
CC(1) = CC(1) / BB(1)
XX(1) = XX(1) / BB(1)
```

## Computer-Aided Thermofluid Analyses Using Excel

```
' loop from 1 to N - 1
For ic = 2 To (N - 1)
M = 1# / (BB(ic) - AA(ic) * CC(ic - 1))
CC(ic) = CC(ic) * M
XX(ic) = (XX(ic) - AA(ic) * XX(ic - 1)) * M
Next ic
M = 1# / (BB(N) - AA(N) * CC(N - 1))
XX(N) = (XX(N) - AA(N) * XX(N - 1)) * M

' loop from N - 1 to 1
For ic = (N - 1) To 1 Step -1
XX(ic) = XX(ic) - CC(ic) * XX(ic + 1)
Next ic

tdma = XX
End With
End Function
```

### References

- [1] J. Walkenbach, *Excel 2010 Formulas*, Wiley Publishing Inc., 2010
- [2] J. Walkenbach, *Excel 2007 Charts*, Wiley Publishing Inc., 2007

## Subject Index

- Activation of Solver, 52, 55
- Adiabatic process, 229
- air-conditioning, 6, 45, 255
- backward difference, 168
- boundary conditions, 164, 165, 167, 169, 170, 173, 181, 184, 187, 188, 195, 197, 203, 205, 206, 272, 273
- Brayton cycle, 208, 209, 210, 213, 215, 216
- built-in function, 24, 25, 68
- Cascade refrigeration, 234
- cavitation**, 88, 89, 91
- central difference, 168, 186
- centrifugal pump, 38, 111, 112, 113, 115, 116, 119
- Chezy-Manning equation, 9
- Coefficient of performance, 220, 230, 245
- Colebrook equation, 9, 15, 79, 95, 96, 97, 98, 249
- Constrained iterative solutions, 88
- continuity equation, 2, 123, 129, 137, 142, 152, 153, 155, 257, 259, 260, 263, 266, 269
- convection heat-transfer, 10, 101
- Convection heat-transfer analyses, 85
- cross-flow, 13, 14
- Darcy-Weisbach equation, 8, 9, 31, 79, 90
- Diesel cycle, 14, 216, 225, 226
- Dittus-Boelter equation, 11, 86
- economic diameter, 109
- energy equation, 8, 89, 105, 110, 120, 123, 124, 126, 129, 137, 139, 142, 143, 150, 152, 153, 155, 156, 157, 258, 266, 267, 269
- Evolutionary method, 54, 57, 58, 59, 62, 63, 64
- Excel built-in functions, 29
- Excel formula, 24, 31, 41, 68, 69, 96, 211, 249, 250
- Exergy, 19, 208, 220, 221, 222, 223, 245
- feed-water, 5, 6
- Fin, 12, 48, 49, 182, 183, 184, 205, 206, 272, 273, 274, 276, 277
- Finite Difference Method, 182
- formula bar, 23, 24, 25, 28, 29, 39, 68, 87, 90, 250, 253, 254
- forward difference, 63, 168
- forward-in-time, 186
- Fourier number, 187, 194, 199
- friction coefficient, 254, 255
- friction factor, 8, 9, 15, 16, 79, 80, 90, 95, 96, 97, 132, 249, 254
- Functions for matrix operations, 32
- global minimum, 57
- Goal Seek
  - Iterative solution, 18, 19, 23, 38, 39, 40, 41, 43, 44, 47, 50, 52, 79, 80, 81, 82, 84, 85, 87, 88, 93, 97, 98, 100, 101
- GRG Nonlinear method, 54, 55, 57, 58, 59, 62, 63, 64, 76
- Hardy Cross, 257, 263, 265
- Hazen-Williams equation, 9
- heat conduction equation, 36, 182, 199, 205
- Heat generation, 164, 169, 170, 172, 173, 175, 176, 181, 194, 272
- heat-exchanger, 13, 212, 213
- heat-exchangers
  - Optimisation, 13
- ideal gas
  - law, 15, 20, 69, 92
- Ideal-gas mixtures, 82
- insulation, 11, 12, 16, 55
- interpolation functions, 18, 74, 252, 253, 255
- iterative solution
  - Constrained, 80, 82, 88, 91, 93, 98, 100, 101
- Iterative solutions
  - Goal Seek, 16, 95
- labelling, 23, 27, 47, 81
- linear systems, 23, 33, 36
- LMTD method, 100
- Logical functions, 31

## Computer-Aided Thermofluid Analyses Using Excel

- macros, 18
- major friction, 8
- matrix functions, 23, 59
- matrix inversion, 18, 33, 36, 177, 191
- Mean effective pressure, 219, 225
- minor friction, 8, 9
- Moody diagram, 8
- Multi-stage cycle, 20
- Newton-Raphson solver, 18, 74, 79, 98, 249
- NTU method, 100
- Nusselt number, 10, 11, 86
- objective function, 55, 158
- optimisation analyses
  - Solver, 5, 14, 16, 17, 52, 55, 74, 252
- Optimisation analyses, 16
- Otto cycle, 14, 19, 208, 216, 217, 218, 219, 220, 221, 222, 223, 224
- Pipe network, 17, 119, 120, 136, 137, 138, 141, 143, 154, 158, 159, 257, 260, 262
- Prandtl number, 11, 86
- Pump curve, 10, 113, 117, 129
- R134a, 15, 16, 25, 26, 77, 230, 232, 233, 244
- R22, 233, 244, 245
- Rankine cycle, 16, 208
- Raphson, 14, 15, 18, 74, 79, 98, 249
- Reynolds number, 8, 11, 16, 31, 80, 86, 90, 97, 254, 255
- shell-and-tube, 13, 100
- Simplex LP method, 59, 61
- Soave-Redlich-Kwong equation, 74
- TDMA, 186, 191, 192, 278, 281, 282
- Thermal resistance, 12, 85, 87
- Thermax, 18, 19, 51, 52, 70, 71, 74, 75, 82, 84, 96, 107, 208, 210, 211, 212, 215, 219, 222, 223, 224, 225, 228, 230, 231, 232, 233, 236, 237, 243, 244, 249, 252, 256
- Tri-diagonal matrix algorithm, 186, 191, 281
- vapour-compression refrigeration
  - Cycle, 228, 229, 230, 231, 232, 245
- VBA, 18, 64, 65, 66, 67, 69, 74, 75, 77, 96, 224